

**Water Resources Research Institute of the
University of North Carolina
Annual Technical Report
FY 2012**

Introduction

During 2012-2013 (Fiscal Year 2012), the Water Resources Research Institute (WRRI) of The University of North Carolina System was responsible for fostering and developing a research, training, and information dissemination program responsive to the water problems of the State and region. To develop its programs, the Institute maintains an aggressive effort to interact and communicate with federal, state, and local water managers. The close contact with water managers is a basis for determining the ever-changing water research priorities.

Research priorities continue to be identified by the WRRI Advisory Committee, composed of representatives of several federal and state agencies, local governments, industries, and non-governmental environmental organizations (NGOs), as well as by other water resource experts in the state with whom WRRI has close relationships. A technical review committee is also convened on an annual basis to advise WRRI staff on the scientific merit of research proposals submitted for funding. Full-time faculty members from all North Carolina institutions of higher education are eligible to receive grants from WRRI.

The information transfer program continued to focus on disseminating results of sponsored research and providing information on emerging water issues, solutions, and regulations. Results of research are disseminated by publication of technical completion reports, summaries in the WRRI newsletter, publication of summaries on the WRRI website, and presentations by investigators at the WRRI Annual Conference and individual group meetings where appropriate. WRRI continues to be a sponsor of continuing education credits by the NC Board of Examiners of Engineers and Surveyors and the NC Board of Landscape Architects. This allows WRRI to offer Professional Development Hours (PDHs) and contact hours for attendance at the WRRI Annual Conference and other workshops and seminars that WRRI sponsors.

WRRI continues to adapt to changes in the landscape of its home institution, NC State University, by consolidating its operations and maximizing staff efficiencies and outputs. They continue to leverage funds from a variety of sources to expand the reach and impact of research and outreach activities, and grow their involvement in and support of water-related research and outreach across the state.

Research Program Introduction

During 2012-2013 (Fiscal Year 2012), WRRI continued its regular program of fostering research, training, and information transfer responsive to water issues of the state and region. Results from Institute-supported research efforts are expected to assist local, municipal, state, regional and federal agencies improve their decision-making in the management and stewardship of their water resources. To help it chart and sponsor a research program responsive to the water resource issues and opportunities in North Carolina, WRRI interacts closely with the N.C. Department of Environment and Natural Resources, other agencies, water and power utilities, and an array of research and outreach programs within the UNC system and at private higher educational institutions across North Carolina. A research advisory committee provides input, guidance, and review of the Institute's research priorities on an annual basis. This committee is composed of representatives of several federal and state agencies, local governments, industries, and non-governmental environmental organizations (NGOs).

The results of this process are shared with prospective investigators as part of WRRI's annual call-for-proposals. Proposals that address the annual priorities and meet peer review and other criteria receive preferential consideration for funding. Research priorities, as determined via the above process, are incorporated into our Section 104 Objectives on an annual basis. The proposal solicitation, as in the past, is sent to relevant contacts at colleges and universities across North Carolina to apprise them of the opportunity to submit proposals. The call for proposals is also sent to an email distribution list of approximately 180 university faculty across North Carolina. Full-time faculty members from all North Carolina institutions of higher education are eligible to receive grants from WRRI.

The proposals received are sent to a Technical Committee and to external peer reviewers to determine the relevancy, need for the proposed research and relative strength and weaknesses. The Technical Committee convenes on an annual basis to review all comments made by reviewers, advise WRRI staff on the scientific merit of research proposals, and make recommendations regarding proposal funding.

Efforts were made to maintain a consolidated, refined, and focused list of FY12-13 research priorities based on in-depth discussions of the most significant water research needs and priorities for the state of North Carolina. These priorities were included in the annual call for FY 2012-2013, and the projects resulting from this annual call will be funded from March 1, 2013 to February 28, 2014 and will be reported in the next USGS Annual Report.

The FY 2012-2013 research priorities were:

- quantifying the economic value of water quality
- quantifying sources, transport, and fate of nutrients and sediments in surface waters, and water quality changes in NC watersheds in which TMDLs and nutrient management plans have been implemented
- defining and evaluating in-stream flow needs and aquatic ecosystem function
- groundwater flow and quality, human impacts
- evaluation of methods for quantifying pollutant removal from stream restoration practices and projects
- defining and evaluating different stormwater control measures, their relative pros and cons, and appropriate pollutant removal credits for these measures as they relate to sediment, nitrogen, phosphorous, pathogens/bacteria, and other stormwater contaminants in urban stormwater systems
- defining and evaluating realistic management measures that can quantifiably mitigate the effects of impervious cover on aquatic life, in different urban settings and stormwater systems
- understanding, quantifying, and managing risks and uncertainties in public water supplies, in the face of changing population, land use, climate, and regulations
- setting rates and financing capital improvements for water and/or sewer utilities, in the face of changing population, land use, climate, and regulations
- applying social science and economic valuation methodologies to help utilities better understand customers' level-of-service expectations, their motivations, and willingness to pay for services, as well as understand customer perceptions, attitudes, opinions and beliefs related to water, wastewater, and reclaimed water
- identifying, understanding, and applying innovative processes and

Research Program Introduction

technologies for water and wastewater treatment, plant operation, distribution systems, and potable and reclaimed water supply and waste discharge management •evaluation of alternative water sources (e.g., graywater or harvested rainwater) for differing consumptive uses (e.g., home irrigation), health risks of alternative sources, and potential impacts of alternative water use on overall water supply and demand

Identification of membrane foulants and optimum cleaning strategies for nanofiltration and reverse osmosis membranes treating groundwaters from the Castle Hayne and Peedee aquifers

Basic Information

Title:	Identification of membrane foulants and optimum cleaning strategies for nanofiltration and reverse osmosis membranes treating groundwaters from the Castle Hayne and Peedee aquifers
Project Number:	2011NC160B
Start Date:	6/15/2011
End Date:	6/14/2012
Funding Source:	104B
Congressional District:	NC004
Research Category:	Engineering
Focus Category:	Treatment, Groundwater, Water Supply
Descriptors:	None
Principal Investigators:	Orlando Coronell

Publications

There are no publications.

CONFIDENTIAL

Identification of membrane foulants and optimum cleaning strategies for nanofiltration and reverse osmosis membranes treating groundwaters from the Castle Hayne and Peedee aquifers: Final Report
(WRRRI project#11-03-W, Sub-award agreement#2011-1481-02)

Prepared by:

Orlando Coronell, Assistant Professor, PI
Alexander Gorzalski, Graduate Research Assistant

PI's contact information:

Orlando Coronell, coronell@unc.edu
163B Rosenau Hall, CB#7431
Department of Environmental Sciences and Engineering
University of North Carolina at Chapel Hill
Chapel Hill, NC 27599-7431
Tel: 919-0966-9010
Fax: 919-966-7911

Submitted to:

Mary Beth Barrow
North Carolina Water Resources Research Institute

March 29, 2013

Abstract

Membrane fouling consists of the accumulation of solutes and/or particulate matter on the membrane surface, resulting in decreased performance in terms of permeate water flux and/or solute rejection. Given the rising number of nanofiltration (NF) and reverse osmosis (RO) installations throughout North Carolina, studies on the fouling properties of local source waters and corresponding cleaning strategies are needed. Accordingly, we have identified foulants and optimum cleaning strategies for membranes collected from the Cape Fear Public Utility Authority (CFPUA) NF plant, which treats water from the Castle Hayne and Peedee aquifers. Castle Hayne foulants included dissolved organic matter and inorganic species, primarily calcium, silica, aluminum, and iron. Peedee foulants contained low concentrations of organic matter, and relatively high concentrations of calcium and silica. Alkaline cleaning solutions, particularly basic solutions containing ethylenediaminetetraacetic acid (EDTA), were shown to be more effective than acidic solutions at increasing water productivity in membrane samples fouled at the CFPUA treatment plant. In addition, membranes obtained directly from the manufacturer (not used in the CFPUA treatment plant) were fouled in the laboratory using waters collected at the CFPUA NF plant. The fouling produced in the laboratory could not be reversed using the cleaning solutions that successfully reversed fouling on membranes fouled at full-scale; this indicates that for the waters tested in this study, fouling in the laboratory is not representative of full-scale processes. Pretreatment of source waters was performed to simulate sand filtration, microfiltration, and ultrafiltration; the various filtration treatments were found to be ineffective at removing dissolved constituents that resulted in membrane fouling. Although membrane fouling significantly increases power consumption by the pumps in the membrane stages of the CFPUA treatment plant, increasing cleaning frequency above the current average of two times per year would result in limited energy savings compared to chemical and labor costs.

Table of Contents

ACKNOWLEDGMENTS	1
1. INTRODUCTION	2
2. METHODS	4
2.1. Treatment Plant Configuration.....	4
2.2. Water Collection and Prefiltration	4
2.3. Water Quality Analyses	5
2.4. Collection of Membrane Elements and Preparation of Cleaning Solutions.....	7
2.5. Characterization of Membranes and Foulant Layers	8
2.6. Membrane Cleaning and Performance Testing in Dead-end Configuration.....	9
2.7. Membrane Cleaning and Performance Testing Using in Cross-Flow Configuration	10
2.8. Other Data Sources.....	12
3. RESULTS.....	14
3.1. Source Water Quality and Prefiltration.....	14
3.2. Full-Scale Membrane System Performance.....	22
3.3. Comparison between the Performance of Fouled Membranes in Dead-End and Cross-Flow Filtration.....	30
3.4. Characterization of Membrane Foulants	32
3.5. Recreating Full-Scale Fouling in a Cross-Flow System	44
3.6. Comparing Dead-End and Cross-Flow Cleaning.....	47
3.7. Effect of Chemical Cleaning on Foulant Removal	48
3.8. Effect of Chemical Cleaning on Membrane Performance	56
3.9. Membrane Longevity	59
3.10. Optimizing Full-Scale Cleaning Frequency.....	61

4. DISCUSSION.....	68
4.1. Identification of Membrane Foulants.....	68
4.2. Potential Removal of Membrane Foulants by Prefiltration	69
4.3. Preventing Full-Scale Membrane Fouling	70
4.4. Comparison of Dead-End and Cross-Flow Systems for Testing Membrane Performance and Cleaning Efficiency	71
4.5. Evaluating Membrane Cleaning Solutions.....	72
4.6. Optimizing Cleaning Frequency	73
4.7. Determining the Applicability of XPS and RBS for the Identification of Membrane Foulants	74
4.8. Challenges in Replicating Full-Scale Fouling in Laboratory Cross-Flow Systems.....	76
4.9. Fluorescence Characterization of Organic Matter in Source Waters, Membrane Permeate Water, and Membrane Fouling Layers.....	77
5. SUMMARY.....	78
6. CONCLUSIONS	79
7. RECOMMENDATIONS.....	80
REFERENCES	81
Appendix 1: Abbreviations and Units.....	87
Appendix 2: Publications, Patents, Technology Transfer and Others	89
Appendix 3: Particle Size Distributions.....	90
Appendix 4: Effect of Dissolved Iron on Fluorescence Measurements	91
Appendix 5: Performance of Elements Collected from the Peedee Second Stage Cleaned with STPP+EDTA	92
Appendix 6: Additional SEM Images of Fouled Membranes	93
Appendix 7: Comparing EDX Results for Two Regions of the Same Sample	95
Appendix 8: Choosing a Clean Membrane Baseline – Comparison of TFC-ULP and TFC-S Elements.....	97
Appendix 9: Individual RBS Spectra.....	99

Appendix 10: Eluted Concentrations of Membrane Foulants Using Two Cleaning Solutions .	103
Appendix 11: SEM Images of Cleaned Membranes.....	104
Appendix 12: XPS Results for Cleaned Membranes.....	109
Appendix 13: EDX Results for Cleaned Membranes	113
Appendix 14: ATR-FTIR Results for Cleaned Membranes	117
Appendix 15: Chloride Rejection by Cleaned Elements	121

Acknowledgments

Funding for this research was provided by the State of North Carolina and the United States Geological Survey (USGS) through the Water Resources Research Institute of The University of North Carolina. Our partners at the Cape Fear Public Utility Authority, John Malone and Anthony Colon, were instrumental in sample collection, sharing of data, and advised the authors throughout the project. Dr. Carrie Donley at the Chapel Hill Analytical and Nanofabrication Laboratory (CHANL) graciously helped train the authors on SEM and EDX analyses, and processed XPS samples. FTIR analyses were performed using instrumentation belonging to the University of North Carolina's Energy Frontier Research Center. Professional Water Technologies (PWT) generously donated Lavasol 7 and OptiClean F membrane cleaning solutions, and Koch Membrane Systems donated a sheet of TFC-ULP membrane. The authors would also like to thank Dao Janjaroen at the University of Illinois at Urbana-Champaign for performing particle size distribution analyses on water samples, and Dr. Rose Cory and Katie Harrold for training on the use of fluorescence instrumentation and analyses and interpretation of fluorescence data. The RBS measurements were carried out in the Triangle Universities Nuclear Laboratories (TUNL), Durham, NC. The authors acknowledge Joshua Powell, Lin Lin, Eliot Meyer, Dr. Thomas Clegg and John Dunham for their assistance in analyzing samples using RBS.

1. Introduction

Over half of North Carolina's population relies on groundwater for their water supply (DWR, 2001), and in the Coastal Plain region, this figure is approximately 90% (NCDENR, 2010a). Population growth and changes in land use have increased demand and extraction of water from coastal aquifers, including the Lower Cape Fear, Upper Cape Fear, Black Creek, Peedee, Beaufort, Castle Hayne, Yorktown, and Surficial aquifers (DWR, 1991; DWR, 2001; DWR, 2002). In turn, increased extraction has resulted in declining groundwater levels and salt intrusion (DWR, 2008a; DWR 2008b; DWR 2009). To mitigate these problems, state regulators have restricted groundwater withdrawals in certain areas, forcing some water utilities to use non-ideal groundwaters that require more intensive treatment (DWR, 1991; DWR, 2001; DWR, 2002; DWR, 2008a).

Salt intrusion, or its predicted occurrence, is a main concern for drinking water production in the Coastal Plain (DWR, 2008a; DWR, 2008b; DWR, 2009). Water has been deemed salty (i.e., >250 ppm) in over 30% of the area of at least six of the main aquifers (NCDENR, 2010b). Additionally, new and upcoming drinking water quality regulations (USEPA, 1993; USEPA, 2001; USEPA, 2006) pose the challenge to utilities of ensuring the removal of a broad variety of contaminants and the control of disinfection byproducts. With evolving regulations, nanofiltration (NF) and reverse osmosis (RO) have become increasingly attractive treatment options as they can remove a broad range of contaminants in one treatment step (Mulder, 1996). By 2002, RO treatment of groundwater had already become a primary method for production of potable water in Dare, Currituck, and Hyde Counties with installed capacity of nearly 11 MGD (DWR, 2001; DWR, 2008a). Approximately ten RO and NF installations are currently being used throughout the state (Malone, 2010), with more expected in the future.

The primary challenge in membrane filtration is the phenomenon of fouling which consists of solute or particle deposition on the membrane surface or pores (Schafer et al., 2005; Al-Amoudi et al., 2007). Fouling results in decreased membrane performance as quantified by water productivity and salt rejection, and thus optimized membrane cleaning strategies are essential to recover performance and maximize membrane life. Optimum cleaning strategies, however, depend on the foulants present (Schafer et al., 2005; Al-Amoudi et al., 2007), and unfortunately there is limited information available on the foulants present and fouling properties of waters from North Carolina. Accordingly, there is a need to identify the main foulants and optimum membrane cleaning strategies for North Carolina waters.

For example, given that hardness, iron, and manganese are the main constituents of concern in the waters of the Castle Hayne and Peedee aquifers that feed the 6-MGD NF plant of the Cape Fear Public Utility Authority (CFPUA) in Wilmington, NC (Malone, 2010), acidic solutions were expected to be optimum cleaning agents (Schafer et al., 2005; Al-Amoudi et al., 2007); however, acid cleaning was ineffective. It was thus theorized that organics or their interactions with inorganic species (Contreras et al., 2009; Law et al., 2007; Lee, et al. 2005; Kim et al. 2009) may have caused the observed fouling, and thus alkaline cleaning was tested and found to recover membrane performance (Malone, 2010). Nevertheless, the foulants responsible for performance decrease were not identified, the pH of cleaning solutions had to be pushed to the limits of membrane tolerance (Malone, 2010; Koch, 2010a and 2010b), and it was unknown whether

using these cleaning solutions with pH conditions at the limits of membrane tolerance will result in long-term membrane damage. In order to avoid early membrane replacement at the CFPUA NF plant which serves 31,500 North Carolinians, there was a need to identify both the main membrane foulants in the Castle Hayne and Peedee waters and the corresponding optimum membrane cleaning strategies. Given the increasing number of NF/RO plants treating groundwaters in the Coastal Plain (DWR, 2001; DWR, 2008a), future NF/RO facilities will likely face similar problems as those observed by the CFPUA NF plant. The same problems are perhaps also currently faced by other NF/RO plants. As a result, studying the membrane fouling characteristics of the Castle Hayne and Peedee aquifers, and corresponding optimum membrane cleaning strategies, was of regional importance.

Accordingly, our goal in this study was to identify membrane foulants and optimum cleaning strategies for NF/RO membranes treating groundwaters from the Castle Hayne and Peedee aquifers. We present analyses of source water quality and pretreatment strategies, as well as the identification of membrane foulants and optimum cleaning strategies for utilities using NF/RO membranes to treat waters from the Castle Hayne and Peedee aquifers. We also compare the properties of foulant layers obtained in membranes fouled at the full-scale treatment plant and in the laboratory. A technique previously used to characterize unfouled membranes, Rutherford backscattering spectrometry (RBS), was introduced for fouled membrane characterization, and X-ray photoelectron spectroscopy (XPS), previously used for characterization of unfouled membranes and to a limited extent for characterization of foulant layers, was used extensively for characterization of fouled membranes. A study of the long-term effects on membrane performance of membrane cleaning using solutions with pH values above the limits recommended by manufacturers is also presented.

2. Methods

2.1. Treatment Plant Configuration

The top row of Figure 1 is a process flow diagram of the various treatment steps at the nanofiltration plant operated by the Cape Fear Public Utility Authority (CFPUA) at Wilmington, NC, which serves approximately 31,500 customers. The treatment plant has separate treatment trains for the Castle Hayne and Peedee aquifers. Water is pumped from each aquifer to the treatment plant, where sulfuric acid and a proprietary antiscalant are added to prevent the formation of inorganic precipitates. This conditioned, unfiltered water passes through 5 μm prefilters to remove suspended particulate matter that can result in rapid fouling of nanofiltration membranes. Following prefiltration, feed water is pumped at high pressures through two stages of nanofiltration elements arranged in series, with each stage containing six four-foot long membrane elements in series. Overall water recovery from both stages of the treatment plant is 80%, while the other 20%, referred to as membrane concentrate, is discharged to waste. The percent water recovery is thus calculated as

$$\text{Recovery (\%)} = \frac{\text{Permeate Flow Rate}}{\text{Feed Flow Rate}} \times 100 . \quad (1)$$

The membranes in all nanofiltration stages are polyamide thin-film composite membranes. The first stage of nanofiltration for the Castle Hayne water has ultra-low pressure membranes (TFC-ULP, Koch Membrane Systems, Wilmington, MA) which have 98.5% chloride rejection (Koch, 2010b). The Castle Hayne second stage, Peedee first stage, and Peedee second stage have softening membranes (TFC-S, Koch Membrane Systems) which have 85% chloride rejection (Koch, 2010a).

2.2. Water Collection and Prefiltration

A process flow diagram of the treatment plant and sample collection locations is shown in Figure 1. Water pumped directly from the aquifers before any treatment will be referred to as ‘plant intake’. Water collected after the water conditioning step at the treatment plant (i.e., pH adjustment and antiscalant addition) will be referred to as ‘unfiltered’ water. The ‘5 μm permeate’, ‘Peedee concentrate’ and ‘Castle Hayne concentrate’ labels describe the location where corresponding water samples were collected at the plant. Peedee concentrate and Castle Hayne concentrate were sampled from the first stage and second stage, respectively, of the nanofiltration stages. Unfiltered water samples were also filtered in the laboratory through 1.2 μm , 0.1 μm , or 100 kDa filters, and corresponding permeate samples were labeled accordingly (see Figure 1). The filter ratings used represent conventional sand filtration (1.2 μm), microfiltration (0.1 μm), and ultrafiltration (100 kDa) pretreatment steps (Kumar et al., 2006). The 1.2 μm , 0.1 μm , or 100 kDa filtered samples were referred to as ‘prefiltered’ waters because, if applied in the treatment plant, these prefiltration treatments would occur before nanofiltration.

Water samples were collected on August 18 and September 21 of 2011. All nanofiltration concentrate samples were collected in September and additional nanofiltration feed and permeate samples were collected on February 10, 2012. Samples were collected in 5-gallon polyethylene collapsible containers and immediately transferred from the treatment plant to the University of North Carolina at Chapel Hill, an approximately four hour drive. At the university, samples were immediately stored at 4°C until used. Collapsible containers were used to eliminate head space in the container to minimize iron precipitation during transport and storage.

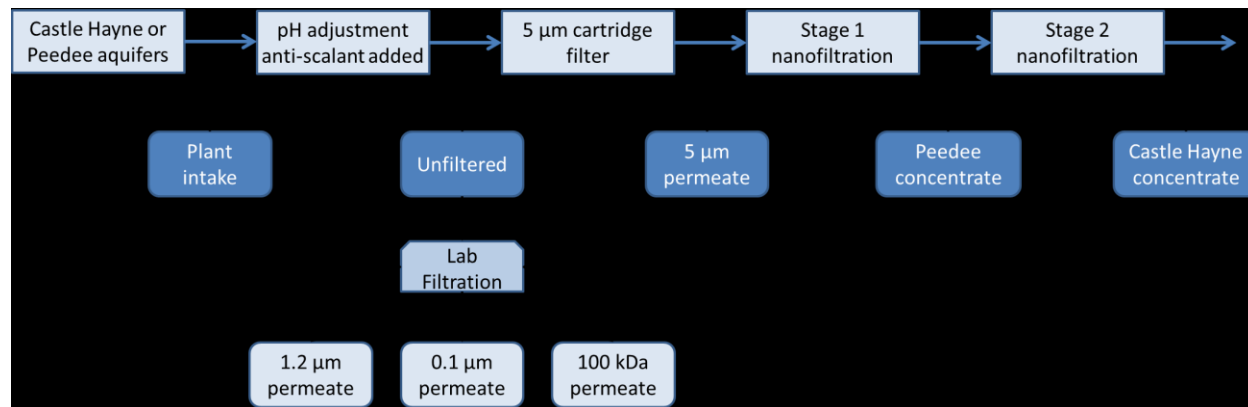


Figure 1. Process flow diagram of water treatment at the Cape Fear Public Utility Authority (CFPUA) Groundwater Nanofiltration Treatment Plant (Wilmington, NC) and locations of the collection of water samples . In the first two rows, white boxes depict treatment processes at the plant, and blue boxes depict sampling locations. Unfiltered samples collected after water conditioning were filtered at the laboratory using membranes with nominal pore sizes of 1.2 µm, 0.1 µm, or 100 kDa. The Pee Dee water treatment train uses TFC-S membranes (Koch Membrane Systems, Wilmington, MA) in both nanofiltration stages. The Castle Hayne water treatment train uses TFC-ULP membranes (Koch Membrane Systems) and TFC-S membranes in the first stage and second stage, respectively, of nanofiltration.

2.3. Water Quality Analyses

Water quality analyses were divided into three groups: (1) conventional water quality parameters, (2) dissolved inorganic species, and (3) organic parameters. Membrane filters that minimized protein binding that would bias the measurement of organic parameters were selected for laboratory use. Table 1 lists materials and methods used to measure water quality parameters and simulate prefiltration processes. The rejection of each water quality parameter by prefiltration was calculated as

$$Rejection (\%) = \left(1 - \frac{Permeate\ Value}{Feed\ Value}\right) \times 100 \quad (2)$$

Table 1. Materials and methods for measuring water quality parameters and performing laboratory filtration tests.

Water Quality Parameter	Instrument/Method
Conventional Parameters	
Turbidity	Portable turbidimeter - Hach 2100P (Loveland, CO)
Silt density index (SDI)	Standard methods (ASTM, 2002)
Total suspended solids (TSS)	Standard methods (AWWA, 2006)
Hardness	Total hardness test kit - Hach (Loveland, CO)
Alkalinity	Standard methods (AWWA, 2006)
Conductivity	Benchtop conductivity meter - Mettler Toledo (Columbus, OH) Accumet Excel XL60 conductivity meter – Fisher Scientific (Pittsburgh, PA)
pH	Accumet AB15 pH meter - Fisher Scientific (Pittsburgh, PA)
Particle size distribution	Zetasizer Nano ZS90 - Malvern Instruments (Worcestershire, United Kingdom)
Dissolved Inorganics	
Dissolved ions	Al, Ca, Fe, Mn, Mg, Si, Na: ICP-MS - Agilent Technologies (Santa Clara, CA) Chloride: Ion selective electrode - Accumet/Fisher (Pittsburgh, PA) Sulfate: Standard Methods (AWWA, 2006)
Organic Parameters	
Dissolved organic carbon (DOC)	Total organic carbon analyzer - Shimadzu TOC-V SPH (Columbia, MD)
Ultraviolet absorbance (UVA)	Diode array spectrophotometer - Hewlett Packard (Palo Alto, CA)
Excitation-emission matrices (EEMs)	Fluorog-321 spectrofluorometer with xenon arc lamp, synapse CCD detector - HORIBA Jobin Yvon (Edison, NJ)
Laboratory Pretreatment	
Conventional sand filtration	1.2 μm cellulose acetate filter - General Electric (Tervose, PA)
Microfiltration	0.1 μm polyvinylidene fluoride (PVDF) filter - Millipore (Billerica, MA)
Ultrafiltration	100 kDa regenerated cellulose filter - Millipore (Billerica, MA)

Organic parameters were used to calculate a series of indicator parameters descriptive of the type of organics present in the water samples analyzed, including specific ultraviolet absorbance (SUVA), slope ratio (Sr), fluorescence index (FI), and intensity of specific fluorescence peaks. SUVA is calculated as UVA divided by DOC and serves as an indicator of the aromaticity of organics. Slope ratio (Sr) is used as an indicator of molecular weight (Helms et al., 2008), and is calculated by dividing the slope of the UV absorbance in the 275-295 nm wavelength range by the corresponding slope in the 350-400 nm range. Fluorescence index and intensity of fluorescent peaks are calculated based on EEMs data. Fluorescence index (FI) is a proxy for organic matter source and is calculated as the ratio of 470 nm emission intensity over 520 nm emission intensity at an excitation wavelength of 370 nm. The fluorescent signature of organic matter can be separated into a number of components, as shown in Figure 2. Components one, two, and three are associated with organic matter from plants and soil, bio-available and nitrogen-containing organic matter, and microbially-derived materials, respectively.

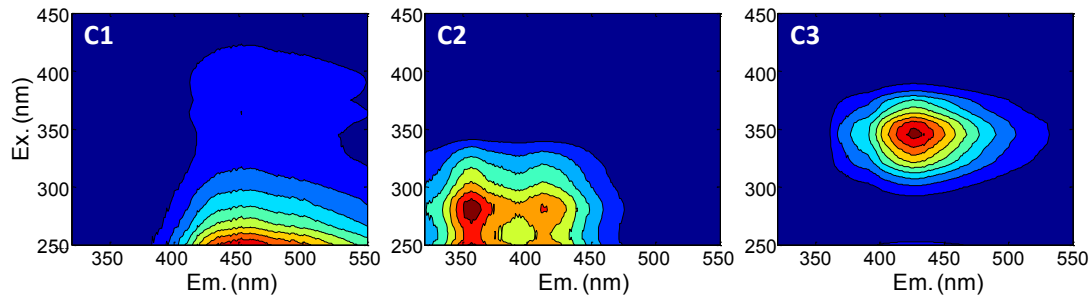


Figure 2. Fluorescence excitation-emission matrices (EEMs) showing the main components in the fluorescent signature of organic matter. Color represents fluorescence intensity in Raman units with blue and red denoting the least and most intense, respectively. Component 1 (C1) is associated with higher plants and soil precursor material, Component 2 (C2) with bio-available organic matter and organic nitrogen, and Component 3 (C3) with microbially-derived material. (Image courtesy of Dr. Rose Cory.)

2.4. Collection of Membrane Elements and Preparation of Cleaning Solutions

For each the Castle Hayne and Peedee treatment trains, the lead element from the first stage and tail element from the second stage were collected as shown in Figure 3. Metal oxide and colloidal fouling typically appear in the first element, while mineral scaling and polymerized silica are most severe in the last element; organic fouling is common in all stages (Nitto Denko, 2011). Figure 4 presents photographs illustrative of open pressure vessels showing membrane elements before collection.

Membrane cleaning tests in the laboratory were performed with the following four standard cleaning solutions (Nitto Denko, 2011):

- 2% citric acid, pH = 2.5 (acidic, gentle)
- 2% STPP with 0.8% EDTA (STPP+EDTA), pH = 10 (basic, gentle)
- 0.5% HCl, pH = 2.5 (acidic, harsh)
- 0.1% NaOH with 0.03% SDS (NaOH+SDS), pH = 11.5 (basic, harsh)

In addition, membranes were also cleaned with sodium hydroxide (NaOH) at pH 11, as well as with Lavasol 7 and OptiClean F which are proprietary alkaline cleaning solutions generously provided by PWT chemicals (Vista, CA). We used these two proprietary cleaning solutions because the treatment plant previously used Lavasol 7 before switching to OptiClean F. The primary components of Lavasol 7 are potassium hydroxide (KOH) and EDTA, while OptiClean F contains sodium metasilicate (Russell, 2012; Furukawa, 2012). Both Lavasol 7 and OptiClean F contain unknown builders (i.e., chemicals that soften water via complexation or precipitation and which are often detergents such as STPP). The results obtained with Lavasol 7 and OptiClean F allowed us to compare the cleaning agents used by the treatment plant to four potential standard alternatives (citric acid, STPP+EDTA, HCl, and NaOH+SDS). In general, acidic cleaners are used for carbonate scales, metal oxides/hydroxides, and inorganic colloids

while basic cleaners are used for mixed inorganic/organic colloids, polymerized silica, biological matter, an natural organic matter (Nitto Denko, 2011).

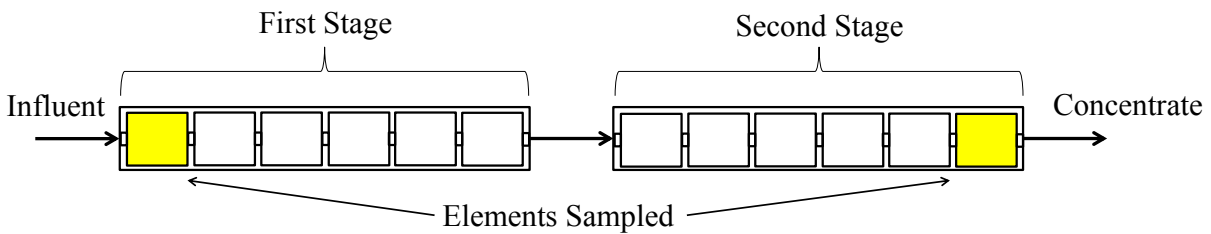


Figure 3. Schematic of membrane sampling locations in each the Castle Hayne and Peedee treatment trains.



Figure 4. Membrane elements collected from the Castle Hayne (left) and Peedee (right) treatment trains.

2.5. Characterization of Membranes and Foulant Layers

SEM/EDX Analyses: Scanning electron microscopy (SEM) and energy dispersive X-ray spectroscopy (EDX) analyses were performed using a Helios Nanolab 600 dual beam system (FEI, Hillsboro, OR) equipped with an INCA X-ray microanalysis system (OXFORD Instruments, United Kingdom) having a Si(Li) INCA PentaFET-x3 detector. An accelerating voltage and current of 20 kV and 0.34 nA, respectively, were used. All samples were coated with 2 nm of Au/Pd to prevent charging. In a small number of samples, current was adjusted to maximize signal, but all currents were within one order of magnitude of 0.34 nA.

FTIR Analyses: Each attenuated total reflectance Fourier transform infrared spectroscopy (ATR-FTIR) spectrum reported here was obtained as the average of five replicate spectra, with

each spectrum being collected as the average of 24 scans in the 375–4000 cm⁻¹ wavenumber range at 1.5 cm⁻¹ resolution. Membrane samples were first dried in air at 35°C, and then in vacuum for 24 hours before performing ATR–FTIR analyses using a Bruker Scientific Alpha FT-IR Spectrometer (Ettlingen, Germany) equipped with OPUS 5.0 software.

RBS Analyses: Rutherford backscattering spectrometry (RBS) analyses were conducted at the Triangle Universities Nuclear Laboratory (TUNL). Samples were irradiated to a fluence of 5×10^{13} ions/cm² using a 2 MeV ⁴He⁺ ion beam, a sample–detector distance of 75 mm, and incident, exit, and scattering angles of 22.5°, 42.5°, and 160°, respectively. The experimental setup was described in greater detail by Attayek et al. (2012).

XPS Analyses: We used X-ray photoelectron spectroscopy (XPS) to quantify membrane surface elemental compositions. Prior to XPS analyses, samples were vacuum-dried for ≈24 h. XPS data was taken on a Kratos Axis Ultra DLD system with a monochromatic Al K α X-ray source operated at 150 W. High resolution scans were obtained at a pass energy of 20 eV, and the area of analysis was 300 μ m \times 700 μ m. Scans were collected for carbon (C1s), oxygen (O1s), nitrogen (N1s), iron (Fe2p), calcium (Ca2p), silicon (Si2p), sulfur (S2p), aluminum (Al2p), magnesium (Mg1s), manganese (Mn2p), chlorine (Cl2p), and sodium (Na1s). XPS results describe the near-surface region (top <10 nm) of the polyamide active layer for unfouled membranes, and the near-surface region of fouling layers for fouled membranes.

2.6. Membrane Cleaning and Performance Testing in Dead-end Configuration

Membrane cleaning was performed with cleaning solutions heated (see Section 2.4) to a temperature of 38°C in an incubator. Full-scale fouled and laboratory cross-flow fouled samples were submerged in the heated cleaning solution and soaked for one hour. Following cleaning, samples were rinsed thoroughly with ultrapure water (>18 M Ω ·cm) water. The performance of fouled membranes in terms of water permeability and salt rejection was tested before and after cleaning. A subset of membrane samples was soaked in cleaning solution at room temperature for one hour and gently scrubbed with a soft sponge to maximize physical foulant removal prior to surface characterization.

Water permeability and salt rejection were tested using a 300 mL stirred dead-end filtration cell (Sterlitech HP4750, Kent, WA). The cell was filled with an electrolyte solution containing 100 mg/L NaCl, and conductivity of the permeate and feed solutions was measured. Sodium chloride concentrations were linearly correlated with conductivity measurements over the range of concentrations tested (data not shown), which allowed for the calculation of chloride rejection from conductivity measurements as given by

$$\text{Chloride Rejection} = 1 - \frac{[Cl]_{\text{Permeate}}}{[Cl]_{\text{Feed}}} \approx 1 - \frac{\text{Conductivity}_{\text{Permeate}}}{\text{Conductivity}_{\text{Feed}}} . \quad (3)$$

Water permeability and salt rejection tests were performed at 95 psi with samples collected over an integrated period of 10 minutes for a minimum of 30 minutes (i.e. 0-10, 10-20, and 20-30 minutes). The first two measurements (0-10 and 10-20 minutes) were used to verify stable performance, while the final sample (20-30 minutes) was used to calculate water permeability and chloride rejection.

Membrane water flow rate ($\text{m}^3 \cdot \text{s}^{-1}$) was calculated as the ratio between the permeate water volume collected and the time (10 min) during which that volume was collected. The permeate water volume collected was determined using the measured weight of the collected sample and the density of water (1 g/cm^3). The water flow rate was then divided by the area of the membrane sample tested (14.6 cm^2) to obtain membrane water flux, J ($\text{m}^3 \cdot \text{m}^{-2} \cdot \text{s}^{-1}$). The water flux, J , through a membrane is given by

$$J = A(\Delta P - \Delta \pi) , \quad (4)$$

where ΔP is the applied transmembrane pressure, $\Delta \pi$ is the transmembrane osmotic pressure, and A is the specific permeability, also referred to as the water permeability coefficient.

2.7. Membrane Cleaning and Performance Testing Using in Cross-Flow Configuration

2.7.1. Cross-Flow System

A schematic of the bench-scale, cross-flow membrane filtration system used for laboratory tests is shown in Figure 5. Feed water temperature and pH were controlled via a recirculating chiller (Neslab Thermoflex 900, Thermo Fisher, Newington, NH) and pH controller (Alpha 190, Eutech Instruments, Vernon Hills, IL), respectively. Feed water was pumped into two cross-flow SEPA membrane cells (Osmonics, Minnetonka, MN) connected in parallel which allowed for simultaneous testing of two membrane samples. Water was pumped using a plunger pump (Model 231, Cat Pumps, Minneapolis, MN) driven by a 1/2 HP variable speed DC motor (Dayton Electric Manufacturing Co., Niles, IL). Both the permeate and concentrate from the system were recycled back to the feed reservoir. This allowed for continuous operation of the membrane system under controlled conditions.

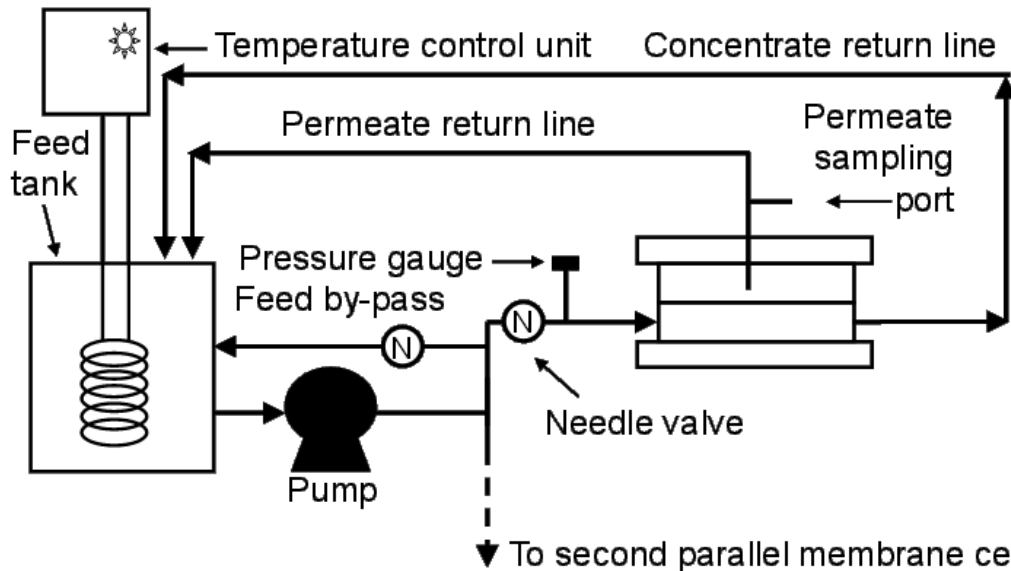


Figure 5. Schematic of bench-scale cross-flow membrane filtration system. Two membrane cells were operated in parallel, with the second cell not shown.

2.7.2. Cross-Flow Fouling Experiments

Lab-scale fouling experiments were conducted with the cross-flow system depicted in Figure 5 using Castle Hayne concentrate collected from the CFPUA treatment plant. To simulate average conditions in the treatment plant, feed pH and temperature were maintained at 6.5 ± 0.2 and $13.0 \pm 0.5^\circ\text{C}$, respectively. A feed pressure of 120 psi and cross-flow velocity of 0.15 m/s were used. Fouling runs for any given membrane sample tested lasted for a minimum of 24 continuous days.

2.7.3. Cross-Flow Cleaning Experiments

In addition to the cleaning tests in dead-end configuration, cleaning experiments were also performed in the cross-flow system to emulate full-scale turbulence during chemical cleaning. The cross-flow cleaning tests were performed with full-scale plant-fouled membranes collected from the CFPUA treatment plant as well as with one membrane fouled in the laboratory using the cross-flow system (Section 2.7.2). The cross-flow fouled membrane was cleaned with STPP+EDTA, while all four plant-fouled membranes were cleaned using both STPP+EDTA and citric acid.

Chemical cleaning solutions were heated to 32°C and then circulated through the membrane cells for one hour at a cross-flow velocity of 0.15 m/s and pressure of 25 PSI. Membranes were then soaked in the cleaning solution for 1 hour by filling the pipes, closing the valves and turning off the pump. Then, a one-hour rinse with deionized water at 25 PSI with a cross-flow velocity of 0.15 m/s was performed. These conditions replicated those in the CFPUA treatment plant during chemical cleaning (Malone, 2012).

2.7.4. Cross-Flow Membrane Performance Measurements

Membrane performance was tested in the cross-flow system depicted in Figure 5 via water permeability and chloride rejection measurements in a similar manner as described in Section 2.6. Water permeability and chloride rejection were evaluated before and after membrane fouling and/or cleaning until readings stabilized.

2.8. Other Data Sources

The CFPUA treatment plant has a supervisory control and data acquisition (SCADA) system that logs operational information. Hourly readings of key parameters from the year preceding membrane element collection were provided by CFPUA personnel for the membrane skids from which elements were sampled. Parameters included feed flow rate, feed pressure, permeate flow rate, concentrate flow rate, temperature, feed pH, feed conductivity, and permeate conductivity.

The SCADA system collected data whether or not the system was operational. Analysis was restricted to periods where each skid was in use by considering only data points with feed pressures of 80 PSI or greater. Noise reduction was achieved for each time point by taking a moving average of ten data points, including the nine points preceding the time point of interest.

Reference performance values for water permeability and salt rejection of unfouled TFC-S membranes was not obtained in the laboratory because at the time of this study the manufacturer (Koch Membrane Systems) had already discontinued production of these membranes. Similarly, for the TFC-ULP membranes, the manufacturer informed us in personal communication that the formula for the TFC-ULP membrane had been altered compared to the formula used at the time of production of the membranes that were installed in the CFPUA treatment plant. We, however, tested the new TFC-ULP in the laboratory and obtained a water permeability value 11.6% lower than the range of permeability indicated in the specifications (Koch, 2010b) provided to the CFPUA treatment plant for the TFC-ULP membranes installed at the plant. The chloride rejection of the new TFC-ULP tested in the laboratory was 92.9%, compared to 98.5% reported in the specifications provided to the CFPUA treatment plant (Koch, 2010b).

Due to the inability to use the performance of new membranes tested in the laboratory as reference values to evaluate the performance decrease of fouled membranes collected from the treatment plant, or the extent of performance recovery of these membranes after being subjected to cleaning procedures, we used as reference performance of unfouled membranes the water permeability and salt rejection reported in the membrane specifications (Koch, 2010a and 2010b) provided by the manufacturer to the CFPUA for the membrane elements installed in the treatment plant. Chloride rejection was assumed to be independent of test conditions: 98.5% and 85% for TFC-ULP and TFC-S, respectively. The clean water permeability of TFC-ULP and TFC-S membranes were calculated as 0.0118 m/d/psi and 0.0138 m/d/psi, respectively, taking into account concentration polarization and the test conditions reported in the specification sheets

(Koch, 2010b and 2010a). Chloride rejection and water permeability values of cleaned membranes were compared to those of unfouled membranes to evaluate cleaning effectiveness.

Specifications from the manufacturer indicate that membrane water productivity may vary by as much as -15%/+20 of the average productivity reported in the specifications, thus figures showing normalized water permeability in this report indicate with dashed lines upper (+20%) and lower (-15%) limits for the expected water permeability of unfouled membranes (Koch, 2010a and 2010b). The manufacturer obtained the -15%/+20% range of water permeability variability for membrane elements with a total membrane area of 37.2 m². As a result, the variability in the water permeability of membrane samples of the sizes used in this project (140 cm² and 14.6 cm² for dead-end and cross-flow samples, respectively) may be greater.

3. Results

3.1. Source Water Quality and Prefiltration

Numerous water quality parameters were evaluated to identify potential membrane foulants. The water quality parameters were divided in three groups: (1) conventional water quality parameters, (2) dissolved inorganic species, and (3) organic parameters. Conventional parameters consisted of turbidity, alkalinity, silt density index (SDI), hardness, conductivity, total suspended solids (TSS), and pH. Dissolved inorganics measured include aluminum, chloride, calcium, iron, magnesium, manganese, silicon, sodium, and sulfate. Organic parameters consisted of dissolved organic carbon (DOC), UV absorbance at 254 nm (UVA), specific UV absorbance (SUVA=UVA/DOC), excitation-emission matrices (EEMs), fluorescence index (FI), slope ratio (Sr), and fluorescence ratios of peaks of particular interest in EEMs. Results of water quality measurements for Castle Hayne and Peedee waters are shown in Table 2. Castle Hayne and Peedee source waters were also filtered to represent cartridge filters used by CFPUA (5 μm), conventional sand filtration (1.2 μm), microfiltration (0.1 μm), and ultrafiltration (100 kDa) pretreatment steps (Kumar et al., 2006). Percent reduction in parameters from Table 2 following filtration are shown in Table 3.

3.1.1. Conventional Water Quality Parameters

Recommendations by the manufacturer (Koch Membrane Systems) of the membranes used in the treatment plant state that turbidity of feed water should not exceed 1 NTU (Koch, 2010a and 2010b). Turbidity in water from the plant intake was 0.088 NTU in the Castle Hayne and 0.105 NTU in the Peedee aquifer at the time of collection (see Table 2). Turbidity measured in the laboratory was much higher, likely due to precipitation of dissolved species during transport. Since samples were filtered in the laboratory following transport, feed turbidity measurements taken in the laboratory for unfiltered water were used to calculate turbidity rejection during filtration tests (see Table 3). Even with the precipitation that occurred during transport and storage, and the corresponding relatively high turbidity it produces, the 5 μm cartridge filters currently used for prefiltration were sufficient to reduce turbidity below 1 NTU.

Silt density index (SDI) in feed water should be less than or equal to 5 to prevent particulate fouling, according to the membrane manufacturer (Koch, 2010a and 2010b). SDI was measured at the treatment plant for plant intake with both Castle Hayne and Peedee waters, and was found to be less than 2. Measurements obtained at the laboratory were higher than on site (see Table 2) likely due to precipitation during transport, not to particulate matter in the source water.

Particle size distributions (see Appendix 3) were measured before and after filtration for both the Castle Hayne and Peedee waters. Filtration with 1.2 μm filters resulted in minimal change in average particle diameter, while 0.1 μm filtration noticeably reduced particle size for both waters. Ultrafiltration with 100 kDa filters reduced average particle diameter below the lower detection limit (i.e., a few nanometers) of the instrument (Zetasizer Nano ZS90 - Malvern Instruments).

Minimal changes in hardness alkalinity, and conductivity following filtration were observed. Changes in pH following filtration were likely due to equilibration of the water with the atmosphere. Groundwaters, especially those whose pH has been adjusted by acid addition (i.e., Castle Hayne water), are typically saturated with carbonic acid, which volatilizes in the form carbon dioxide when exposed to the atmosphere. The loss of carbonic acid is likely the cause of the increasing pH observed with filtration. The concentration of total suspended solids (TSS) was below the limit of quantification following all forms of filtration.

Table 2. Water quality parameters for Castle Hayne and Peedee groundwaters.

	Castle Hayne			Peedee		
	Average	Standard Deviation	Note	Average	Standard Deviation	Note
Conventional Parameters*						
Turbidity (NTU)	0.088	-	[1]	0.105	-	[1]
Alkalinity (mg/L as CaCO ₃)	94.6	0.6		180.5	0.7	
SDI	5.4	-	[2]	3.5	-	[2]
Hardness (mg/L as CaCO ₃)	281.4	3.1		262.1	2.7	
Conductivity (µs/cm)	570.3	5.5		578.0	1.0	
TSS (mg/L)	1.8	0.7		Below LOQ	Below LOQ	[3]
pH	5.99	0.05		6.67	0.03	
Dissolved Inorganics (mg/L)**						
Aluminum	0.015	0.011		0.011	0.012	
Chloride	29.4	-	[4]	51.6	-	[4]
Calcium	105.5	-	[4]	93.5	-	[4]
Iron	5.7	1.1		0.09	0.03	
Magnesium	2.2	0.1		7.4	0.6	
Manganese	0.084	0.009		0.011	0.000	
Silicon	8.0	8.8		5.9	7.1	
Sodium	8.4	0.4		19.6	1.5	
Sulfate	231.4	-	[4]	103.1	-	[4]
Organic Parameters***						
DOC (mg/L)	7.9	1.0		4.4	1.1	
UVA 254 (m ⁻¹)	35.3	4.2		12.2	3.4	
SUVA (L/mg-m)	4.5	0.04		2.8	1.5	
Slope ratio	0.7	0.05		1.0	0.2	
Fluorescence index	1.55	0.05		1.53	0.01	
Peak C1 Intensity	3.05	0.31		2.14	0.52	
Peak C2 Intensity	0.32	0.05		0.21	0.03	
Peak C3 Intensity	1.17	0.15		0.74	0.18	

*Conventional parameters were calculated from technical replicates of samples collected in August 2011.

**Averages and standard deviations for dissolved inorganics were calculated from samples collected in August 2011 and February 2012.

***Averages and standard deviations for organic parameters were calculated from samples collected in August 2011 and September 2011.

[1] Measured at treatment plant to avoid precipitation during transport. Sample collected February 2012 prior to antiscalant addition, pH adjustment.

[2] SDI requires approximately 5 gallons of water per test; replicates were not performed due to limited sample volume.

[3] TSS measurements for Peedee Waters were below the limit of quantification (LOQ) of 1.66 mg/L.

[4] Calculated as average of multiple instrument readings from the same sample.

Table 3. Approximate reduction in the values of water quality parameters (i.e. rejection) for various pretreatment alternatives tested in the laboratory.

	Castle Hayne				Peedee			
	5µm	1.2µm	0.1µm	100kDa	5µm	1.2µm	0.1µm	100kDa
Conventional Parameters								
Turbidity [1]	99%	100%	100%	100%	0%	63%	54%	93%
Alkalinity	8%	6%	2%	3%	0%	0%	3%	1%
SDI	1%	37%	68%	[2]	59%	73%	73%	[2]
Hardness	1%	4%	1%	4%	0%	0%	0%	2%
Conductivity	0%	0%	2%	0%	0%	3%	0%	2%
TSS [3]	< LOQ	< LOQ	< LOQ	< LOQ	< LOQ	< LOQ	< LOQ	< LOQ
pH [4]	5.99 - 6.22	5.99 - 6.20	5.99 - 6.19	5.99 - 6.43	6.67 - 7.08	6.67 - 7.25	6.67 - 6.87	6.67 - 7.01
Dissolved Inorganics								
Aluminum	-	-	21%	53%	-	-	22%	0%
Chloride	-	-	0%	0%	-	-	0%	0%
Calcium	-	-	1%	4%	-	-	0%	2%
Iron	-	-	1%	2%	-	-	19%	18%
Magnesium	-	-	1%	1%	-	-	5%	2%
Manganese	-	-	0%	7%	-	-	0%	0%
Silicon	-	-	0%	7%	-	-	2%	10%
Sodium	-	-	0%	2%	-	-	4%	3%
Sulfate	-	-	3%	4%	-	-	2%	0%
Organic Parameters								
DOC	-	-	0%	0%	-	-	2%	0%
UVA 254	0%	2%	0%	4%	0%	0%	0%	0%
SUVA	-	-	0%	0%	-	-	9%	0%
Slope ratio	7%	7%	8%	3%	14%	13%	16%	15%
Fluorescence index	1%	2%	1%	2%	-1%	-1%	0%	-1%
Peak C1 Intensity	0%	0%	0%	0%	0%	0%	0%	0%
Peak C2 Intensity	0%	2%	0%	2%	0%	0%	0%	0%
Peak C3 Intensity	0%	1%	1%	0%	0%	0%	0%	0%
[1] Turbidity rejection was calculated from unfiltered water (Castle Hayne: 18.2 NTU; Peedee: 0.24 NTU) and permeate water measured in the laboratory following transport.								
[2] SDI requires approximately 5 gallons of water per test; tests were not performed due to limited sample volume.								
[3] All TSS measurements for filtered samples were below the limit of quantification (LOQ) of 1.66 mg/L.								
[4] pH measurements displayed in "unfiltered - filtered" format for pH before and after filtration, respectively.								

3.1.2. Dissolved Inorganic Species

Tables 2 and 3 present the concentrations of dissolved inorganic species measured in source waters and rejection following prefiltration. Water from the Castle Hayne aquifer had high concentrations of dissolved calcium, iron, silicon, and sulfate which are known membrane foulants. The CFPUA adds sulfuric acid to the Castle Hayne water to prevent the formation of inorganic precipitates, but this results in an increased sulfate concentration. High concentrations of calcium and silicon were observed in water from the Peedee aquifer, and manganese concentrations were much lower (0.011 mg/L) than expected; at the time of treatment plant design, manganese was measured at 0.14 mg/L (Membrane Systems, Inc.). Concentrations of dissolved silicon and aluminum had large standard deviations relative to the average concentration, suggesting temporal variability in concentration (i.e., the values shown in Table 2 are the average of results obtained for samples collected in September 2011 and February 2012).

The rejection of inorganic species was only analyzed for 0.1 μm and 100 kDa filtered samples because all samples had to be filtered through 0.2 μm filters to protect the ICP-MS instrument. The only species whose concentrations were reduced by at least 10% by filtration were aluminum in both waters, and iron and silicon (100 kDa only) in the Peedee water. These results indicate that prefiltration would not be effective at removing dissolved inorganic species, and thus that it would not contribute to minimization of inorganic fouling (i.e., scaling).

3.1.3. Organics and Fluorescence Parameters

Natural organic matter in the tested waters was characterized by measuring dissolved organic carbon (DOC), UV absorbance (UVA) and fluorescence excitation-emission matrices (EEMs), and by calculating the specific UV absorbance (SUVA), slope ratio (Sr), fluorescence index (FI) and fluorescence peaks of particular interest in EEMs. EEMs can be used to characterize the relative abundance of hydrophobic molecules, biopolymers, and humics which are likely to cause membrane fouling (Amy, 2008). Values of SUVA are strongly correlated with percent aromaticity (Weishaar et al., 2003), and thus hydrophobicity, with high SUVA values often indicating a larger hydrophobic fraction of organic matter, and suggesting a greater potential for membrane fouling (USEPA, 2005).

Slope ratio (Sr) is used as an indicator of molecular weight (Helms et al., 2008). Samples with a higher content of low-molecular weight organics have a high slope ratio, while low slope ratio indicates high molecular weight. Fluorescence index (FI) is a proxy for organic matter source. An FI of approximately 1.9 indicates a significant organic content of microbial origin while an FI of 1.40 indicates terrestrially derived organic matter (McKnight et al., 2001).

Table 2 indicates that water from the Castle Hayne aquifer contains almost twice the dissolved organic carbon (DOC) and absorbs almost three times as much ultraviolet light (UVA 254) as water from the Peedee aquifer. Higher SUVA and lower slope ratio in the Castle Hayne water than in the Peedee water indicates that the organic matter in the Castle Hayne aquifer is more aromatic, thus hydrophobic, and may lead to a higher propensity for organic fouling of membranes. Consistent with the DOC and SUVA values in Castle Hayne and Peedee waters, as

shown in Section 3.4.6, Castle Hayne fouling layers contained higher concentrations of organic matter than the Peedee fouling layers.

EEMs for the Castle Hayne and Peedee waters following prefiltration are shown in Figures 6 and 7, respectively. These figures demonstrate that the fluorescence signature of both waters does not change significantly with filtration, and therefore filtration does not significantly remove fluorescent natural organic matter. Figures 6 and 7 also visually illustrate the relative fluorescence of components C1, C2, and C3. Fluorescence components C1, C2, and C3 were about 150% more intense in the Castle Hayne water than in the Peedee water, but were present in similar ratios. The order of peak intensity is $C1 > C3 > C2$, which suggests that organic matter was mostly associated with higher plants and soil material, followed by microbially-derived material and bio-available organic matter and organic nitrogen.

The Peedee water has a higher Sr than the Castle Hayne water, suggesting that the Peedee water has a higher proportion of low-molecular weight organics. Measurements of fluorescence index (FI) are similar for the two waters and indicate primarily terrestrial sources of organic matter.

Table 3 indicates minimal change in organic parameters following filtration. These results suggest that most of the organic matter was smaller in size than the smallest filter used (100 kDa). Because dissolved iron has been shown to influence fluorescence parameters (Pullin et al., 2007), the effect of increasing dissolved iron concentrations on fluorescence parameters was tested for the Castle Hayne and Peedee waters (see Appendix 4). Increasing iron concentration increased UVA 254, but had a minor effect on fluorescence parameters and did not affect the trends observed (e.g., $C1 > C3 > C2$ for both Castle Hayne and Peedee waters, Sr is higher for Castle Hayne water than for Peedee water, etc.).

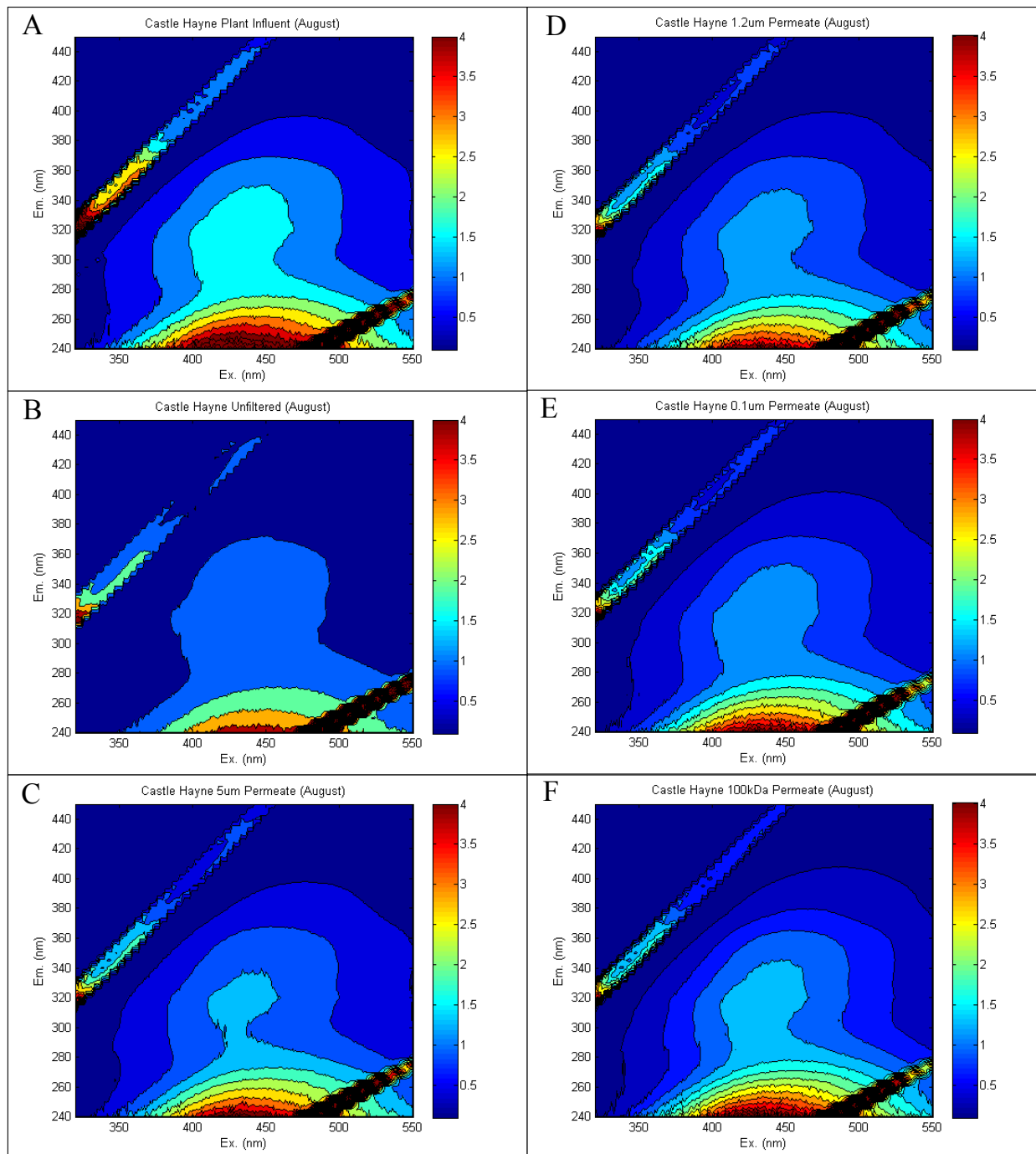


Figure 6. Excitation-Emission Matrices (EEMs) for water samples collected from the Castle Hayne treatment train in August 2011. Samples include (A) plant influent, (B) influent after pH adjustment and antiscalant addition, (C) 5 μm cartridge filter effluent, (D) 1.2 μm filter effluent, (E) 0.1 μm filter effluent, and (F) 100 kDa filter effluent. For (C) through (F), filtration tests were performed in the UNC laboratories using the water shown in (B) as influent.

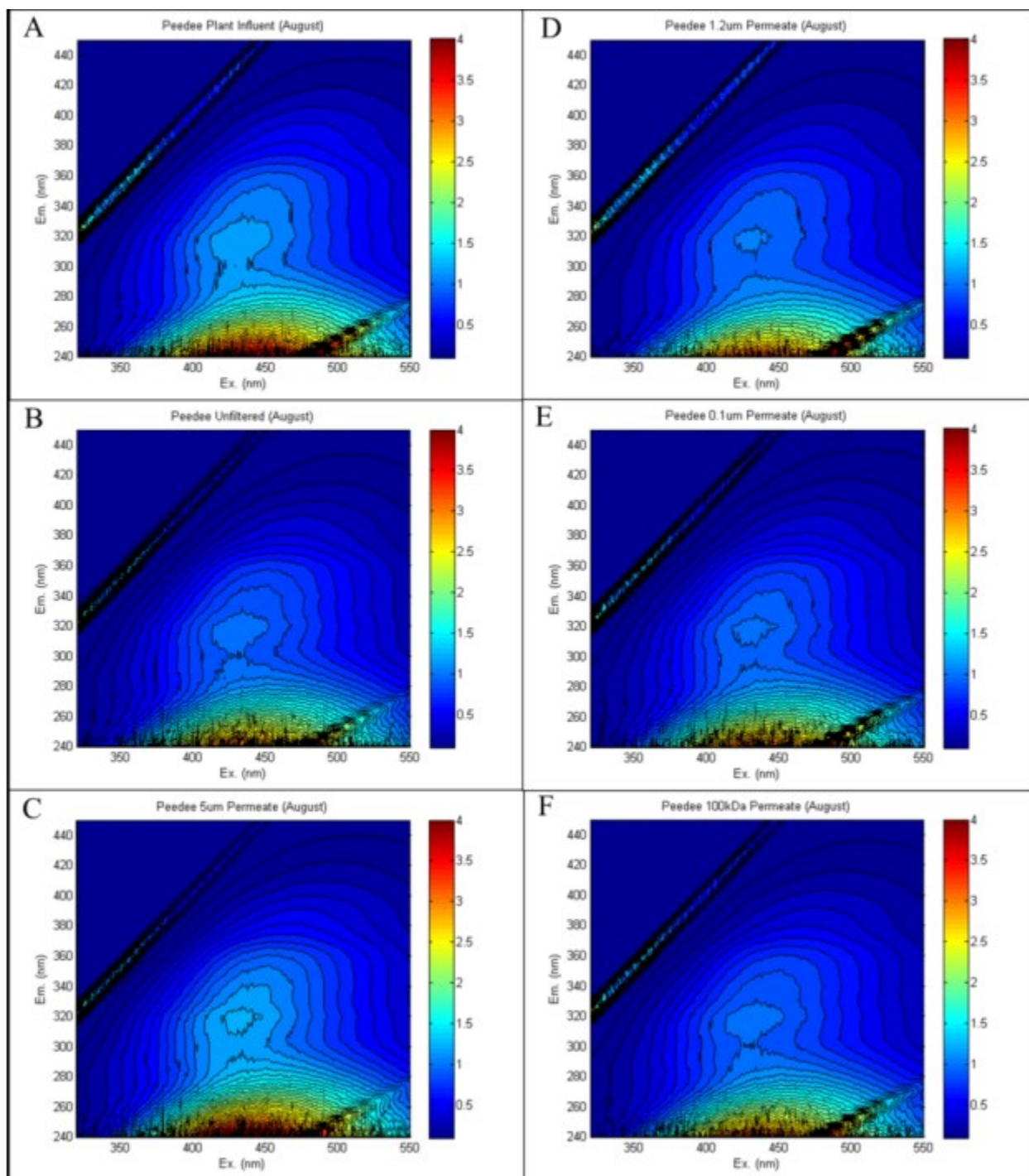


Figure 7. Excitation-Emission Matrices (EEMs) for water samples collected from the Peedee treatment train in August 2011. Samples include (A) plant influent, (B) influent after pH adjustment and antiscalant addition, (C) 5 μm cartridge filter effluent, (D) 1.2 μm filter effluent, (E) 0.1 μm filter effluent, and (F) 100 kDa filter effluent. For (C) through (F), filtration tests were performed in the UNC laboratories using the water shown in (B) as influent.

3.2. Full-Scale Membrane System Performance

Feed, permeate, and concentrate water samples were collected in February 2012 from both the Castle Hayne and Peedee membrane treatment trains. The Castle Hayne treatment train has two different membrane types: TFC-ULP in the first stage and TFC-S in the second stage. For this reason, permeate water samples were collected from both stages of the Castle Hayne treatment train whereas only total permeate (i.e., combined permeate from both stages) was collected from the Peedee treatment train. Results from water quality analyses of the samples collected and data from the treatment plant's SCADA system were used to evaluate performance of the full-scale membrane system.

3.2.1. Full-Scale Rejection of Dissolved Constituents

Permeate water samples were tested for various water quality parameters and the results were compared to corresponding values for feed water samples to determine rejection of dissolved constituents (see Section 2.3). Table 4 shows observed rejection of dissolved species. Recovery of 50% from the Castle Hayne first stage, based on treatment plant design values, was used to calculate the water quality of the influent to the Castle Hayne second membrane stage. For example, if the Castle Hayne feed water entering the first membrane stage contained 105.5 mg/L of calcium (see Table 2), the concentration of calcium entering the second stage would be 196.2 mg/L because the first stage had 50% recovery and 93% rejection (see Table 4).

The rejection of dissolved ions in Table 4 was comparable to the rejection reported by the manufacturer in the specification sheets for the TFC-ULP and TFC-S membranes provided to the CFPUA ref: 98.5% chloride rejection for TFC-ULP, and 85%, 98.5%, and 98.5% rejection of chloride, total hardness, and magnesium sulfate, respectively for TFC-S (Koch, 2010b and 2010a). However, it should be noted that the rejection data in the manufacturer's specifications were collected during testing of the membrane elements with 15% water recovery, while the CFPUA treatment plant operates at a total recovery for each the Castle Hayne and Peedee treatment trains of 80%.

Table 4 also indicates that, in general, the rejection of monovalent ions, sodium and chloride, was lower than rejection for polyvalent ions, as expected. We observed excellent rejection (93-99%) of polyvalent ions such as iron, magnesium, and manganese; however, the rejection of calcium and aluminum was relatively low with values as low as 57% for calcium and negligible rejection for aluminum. Given that most of the hardness in Castle Hayne water comes from calcium content (see Table 2), total hardness rejection was similarly poor. With the exception of calcium rejection in the Castle Hayne first stage, calcium and aluminum rejection were lower than sodium and chloride rejection in all membrane stages.

Table 4. Observed rejection of various water quality parameters in the membrane filtration stages of the CFPWA Groundwater Nanofiltration Treatment Plant (Wilmington, NC) relative to feed water concentration.

	Castle Hayne		Peedee
	Stage 1 Permeate (TFC-ULP)	Stage 2 Permeate (TFC-S)	Total Permeate (TFC-S)
Conventional Parameters			
Hardness	93%	75%	60%
Conductivity	96%	95%	90%
Dissolved Inorganics			
Aluminum	53%	-12%	64%
Chloride	BLD, >88% [1]	77% [2]	76%
Calcium	93%	71%	57%
Iron	99%	96%	93%
Magnesium	99%	97%	96%
Manganese	99%	97%	94%
Silicon	98%	88%	82%
Sodium	75%	68%	70%
Sulfate	100%	100%	99%
Organic Parameters			
DOC	BLD, >99% [1]	99% [3]	77%
UVA 254	99%	99%	58%
SUVA	N/A [4]	7%	-83%
Slope ratio	-295%	33% [5]	-39%
Fluorescence index	-1%	4% [5]	-1%
Peak C1 Intensity	100%	100%	98%
Peak C2 Intensity	99%	99%	96%
Peak C3 Intensity	100%	100%	99%
[1] Measurements that were below the limit of detection (BLD)			
[2] First stage chloride rejection assumed to be 90%.			
[3] First stage DOC rejection assumed to be 100%.			
[4] SUVA cannot be calculated as DOC was below detection.			
[5] Second stage influent assumed to be equal to first stage influent.			

Both stages of the Castle Hayne treatment train exhibited excellent rejection of DOC, UVA 254, and all three fluorescence peaks. DOC rejection in both Castle Hayne stages was 99% or greater, which exceeds the DOC rejection by nanofiltration membranes reported by Peiris et al. (2010) (92.7-95.8%) and Jarusutthirak et al. (2007) (94.9-97.0%). DOC rejection by nanofiltration in the Peedee treatment train was only 77%, which is lower than rejections reported in literature. The observed rejection of UVA by TFC-S membranes was 58% and 99% for Peedee water and Castle Hayne water, respectively, consistent with the range of approximately 50-80% reported by Yoon et al. (2005). The lower rejection of organics observed in the Peedee treatment train,

compared to in the Castle Hayne treatment train, was consistent with the higher slope ratio (0.7), and thus lower molecular weight organics, obtained for the Peedee water compared to the slope ratio (1.0) obtained for the Castle Hayne water (Section 3.1.1.).

Figure 8 shows EEMs of the three permeate waters. While the permeate water from the Castle Hayne first stage has little fluorescence, the permeate water from the second stage has visible fluorescence in all three peak areas (C1, C2, and C3). The analysis of the relative fluorescence intensities of Peaks C1, C2 and C3 in the feed (Figure 8A) and second stage permeate (Figure 8C) samples of Castle Hayne water indicates that the fluorescence intensity of Peak C2 is more permeable than that of Peaks C1 and C3. This suggests that the organic matter that makes up peak C2 might be more permeable than the organic matter that makes up the other peaks. Similarly, for Peedee water, it appears that the organic matter that makes up Peak C1 is more permeable than the organic matter that makes up Peak C3.

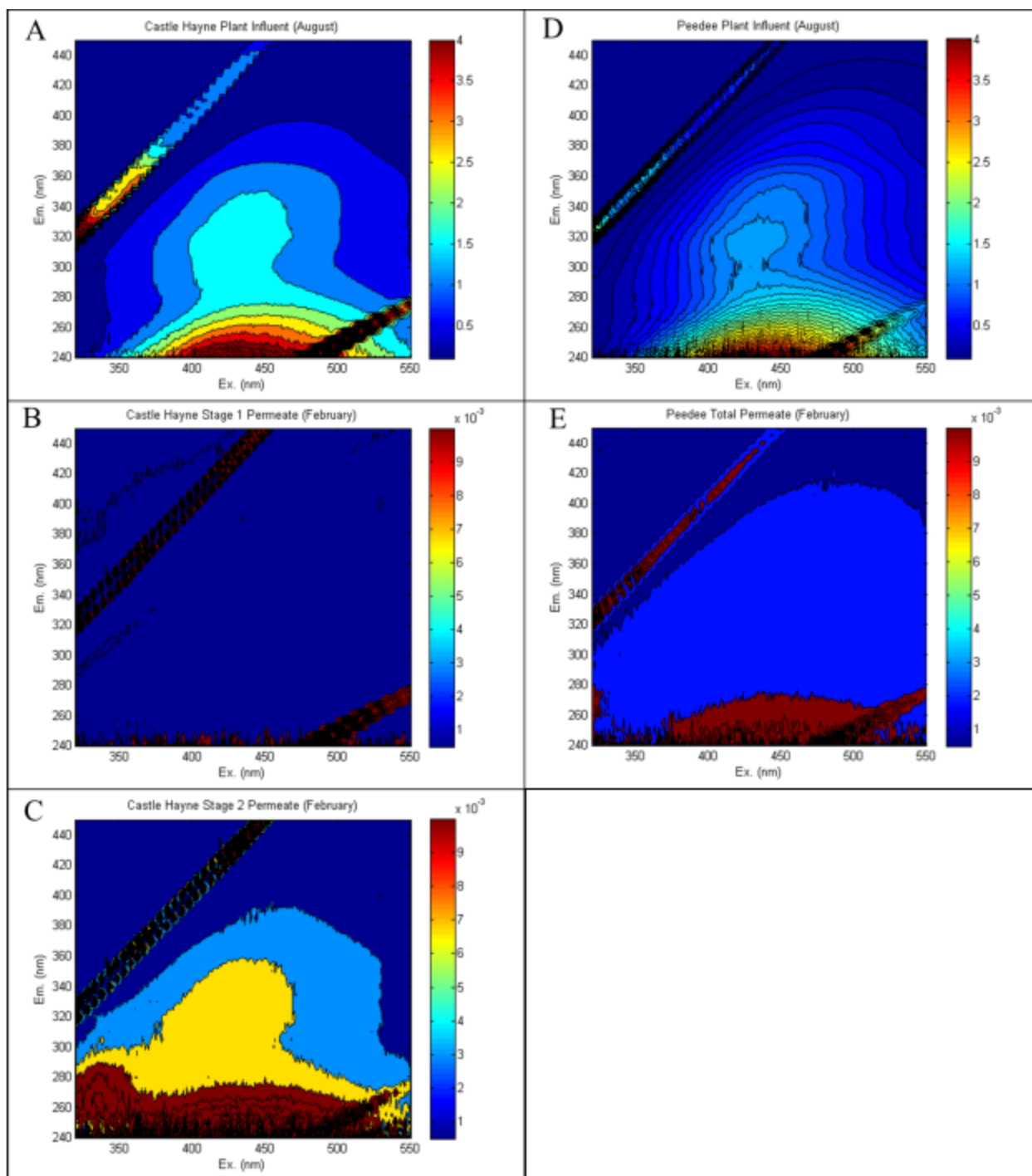


Figure 8. Excitation-Emission Matrices (EEMs) for unfiltered and membrane permeate water samples. Samples include (A) Castle Hayne plant influent (B) Castle Hayne stage 1 permeate, (C) Castle Hayne stage 2 permeate, (D) Peedee plant influent, and (E) Peedee total permeate. Note that the fluorescence scale is three orders of magnitude lower for membrane permeate samples (B, C, E) than for treatment plant influent (A, D).

3.2.2. Full-Scale Operational Parameters

The treatment plant's SCADA system logs important operational parameters. A subset of these parameters was obtained from plant personnel (Malone, 2012), including:

- Feed pressure
- Permeate and concentrate flow rate
- Feed and permeate conductivity
- Feed temperature
- Feed pH
- Water pressure before 5- μ m filters
- Pressure loss across 5- μ m filters
- Percent of maximum motor speed used to drive the feed pumps for membrane stages

These data from the SCADA system can be used to calculate water recovery, conductivity rejection, and overall membrane water permeability. Water recovery was calculated as

$$\text{Recovery (\%)} = \frac{\text{Permeate flow rate}}{\text{Permeate flow rate} + \text{Concentrate flow rate}} \times 100 . \quad (5)$$

Figures 9 and 10 show permeate water flow rate and percent water recovery for the nanofiltration treatment trains treating Castle Hayne and Peedee water in the CFPUA treatment plant from April 2011 through May 2012. Figures 9 and 10 indicate that water recovery during operation is very close to the treatment plant's target of 80%. The Castle Hayne treatment train has more pressure vessels, thus more membranes and more membrane area than the Peedee train. For this reason, 80% recovery corresponds to a permeate water flow rate (i.e., water production rate) of approximately 1,040 GPM for the Castle Hayne system and 835 GPM for the Peedee system.

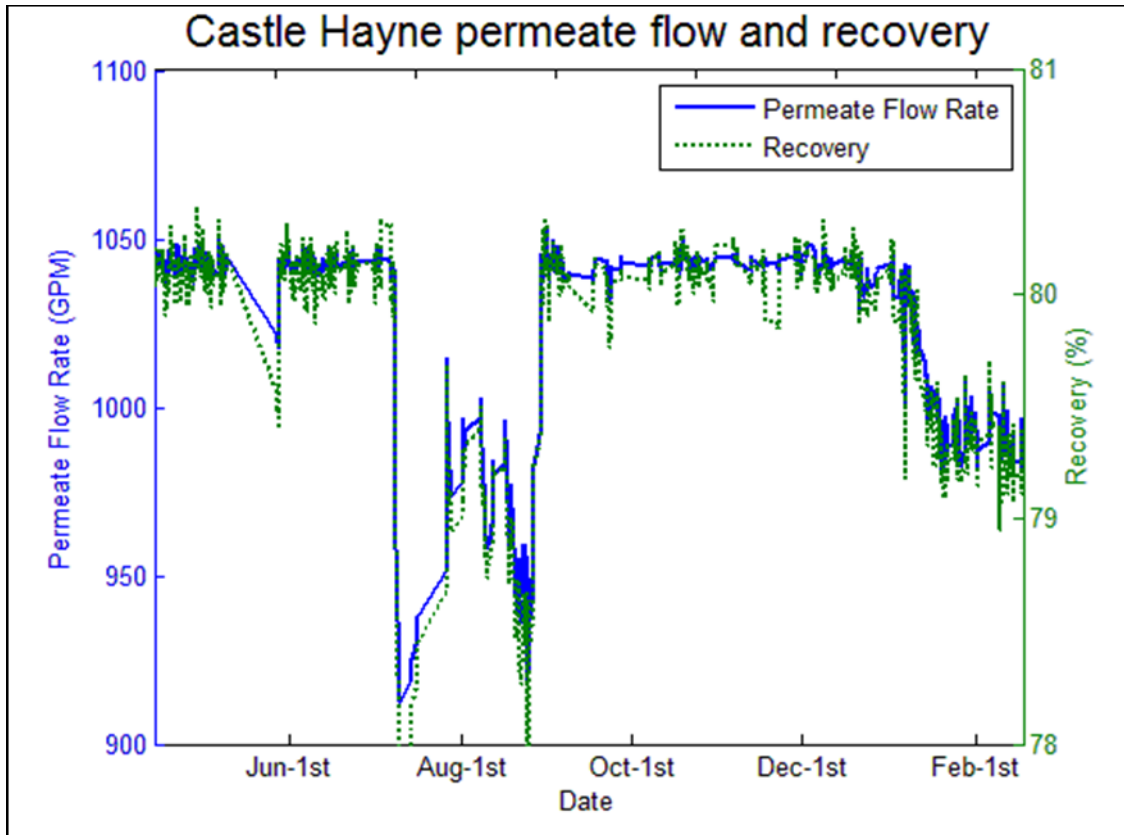


Figure 9. Permeate water flow rate and water recovery for the Castle Hayne treatment train in the CFPWA Groundwater Nanofiltration Treatment Plant from April 2011 through February 2012.

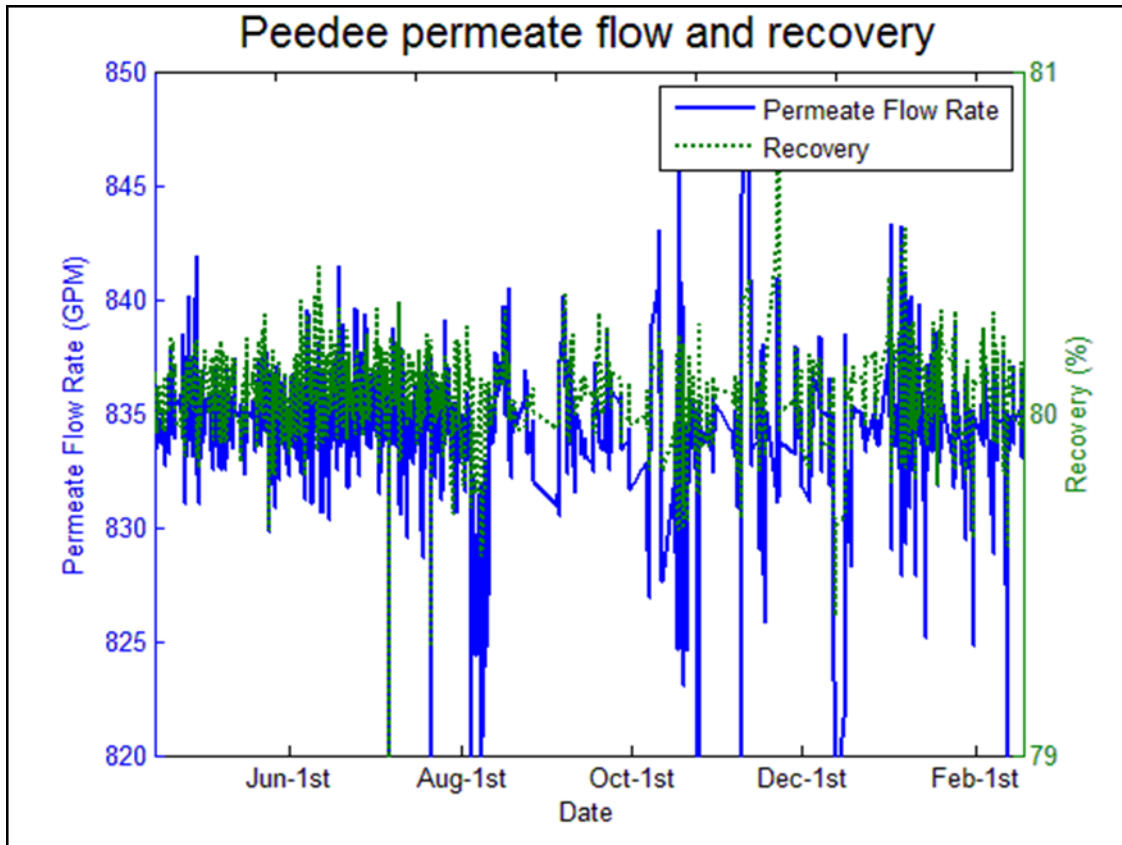


Figure 10. Permeate water flow rate and water recovery for the Peedee treatment train in the CFPUA Groundwater Nanofiltration Treatment Plant from April 2011 through February 2012.

The CFPUA treatment plant operates under constant flux conditions, where feed pressure is increased as the membrane fouls to maintain a constant permeate flow rate. Figure 11 shows the feed pressure in the Castle Hayne and Peedee treatment trains over time. Feed pressure was increased as fouling increased in severity to maintain the consistent permeate water production shown in Figures 9 and 10. Cleaning is also evident from the feed pressure plots, as reductions in operating pressure of 70 and 35 PSI followed cleaning in the Castle Hayne and Peedee systems, respectively.

Although treatment plant cleaning procedures allowed significant reductions in feed pressure, treatment plant personnel still had to contend with detrimental effects on system performance caused by fouling. The permeate flow rate in the Castle Hayne system (see Figure 10) from early July to late August was 10-15% below the typical production rate. Similar but less severe permeate shortfalls were observed in early August in the Peedee system. High feed pressure also resulted in the rupture of several seals within the system, which were not rated for the pressures applied (Malone, 2012). These experiences demonstrated the need to identify optimum cleaning strategies and explore measures that may delay fouling.

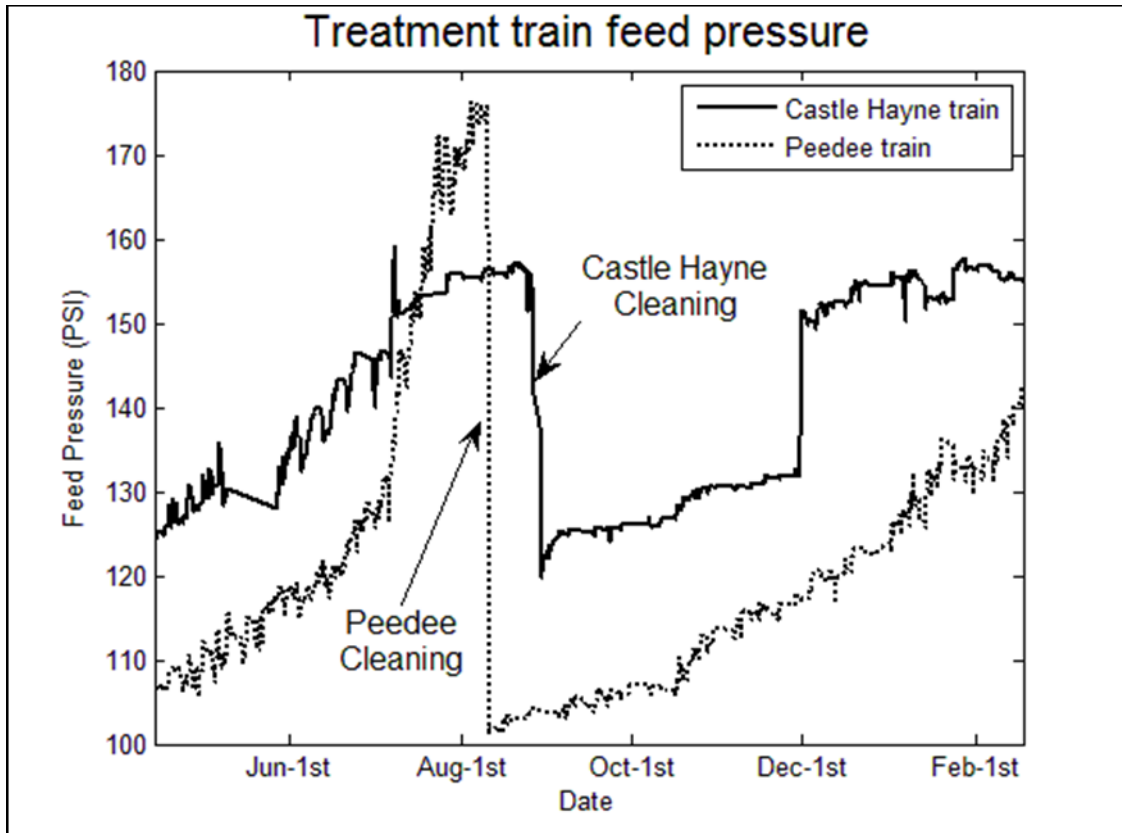


Figure 11. Feed water pressure in the Castle Hayne and Peedee treatment trains in the CFPUA Groundwater Nanofiltration Treatment Plant from April 2011 through February 2012.

Conductivity rejection in the Peedee treatment train improved from 76 to 83 % as fouling increased in severity, as shown in Figure 12. Following cleaning, conductivity rejection dropped to 73.5%, before increasing again to 76% as foulants accumulated. No similar correlation with conductivity rejection and cleaning was observed for the Castle Hayne system. Conductivity rejection in the Castle Hayne system was approximately 95%, compared with 76% in the Peedee system.

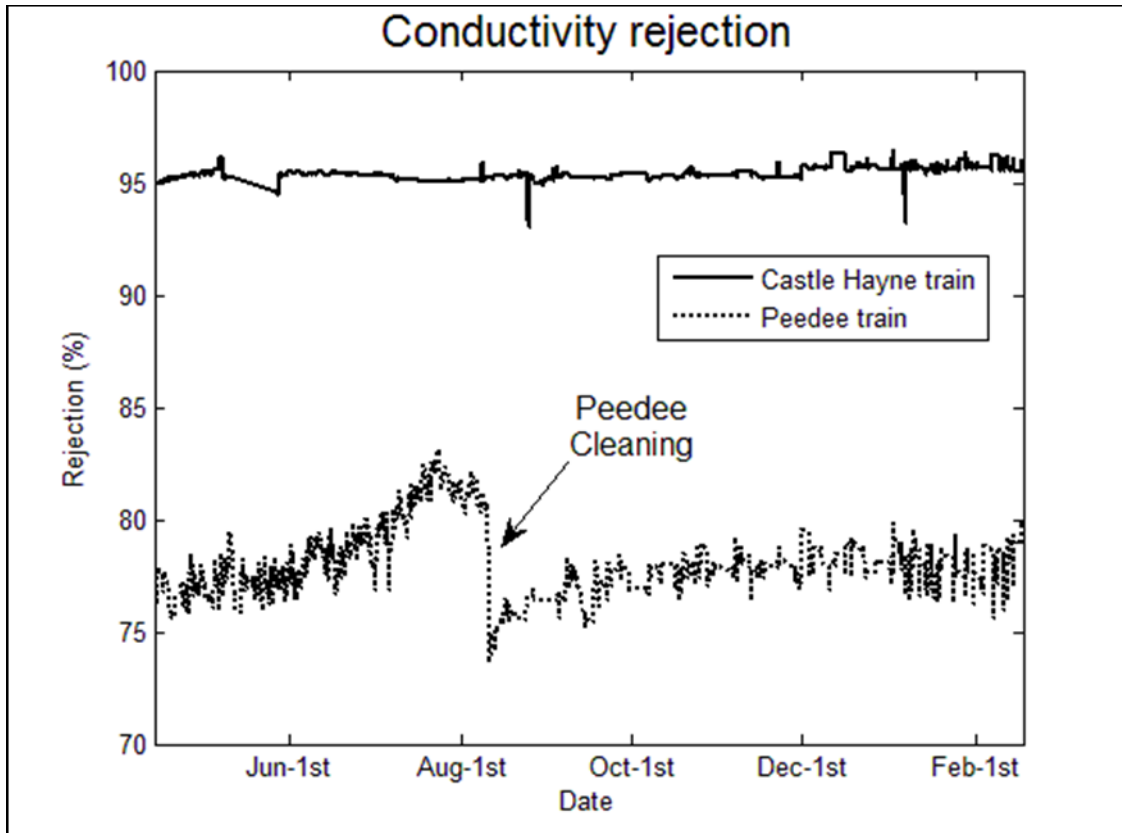


Figure 12. Conductivity rejection in the Castle Hayne and Peedee treatment trains in the CFPUA Groundwater Nanofiltration Treatment Plant from April 2011 through February 2012.

3.3. Comparison between the Performance of Fouled Membranes in Dead-End and Cross-Flow Filtration

Elements from the lead position of the first stage and the tail position of the second stage (i.e. first and last elements in the treatment train) were collected from the Castle Hayne and Peedee treatment trains as detailed in Section 2.4. Membrane samples were cut from the elements, and tested using both dead-end and cross-flow filtration. As shown in Figure 13, dead-end and cross-flow tests yielded similar specific water permeability results, using the temperature correction procedure described by MWH (2005). Since water permeability results using dead-end and cross-flow filtration are comparable, then cleaning effectiveness (measured as the increase in membrane water permeability caused by cleaning) was evaluated using dead-end filtration as opposed to the more time-consuming cross-flow filtration (Section 3.6). From Figure 13, we also see that elements from the Castle Hayne second stage are the most severely fouled in the treatment plant.

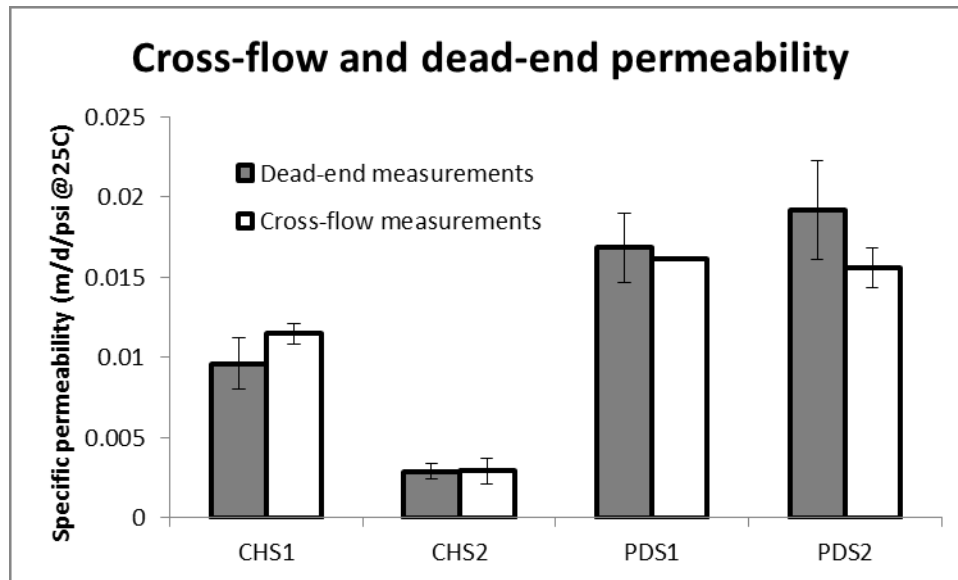


Figure 13. Specific water permeability of full-scale fouled elements tested using the dead-end apparatus and cross-flow system. Note: Peedee second stage membranes were damaged as evidenced by significantly low chloride rejection results (see Figure 14), thus caution should be used when interpreting results for these membranes.

Chloride rejection was also tested using the two setups, and corresponding results are shown in Figure 14. While the conductivity rejection for tests with membranes from the Castle Hayne treatment train were statistically the same for tests in the dead-end apparatus and cross-flow system, there was a difference of about 7.7 percentage points between conductivity rejections obtained in dead-end and cross-flow operation for membranes from the Peedee first stage. This indicates that conductivity rejection results from dead-end experiments may not be representative of those obtained in a cross-flow system. One potential explanation for this observation is that turbulence at the membrane surface was different in the dead-end apparatus than the cross-flow system. Concentration polarization is minimized in the cross-flow system by shearing forces generated as water flows through the feed spacer, increasing turbulence at the membrane surface and carrying away solutes. The dead-end cell has a stir bar inside (and not touching the membrane surface), which was operated at approximately 350 revolutions per minute. The dead-end cell's stir bar may have generated less turbulence than the flow of feed water in the cross-flow system, thus resulting in a relatively stronger concentration polarization effect in the dead-end cell.

Also evident in Figure 14 is the significantly different chloride rejection results for the Peedee stage 2 membranes in dead-end and cross-flow operations. Appendix 5 demonstrates that the significant discrepancy between Peedee stage 2 dead-end and cross-flow chloride rejection can be attributed to differences in location of membrane sample rather than differences in the two setups.

Numerous samples from the Peedee second stage were used in the calculation of chloride rejection in Figure 14 (n=17). A similar number (n=14 to 18) of samples were used in calculating average and standard deviation of chloride rejection for the other three sampled membranes. Peedee Stage 2 samples appear to be damaged, as the manufacturer lists chloride rejection as

85% (Koch, 2010a) and laboratory tests for 17 fouled samples resulted in chloride rejections of 50% on average with values as low as 31%. The low rejection and high standard deviation obtained for membrane samples from the Peedee second stage demonstrated that Peedee second stage membranes were damaged, and that this damage resulted in chloride rejection and water flux results more spatially variable than in the other membranes sampled.

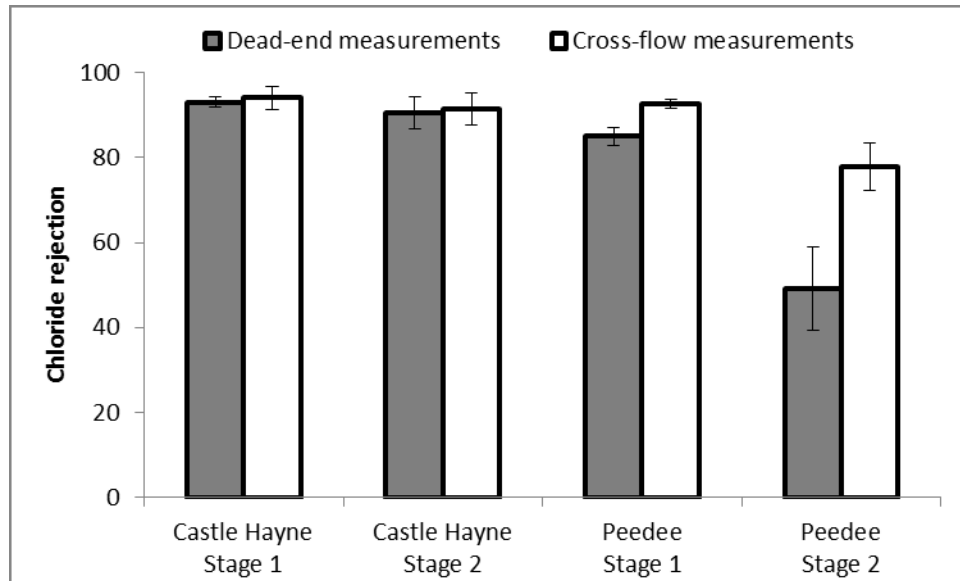


Figure 14. Conductivity rejection of full-scale fouled elements tested using the dead-end apparatus and cross-flow system. Note: Peedee second stage membranes were damaged as evidenced by high flow rate and low chloride rejection, thus caution should be used when interpreting results for these membranes.

3.4. Characterization of Membrane Foulants

3.4.1. Scanning Electron Microscopy (SEM)

SEM was used to capture high resolution images of unfouled and fouled membranes. Figure 15 shows SEM images of the polyamide active layer of an unfouled TFC-ULP membrane at high resolution (5 μm scale) and low resolution (500 μm scale). The figure shows that while at the at the 5- μm scale the unfouled membrane surface has a textured appearance, at the 500- μm scale it appears smooth. The Castle Hayne stage 1 and stage 2 fouling layers (see Figures 16 and 17, respectively) appear to be continuous scales. The fouling layer of the Castle Hayne first stage has a rough, amorphous texture while the fouling layer of the second stage is smooth. Fractures in the fouling layer of the Castle Hayne second stage may have resulted from the sample drying process during sample preparation.

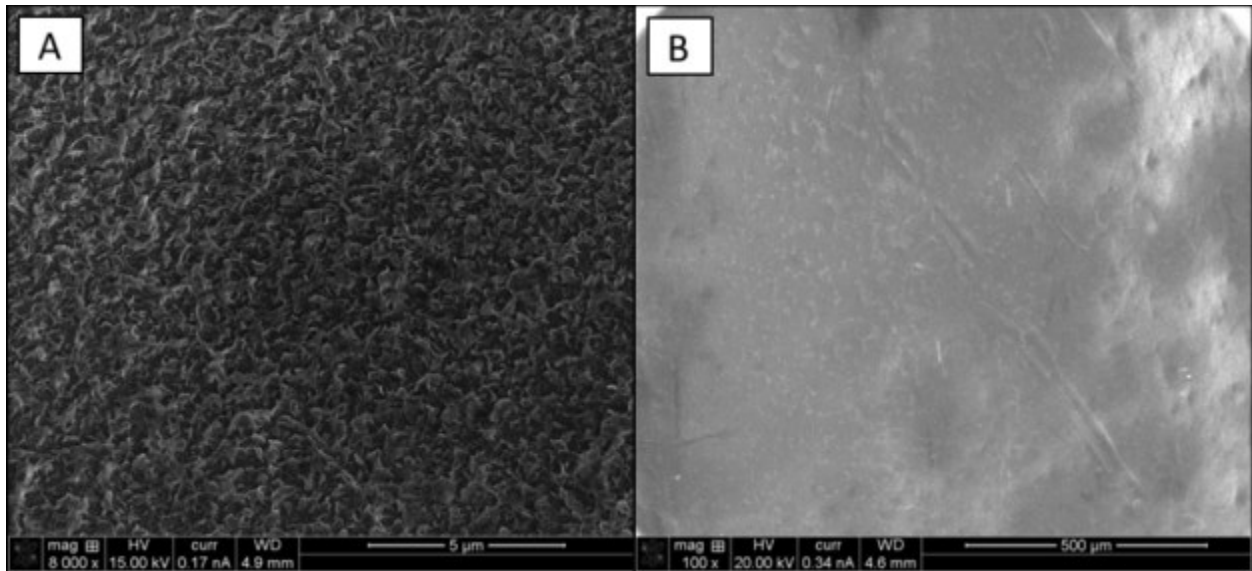


Figure 15. Unfouled TFC-ULP membrane at (A) 5 μm and (B) 500 μm scale.

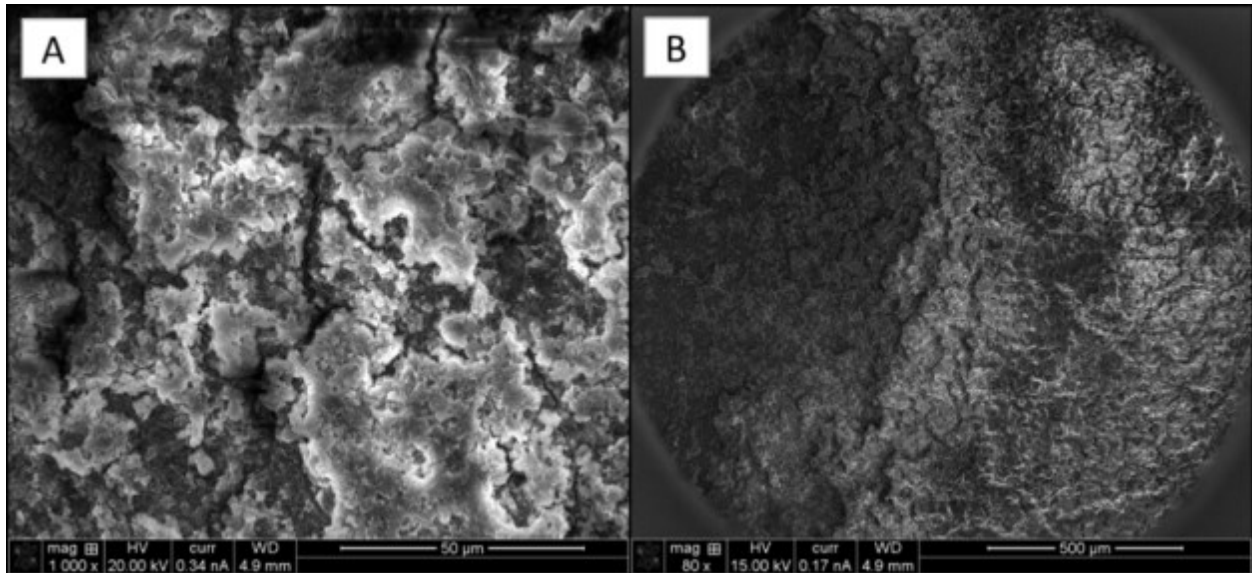


Figure 16. Castle Hayne stage 1 fouled membrane at (A) 50 μm and (B) 500 μm scale.

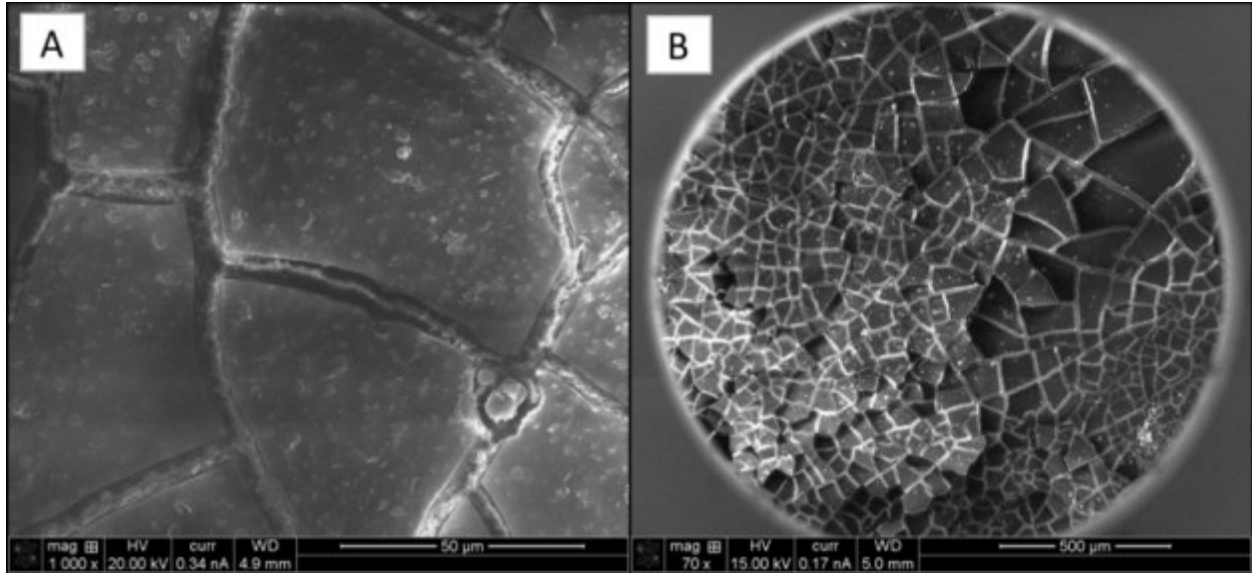


Figure 17. Castle Hayne stage 2 fouled membrane at (A) 50 µm and (B) 500 µm scale.

Figures 18 and 19 show SEM images of the fouling layers on the Peedee first and second stage elements. Although the Peedee first stage fouling layer completely covers the polyamide surface, the fouling layer did not have a distinct morphology. In contrast, the Peedee second stage fouling layer seemed to form in shapes of similar structure approximately 100 µm in diameter. Additional SEM images of fouled membranes at various magnifications, captured at a grazing angle rather than perpendicular to the membrane surface, can be found in Appendix 6. The images provide further visual evidence of the different morphologies of the foulant layers.

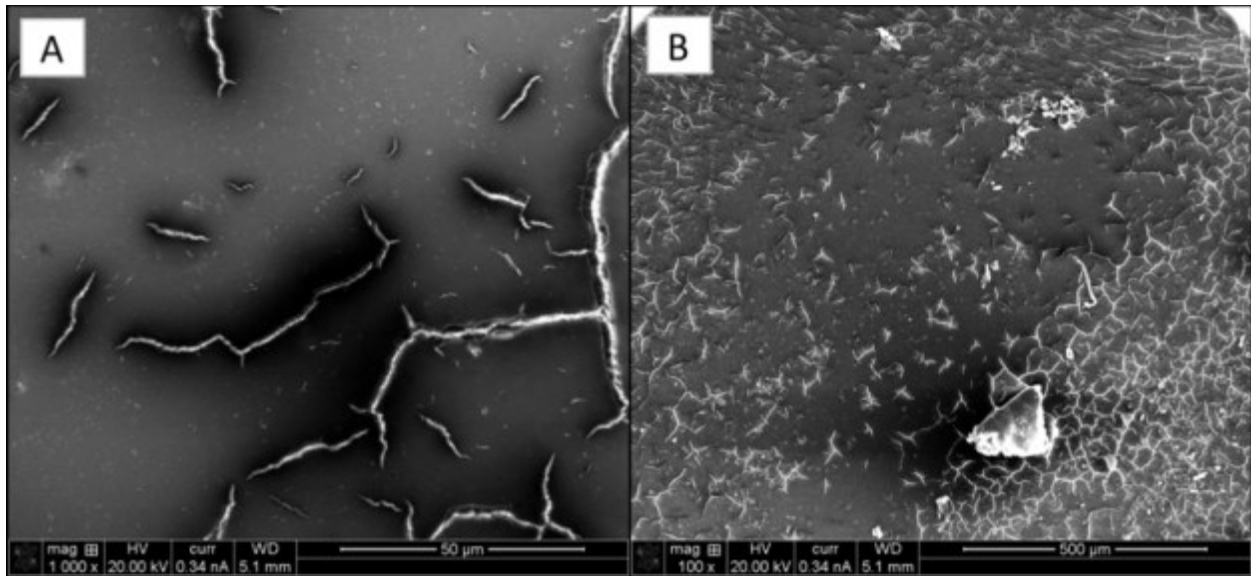


Figure 18. Peedee stage 1 fouled membrane at (A) 50 µm and (B) 500 µm scale.

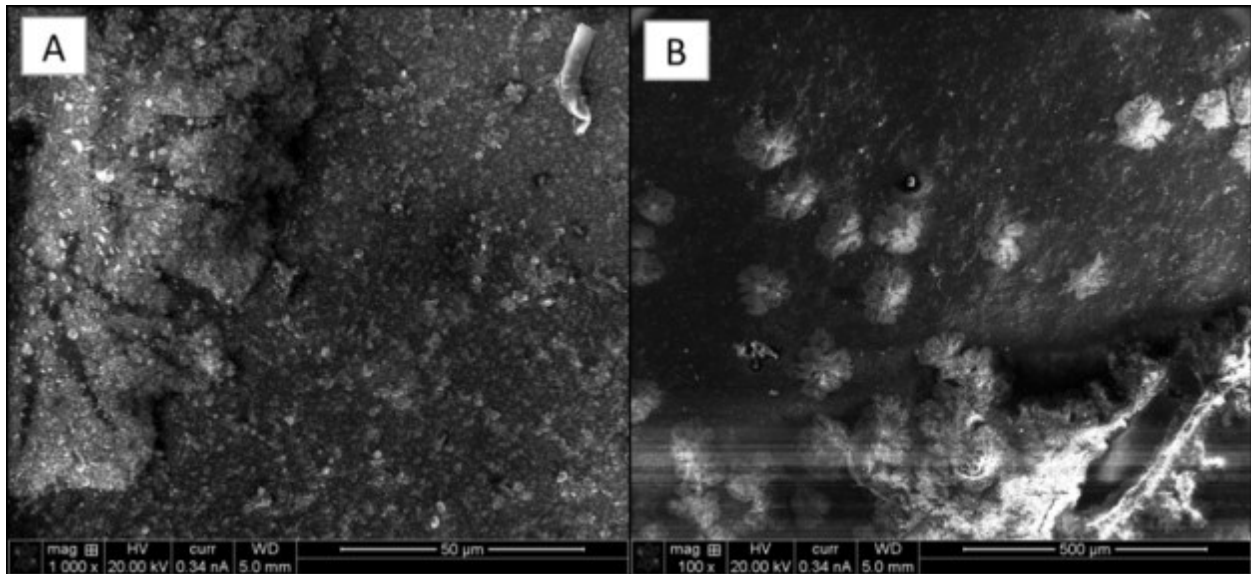


Figure 19. Peedee stage 2 fouled membrane at (A) 50 µm and (B) 500 µm scale.

3.4.2. X-Ray Photoelectron Spectroscopy (XPS)

While SEM was used to visually evaluate the morphology of fouling layers, XPS analysis was used to determine their elemental composition. XPS analysis provides the elemental composition within the first few nanometers from the surface of the sample (Shafer et al., 2006). If a fouling layer is less thick than the analysis depth of XPS (<10 nm), then XPS results would represent the combined signal from foulants and the active layer.

Results for XPS characterization are shown in Figure 20. Error bars correspond to +/- 1 standard deviation as calculated from a minimum of three sample replicates. The presence of a fouling layer is evident by the decrease in carbon and nitrogen content, two elements prevalent in the

membrane itself. All fouled samples show an increase in oxygen concentration, which could be attributed to oxide, hydroxide, carbonate, sulfate, or silicate foulants.

All fouled elements also had detectable concentrations of each inorganic element detected (i.e., iron, calcium, silicon, aluminum, and sulfur) in raw water samples with ICP-MS analysis. The fouled membranes from the two Castle Hayne stages had statistically similar concentrations of calcium and iron, and while the first stage had more silicon and aluminum, the second stage had more sulfur. The Peedee elements had similar iron concentrations, but the first stage had more calcium and the second stage had more silicon and aluminum. Iron concentrations in the Castle Hayne membranes were higher than in the Peedee membranes.

Calcium was observed in significant concentrations in all membranes tested, and sulfur in relatively low concentrations. High silicon concentrations were observed in the Castle Hayne first stage and Peedee second stage elements. Colloidal silica typically fouls the first membranes in a treatment train while polymerized silica commonly precipitates on the last membrane in the treatment train (Nitto Denko, 2011), suggesting that the Castle Hayne first stage contains colloidal silica while the Peedee second stage contains polymerized silica. This hypothesis is supported by physical handling of the two membranes: the Castle Hayne first stage foulant was easily removed by touching the surface or spraying it with water, while the Peedee second stage could not be removed by similar means.

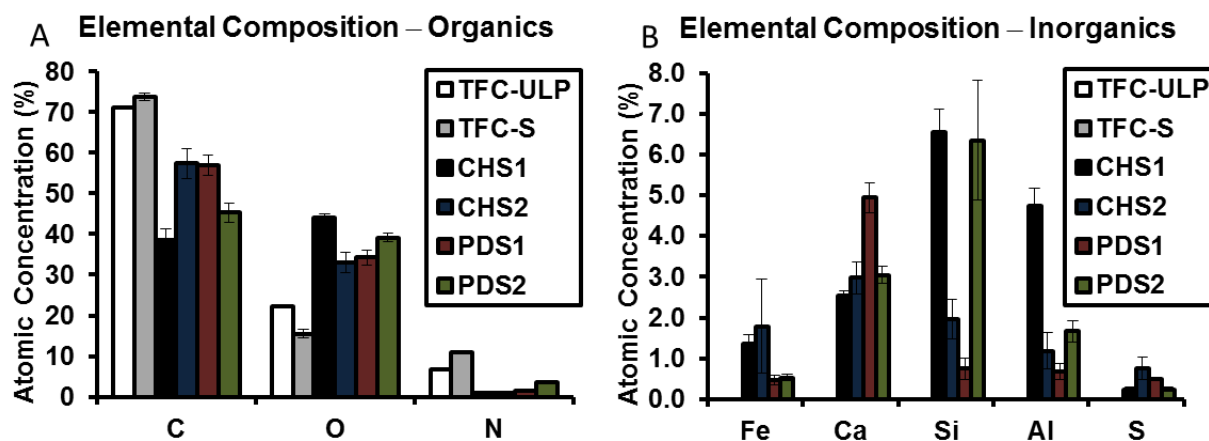


Figure 20. Elemental composition of (A) organics and (B) inorganics in unfouled and fouled membranes determined by XPS. The TFC-ULP membrane was the clean membrane baseline for the Castle Hayne first stage (CHS1) membrane, while TFC-S membrane was the clean membrane baseline for the Castle Hayne second stage (CHS2), Peedee first stage (PDS1), and Peedee second stage (PDS2) membranes .

3.4.3. Energy Dispersive X-Ray Spectroscopy (EDX)

EDX is an analytical technique that yields elemental composition information like XPS, but penetrates approximately 1000 times deeper into the sample – several micrometers (Greenlee et al., 2009). Figure 21 shows the elemental composition of fouled membranes as determined by EDX. As was observed with XPS characterization (Section 3.4.2), fouled membranes analyzed by EDX had lower carbon and higher oxygen content than the unfouled TFC-ULP membrane. In

contrast to XPS measurements, nitrogen was observed at higher concentrations in fouled elements than in the unfouled TFC-ULP.

As was also observed by XPS, EDX results indicate that Castle Hayne foulants contained more iron than the Peedee foulants and that aluminum and silicon were higher in concentration in the fouling layers of the Castle Hayne first stage membranes than in the fouling layers of the second stage membranes. Conversely, the fouling layers of the Peedee first stage membranes showed EDX results significantly lower than XPS results for inorganic constituents. Additionally, the carbon, oxygen and nitrogen content obtained by EDX for the membrane sample from the Peedee first stage were similar to those obtained for the unfouled TFC-ULP membrane. The results thus indicate that the Peedee first stage membrane had a very thin fouling layer that resulted in an EDX signal largely representative of the unfouled membrane (because the analysis depth of EDX is much greater than the fouling layer thickness).

In the TFC-ULP membrane, as well as most of the fouled elements, there are high concentrations of sulfur. This sulfur signal is caused by the polysulfone support layer in the TFC-ULP membrane. Low sulfur signal and similar ratios of inorganics measured by XPS and EDX suggests that the Castle Hayne stage 1 fouling layer is the thickest of the four fouling layers tested which was supported by visual inspection of the fouled membranes.

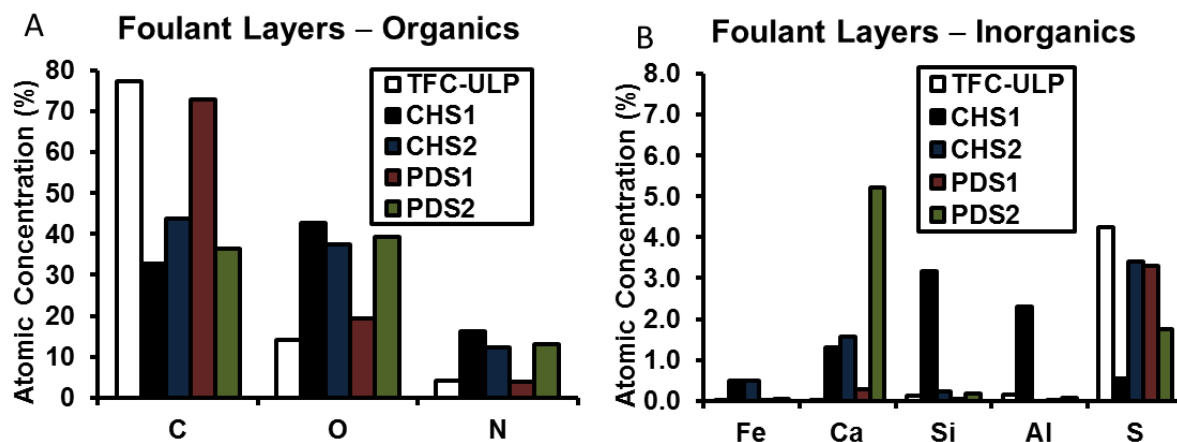


Figure 21. Elemental composition of (A) organics and (B) inorganics in unfouled and fouled membranes determined by EDX. Fouled membranes include the Castle Hayne first stage (CHS1), Castle Hayne second stage (CHS2), Peedee first stage (PDS1), and Peedee second stage (PDS2). TFC-ULP was used as the clean element baseline for all elements because TFC-S was not available from the manufacturer at the time of analysis.

The fouling layer in the Peedee second stage had the most dissimilar elemental composition when measured by XPS and EDX. One possible explanation for the difference in results from the two methods is the ability of EDX to resolve different areas of a heterogeneous fouling layer; while the horizontal spatial resolution of EDX analysis is the same as that of SEM imaging (e.g., tens of microns), the horizontal resolution of XPS analysis is in the several hundreds of microns (see Appendix 7). Given the spatial variability of the Peedee second stage fouling layer, the elemental composition obtained by EDX analysis was highly sensitive to the spot analyzed on the membrane surface.

3.4.4. Attenuated Total Reflectance Fourier Transform Infrared Spectroscopy (ATR-FTIR)

ATR-FTIR provides an additional means to characterize fouled and unfouled membranes. Different bond types absorb energy at a specific wavelength, resulting in characteristic peaks in the ATR-FTIR spectrum. These peaks can be used to identify bond types, and perhaps indicate molecules present rather elemental composition as was determined by XPS and EDX. Figure 22 shows ATR-FTIR spectra for an unfouled TFC-ULP membrane and the four fouled elements. TFC-ULP and TFC-S membranes have very similar ATR-FTIR spectra as shown in Appendix 8, and therefore, TFC-ULP membranes were used as a baseline.

The TFC-ULP peaks indicate the presence of certain compounds in the membrane. For example, peaks at 1587, 1504, and 1488 cm^{-1} correspond to the polysulfone support layer, and peaks at 1663, 1609, and 1541 cm^{-1} indicate that the active layer is composed of polyamide (Tang et al., 2009). A similar approach can be used to identify membrane foulants. For the Castle Hayne first stage sample, two peaks are evident at wavenumbers of 1032 and 1007 m^{-1} . These peaks correspond to stretching of the Si-O bond, suggesting that the first stage Castle Hayne elements are fouled by silicates (Saikia et al. 2010, Vaculikova et al. 2011). Similarly, the peak around 912 m^{-1} represents deformation of an OH group linked to two Al^{3+} , and the peaks around 468 and 535 m^{-1} represent Si-O-Si bending and Si-O-Al stretching, respectively (Saikia et al. 2010, Vaculikova et al. 2011). All of these bonds are present in theoretical kaolinite, and therefore the fouling layer most likely contains kaolinite. Gabelich et al. (2005) also showed that the precipitate foulants most likely to form in membrane systems from dissolved aluminum and silica are kaolinite and muscovite. The peaks mentioned above could also represent aluminum silicate, which has a similar chemical structure to kaolinite.

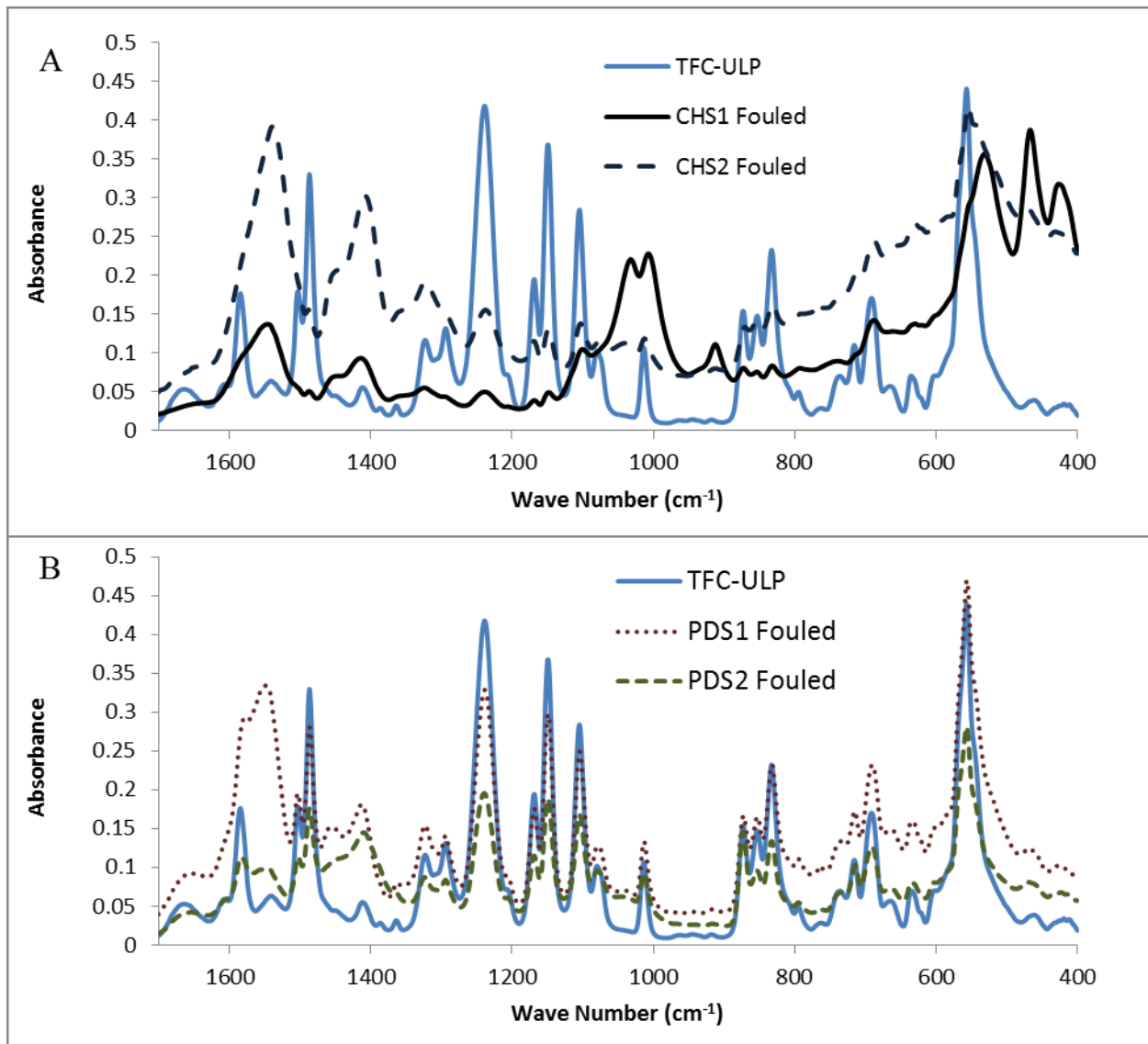


Figure 22. ATR-FTIR spectra for a sample of the unfouled TFC-ULP membrane and fouled membrane samples from the (A) Castle Hayne treatment train and (B) Peedee treatment train.

All fouled samples had an absorbance peak around 1440 m^{-1} , which is characteristic of calcium carbonate (Stein, 2012). The Castle Hayne second stage sample has peaks in similar locations to the first stage with different magnitudes of absorbance. Peaks that were more prominent in the Castle Hayne second stage sample included those at 1408 and 1540 m^{-1} ; however, these peaks could not be matched to particular bonds. ATR-FTIR spectra of fouled elements from the first and second Peedee stages had FTIR spectra that more closely aligned with the unfouled TFC-ULP element, indicating thinner fouling layers that resulted in a large portion of the FTIR signal coming from the membrane itself as opposed to from the fouling layer. Other prominent peaks could not be linked to potential foulants.

3.4.5. Rutherford Backscattering Spectrometry (RBS)

RBS provides another means to characterize the elemental composition of membrane samples. Unlike XPS, RBS can characterize the full depth of the membrane's active layer. RBS is also more sensitive than EDX, allowing for the detection of elements present in relatively low concentration. Figure 23 shows RBS spectra for an unfouled TFC-ULP membrane sample and a sample of the Castle Hayne first stage fouled membrane, while Figure 24 shows spectra for an unfouled TFC-S membrane sample and samples of the Castle Hayne first stage, Peedee first stage, and Peedee second stage fouled membranes.

From Figures 23-24, we see that all four elements have peaks that indicate the presence of aluminum, silicon, calcium, and iron as was observed by XPS (see Figure 20), in addition to the expected constituents of organic matter and polymers carbon, oxygen and nitrogen. Additional spectra are shown in Appendix 9. Although spectra for all four fouled elements indicate the presence of the same elements, relative concentrations of each element vary significantly. The distinct calcium peak (as opposed to a plateau as in the other fouled samples) in the Peedee first stage RBS spectrum (see Figure 24) indicates that the (calcium-containing) fouling layer is thin enough that RBS can 'see' the surface and backside of it. XPS results also indicated that calcium was the primary foulant in the Peedee first stage (see Figure 20). Since the analysis depth of RBS is about 2 μm , then the thickness of the fouling layer in the Peedee first stage is less than $\approx 2 \mu\text{m}$; based on the thickness of the calcium peak, the thickness of the fouling layer in the Peedee first stage membranes can be estimated as $< 200\text{nm}$.

The analysis of the Peedee second stage RBS spectrum in Figure 24 indicates that all RBS signal comes from the fouling layer, which means that the fouling layer thickness is larger than 2 μm . The analysis of the RBS spectrum indicates that the fouling layer is composed of at least three sub-layers containing carbon, oxygen, silicon, aluminum, calcium, and iron. The top sub-layer ($< 40 \text{ nm}$ thick) is rich in iron compared to the two bottom sub-layers, and the top two sub-layers are rich in calcium and silicon compared to the third sub-layer. The thickness of the top two sub-layers combined is $< 300 \text{ nm}$ thick.

The RBS spectra for the Castle Hayne fouled membrane samples in Figures 23 and 24 indicate that the fouling layers in both Castle Hayne stages are thicker than 2 μm . The spectra also show that iron, calcium and carbon content is higher at the surface of the Castle Hayne stage two sample than at the surface of the Castle Hayne stage one sample. The RBS spectrum for the fouling layer of the Castle Hayne stage one sample shows a top sub-layer less than 300-nm thick rich in silicon followed by a thick fouling layer. Similarly, the RBS spectrum for the fouling layer of the Castle Hayne stage two sample shows a top sub-layer less than 500-nm thick rich in calcium, silicon and probably aluminum.

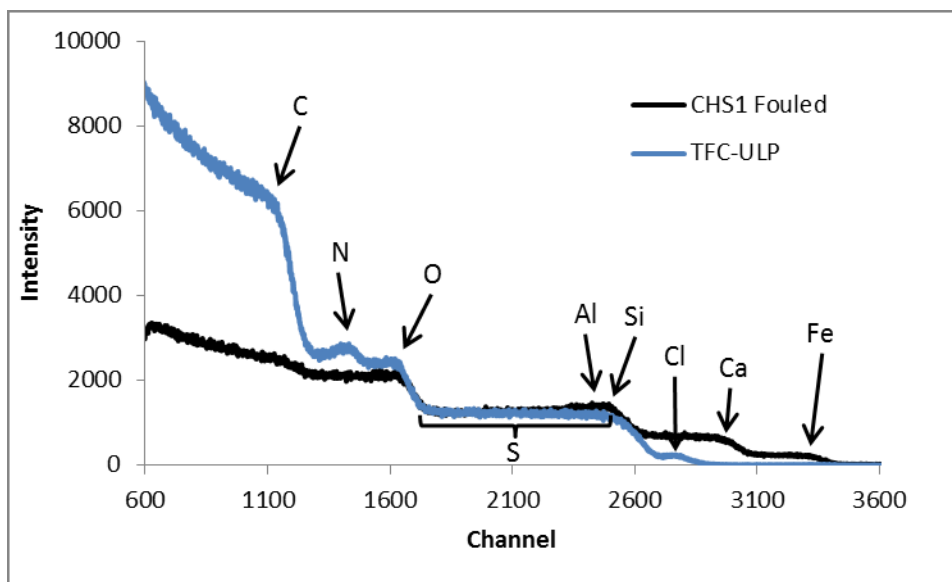


Figure 23. RBS spectra for samples of the Castle Hayne first stage (CHS1) fouled membrane and unfouled TFC-ULP membrane.

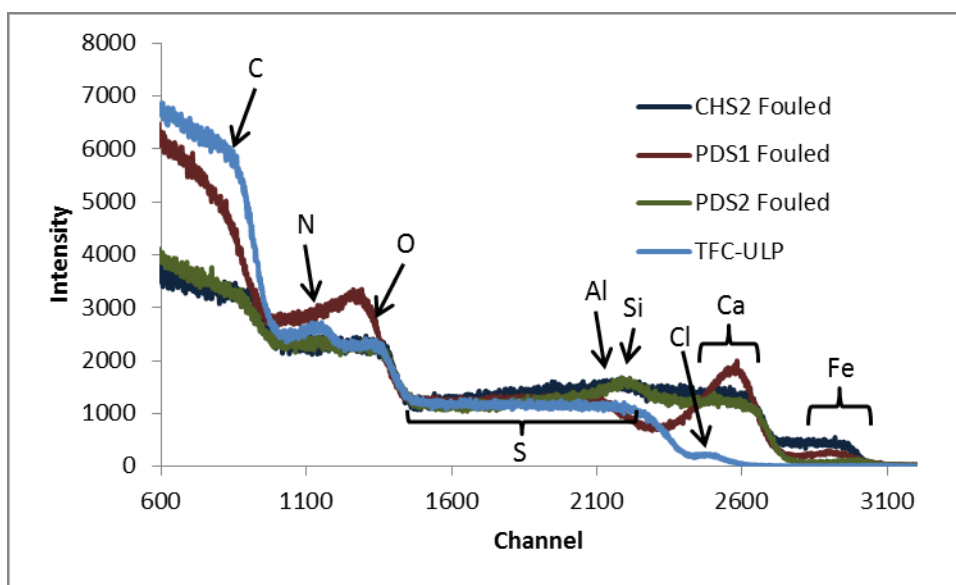


Figure 24. RBS spectra for samples of the Castle Hayne second stage (CHS2), Peedee first stage (PDS1), and Peedee second stage (PDS2) fouled membranes and an unfouled TFC-S membrane sample.

3.4.6. Analysis of Extracted Foulants

Although, XPS, EDX, and RBS can all determine elemental composition, these techniques are best suited for the identification of inorganic foulants. XPS, EDX, and RBS cannot distinguish carbon, oxygen, and nitrogen atoms present in the membrane from those present in organic foulants. While ATR-FTIR can indicate the presence of bonds typically found in organics, the complex nature of the foulants observed in the four membranes tested prevented the identification of individual molecules from ATR-FTIR spectra. In addition, relating ATR-FTIR absorbance to foulant concentration provides further challenges. As a result, to better

characterize the composition of the fouling layers, we analyzed cleaning solutions for DOC and dissolved ions to measure the concentration of foulants extracted during the cleaning process.

Organic matter can be extracted from membrane foulant layers by soaking fouled membrane samples in sodium hydroxide solutions (Ivnitsky et al., 2005; Cho et al., 1998). Following membrane cleanings with sodium hydroxide (pH=11) (See Section 3.7), the concentration of dissolved organic carbon (DOC) in the cleaning solution was measured. Using the area of the membrane sample cleaned and the volume of the cleaning solution used, we calculated the areal concentration (g/m^2) of organic matter on the fouling layer on the membrane surface. The results obtained for membrane samples from both stages of the Castle Hayne and Peedee treatment trains are presented in Figure 25. From these results, it was evident that the Castle Hayne membranes had more significant organic fouling than the Peedee elements, particularly the membranes from the Castle Hayne second stage.

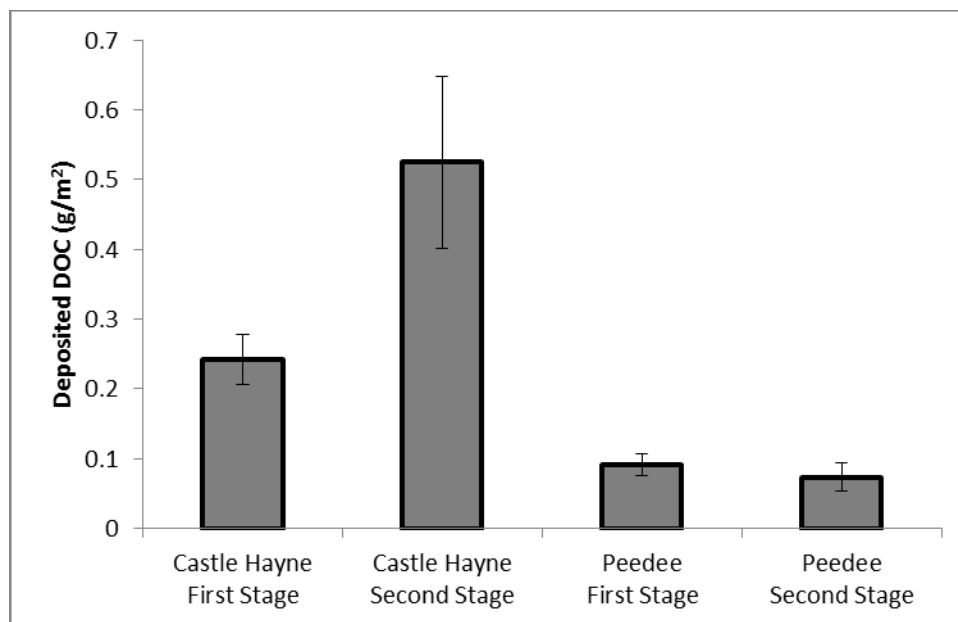


Figure 25. Deposited organic carbon (measured as DOC in the cleaning solutions) extracted during cleaning with sodium hydroxide at pH=11.

To determine if the fouling layers contained more organic or inorganic fouling, concentrations of inorganic foulants in the cleaning solutions following chemical cleaning were measured by ICP-MS. Measurements of inorganics were performed using cleaning solutions that most effectively removed the membrane fouling layer (see Section 3.7); STPP+EDTA and Lavasol 7 cleaning solutions were used as sodium hydroxide was less effective at removing inorganics (see Appendix 10). Results of inorganic extractions are shown in Figure 26.

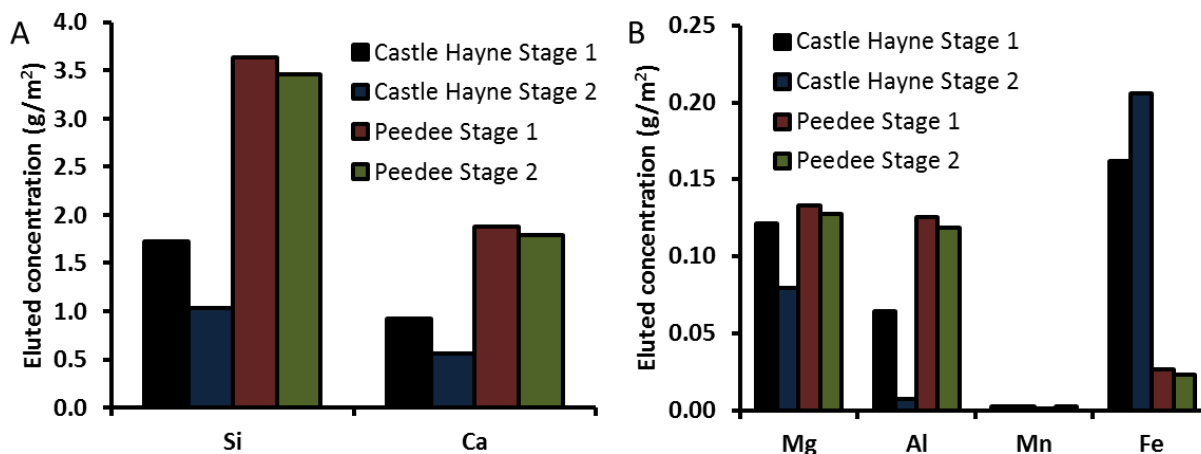


Figure 26. Deposited inorganic foulants extracted during cleaning with the most efficient cleaning solution (STPP+EDTA for the Castle Hayne elements, Lavasol 7 for the Peedee).

From Figures 25 and 26, we can infer the relative mass contribution of inorganic and organic constituents to the foulant layer. For both Castle Hayne elements, the presence of foulants in order of decreasing mass concentration was silicon, calcium, organic matter, iron, magnesium, aluminum, manganese. Similarly, the order for Peedee was silicon, calcium, magnesium, aluminum, organic matter, iron, and manganese.

The results also show that silicon, calcium, and aluminum are in general present in higher concentration in the Peedee fouling layers than in the Castle Hayne fouling layers, and that the opposite is true for iron. These findings generally agree with XPS results, although aluminum concentration in the foulants extracted from membranes from the Castle Hayne first stage compared to the corresponding concentration in the Castle Hayne and Peedee second stage samples is lower than what was expected from XPS results. This could indicate that the aluminum present in the Castle Hayne first stage fouling layer is colloidal in nature, and thus filtered by the 0.2 μm prefilter used to protect the ICP-MS instrument.

Further analysis of organic matter extracted from fouled elements is shown in Table 5. Castle Hayne foulants are more UV absorbent, as determined by SUVA values. Additionally, SUVA measurements were lower in extracted organic matter than was observed in the source water (see Table 2), indicating that the less aromatic organic matter fraction contributes most to fouling. Her et al. (2010) also reported lower SUVA in extracted foulants than the source water as a whole. Extracted organic matter from the Castle Hayne first stage, Peedee first stage, and Peedee second stage fouled elements had a higher slope ratio than the respective source waters, suggesting lower molecular weight organics in the foulant layer than the overall source water. These findings suggest that organic foulants had lower molecular weight and were less hydrophobic than the source water as a whole. Despite DOC concentrations of 1 to 12 mg/L in the extracted foulants, very little of the organic matter present was fluorescent as evidenced by low fluorescence intensity of peaks C1, C2, and C3.

Table 5. Organic parameters for extractions performed using NaOH at pH=11. Prior to fluorescence analysis, samples were neutralized to pH=7.

	Castle Hayne First Stage		Castle Hayne Second Stage	
	Average	Standard Deviation	Average	Standard Deviation
Organic Parameters				
DOC (mg/L)	4.6	0.7	9.9	2.3
UVA 254 (m ⁻¹)	7.9	0.1	11.8	2.7
SUVA (L/mg-m)	1.7	0.2	1.2	0.0
Slope ratio	1.25	0.43	0.54	0.00
Fluorescence index	1.24	0.037	1.28	0.053
Peak C1 Intensity	0.068	0.020	0.058	0.018
Peak C2 Intensity	0.076	0.025	0.045	0.016
Peak C3 Intensity	0.030	0.009	0.017	0.002
	Peedee First Stage		Peedee Second Stage	
	Average	Standard Deviation	Average	Standard Deviation
Organic Parameters				
DOC (mg/L)	1.7	0.3	1.4	0.4
UVA 254 (m ⁻¹)	2.2	1.2	2.0	0.0
SUVA (L/mg-m)	1.3	0.9	1.5	0.4
Slope ratio	2.05	0.23	2.31	1.71
Fluorescence index	1.17	0.082	1.22	0.060
Peak C1 Intensity	0.030	0.013	0.073	0.012
Peak C2 Intensity	0.080	0.045	0.090	0.019
Peak C3 Intensity	0.008	0.001	0.020	0.001

3.5. Recreating Full-Scale Fouling in a Cross-Flow System

While we initially intended to analyze cleaning efficiency using membranes fouled in the laboratory with water collected at the CFPUA treatment plant, it was determined that fouling in the laboratory was not representative of full-scale fouling. Castle Hayne second stage concentrate was chosen for fouling experiments because it had the highest fouling potential of any water collected from the treatment plant. Additionally, laboratory fouling results obtained with Castle Hayne second stage water could be directly compared to the fouling layer characterization results obtained with the membrane element collected from the second stage of the Castle Hayne treatment train at the treatment plant; the Castle Hayne second stage element filtered water that was essentially the same membrane concentrate used for the laboratory fouling studies.

Fouling tests were conducted at 13°C and a pH of 6.5 to simulate treatment plant conditions. Two membrane samples were tested in parallel in the cross-flow filtration system depicted in Figure 3. Fouling tests lasted for a minimum of 24 days until a decrease in flux of 20% was observed. One of the two membranes tested in parallel was then collected and cut into 4 pieces, and one of the four pieces was used to test cleaning efficiency in dead-end configuration. The remaining three pieces were used for characterization by XPS, ATR-FTIR and/or RBS. The second membrane was left in the cross-flow system and cleaned in place using STPP+EDTA. Results of membrane characterization tests for the membranes fouled in the cross-flow system including XPS, RBS, and ATR-FTIR are shown in Figures 27-29, and are compared to results obtained for the membranes collected from the second stage of the Castle Hayne treatment train at the treatment plant.

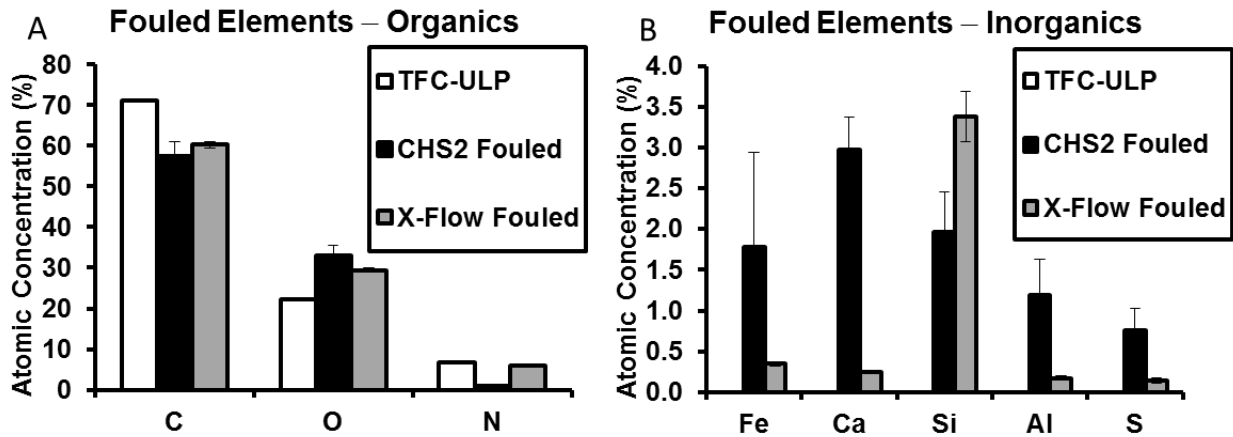


Figure 27. Comparison of fouling layer elemental composition, as quantified using XPS, for membranes fouled at full-scale (CHS2) and in the laboratory cross-flow system (X-Flow) using concentrate water from the second stage of the Castle Hayne treatment train.

Figure 27 indicates that the fouling layer generated by the laboratory cross-flow system contained more silicon than the fouling layer on Castle Hayne second stage membranes and less of all other inorganic constituent, as measured by XPS. Dissimilar RBS and ATR-FTIR spectra in Figures 28 and 29, respectively, between the membrane samples fouled at full-scale and in the laboratory also indicate that cross-flow fouling experiments conducted in the laboratory were not representative of full-scale fouling.

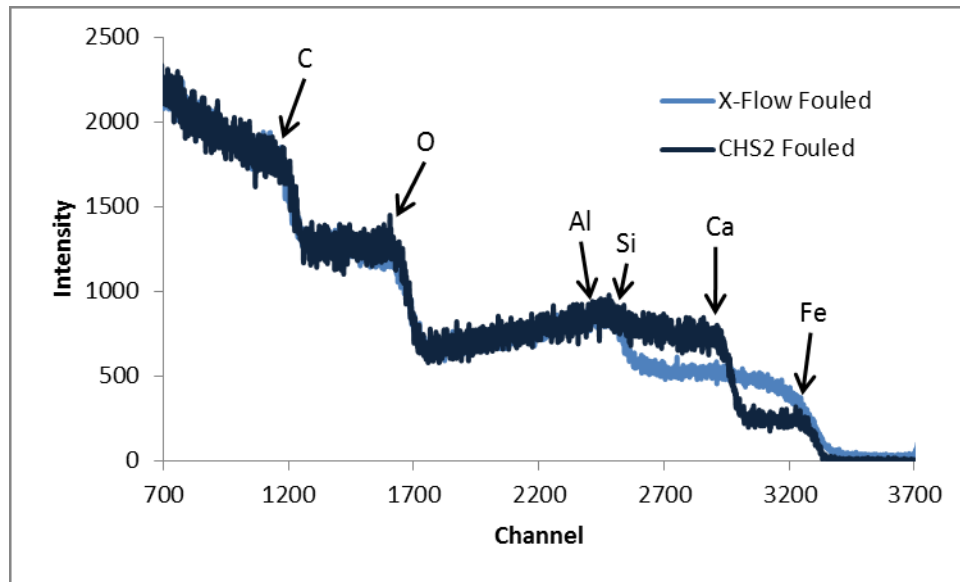


Figure 28. RBS spectra of membranes fouled at full-scale (CHS2) and in the laboratory cross-flow system (X-Flow) using Castle Hayne concentrate.

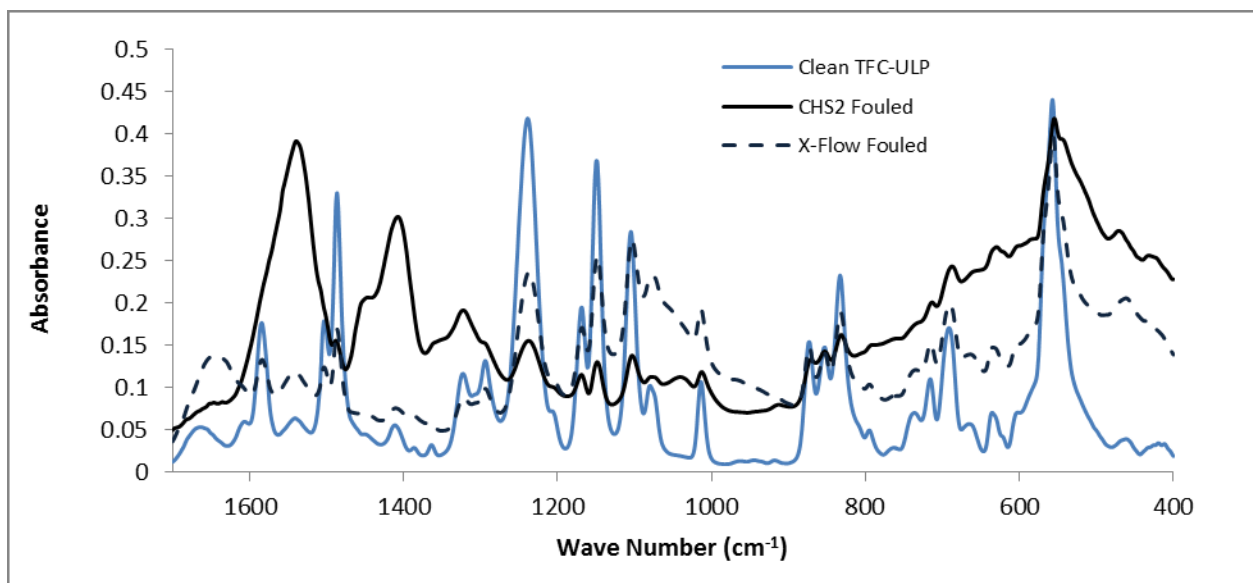


Figure 29. ATR-FTIR spectra of membranes fouled at full-scale and in the laboratory cross-flow system (X-Flow) using Castle Hayne concentrate.

Laboratory cross-flow fouled membranes were cleaned using citric acid, HCl, STPP+EDTA, NaOH+SDS, NaOH (pH=11), Lavasol 7, and OptiClean F. None of the cleaning solutions tested produced significant improvement in membrane permeability following cleaning (data not shown). In contrast, seven solutions were tested on the Castle Hayne second stage membrane samples fouled at full scale (see Section 3.8), and all seven resulted in significant flux improvement with five of the seven solutions returning membrane permeability to values representative of an unfouled membrane.

Two potential explanations for the difference in foulants deposited at full scale and in the cross-flow system are the absence of an antiscalant in the cross-flow system and that Castle Hayne

water changes significantly in quality when exposed to the atmosphere. Antiscalant could not be fed practically in the laboratory because it would have needed to be added continuously, diluting the feed solution, and elevating the antiscalant degradation products to levels not present at the treatment plant. Addition of an antiscalant is impractical, and therefore is not done in laboratory settings. Castle Hayne water also contains high concentrations of dissolved iron, which precipitate when exposed to oxygen from the atmosphere. Iron concentrations in water samples from the second stage concentrate in the Castle Hayne treatment train decreased from 13.3 mg/L to 0.06 mg/L after exposure to the atmosphere prior to use in cross-flow filtration system.

3.6. Comparing Dead-End and Cross-Flow Cleaning

As was shown in Section 3.5, producing fouled membranes in the laboratory resulted in fouling characteristics not representative of fouling at full-scale. Thus, the appropriate way to test cleaning effectiveness was to clean the full-scale fouled membranes collected from the treatment plant.

Dead-end cleaning and performance testing allows for faster sample processing than cross-flow cleaning and testing, and thus more cleaning solutions can be tested using the dead-end setup. As a result, to determine if dead-end and cross-flow cleaning yielded comparable results, we evaluated membrane performance in terms of water permeability following cleaning using both configurations.

Cleaning effectiveness in dead-end and cross-flow setups was tested for two cleaning solutions: one basic (STPP+EDTA) and one acidic (citric) cleaning solution. Results of these cleanings tests are shown in Figures 30 and 31. Cleaning was similarly effective for the dead-end and cross-flow cleaning configurations of full-scaled fouled membrane samples as depicted by the similar specific water permeability values shown in Figures 30-31 for both configurations. Accordingly, dead-end cleanings were used to obtain the results for foulant removal and performance recovery in Sections 3.7 and 3.8, respectively. As described in Section 3.3 above, we found that the membrane element collected from the second stage of the Peedee treatment train was defective, yielding highly variable water permeability and chloride rejection values that depended on the location sampled in the membrane element. While the permeability results for both setups were similar following cleaning with STPP+ EDTA, there was a discrepancy following cleaning with citric acid that was attributed to spatial variability in membrane damage.

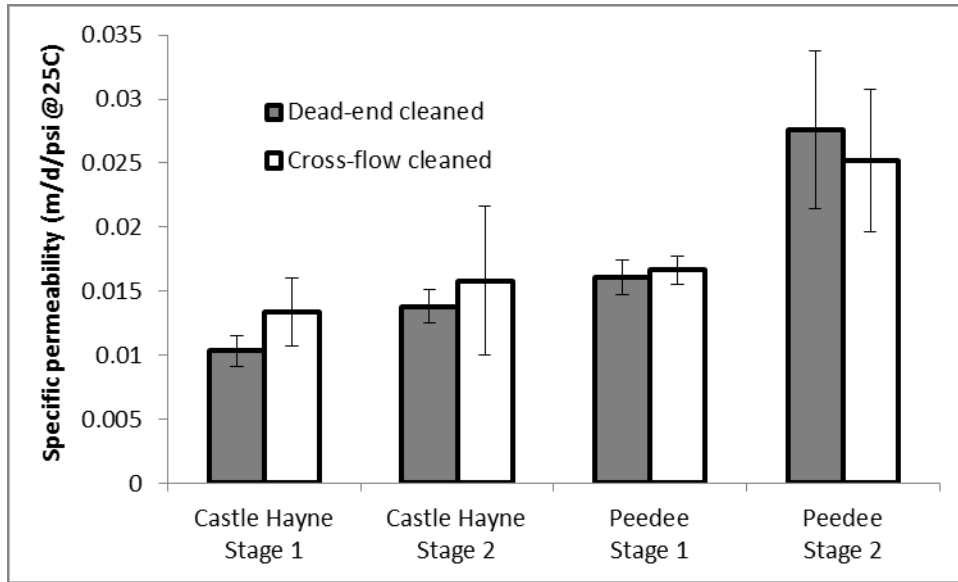


Figure 30. Specific permeability of plant-fouled membranes cleaned with STPP+EDTA in dead-end and cross-flow configurations. Note: Peedee second stage membranes were damaged as evidenced by high flow rate and low chloride rejection, thus caution should be used when interpreting results for these membranes.

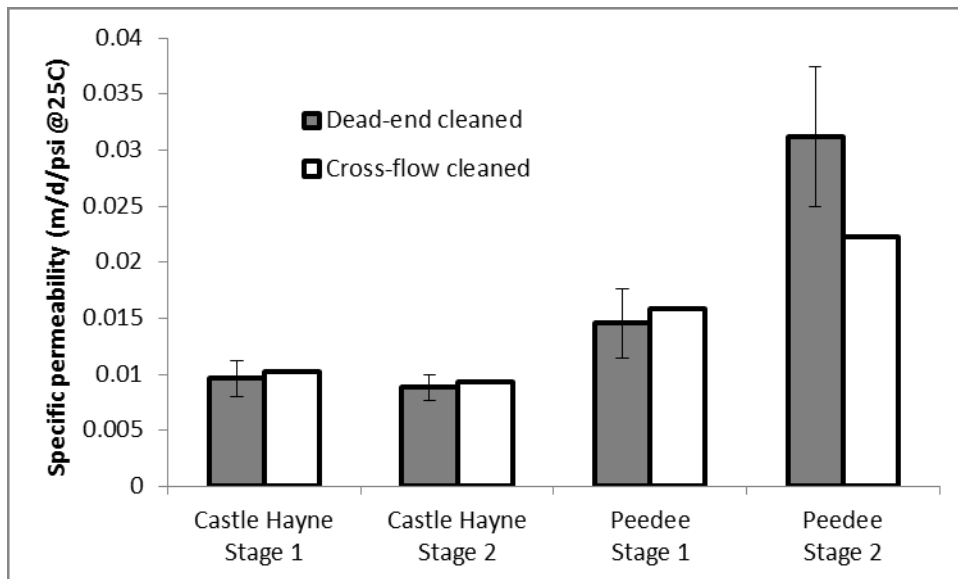


Figure 31. Specific permeability of plant-fouled membranes cleaned with citric acid in dead-end and cross-flow configurations. Cross-flow cleanings with citric acid were not conducted in duplicate, and therefore do not have error bars. Note: Peedee second stage membranes were damaged as evidenced by high flow rate and low chloride rejection, thus caution should be used when interpreting results for these membranes.

3.7. Effect of Chemical Cleaning on Foulant Removal

A number of chemical cleaning solutions were tested for their effectiveness at reversing membrane fouling. Effectiveness of cleaning solutions was determined by comparing the results for cleaned elements to those for unfouled TFC-ULP and TFC-S membranes. STPP+EDTA was

found to be effective for all membranes tested, and therefore we use the corresponding results as illustrative results in this section, with similar results contained in the appendices for the other cleaning solutions. Lavasol 7 was generally found to be equally or more effective than STPP+EDTA at reversing membrane fouling. However, the CFPUA switched from Lavasol 7 to OptiClean F because Lavasol 7 was impractical and hazardous for treatment plant personnel to handle. Lavasol 7 results are provided for comparison with STPP+EDTA results, but are not the focus of this section as the utility has already decided not to use this cleaning solution.

3.7.1. Scanning Electron Microscopy (SEM)

SEM images provide a simple means for analyzing foulant removal from a fouled membrane by determining if the textured polyamide surface typical of unfouled active layers is visible following cleaning. As shown in Figure 32, cleaning using STPP+EDTA reversed membrane fouling such that the active layer was visible in all four fouled membranes imaged after cleaning. Appendix 11 contains further SEM images for membranes cleaned with other cleaning solutions. These images demonstrated that acidic cleaners, including citric acid and HCl, were not as effective as basic cleaners at removing the fouling layer.

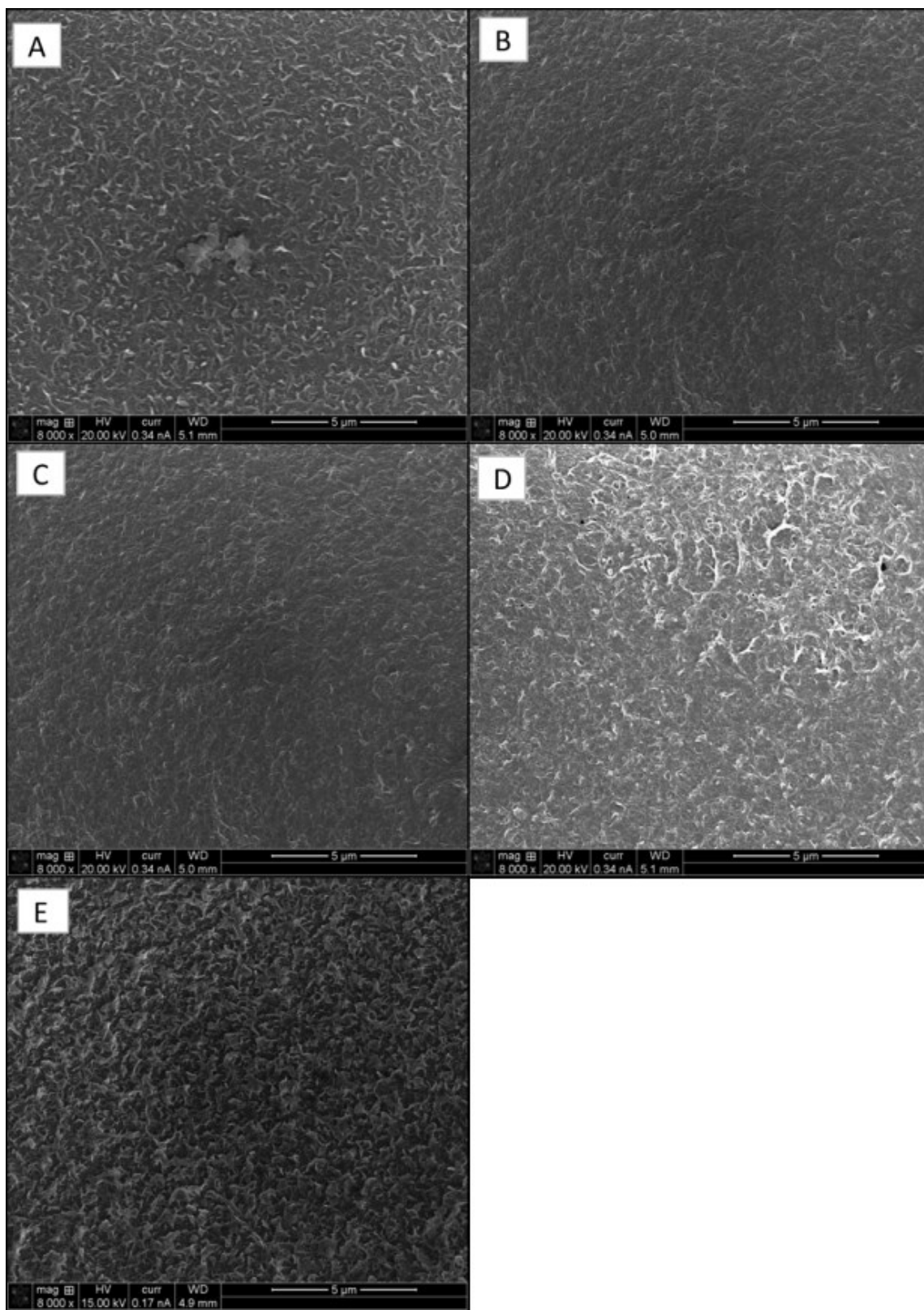


Figure 32. SEM images at 5 μm scale of (A) Castle Hayne first stage, (B) Castle Hayne second stage, (C) Peedee first stage, and (D) Peedee second stage membrane samples cleaned using STPP+EDTA. For comparison, Panel (E) shows an unfouled TFC-ULP membrane at 5 μm scale.

3.7.2. X-Ray Photoelectron Spectroscopy (XPS)

XPS was used to determine the elemental composition of the membrane surface following cleaning. As shown in Figure 33, STPP+EDTA removed foulants such that the elemental composition of cleaned membranes was similar to that of the unfouled membranes, TFC-ULP and TFC-S. The most notable exception is perhaps the inability of STPP+EDTA to remove all silicon and aluminum from the foulant layers of the Castle Hayne Stage 1 membranes. Appendix 12 shows XPS results for membranes cleaned with all other cleaning solutions. From the figures in Appendix 12, it is evident that acidic cleaners were ineffective at removing silicon and aluminum from the fouling layers in both Castle Hayne membranes. NaOH+SDS performed poorly at removing calcium and iron from the fouling layer of the Castle Hayne second stage. In the Peedee second stage, it was evident that citric acid was not effective at removing silicon, nor was NaOH+SDS at removing calcium or silicon.

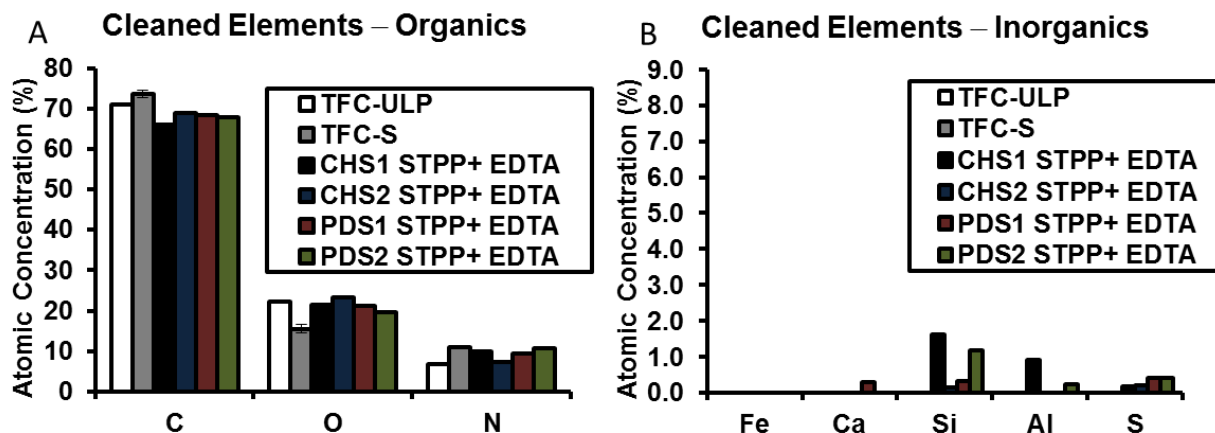


Figure 33. Surface atomic concentrations of (A) organics and (B) inorganics in unfouled and fouled membranes determined by XPS. The TFC-ULP membrane was the clean membrane baseline for the Castle Hayne first stage (CHS1) membrane samples, while the TFC-S membrane was the baseline for the Castle Hayne second stage (CHS2), Peedee first stage (PDS1), and Peedee second stage (PDS2) membrane samples.

3.7.3. Energy Dispersive X-Ray Spectroscopy (EDX)

As was shown in the previous section, cleaning with STPP+ EDTA removes most of the foulant layer from all four membranes tested. Since EDX is less sensitive to surface foulants than XPS, foulant removal appears even greater as shown in Figure 34. However, this is an artifact of EDX penetrating deepert into the sample and characterizing more of the membrane than of the foulant layer. From Figures 33 and 34, it is evident that XPS is a more appropriate technique than EDX for characterizing foulants that remain after cleaning. The high sulfur signal in Figure 34 results from the fact that most of the EDX signal comes from the polysulfone support rather than from the active layer. EDX results for membranes cleaned with other solutions are shown in Appendix 13.

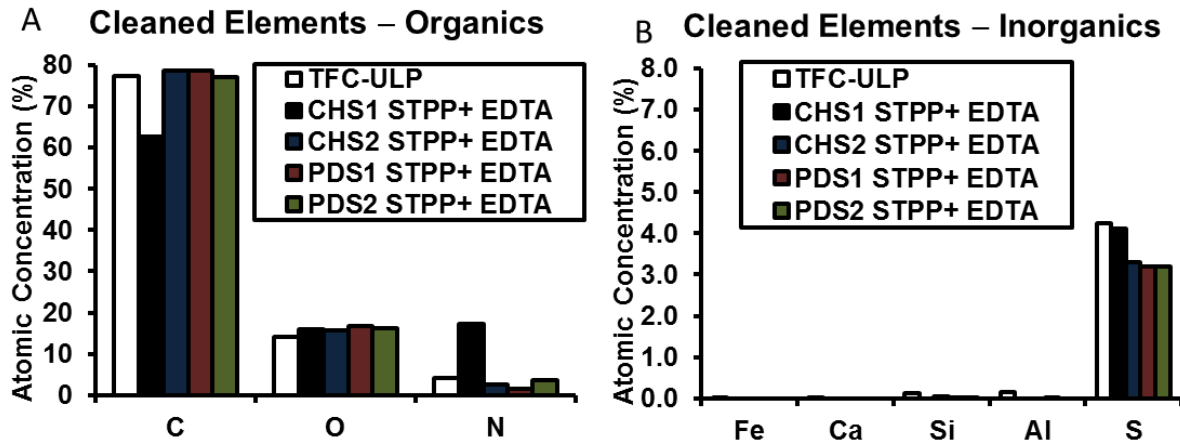


Figure 34. Atomic concentration of (A) organics and (B) inorganics in unfouled and fouled membranes determined by EDX. The TFC-ULP membrane was used as the clean element baseline for all membranes because the TFC-S membrane was not available from the manufacturer at the time of analysis.

3.7.4. Attenuated Total Reflectance Fourier Transform Infrared Spectroscopy (ATR-FTIR)

ATR-FTIR provides further evidence that STPP+EDTA was effective at removing foulants present in all membranes tested (see Figure 35). The spectra of cleaned elements in Figure 35 closely match that for the unfouled TFC-ULP membrane, which is used as a reference. ATR-FTIR results for all solutions tested are shown in Appendix 14.

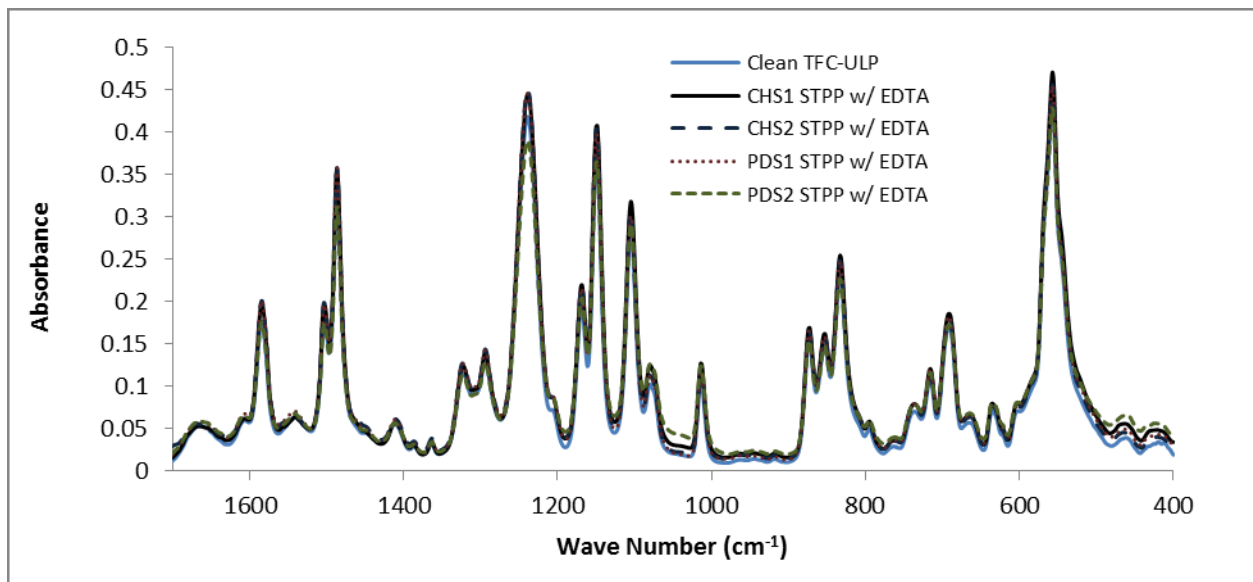


Figure 35. ATR-FTIR spectra of an unfouled TFC-ULP membrane sample as well as of samples of Castle Haye first stage (CHS1), Castle Haye second stage (CHS2), Peedee first stage (PDS1), and Peedee second stage (PDS2) membranes cleaned using STPP+EDTA.

3.7.5. Rutherford Backscattering Spectrometry (RBS)

RBS spectra of fouled membranes before and after cleaning with STPP+EDTA are shown in Figures 36-39. Spectra of fouled membranes cleaned with STPP+EDTA generally align well with the spectra of the unfouled membranes, thus indicating that STPP+EDTA removed most of the fouling layers leaving behind traces of the fouling layers only a few nanometers thick. Nevertheless, we see that small concentrations of calcium remain in both Castle Hayne membranes and in the Peedee first stage membrane. Similarly, traces of iron remain in the membranes of the second stage of both the Castle Hayne and Peedee treatment trains. Silicon and aluminum were found to be still present on the Peedee second stage membrane.

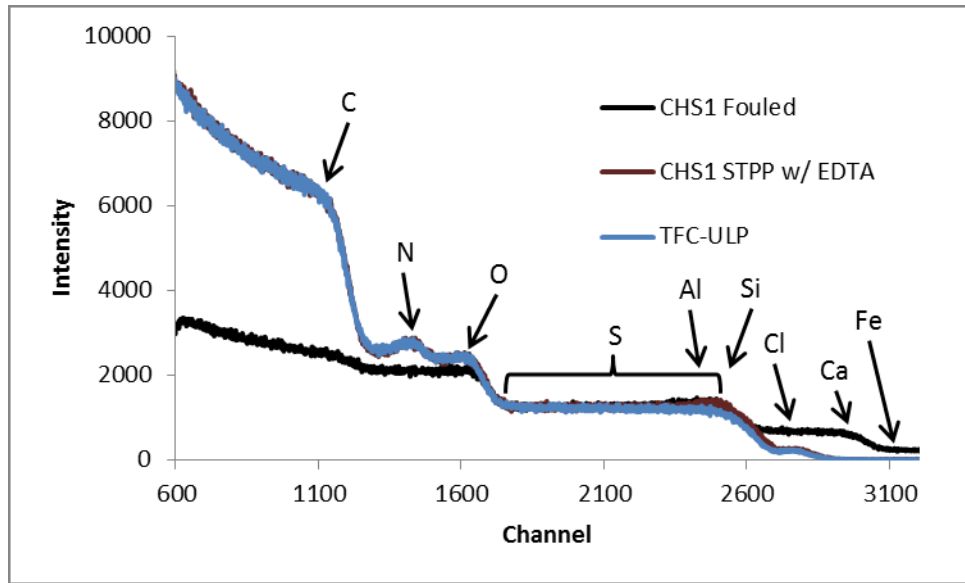


Figure 36. RBS spectra of a Castle Hayne first stage (CHS1) element before and after cleaning with STPP+EDTA. Cleaning returned the membrane to a condition similar the unfouled baseline (TFC-ULP).

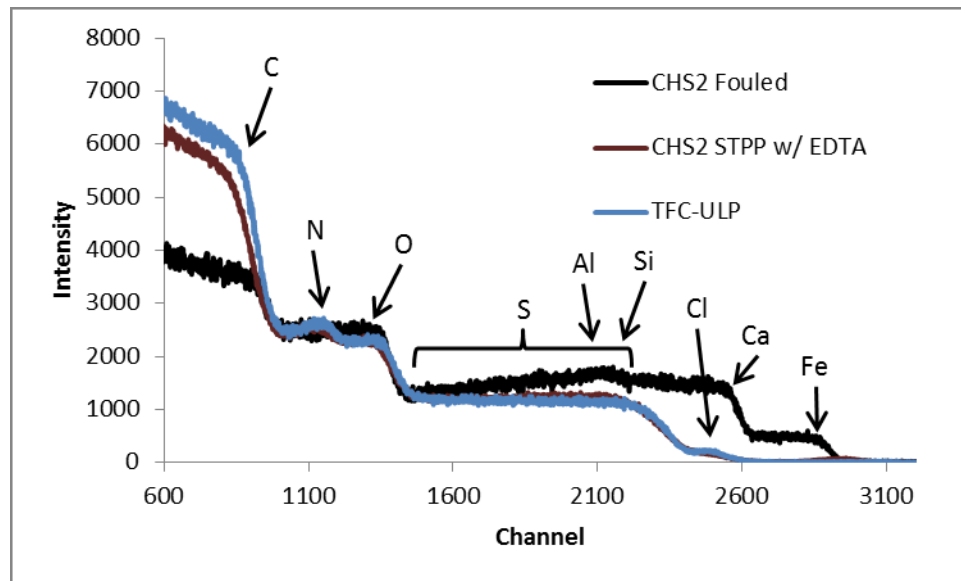


Figure 37. RBS spectra of a Castle Hayne second stage (CHS2) element before and after cleaning with STPP+EDTA. Cleaning returned the membrane to a condition similar the unfouled baseline (TFC-S).

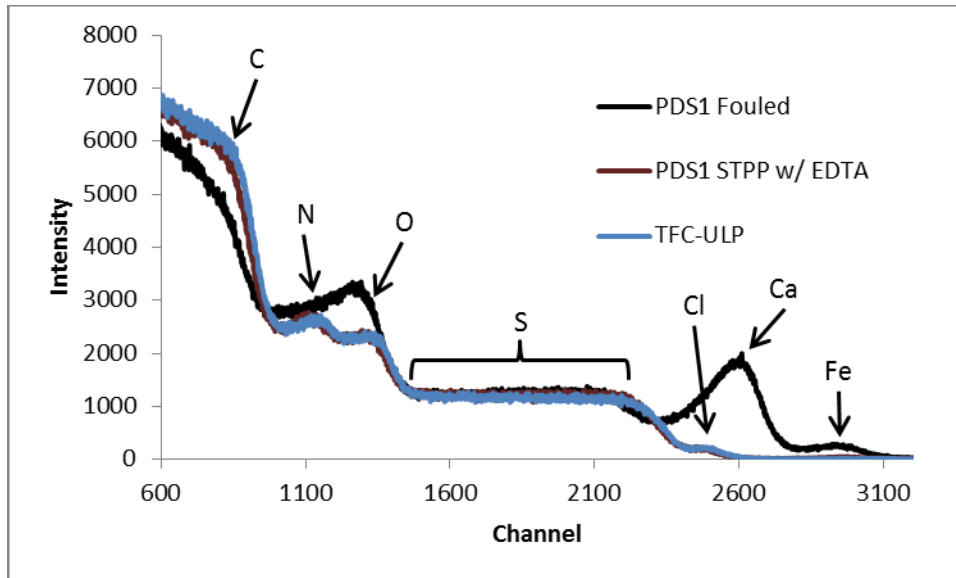


Figure 38. RBS spectra of a Peedee first stage (PDS1) element before and after cleaning with STPP+EDTA. Cleaning returned the membrane to a condition similar the unfouled baseline (TFC-S).

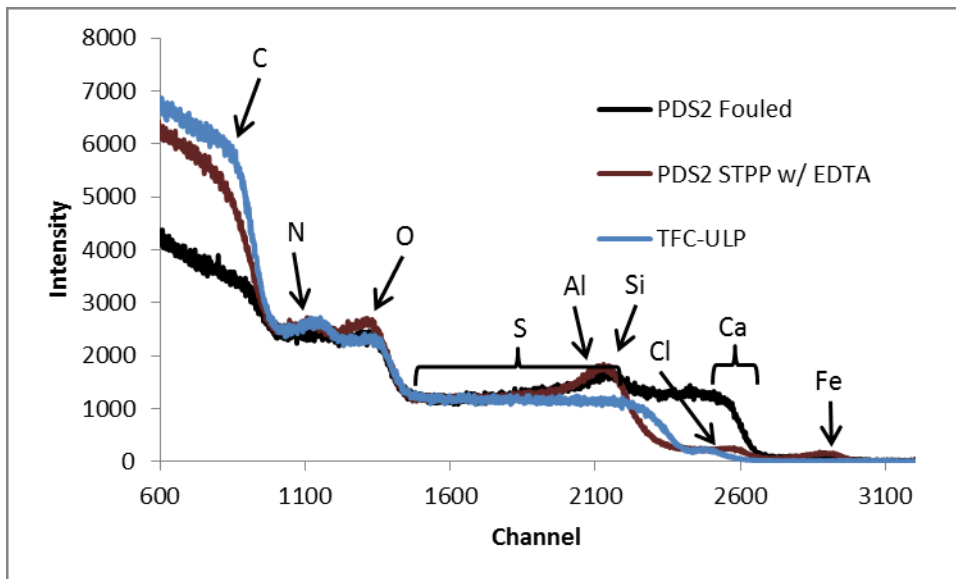


Figure 39. RBS spectra of a Peedee second stage (PDS2) element before and after cleaning with STPP+EDTA. The peak that still remains in the fouled sample is composed of aluminum and or silica.

3.7.6. Comparing Effectiveness of Lavasol 7 and OptiClean F at Removing Foulants

Lavasol 7 was previously used at the treatment plant before switching to OptiClean F due to safety hazards handling concentrated Lavasol 7. Comparing Lavasol 7 and OptiClean F, it was evident that the two solutions were similarly effective at removing foulant layers from fouled membranes from the Castle Hayne first and second stage as well as from the Peedee first stage (see Appendices 12 and 13). By contrast, OptiClean F was shown to be less effective at removing foulants present in the Peedee second stage membranes than Lavasol 7. As Figure 40

shows, much of the foulant layer still remained following cleaning with OptiClean F whereas Lavasol 7 returned the membrane to its original unfouled state. This difference can also be seen in the corresponding ATR-FTIR spectra (see Figure 41). The FTIR peaks characteristic of the polysulfone support are muted in fouled samples and those cleaned with OptiClean F; however, the polysulfone peaks are similar in the spectra of the unfouled TFC-ULP membrane and in fouled samples cleaned with Lavasol 7.

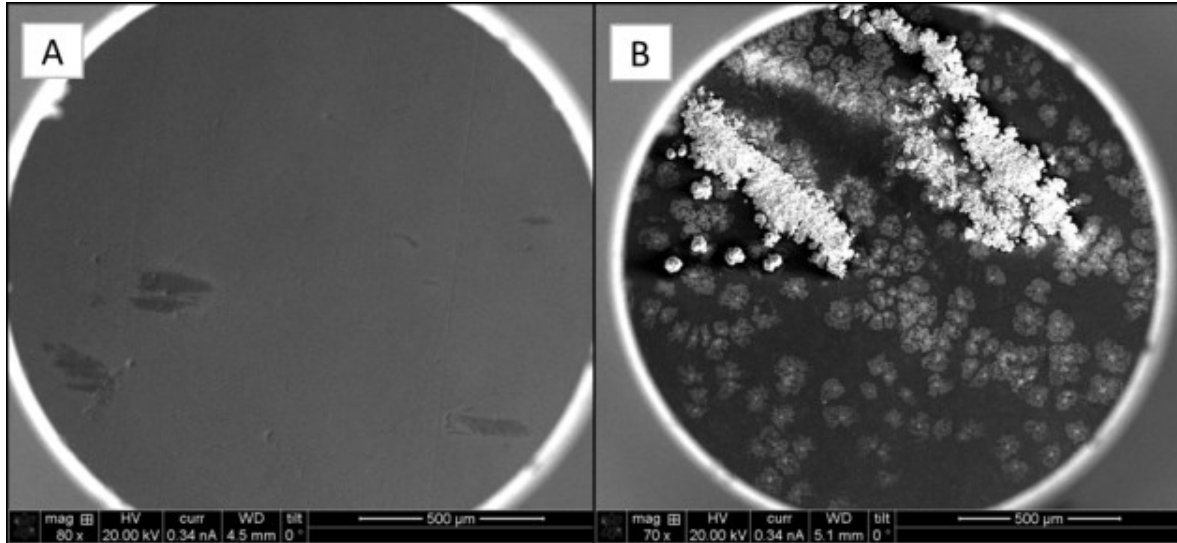


Figure 40. SEM images of Peedee second stage membrane samples cleaned with (A) Lavasol 7 and (B) OptiClean F.

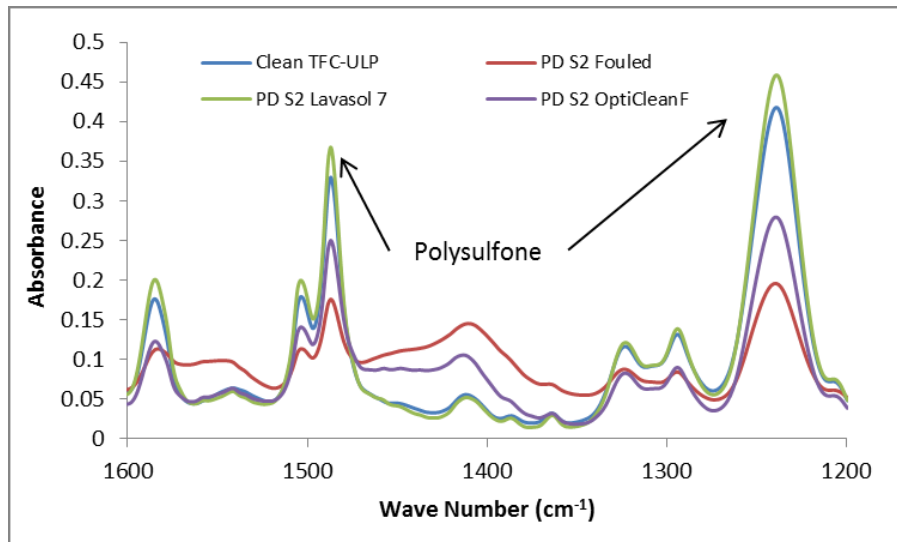


Figure 41. ATR-FTIR results for Peedee Second stage membrane samples cleaned with Lavasol 7 and OptiClean F.

3.8. Effect of Chemical Cleaning on Membrane Performance

Each of the four fouled membranes sampled were cleaned in the dead-end configuration using citric acid, STPP+EDTA, NaOH at pH=11, Lavasol 7, and OptiClean F. Citric acid and STPP+EDTA were tested because they were found to be more effective at removing foulants than HCl and NaOH+ SDS, respectively. NaOH at pH=11 was chosen to test the effectiveness of solely increasing pH. Lavasol 7 and OptiClean F were chosen so that alternative cleaning solutions could be compared to those solutions used at the treatment plant. Permeability and chloride rejection were measured before and after cleaning. When prepared without pH adjustment, Lavasol 7 and OptiClean F solutions had pH values of approximately 12.5 and 12.0, respectively. The membrane manufacturer specified a maximum pH of 11.0 during cleaning for both TFC-ULP and TFC-S membranes (Koch, 2010b and 2010b). For this reason, Lavasol 7 and OptiClean F were also tested with an adjusted pH of 11.0.

Figure 42 shows water permeability results for Castle Hayne first stage membranes before and after cleaning normalized to the water permeability for new TFC-ULP membranes reported in the manufacturer’s specifications (0.0118 m/day/psi) (see Section 2.8). Each of the seven cleaning solutions tested resulted in statistically similar water permeability values. Cleanings were observed not to have a significant impact on chloride rejection (see Appendix 15).

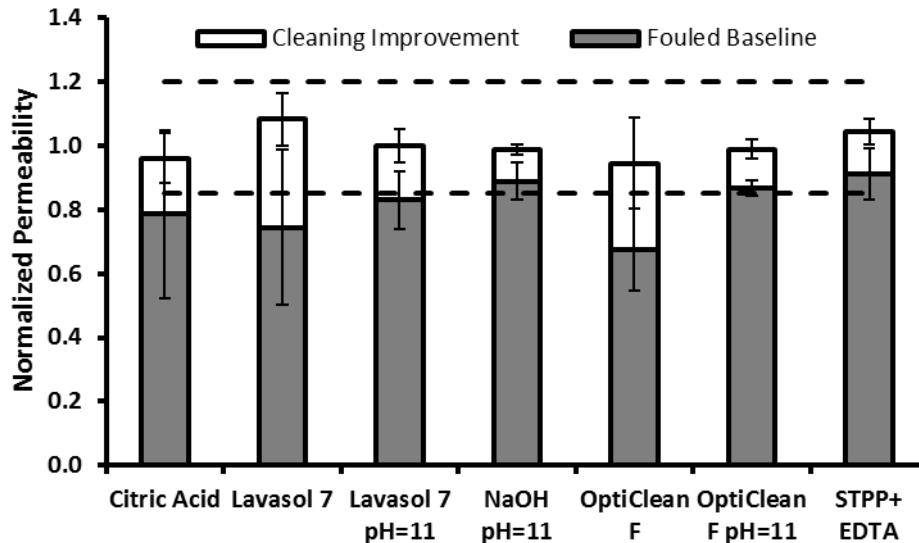


Figure 42. Water permeability of Castle Hayne first stage fouled membranes before and after cleaning with various cleaning solutions. Permeability measurements were normalized to the water permeability for new TFC-ULP membranes reported in the manufacturer’s specifications. Dashed lines represent the range of expected permeability for new TFC-ULP membranes (see Section 2.8). Lavasol 7 and OptiClean F were prepared with and without pH adjustment, resulting in an adjusted pH values of 11 for both cleaning solutions and unadjusted Lavasol 7 and OptiClean F pH values of approximately 12.5 and 12.0, respectively.

Cleaning results for fouled membranes collected from the Castle Hayne second stage are shown in Figure 43. Permeability results were normalized to the water permeability for new TFC-S membranes reported in the manufacturer’s specifications (0.0138 m/day/psi) (see Section 2.8). Unlike the results obtained for the Castle Hayne first stage membranes, citric acid was observed

to perform significantly worse than the basic cleaning solutions for the Castle Hayne second stage membranes. The cleaning efficacy of Lavasol 7 and OptiClean F decreased when the pH was reduced to 11.0 compared to when the pH was not adjusted (i.e., pH~12-12.5). Using NaOH at pH=11 was shown to be similarly effective at recovering membrane performance as STPP+EDTA and Lavasol 7 at pH=11.0. OptiClean F at pH=11 was less effective than other basic solutions. Cleaning did not affect chloride rejection, as shown in Appendix 15.

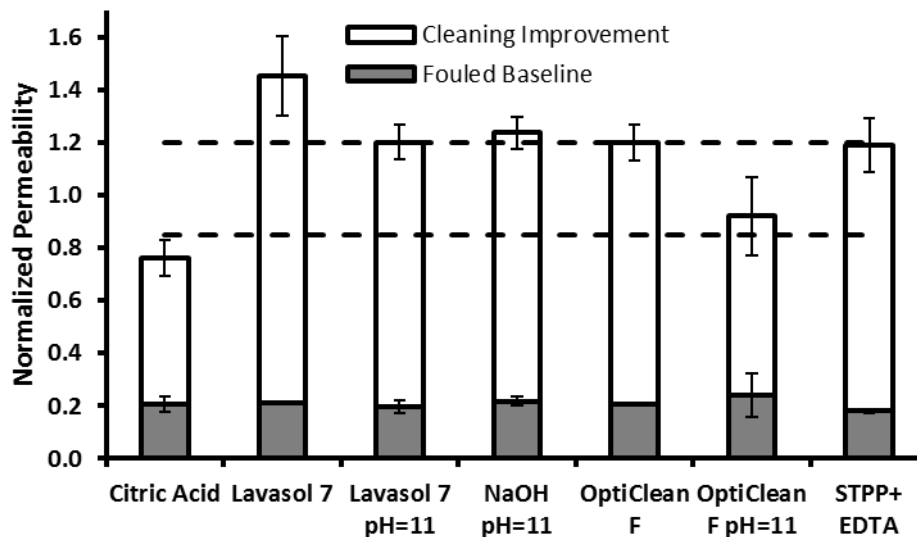


Figure 43. Water permeability of Castle Hayne second stage fouled membranes before and after cleaning with various cleaning solutions. Permeability measurements were normalized to the water permeability for new TFC-S membranes reported in the manufacturer specifications. Dashed lines represent the range of expected permeability for new TFC-S membranes (see Section 2.8). Lavasol 7 and OptiClean F were prepared with and without pH adjustment, resulting in an adjusted pH values of 11 for both cleaning solutions and unadjusted Lavasol 7 and OptiClean F pH values of approximately 12.5 and 12.0, respectively.

Water permeability results for Peedee first stage membrane samples before and after cleanings are shown in Figure 44. The Peedee first stage was the least fouled of the four membranes tested. Most of the basic cleaners tested were similarly effective at improving water permeability; however, citric acid cleaning resulted in no improvement in water permeability. Membrane cleaning did not significantly affect chloride rejection, as shown in Appendix 15.

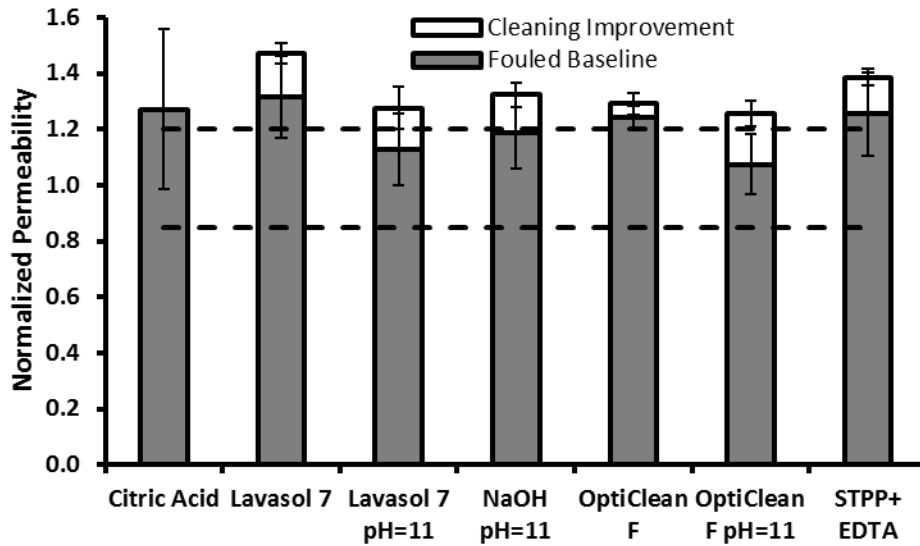


Figure 44. Water permeability of Peedee first stage fouled membranes before and after cleaning with various cleaning solutions. Permeability measurements were normalized to the water permeability for new TFC-S membranes reported in the manufacturer’s specifications. Dashed lines represent the range of expected permeability for new TFC-S membranes (see Section 2.8). Lavasol 7 and OptiClean F were prepared with and without pH adjustment, resulting in an adjusted pH values of 11 for both cleaning solutions and unadjusted Lavasol 7 and OptiClean F pH values of approximately 12.5 and 12.0, respectively.

Figure 45 shows fouled and cleaned normalized water permeability results for Peedee second stage membrane samples. As described in Section 3.3, due to damaged membranes permeability of cleaned elements was well above the range expected for unfouled elements, and chloride rejection was much lower as well (see Appendix 15) with average chloride/conductivity rejections of 50% compared to the 85% indicated in the manufacturer’s specifications. Although the damage to these membrane samples complicates interpretation of the results, we see that all cleaning solutions tested significantly improved permeability except for OptiClean F, particularly at pH= 11.0.

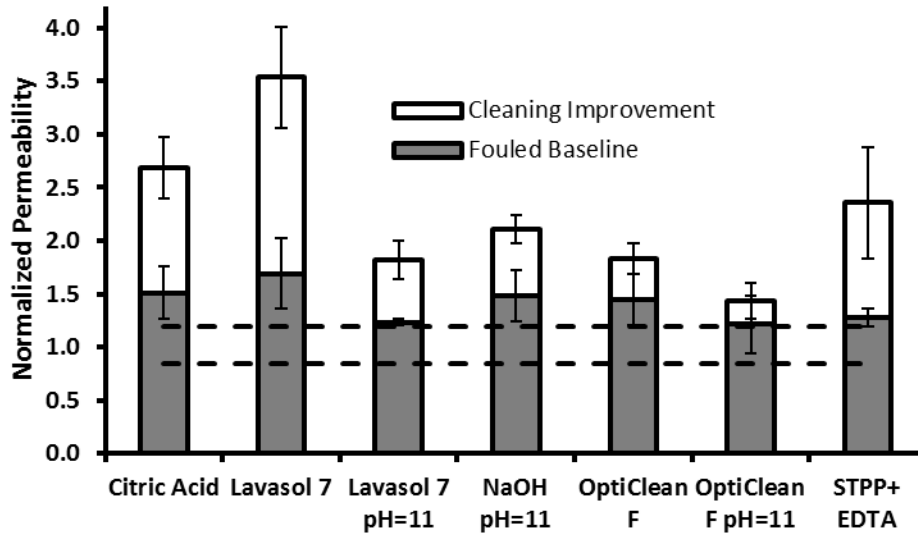


Figure 45. Permeability of Peedee second stage fouled membranes before and after cleaning with various cleaning solutions. Permeability measurements were normalized to the water permeability for new TFC-S membranes reported in the manufacturer specifications. Dashed lines represent the range of expected permeability for new TFC-S membranes (see Section 2.8). Lavasol 7 and OptiClean F were prepared with and without pH adjustment, resulting in an adjusted pH values of 11 for both cleaning solutions and unadjusted Lavasol 7 and OptiClean F pH values of approximately 12.5 and 12.0, respectively. Note: Peedee second stage membranes were damaged as evidenced by high flow rate and low chloride rejection, thus caution should be used when interpreting results for these membranes.

3.9. Membrane Longevity

To determine if prolonged exposure to membrane cleaning solutions from repeated cleanings would affect membrane performance, membrane longevity tests were conducted. Longevity tests were performed by exposing TFC-ULP elements obtained from the manufacturer to cleaning solutions at 38°C and then testing performance after varied exposure periods. Given that at the CFPUA treatment plant cleanings occur approximately biannually (see Figure 10) for a minimum of two hours, 40 hours of cleaning solution exposure is analogous to 10 years of cleaning.

Figures 46 and 47 show normalized water permeability and chloride rejection, respectively, for membranes exposed to three cleaning solutions: STPP+EDTA, Lavasol 7, and OptiClean F. These three cleaning solutions were selected for the membrane longevity tests because STPP+EDTA was the most effective non-proprietary cleaning solution for all four fouled membrane samples and Lavasol 7 and OptiClean F have been used by the treatment plant. Lavasol 7 and OptiClean F were prepared without pH adjustment resulting in corresponding pH values of approximately 12.5 and 12.0 which exceed the membrane manufacturer’s recommendation of 11.0 for cleaning (Koch, 2010a and 2010b). The pH of STPP+EDTA was adjusted to 10.5. From Figure 46, it was evident that Lavasol 7 increased membrane permeability by approximately 20% for all exposure periods tested, as did OptiClean F for exposures over 40 hours. For periods of exposure greater than 40 hours, membranes exposed to both Lavasol 7 and OptiClean F had

chloride rejections 4-5 percentage points lower than membranes exposed to STPP+EDTA and deionized water for which chloride rejection remained statistically constant over the exposure period. Water permeability of TFC-ULP membranes exposed to deionized water and STPP+EDTA demonstrated reduced permeability over time, possibly due to membrane compression effect.

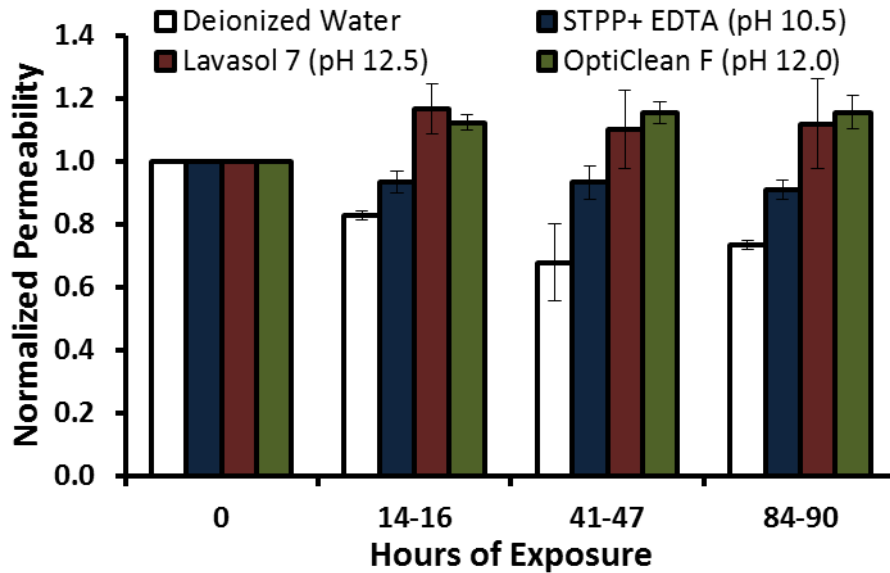


Figure 46. Normalized water permeability of membranes exposed to cleaning solutions for varying amounts of time. Samples were normalized to the initial membrane water permeability at time 0 hours. Cleaning solution pH was approximately 10.5 for STPP+EDTA, 12.5 for Lavasol 7, and 12.0 for OptiClean F.

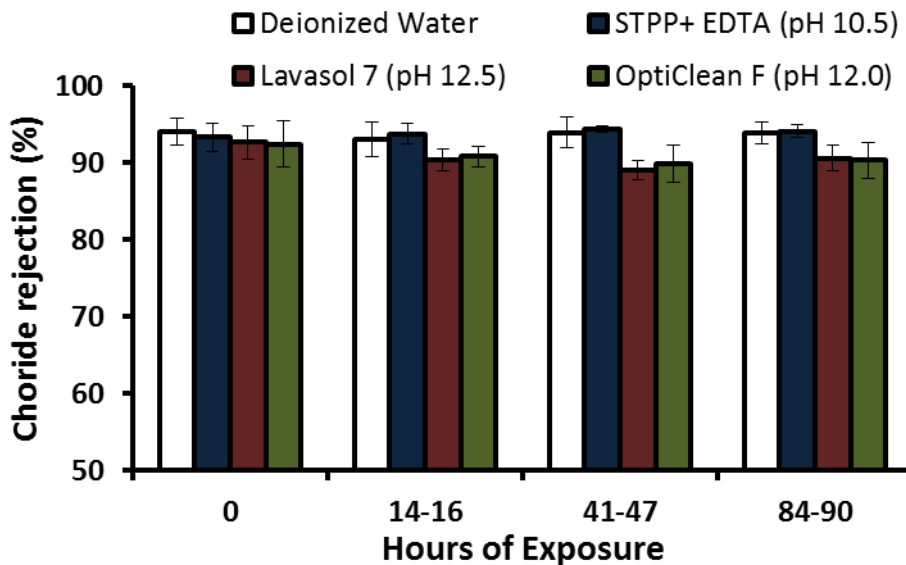


Figure 47. Chloride rejection of membranes exposed to cleaning solutions for varying amounts of time. Cleaning solution pH was approximately 10.5 for STPP+EDTA, 12.5 for Lavasol 7, and 12.0 for OptiClean F.

3.10. Optimizing Full-Scale Cleaning Frequency

Over a one month period spanning June and July of 2012, the average daily electricity cost to operate the treatment plant, including pumping water from the Castle Hayne and Peedee aquifer wells to the treatment plant, was \$1,283.32 (Malone, 2013). Excluding seasonal differences in water demand, the extrapolated annual electricity cost is over \$468,000. Producing water as fouling progresses requires more energy as feed pressure is increased to maintain constant flux. Therefore, we considered optimizing cleaning frequency to reduce energy consumption, thereby reducing energy costs. To optimize full-scale cleaning frequency, we compared the cost of chemical cleaning, including chemical costs and labor costs, to the variable energy costs during periods of fouling. We did not take into account depreciation or maintenance costs of equipment used during cleaning or filtration operations.

3.10.1. Labor and Chemical Costs

Chemical cleanings incur costs in the form of labor and chemicals used. Chemical cleaning requires 4 man-hours of preparation the day prior to cleaning, and 12 man-hours the day of cleaning, resulting in a total labor cost of \$408 per cleaning (Malone, 2013). Cleanings performed with OptiClean F use three 10-gallon pails of powdered chemical at a cost of \$103 per pail, or a total chemical cost of \$309. Lavasol 7 is more expensive, requiring six 5-gallon buckets of liquid chemical at \$205 per bucket, or a total chemical cost of \$1,230. Summing labor and chemical costs, the total cleaning costs using OptiClean F and Lavasol 7 are \$717 and \$1,638, respectively.

3.10.2. Well Field Pumping Costs

Water is pumped from the Castle Hayne and Peedee well fields to treatment plant. Although pumping water to the facility is independent of membrane fouling, understanding energy use by well field pumps is important for two reasons. First, it is important to understand what portion of energy use is fixed. Based on a one month period of June and July, 2012, well field pumps cost \$419 per day to operate, or 33% of overall electricity costs (Malone, 2013). Second, pressure output by the well field pumps provides the baseline of feed pressure for the membrane system. Water pumped to the treatment plant typically has a pressure of 45 psi at the treatment plant entrance (Malone, 2013). Some pressure is lost in the 5 μ m prefilters before the membrane feed pumps boost the feed pressure high enough to achieve 80% recovery in the nanofiltration system (see Section 3.2.2).

Relevant well field operational data are summarized in Table 6. Pumps are submerged in the well at a given ‘pump depth’, and when pumps are not in operation, the water rises to the ‘static water level’. When wells are turned on, a cone of depression forms around the pump, lowering the level of water in the well to the ‘pumping water level’ which corresponds to the head required to lift water to the surface and is expressed in Table 6 as head and pressure (e.g., ‘depth (pressure)’). Well pumps provide head to lift water to the surface, plus a residual pressure of 45 psi entering the treatment plant. Summing the pressure heads for lifting the water (i.e., ‘pumping water

level') and residual mechanical pressure (i.e., pressure at membrane feed pump'), the total head delivered by the Castle Hayne well field pumps is 61.3-66.4 psi and the corresponding head delivered by the Peedee well field pumps is 62.7-72.0 psi.

Table 6. Well field operational data for the Castle Hayne and Peedee aquifers (Malone, 2013). Pump depth, static water level, and pumping water level ranges were provided through personal communication with the treatment plant (Malone, 2013). Pressure at the membrane feed pump was determined from SCADA data, and total head delivered by the well pump was calculated as the sum of pressure head needed to lift water to the surface (pumping water level) and pressure at the membrane feed pump.

	Castle Hayne Well Field	Peedee Well Field
Pump depth in well	60 ft	100 ft
Static water level (feet)	18 - 23	40-45
Pumping water level	42 – 45 ft (18.2 - 19.5 psi)	45 - 60 ft (19.5-26.0 psi)
Pressure at membrane feed pump	45.0 +/- 1.91 psi	45.0 +/- 1.85 psi
Total head delivered by well pump	61.3 – 66.4 psi	62.7 – 72.9 psi

3.10.3. Modeling Membrane Feed Pump Performance

To determine the cost of operating a membrane feed pump at varying degrees of fouling, we must know the power delivered by the pump, the pump efficiency, and the efficiency of the electric motor driving the pump. The power delivered by a pump is calculated as described by Munson et al. (2005)

$$P_D = Q\rho gh , \quad (6)$$

where the power delivered, P_D , is the product of Q , the volumetric flow rate, ρ , the density of the fluid, g , gravitational acceleration, and h , the pressure head delivered by the pump.

To calculate the electrical power consumed by the motor, P_C , the power delivered by the pump, P_D , is divided by the mechanical efficiency of the pump, η_p , and the efficiency of the electric motor, η_m , as expressed by Munson et al. (2005)

$$P_C = \frac{P_D}{\eta_p \eta_m} . \quad (7)$$

The motors that drive the membrane feed pumps are manufactured by U.S. motors and deliver 125 HP at 1785 RPM, and operate using 460 volt, 3-phase, 60 Hertz electricity (Malone, 2013). Efficiency of the motor could not be determined during operation, and thus a constant efficiency of 95% was assumed.

We used pump curve information obtained from the manufacturer (Afton Pumps, Houston, TX) for the individual pumps installed in the Peedee treatment train (Malone, 2013) to obtain the pump efficiency (η_p) values required to calculate the power consumed by the motors. The pumps used in the treatment plant were performance tested prior to delivery. Figure 48 shows mechanical pump efficiency (η_p) as a function of the fraction of maximum motor speed (i.e., fraction of 1785 RPM). While pumping in both systems is equally efficient at full motor speed, the Castle Hayne system has a lower efficiency at all other motor speeds, thus requiring more power than the Peedee system.

We evaluated the accuracy of the η_p values obtained in Figure 48 by comparing in Figure 49 the total dynamic head (TDH) values obtained with the same model to the corresponding values observed in the treatment plant. Observed TDH was calculated using data gathered by the SCADA system (Malone, 2013). SCADA measures fraction of motor speed (i.e., the input for the model), and also pressure of plant influent, headloss across the membrane prefilters, and membrane feed pressure. Observed TDH was calculated as the sum of membrane feed pressure and headloss across the prefilters minus pressure of plant influent. Modeled TDH values as a function of the fraction of maximum motor speed are presented in Figure 48. From this plot, we see that increasing motor speed increases feed pressure up to approximately 120 psi and 140 psi for the Castle Hayne and Peedee systems, respectively. The reason the same pump model in the Castle Hayne system has a lower modeled pressure than a Peedee pump at the same motor speed is that the flow rate delivered by the Castle Hayne pump (1,300 GPM) is greater than the flow rate delivered by the Peedee pump (1,040 GPM). Figure 49 shows that the model underestimates the power delivered by the Castle Hayne pumps and overestimates by the power delivered by the Peedee pumps. However, this discrepancy is relatively minor and gave us confidence that modeled η_p and TDH were descriptive of the actual η_p and TDH in the system.

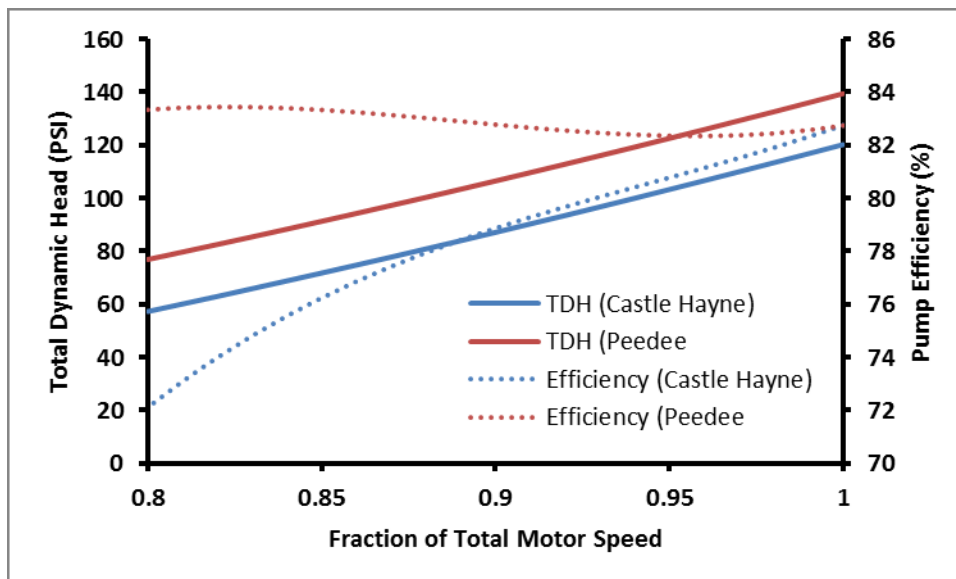


Figure 48. Modeled total dynamic head and pump efficiency as a function of fraction of total motor speed.

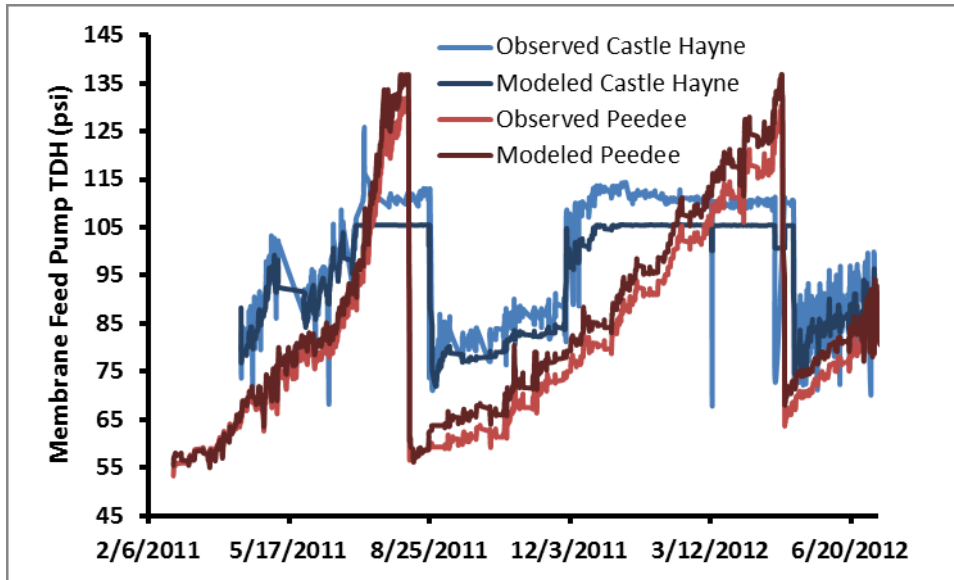


Figure 50. Comparison of observed and modeled pump total dynamic head (TDH) delivered by the Castle Hayne and Peedee membrane feed pumps over time.

The power consumed by the membrane feed pumps was modeled using Equation 7. Results are shown in Figure 50. Power consumption by the Peedee membrane pumps increased from 32.7 kW after cleaning to a maximum of 79.1 kW when fouling was most severe, while power consumption by the Castle Hayne membrane pumps increased from 56.1 kW to 77.5 kW during fouling events. Even after cleaning, the Castle Hayne treatment train is operated at a higher pressure than the Peedee (see Figures 12 and 50) because the Castle Hayne system has TFC-ULP membranes in its first stage, which are less productive than TFC-S which is in the first stage of the Peedee. This difference in feed pressure leads to nearly double the power consumption (32.7 vs. 56.1 kW) due to differences in mechanical efficiency (see Figure 48).

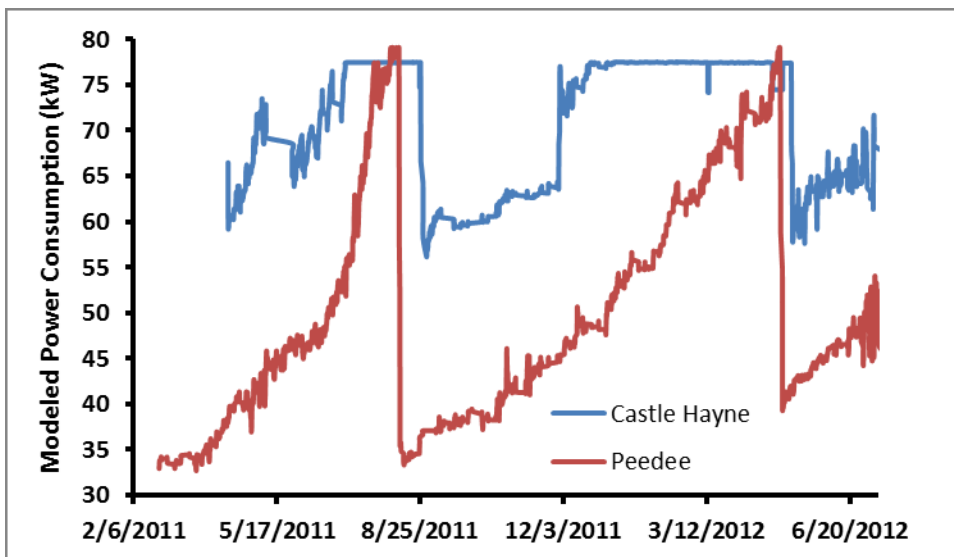


Figure 50. Modeled power consumption by the Castle Hayne and Peedee feed pumps over time.

3.10.4. Estimating Savings in Energy Cost for Varying Cleaning Regimens

To determine energy savings with various cleaning regimens, we needed to determine the change in energy consumption and multiply it by the price of electricity. Taking the average of on-peak and off-peak energy cost at the treatment plant in June and July of 2012 (Malone, 2013) resulted in a price of \$0.046/kWh, which was used to estimate cost savings. For the purpose of this analysis, it was assumed that successive cleanings are equally effective at returning treatment trains to their previous level of performance. SCADA results were gathered at one-hour time steps, and differences in power usage (kW) were multiplied by this time step to get energy consumption (kWh) for the base cleaning scenario (i.e., the actual scenario used in the treatment plant) and other scenarios that assumed more frequent cleaning.

The Castle Hayne system frequently encounters periods of rapid fouling, where feed pressure increases significantly in a very short period of time. As shown in Figure 51 in the baseline scenario, one hour after system startup on the morning of November 30, 2011, feed pressure increased from 130 to 150 psi within a one hour period and did not decrease until cleaning in May of 2012. Figure 51 shows modeled power consumption for a period of eight months for the observed baseline scenario (i.e., no cleaning events), and a scenario with more frequent cleaning (i.e., two cleaning events occurring after a time period equal to the onset of rapid fouling in the baseline scenario). For the scenario with more frequent cleaning events, it was assumed that fouling would progress at the same rate observed in the treatment plant before the rapid fouling event of November, 2011. Compared to the baseline scenario, the scenario with increased cleaning frequency reduced the average energy use over the 8-month time period studied in Figure 51 from 71.7 ± 7.6 kW to 61.1 ± 7.7 kW. Cleaning resulted in an overall energy savings of 18,300 kWh, equivalent to an energy cost savings of \$841.

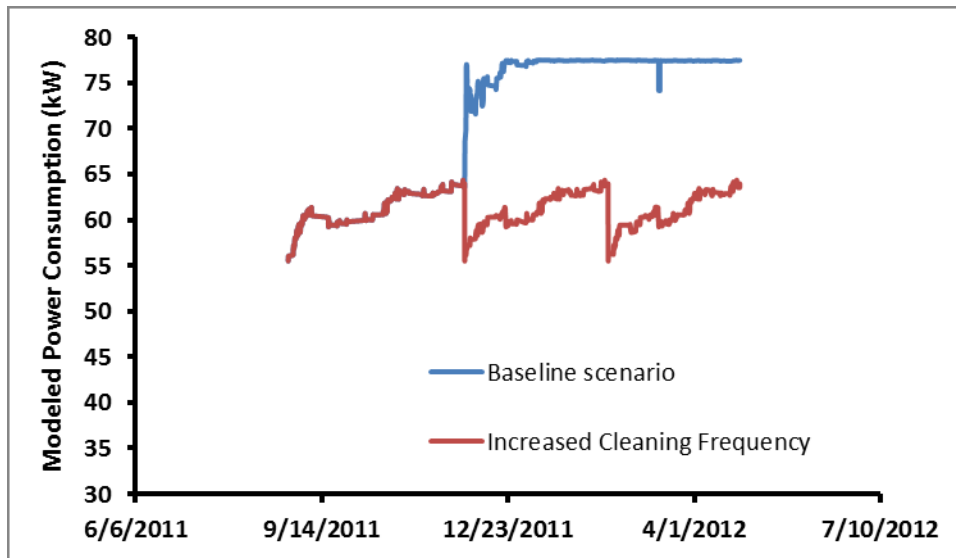


Figure 51. Comparison of modeled power consumption in the Castle Hayne treatment train for the baseline scenario observed at the treatment plant and a scenario with more frequent cleaning.

A similar approach was taken in modeling energy savings for the Peedee treatment train. Since there were no periods of rapid fouling in the Peedee treatment train like those observed in the Castle Hayne system, a different set of cleaning criteria were needed. Typically, nanofiltration

membranes are cleaned following a 10-30% decrease in flux (Shafer et al., 2006). Thus, we modeled power consumption assuming cleanings after 10%, 20%, and 30% increases in feed pressure as shown in Figure 52. Cleaning reduced the average energy consumption from 54.0 ± 13.4 kW in the baseline scenario to 38.1 ± 2.3 kW, 39.9 ± 3.6 kW, and 42.2 ± 5.0 kW for the three cleaning scenarios. These reduced power consumptions correspond to energy cost savings of \$1,238, \$1,103, and \$922 for cleanings following an increase in feed pressure of 10%, 20%, and 30%, respectively.

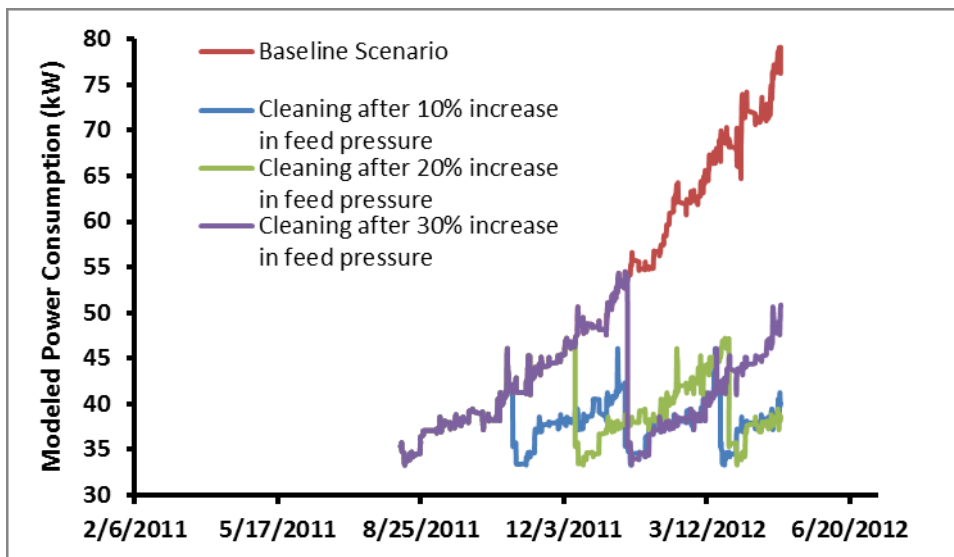


Figure 52. Comparison of modeled power consumption in the Peedee treatment train for the baseline scenario observed at the treatment plant and scenarios with cleaning events after a 10%, 20%, and 30% increase in feed pressure.

3.10.5. Comparing Cleaning Costs with Energy Savings

To determine the optimum cleaning frequency, cost of chemical cleanings (Section 3.10.1) were compared to energy savings from increased cleaning frequency (Section 3.10.4). Table 6 summarizes the costs and savings associated with increasing cleaning frequency. Cleaning with Lavasol 7 (\$1,638/cleaning) was much more expensive than cleaning with OptiClean F (\$717/cleaning). As a result, net savings from cleaning with OptiClean F were always greater than cleaning with Lavasol 7 as the two were assumed to be equally effective cleaning agents. The only cleaning scenario with positive net savings was cleaning of the Peedee treatment train after a 30% increase in feed pressure using OptiClean F. These results suggest that more frequent cleanings would generally cost more in labor and chemical costs than the associated savings in energy costs.

Table 6. Energy costs savings, cleaning costs, and net savings for different cleaning scenarios over the period between cleaning events.

	Castle Hayne - Immediately After Rapid Fouling	Peedee - 10% Feed Pressure Increase	Peedee - 20% Feed Pressure Increase	Peedee - 30% Feed Pressure Increase
Energy Savings	\$840.80	\$1,238.45	\$1,102.53	\$921.81
Number of Cleanings	2	3	2	1
Days Between Cleaning Events	95	78	122	159
OptiClean F Total Cleaning Costs	\$1,434.00	\$2,151.00	\$1,434.00	\$717.00
Lavasol 7 Total Cleaning Costs	\$3,276.00	\$4,914.00	\$3,276.00	\$1,638.00
Net savings from OptiClean F Cleaning	-\$593.20	-\$912.55	-\$331.47	\$204.81
Net savings from Lavasol 7 Cleaning	-\$2,435.20	-\$3,675.55	-\$2,173.47	-\$716.19

4. Discussion

4.1. Identification of Membrane Foulants

Five membrane characterization techniques – SEM, XPS, EDX, ATR-FTIR, and RBS – were used to identify membrane foulants in the sections and figures described below:

- SEM: Section 3.4.1, Figures 15-19
- XPS: Section 3.4.2, Figure 20
- EDX: Section 3.4.3, Figure 21
- ATR-FTIR: Section 3.4.4, Figure 22
- RBS: Section 3.4.5, Figures 23 and 24

Membrane cleaning solutions were also analyzed to determine the concentrations of extracted inorganic foulants and organic matter as shown in Section 3.4.6, Figures 25 and 26. Of the characterization techniques listed above, XPS, EDX, and extraction analysis can quantify the elemental composition and/or concentrations of foulants in the fouling layers. Table 7 shows elements ranked by decreasing order of concentration as obtained for XPS, EDX, and foulant extraction analyses. From these results, it was evident that XPS and EDX yield similar results regarding the relative concentration of foulant elements. However, the absolute concentrations of foulants were much lower for EDX than for XPS because EDX penetrates a few microns (Greenlee et al., 2009) into the sample, therefore characterizing a larger portion of the membrane itself together with the fouling layer, while XPS only penetrates a few nanometers thus characterizing mainly the fouling layer (Shafer et al., 2006).

Table 7. Ranking in order of decreasing concentrations in the fouling layers of foulant elements as determined by XPS, EDX, and foulant extraction analyses.

	XPS	EDX*	Foulant Extraction**
Castle Hayne 1 st Stage	O>Si>Al>Ca>Fe>S	O>Si>Al>Ca>Fe	Si>Ca>OM>Fe>Al
Castle Hayne 2 nd Stage	O>>Ca>>Si>Fe>Al>S	O>Ca>Fe>Si>Al	Si>Ca>OM>Fe>Al
Peedee 1 st Stage	O>Ca>Si>Al>S>Fe	O>Ca>Si>Al> Fe	Si>Ca>Al>OM>Fe
Peedee 2 nd Stage	O>Si>Ca>Al>Fe>S	O>Ca>Si>Al>Fe	Si>Ca>Al>OM>Fe

*EDX cannot be used to determine the presence of sulfur in the fouling layer, as it penetrates into the polysulfone support and signal from the support cannot be separated from the signal from the foulant layer.

**Foulant extractions cannot measure the presence of oxygen; magnesium results excluded; OM indicates organic matter.

Extraction with sodium hydroxide may underestimate organic fouling, because increasing pH alone may not remove organic matter as well as solutions that include a chelating agent such as EDTA (Ang et al. 2006; Hong and Elimelech, 1997). However, organic matter extracted from the membrane surface could not be accurately quantified in cleaning solutions containing EDTA because EDTA is itself an organic molecule. For example, STPP+EDTA contained 0.8 percent EDTA, or 8,000 mg/L EDTA, which is orders of magnitude larger than the organic matter concentration in the cleaning solution due to membrane foulants (~12 mg/L of DOC in the most concentrated sample extracted with NaOH at pH=11).

ATR-FTIR spectra of fouled elements yielded absorbance peaks at specific wave numbers characteristic of certain bond types (see Figure 22). All fouled samples had an absorbance peak around 1440 m^{-1} , which is characteristic of calcium carbonate (Stein, 2012). The Castle Hayne first stage had absorbance peaks characteristic of Si-O, Si-O-Si, and Si-O-Al bonds. When considered together, these bonds may represent kaolinite, a clay that could have been deposited in colloidal form or precipitated on the membrane surface. These bonds could also be characteristic of other aluminum and silicate colloids. Spectra for fouled elements from the Castle Hayne first stage contained an array of absorbance peaks from a heterogeneous fouling layer which complicate foulant identification. The other three fouled membranes tested contained prominent peaks that could not be linked to specific molecules containing the elements identified by EDX and XPS.

Individual elements present in fouling layers were also identified by RBS. From Figure 24, we determined that the Peedee first stage and second stage fouling layers had thicknesses of less than 200 nm and 300 nm, respectively. The Peedee first stage fouling layer had a relatively high calcium content. The Peedee second stage had three distinct layers, the top layer (<40nm) having a relatively high iron content, and the bottom two layers having a mixture of carbon, oxygen, silicon, aluminum, calcium, and iron. The two Castle Hayne fouling layers are thicker than $2\text{ }\mu\text{m}$ (see Figures 23 and 24). The Castle Hayne second stage fouling layer contains more iron, calcium, and carbon than the fouling layer of the first stage. The Castle Hayne first stage fouling layer has a thin surface layer rich in silicon less than 300-nm thick atop a thick fouling sublayer.

Compared to other polyvalent cations, calcium and aluminum were poorly rejected in the full-scale system (see Table 4). One potential explanation for poor aluminum and calcium rejection is concentration polarization, but concentration polarization alone would have also resulted in similarly poor rejection of other dissolved constituents. Another explanation could be that calcium and aluminum are preferentially present in the fouling layer at the membrane surface. This hypothesis is supported by the observed presence of aluminum, calcium, and silicon in the fouling layers of all membranes tested (see Section 3.4), and is consistent with studies reporting that calcium acts as an intermolecular bridge between nanofiltration membrane surfaces and organic matter (Li and Elimelech, 2004).

Based on the numerous methods used to characterize the membrane fouling layers, we determined that all fouling layers contain iron, aluminum, silicon, calcium, oxygen, and carbon. Organic foulants were detectable in all membranes, but were present in higher concentrations in the Castle Hayne fouled elements than in the Peedee fouled elements. Significant calcium and silicon concentrations were observed in all fouled membranes, possibly indicating silicate and calcium carbonate fouling.

4.2. Potential Removal of Membrane Foulants by Prefiltration

Membrane foulants consisted of a variety of inorganic constituents and organic matter as was discussed in Section 4.1. Prefiltration methods included the treatment plant's existing $5\text{-}\mu\text{m}$ filtration as well as $1.2\text{ }\mu\text{m}$, $0.1\text{ }\mu\text{m}$, and 100 kDa filtration which simulated sand filtration,

microfiltration, and ultrafiltration, respectively. Prefiltration results shown in Section 3.1 indicate that prefiltration removed over 99% of turbidity in Castle Hayne water, and 42-97% (depending on the filter used) in Peedee water (see Table 3). Prefiltration also reduced SDI in both samples. Although prefiltration reduced both turbidity and SDI, the values measured in the source waters were already below the values specified by the manufacturer as the maximum limits that waters should have to be apt to serve as influent to the membrane elements (Koch, 2010a and 2010b).

Of the dissolved ions tested, only aluminum was reduced by at least 20% by prefiltration; this relatively significant aluminum removal may indicate that the aluminum present is colloidal in nature. The other ions tested were not significantly reduced by prefiltration, and neither was the concentration of DOC. This includes calcium, silicon, and iron, which are key inorganic foulants found in the fouling layers, as discussed in Section 4.1.

The inability of sand filtration, microfiltration, and ultrafiltration to remove the dissolved constituents that make up the fouling layers suggests that improving water quality of the membrane feed via pretreatment by prefiltration methods would not significantly reduce the membrane fouling potential of the feed waters.

4.3. Preventing Full-Scale Membrane Fouling

Given that prefiltration was ineffective at removing membrane foulants as described in Section 4.2, other methods for preventing membrane fouling should be considered. Two methods to prevent the formation of membrane foulants are pH control and the addition of an antiscalant. At the treatment plant, Castle Hayne feed water is adjusted to a pH of approximately 6.0 before treatment to prevent the precipitation of inorganic foulants. The pH of Peedee feed water is also adjusted to a value of 6.67. Both the Castle Hayne and Peedee treatment trains use an antiscalant as well.

Silicon was an important membrane foulant identified in all four-fouled membranes tested (see Figures 20, 21, and 26). In the bench-scale fouled membrane, silicon was the predominant membrane foulant and could not be efficiently removed by any of the cleaning agents tested (see Figure 27). Given the silicon concentrations in the influent Castle Hayne and Peedee waters, solubility limit analyses in the membrane concentrate waters indicate that fouling by silicates potentially occurs in both the Castle Hayne and Peedee membranes. Silicate solubility at the temperature (13°C) of influent waters to the membrane stages is approximately 100 mg/L as SiO₂ at pH=7.0 (FILMTEC, 2013). At the pH conditions of the Castle Hayne (pH≈5.99) and Peedee (pH≈6.7) waters in the membrane stages (see Table 2), silicate solubility increases to 112 and 106 mg/L as silicate for Castle Hayne water and Peedee water, respectively. Influent silicon concentrations in the Castle Hayne and Peedee waters were found to be 8.0±8.8 mg/L as Si and 5.9±7.1 mg/L as Si, respectively (see Table 2). Using the 95% upper confidence level of silicon solubility limits for Castle Hayne (16.8 mg/L as Si) and Peedee (13 mg/L as Si) waters, we converted these values to 36.0 mg/L as SiO₂ and 27.8 mg/L as SiO₂, respectively. Given 80% recovery in the system (see Figures 9 and 10), silicate concentrations could potentially increase in the membrane feed channel to 180 mg/L as SiO₂ in the Castle Hayne treatment train and 139

mg/L as SiO₂ in the Peedee treatment train. Both values are above the solubility limit for silicates in their respective waters. Decreasing solution pH only increases silicate solubility by approximately 12% per pH unit (FILMTEC, 2013), thus silicate solubility would only be 136 mg/L at pH=4, making acidification of the feed solution impractical for controlling fouling by silicate. The potential problem of fouling by silicates is compounded by Luo and Wang's (2001) observation that precipitation of silicates also occurred at concentrations below saturation during high-pressure membrane filtration; Luo and Wang suggested catalysis by Al³⁺ and Fe³⁺ ions as the most probable cause. Given the challenges to control silicate solubility by pH adjustment and the possibility of silicate precipitation below saturation conditions, antiscalants are often used to control silicate fouling.

Antiscalants disrupt one or more of the stages of scale formation by (1) increasing the concentration of ions needed for clustering, (2) disrupting nuclei ordering or crystal structure, (3) repelling ions from crystal surfaces to prevent growth, or chelating dissolved ions (Greenlee et al., 2009). The CFPWA uses SpectraGuard™, produced by Professional Water Technologies™, which is supposed to control silica fouling. Although we were unable to test alternative antiscalants or dosing due to challenges recreating fouling in the laboratory (see Sections 3.5 and 4.8), we did see an increase in the presence of silicon in fouling layers when an antiscalant was not added in the laboratory (Figure 27). While we cannot categorically say that the antiscalant used by the treatment facility reduced silicate fouling, we observed significantly high silica concentrations in fouling layers generated in the laboratory when the antiscalant was not added.

4.4. Comparison of Dead-End and Cross-Flow Systems for Testing Membrane Performance and Cleaning Efficiency

4.4.1. Membrane Performance

Membrane water permeability and salt rejection were measured in both dead-end and cross-flow cells. Figure 13 in Section 3.3 shows the results for water permeability tests performed on fouled membranes using the two setups. These results demonstrate that the dead-end and cross-flow cells yield statistically equal values of water permeability, and therefore that water permeability measurements in dead-end configuration are representative of corresponding measurements in cross-flow configuration.

Figure 15 in Section 3.3 shows chloride rejection by fouled membranes using the dead-end and cross-flow configurations. Chloride rejections obtained with both configurations were statistically equal for Castle Hayne fouled membranes. By contrast, dead-end chloride rejections were lower than cross-flow chloride rejections for the Peedee fouled membranes by 8 percentage points and 29 percentage points for first stage membranes and second stage membranes, respectively. As discussed in Section 3.3, however, the membranes from the Peedee second stage were damaged and had a relatively high variability of performance properties with respect to membrane sampling location in the membrane element. Nevertheless, the chloride rejection difference of 8 percentage points obtained for the fouled membranes collected from the Peedee first stage indicate that dead-end chloride rejection may not be representative of cross-flow rejection. For treating freshwaters where the primary constituents of concern are iron and manganese,

differences in chloride rejection of a few percentage points between the two setups may not be as important as these differences would be for e.g. seawater applications.

4.4.2. Cleaning Efficiency

Water permeability was also tested after cleaning fouled membranes in the dead-end and cross-flow configurations to determine if the two cleaning procedures were similarly effective at recovering membrane performance. Figure 30 in Section 3.6 shows that water permeability measurements obtained after cleaning with STPP+EDTA in dead-end and cross-flow configurations were statistically equal. Figure 31 in Section 3.6 compares dead-end and cross-flow cleaning with citric acid. Citric acid cleanings were only performed once in the cross-flow system, but if we assume a standard error equal to that of STPP+EDTA cleaning for the Peedee second stage element (see Figure 30), then the two cleaning setups yield statistically equal permeability. The comparison of water permeability results between membranes cleaned in dead-end configuration and membranes cleaned in cross-flow configuration demonstrate that water permeability measurements in dead-end configuration are representative of corresponding measurements in cross-flow configuration.

While in principle cross-flow cleaning and performance testing is preferred over dead-end cleaning and testing because the cross-flow configuration better represents the fluid dynamics conditions existing in treatment plants, our results above indicate that the results obtained for cleaning efficiency and water permeability in dead-end configuration are representative of those obtained in cross-flow configuration. As a result, we conclude that – for fresh water applications – the dead-end configuration can be used to satisfactorily obtain performance properties of membrane samples and cleaning efficiency of cleaning solutions. Dead-end tests have the added benefit that they are less resource-intensive than cross-flow tests.

4.5. Evaluating Membrane Cleaning Solutions

To determine the effectiveness of membrane cleaning solutions, three factors were considered: foulant removal (Section 3.7), performance recovery (Section 3.8), and long-term effects on membrane longevity (Section 3.9). Performance recovery, specifically improving membrane water permeability while maintaining integrity to reject salts, is the objective of membrane cleaning. However, foulant removal and performance recovery must be considered in concert. For example, given the spatial variability of membrane performance and the uncertainty in cleaned element permeability, flux measurements alone may not fully explain cleaning behavior. Similarly, if flux increases but a portion of the fouling layer remains, fouling may occur more rapidly upon system startup after cleaning. Conversely, the presence of foulants may not severely decrease membrane performance, as was observed in the Castle Hayne and Peedee first stage elements. Longevity tests can then be used to determine the long-term effects of cleaning on membrane integrity.

In general, basic cleaners were found to remove foulants and recover flux better than acidic cleaning agents (Section 3.7 and 3.8). Specifically, Lavasol 7 and STPP+EDTA were found to be the most effective basic solutions from the perspective of foulant removal and flux recovery. For example, cleanings of the Castle Hayne second stage fouled element with Lavasol 7 at pH=11 and STPP+ EDTA increased permeability by 507% and 560%, respectively, compared to citric acid cleaning which increased permeability by 265% (Figure 43 in Section 3.8). Both Lavasol 7 and STPP+EDTA contain EDTA, a chelating agent which sequesters metal ions such as calcium and iron, reducing their interaction with the membrane surface and organic matter. EDTA removes free ions, and ions complexed with organic matter by ligand exchange reactions (Hong and Elimelech, 1997) which reduces intermolecular adhesion forces between organic molecules (Ang et al., 2006) and causes organic molecules to become charged and repel each other. This mechanism of EDTA action is relevant to the fouling layers of membranes treating Castle Hayne and Peedee waters as our results indicate that they contain organic matter and polyvalent cations such as calcium, aluminum and iron.

OptiClean F, which does not contain EDTA, was chosen to replace Lavasol 7 at the treatment plant given operational challenges and hazards to personnel from handling Lavasol 7. OptiClean F was shown to be less effective at removing foulants (Figures 40 and 41 in Section 3.7.6) and recovering membrane performance (Figures 43 and 45 in Section 3.8) than Lavasol 7. Lavasol 7 at pH=11 increased the water flux of Castle Hayne second stage and Peedee second stage fouled membranes by 507% and 48%, respectively, while OptiClean F at pH 11.0 increased fluxed by 283 and 18%, respectively. STPP+EDTA increased flux by 560% and 84% for the second stage elements of the Castle Hayne system and Peedee system, respectively, and could be considered as an alternative cleaning solution.

Membrane longevity tests shown in Section 3.9 demonstrate that prolonged exposure to cleaning solutions at a pH greater than 11.0 (Lavasol 7 and OptiClean F) increases membrane water permeability and decrease chloride rejection relative to cleaning agents with pH values lower than 11.0 (STPP+EDTA). After 14-16 hours of exposure to Lavasol 7 and OptiClean F, normalized water permeability increased by 17% and 12%, respectively, which were 34 and 19 percentage points higher than the deionized water control (see Figure 48). Chloride rejection decreased by 3.6 and 2.5 percentage points after 41-47 hours of exposure to Lavasol 7 and OptiClean F, respectively. These results indicate that cleaning solutions should be neutralized to 11.0 before cleaning to preserve long-term membrane performance. Longevity tests did not include physical cross-flow turbulence, which may influence the extent of damage from high pH solutions.

4.6. Optimizing Cleaning Frequency

Annual energy costs at the treatment facility were approximately \$1,300 per day during June and July of 2012, or an estimated annual cost of \$468,000 (see Section 3.10). Energy consumption increases as membranes foul due to increases in feed pressure required to maintain constant flux. Cleaning costs and modeled reductions in energy use following cleaning were compared for full-scale cleaning. Labor and chemical costs meant that frequent cleaning with either Lavasol 7 or

OptiClean F was more expensive than the corresponding savings in electricity costs (see Table 6). The only scenario where more frequent cleaning resulted in net cost savings was the cleaning of the Peedee treatment trains using OptiClean F after feed pressure was increased by 30% (Table 6), and this was assuming OptiClean F was similarly effective at performance recovery as Lavasol 7, which was shown not to be the case for Peedee second stage elements (Figure 45, Section 3.8).

Despite the fact that cleaning reduces energy consumption for the membrane feed pump by 14.8% for the Castle Hayne cleaning and by 21.9-29.4% for the Peedee cleanings, the total energy cost savings were relatively minor compared to the overall energy cost. One reason for the modest reductions in energy cost is that a large portion of the energy consumption is relatively fixed (i.e., it is not be impacted by membrane performance). As discussed in Section 3.10.2, pumping water to the treatment plant at a pressure of 45 psi accounts for 33% of overall electricity expenditures. Further, an average of 35% of the remaining 67% of energy costs were consumed by the laboratory and maintenance facilities in June/July of 2012. As a result, only 45% of the overall electricity demand occurs in the nanofiltration facility. Daily energy consumption at the nanofiltration facility is monitored by treatment plant personnel.

To improve the economic benefits of cleaning, less expensive basic cleaning solutions containing EDTA (see Section 4.5) might be found; however, increasing the frequency of cleanings does not seem to hold much potential for financial savings. Given the risks of membrane damage through greater exposure to cleaning chemicals (see Section 4.5), increasing cleaning frequency should be avoided unless cleaning solution pH is adjusted prior to cleaning.

4.7. Determining the Applicability of XPS and RBS for the Identification of Membrane Foulants

XPS is a technique commonly used in the characterization of unfouled membranes and RBS has been recently introduced for the same purpose. The use of XPS for characterization of fouling layers has been limited in the literature and RBS has not been used for fouling studies. Searching the database Web of Science in March 2013 with the keywords ‘XPS, FOULING, NANOFILTRATION, CHARACTERIZATION’ yielded eight results, only two of which included characterization of fouled membranes (Song et al., 2004; Mondal and Wickramasinghe, 2008). Of these two publications, one involved the filtration of produced waters generated during oil and gas production (Mondal and Wickramasinghe, 2008), and the other only measured carbon, oxygen, nitrogen and calcium, with calcium concentration being always below 1% (Song et al., 2004). A search for the keywords ‘RBS, FOULING, MEMBRANE’ yielded zero results.

Unfouled NF and RO membranes consist of a polyamide active layer 20-200 nm in thickness, a polysulfone support approximately 30-50 μm thick, and a polyester backing that is approximately 200 μm thick. XPS can only penetrate a few nanometers (Shafer et al., 2006), and thus will only provide information about the active layer. If a membrane fouling layer is more than a few nanometers thick, XPS will only characterize the surface of the fouling layer. If the

fouling layer is thinner than the depth of XPS penetration, XPS results will represent the combined signal coming from both the fouling layer and membrane active layer. EDX penetrates 1,000 times deeper than XPS, a few microns (Greenlee et al., 2009), characterizing the active layer and the polysulfone support in an unfouled membrane. For very thick fouling layers (i.e., tens of microns or more), EDX characterizes only the fouling layer. For fouling layers less than a few microns thick, EDX will characterize the fouling layer, the active layer, and the polysulfone support.

Although the concentrations of foulants obtained by XPS are much higher than those obtained by EDX (see Figures 20 and 21 in Sections 3.4.2 and 3.4.3), the two techniques yielded consistent information about the relative abundance of each element in fouled membranes (see Section 4.1). The observed difference in absolute foulant concentrations between the two techniques, coupled with higher concentrations of sulfur measured by EDX, suggests that the fouling layers are thinner than the depth of EDX penetration, i.e., less than a few microns.

While EDX appears to be a suitable characterization technique for thick fouling layers like that in the Castle Hayne first stage, XPS gives greater sensitivity to analyze thinner fouling layers, such as those from the Castle Hayne second stage and both Peedee stages. If EDX alone was used, we would conclude that the Castle Hayne first stage fouling layer included calcium and small concentrations of iron, the only significant inorganic foulant in the Peedee first and second stage was calcium (see Figure 21). By contrast, XPS (see Figure 20) shows that all four membrane foulant layers contain iron, calcium, silicon, aluminum, and sulfur, a much more diverse group of foulants than determined by EDX.

RBS is a technique recently introduced for the characterization of membranes (Mi et al., 2006) which has not previously been applied to fouled samples. RBS combines the relatively large analysis depth of EDX (i.e., into the polysulfone support) with sensitivity to low foulant concentrations similar to XPS, particularly for atoms with higher atomic weight. For example, Figure 24 (Section 3.4.5) contains the RBS spectra for the Peedee first stage fouled element. Both the sulfur plateau from the polysulfone support and the calcium foulant, which was barely detected by EDX analysis (see Figure 21), are evident in the fouled membrane spectrum, demonstrating simultaneous characterization of the inner membrane and a thin foulant layer. The presence of elemental signals, as peaks instead of as plateaus, also enables the identification of relatively thin fouling layers or sublayers within thick fouling layers as described in Section 3.4.5. Since the analysis depth of RBS is $\approx 2 \mu\text{m}$, then RBS is also well suited for characterization of thick fouling layers. RBS showed also utility for identifying elements that remained on the membrane surface after cleaning procedures (see Section 3.7.5) and that were not observed by XPS.

XPS and RBS allow for the characterization of thin fouling layers, which is important because the thickness of the fouling layer is not necessarily correlated with flux reduction. Consider the Castle Hayne first and second stage fouled elements. We established above that the first stage had a thicker fouling layer than the second stage. Normalized permeability in the first stage fouled element was 10-30% below the average normalized permeability of a new unfouled element (see Figure 42). The thinner second stage foulant had a normalized flux 80% below the normalized average permeability of a new unfouled element (Figure 43). Therefore, it is

important to characterize thin fouling layers, and XPS and RBS show more utility in the characterization of thin fouling layers than EDX.

4.8. Challenges in Replicating Full-Scale Fouling in Laboratory Cross-Flow Systems

As was shown in Section 3.5, attempts to recreate full-scale fouling in the laboratory resulted in a foulant layer unrepresentative of full-scale conditions. Laboratory fouling resulted in a foulant layer containing higher concentrations of silicon and lower concentrations of all other inorganic species than the full-scale fouled element (Figure 27). Reduction in the amount of iron present can be explained by the visible precipitation of iron following exposure to the atmosphere which resulted in a three orders of magnitude reduction in dissolved iron.

However, this finding does not explain the reductions in calcium, aluminum, or sulfur fouling. Reductions in calcium fouling could have been due to a reduction in the concentration of carbonate, as calcium carbonate is a common membrane foulant. The CFPUA plant adds sulfuric acid to reduce iron fouling and the formation of other inorganic precipitates. This acid addition influences carbonate speciation, protonating carbonate ions (CO_3^{2-}) to bicarbonate (HCO_3^-), and bicarbonate further to carbonic acid (H_2CO_3) which seeks equilibrium with dissolved carbon dioxide (CO_2) (Benjamin, 2002). Anoxic waters, such as the Castle Hayne and Peedee aquifers, have poor gas exchange with the atmosphere and may be supersaturated with carbon dioxide prior to extraction and subsequent acid addition. When samples were exposed to the atmosphere, carbon dioxide volatilized from solution, thus decreasing the total carbonate content in solution. The same process may have repeated when acid was added in the cross-flow system to maintain a constant pH, forcing carbonates out of the system, and potentially reducing calcium carbonate fouling.

It is unclear what the reasons are for the differences observed in fouling by other constituents, though the lack of antiscalant addition during laboratory cross-flow fouling tests most likely influenced the fouling layer properties. Antiscalants decay over time, and thus are added at a constant rate in once-through, full-scale systems. In recirculating laboratory systems, it is impractical to dose antiscalants to achieve a consistent concentration, and therefore antiscalants are not employed in laboratory fouling studies. Achieving consistent antiscalant concentrations would require an antiscalant dosing system controlled by online real-time monitoring of the antiscalant concentration. However, the continuous addition of antiscalant in a typical closed-loop laboratory membrane filtration system would result in the buildup of antiscalant degradation products in the feed water which is inconsistent with full-scale conditions.

Regardless of the explanation for differences in foulant layer composition, fouling experiments conducted in the laboratory were not representative of full-scale fouling. The fouling layer generated in the laboratory bench-scale system had a distinctly different elemental composition than the fouling layer in membranes fouled at the treatment plant. Additionally, bench-scale fouling was irreversible as opposed to full-scale fouling which was reversible. Accordingly, caution should be used when studying the fouling propensity of ground waters (e.g., Castle

Hayne and Peedee waters) in laboratory settings as laboratory tests may not recreate conditions encountered in full-scale systems.

4.9. Fluorescence Characterization of Organic Matter in Source Waters, Membrane Permeate Water, and Membrane Fouling Layers

DOC, UVA, and EEMs, as well as subsequently calculated fluorescence indicators (SUVA, Sr, and FI) were used to characterize organic matter in source waters, membrane permeate water, and membrane fouling layers. Water from the Castle Hayne aquifer contains almost twice the DOC and three times the SUVA of water from the Peedee aquifer (see Table 2). In addition to a higher SUVA, the Castle Hayne water also has a lower slope ratio than the Peedee water, indicating more hydrophobic, higher molecular weight organics that have a higher potential for organic fouling (see Table 2). However, organic matter extracted from the membrane fouling layers had lower SUVA and higher slope ratio than organics in the source waters. Her et al. (2010) also observed similar SUVA tendencies between organics in feed waters and fouling layers. The results thus indicate that fouling layers preferentially contain lower molecular weight, more hydrophilic organic matter. These findings are consistent with fouling layers comprised of organic matter organic matter stabilized by calcium, which cleaning solutions containing EDTA are particularly effective at reversing, as explained in Section 4.5.

Rejection of DOC, UV absorbent organic matter (UVA), and fluorescent organic matter were 99% or greater for both stages of the Castle Hayne treatment train when operated at full scale (see Table 4). Rejection of organics was lower in the Peedee aquifer (58-99%) (Table 4). The lower rejection of organics by the membranes in the Peedee stages, and the higher slope ratio for organics in the Peedee source water than for organics in the Castle Hayne feed water (Table 2), indicate that organic matter from the Peedee water is smaller in size than organic matter from the Castle Hayne aquifer, and thus more membrane permeable.

5. Summary

Membrane foulants were identified for membranes treating water from the Castle Hayne and Peedee aquifers. Castle Hayne foulants include calcium, silicon, aluminum, and iron, while Peedee foulants contain primarily silicon, calcium, and aluminum. Castle Hayne fouling layers contained more organic matter than Peedee fouling layers. Prefiltrations were performed to simulate sand filtration, microfiltration, and ultrafiltration. All prefiltration methods tested removed particulate matter, which did not appear to contribute to membrane fouling, but were ineffective at removing dissolved constituents that contributed to fouling.

The Castle Hayne second stage element had the lowest flux of any of the membranes sampled, and thus was the most severely fouled. Membrane cleaning and performance testing was performed in dead-end and cross-flow setups, both of which yielded similar results. Although many cleaning solutions were tested, basic cleaning agents containing EDTA, specifically Lavasol 7 and STPP+EDTA, were the most effective at reversing membrane fouling. STPP+EDTA was shown to cause less long-term change in membrane performance than Lavasol 7, as determined by water permeability and chloride rejection. Lavasol 7 and OptiClean F were shown to increase membrane permeability and decrease salt rejection after prolonged exposure to cleaning solutions at pH values more basic than the limits recommended by the manufacturer.

Our results showed that characterization techniques commonly used to characterize membrane foulants, ATR-FTIR and EDX, had limitations when characterizing membrane fouling layers composed of multiple foulants and thin fouling layers, respectively. We showed that XPS can be used to characterize thin fouling layers and RBS has utility for identifying depth heterogeneous fouling layers. EDX lacks the depth resolution that XPS provides to characterize thin fouling layers; the depth of analysis of RBS allows for the characterization of foulant layers more than a few nanometers thick, which is not possible with XPS.

Laboratory bench-scale fouling tests using feed waters resulted in fouling layers vastly different in composition and susceptibility to cleaning than corresponding full-scale fouling layers. These results indicate that recreating full-scale fouling for academic or design purposes using recirculating systems may not be appropriate for ground waters such as the coastal North Carolina waters tested in this study. We also determined that laboratory fouling tests in the absence of an antiscalant produced irreversible silicate fouling. To prevent fouling, decreasing pH by addition of sulfuric acid may reduce precipitate fouling caused by calcium, iron, and silicates. The use of different antiscalants may also minimize fouling; however, we were unable to test the effect of antiscalant addition in the laboratory.

6. Conclusions

Based on the experimental results in Section 3 and the discussion in Section 4, we were able to conclude the following:

- 1) Prefiltrations simulating sand filtration, microfiltration, and ultrafiltration were ineffective at removing source water constituents that contribute to fouling.
- 2) Basic cleaning agents containing EDTA, specifically Lavasol 7 and STPP+EDTA, were the most effective at reversing membrane fouling.
- 3) Prolonged exposure to chemical cleaning solutions with a pH higher than the manufacturer's cleaning guidelines results in increased water permeability and decreased chloride rejection.
- 4) XPS provides greater sensitivity for thin fouling layers than EDX, and RBS allows for the characterization of depth heterogeneous fouling layers.
- 5) Dead-end membrane performance testing and cleaning was representative of cross-flow testing and cleaning for the fouled membranes tested here.
- 6) The most severe fouling from the perspective of flux decrease was observed in elements collected from the Castle Hayne second stage.
- 7) The main foulants in the Castle Hayne aquifer are calcium, silicon, aluminum, and iron. The Peedee foulants contain primarily silicon, calcium, and aluminum. Organic matter was detected in foulants from all membranes, but concentrations were higher in the Castle Hayne fouling layers than in the Peedee fouling layers.
- 8) Attempts to recreate full-scale fouling in the laboratory produced fouling layers vastly different in composition and susceptibility to cleaning than full-scale fouling layers. Similar challenges might be faced by others in the field trying to test the fouling propensity of the Castle Hayne and Peedee waters (or other ground waters) for academic or design purposes.
- 9) Laboratory fouling experiments conducted in the absence of an antiscalant produced irreversible fouling.

7. Recommendations

Based on the experiments and analysis contained within this report, we recommend:

- 1) Further pH reduction by increased sulfuric acid addition to membrane feed waters may be considered to reduce calcium, iron, and silicate fouling; however, analysis of the potential for precipitation of sulfates (e.g., barium sulfate) must be performed.
- 2) Basic cleaning solutions containing EDTA, such as Lavasol 7 or STPP+EDTA should be used for membrane cleaning.
- 3) The pH of cleaning solutions should be adjusted to or below the maximum pH recommended by the membrane manufacturer to minimize membrane deterioration.
- 4) Scientists and engineers looking to test a wide range of cleaning solutions should determine if dead-end cleanings are representative of cross-flow cleanings for the specific foulant layers of concern. (For this study, both configurations proved to produced similar results)
- 5) An antiscalant effective at preventing silica fouling should be used when treating waters from the Castle Hayne and Peedee aquifers by nanofiltration or reverse osmosis.
- 6) The analysis of the elemental composition of fouling layers on membrane samples should be performed with XPS and/or RBS (as opposed to EDX) when one desires to maximize the accuracy in the identification of the elements that constitute the fouling layer, particularly when fouling layers are thin.
- 7) Caution should be used when extrapolating bench-scale fouling results to full-scale system performance. Bench-scale fouling experiments can result in fouling layers that are dissimilar in composition and susceptibility to cleaning from fouling layers in full-scale fouled membranes.

References

- Al-Amoudi, A.; Lovitt, R.W. (2007). Fouling strategies and the cleaning system of NF membranes and factors affecting cleaning efficiency. *Journal of Membrane Science*, 303, 4-28.
- American Public Health Association (APHA); American Water Works Association (AWWA); Water Environment Federation (WEF). (2006). *Standard Methods for the Examination of Water and Wastewater*; 18 ed.; American Public Health Association: Washington, D.C.
- Amy, G. (2008). Fundamental understanding of organic matter fouling of membranes. *Desalination*, 231(1-3), 44-51.
- Ang, W., Lee, S., Elimelech, M. (2006). Chemical and physical aspects of cleaning of organic-fouled reverse osmosis membranes. *Journal of Membrane Science*, 272, 198-210.
- ASTM Standard D4189, 1995 (2002), "Silt Density Index (SDI) of Water," ASTM International, West Conshohocken, PA, 2002.
- Attayek, P.J.; Meyer, E.S.; Lin, L.; Rich, G.C.; Clegg, T.B.; Coronell, O. (2012). A remotely-controlled, semi-automatic target system for Rutherford backscattering spectrometry and elastic recoiled detection analyses of polymeric membrane samples. *Nuclear Instruments and Methods in Physics A.*, 676, 21-25.
- Benjamin, M. M. (2002). *Water Chemistry*. Long Grove, IL: Waveland Press, Inc.
- Cho, J., Amy, G., Pellegrino, J., Yoon, Y. (1998). Characterization of clean and natural organic matter (NOM) fouled NF and UF membranes, and foulants characterization. *Desalination*, 118, 101-108.
- Contreras, A.E.; Kim, A.; Li, Q. (2005). Combined fouling of nanofiltration membranes: Mechanisms and effect of organic matter. *Journal of Membrane Science*, 327, 87-95.
- Division of Water Resources (DWR), *Currituck County outer banks water supply study*. 1991, North Carolina Department of Environment and Natural Resources (NCDENR): Raleigh, NC.
- Division of Water Resources (DWR), *Central Coastal Plain capacity use area assessment report*. 2008a, North Carolina Department of Environment and Natural Resources (NCDENR): Raleigh, NC.
- Division of Water Resources (DWR), *North Carolina ground water resources monitoring well network 2008 annual report*. 2008b, North Carolina Department of Environment and Natural Resources (NCDENR): Raleigh, NC.

- Division of Water Resources (DWR), *North Carolina ground water resources monitoring well network 2009 annual report*. 2009, North Carolina Department of Environment and Natural Resources (NCDENR): Raleigh, NC.
- Division of Water Resources (DWR), *Proposed Bladen County capacity use investigation scope of work and timeline for completion*. 2002, North Carolina Department of Environment and Natural Resources (NCDENR): Raleigh, NC.
- Division of Water Resources (DWR), *State Water Supply Plain*. 2001. North Carolina Department of Environment and Natural Resources (NCDENR): Raleigh, NC.
- FILMTEC Membranes – Dow Chemical. *Water Chemistry and Pretreatment: Silica Scale Prevention* [Technical Manual]. Available at http://www.dowwaterandprocess.com/support_training/literature_manuals/filmtec_manual.htm (Accessed March 2013).
- Koch Membrane Systems. 2010a. *Fluid Systems TFC-S 8" Elements-Data Sheet*.
- Koch Membrane Systems. 2010b. *Fluid Systems TFC-ULP 8" Elements-Data Sheet*.
- Furukawa, R., *Personal communication*. 2012, Professional Water Treatment Chemicals.
- Gabelich, C. J., Chen, W. R., Yun, T. I., Coffey, B. M., Suffet, I. H. (2005). The role of dissolved aluminum in silica chemistry for membrane processes. *Desalination*, 180, 307-319.
- Greenlee, L., Lawler, D. F., Freeman, B. D., Marrot, B., Moulin, P. (2009). Reverse osmosis desalination: Water sources, technology, and today's challenges. *Water Research*, 43, 2317-2348.
- Helms, J. R., Stubbins, A., Ritchie, J. D., Minor, E. C., Kieber, D. J., & Mopper, K. (2008). Absorption spectral slopes and slope ratios as indicators of molecular weight, source, and photobleaching of chromophoric dissolved organic matter. *Limnology and Oceanography*, 53(3), 955-969.
- Her, N., Amy, G., & Jarusutthirak, C. (2000). Seasonal variations of nanofiltration (NF) foulants: identification and control. *Desalination*, 132(1-3), 143-160.
- Her, N., Amy, G., Plottu-Pecheux, A., Yoon, Y. (2010). Identification of nanofiltration membrane foulants. *Water Research*, 41, 3936-3947.
- Hong, S.; Elimelech, M. (1997). Chemical and physical aspects of natural organic matter (NOM) fouling of nanofiltration membranes. *Journal of Membrane Science*, 132, 159-181.

- Ivnitsky, H., I. Katz, D. Minz, E. Shimoni, Y. Chen, J. Tarchitzky, R. Semiat, C.G. Dosoretz. (2005). Characterization of membrane biofouling in nanofiltration processes of wastewater treatment. *Desalination*, 185(2005) 255-268.
- Jarusutthirak, C., Mattaraj, S., Jiratananon, R. (2007). Influence of inorganic scalants and natural organic matter on nanofiltration membrane fouling. *Journal of Membrane Science*, 287, 138-145.
- Kim, A.S.; Contreras, A.E.; Li, Q.; Yuan, R. (2010). Fundamental mechanisms of three-component combined fouling with experimental verification. *Langmuir*, 25, 7815-7827.
- Kavitha, a L., Vasudevan, T., & Prabu, H. G. (2011). Evaluation of synthesized antiscalants for cooling water system application. *Desalination*, 268(1-3), 38-45.
- Kumar, M., S. S. Adham, & Pearce, W. R. (2006). Investigation of seawater reverse osmosis fouling and its relationship to pretreatment type. *Environmental Science & Technology* 40(6), 2037-2044.
- Law, C.M.C.; Li, X.-Y.; Li, Q. (2010). The combined colloid-organic fouling on nanofiltration membrane for wastewater treatment and reuse. *Separation Science Technology*, 45, 935-940.
- Lee, S.; Cho, J.; Elimelech, M. (2005). Combined influence of natural organic matter (NOM) and colloidal particles on nanofiltration membrane fouling. *Journal of Membrane Science*, 262, 27-41.
- Li, Q. and Elimelech, M. (2004). Organic fouling and chemical cleaning of a nanofiltration membranes: measurements and mechanisms. *Environmental Science and Technology*, 38(17) 4683-4693.
- Luo, M. & Wang, Z. (2001). Complex fouling and cleaning-in-place of a reverse osmosis desalination system. *Desalination*, 141(1) 15-22.
- Malone, J.; Colon, A., *Personal communication*. 2010, North Carolina Cape Fear Public Utility Authority.
- Malone, J.; Colon, A., *Personal communication*. 2011, North Carolina Cape Fear Public Utility Authority.
- Malone, J.; Colon, A., *Personal communication*. 2012, North Carolina Cape Fear Public Utility Authority.
- Malone, J.; Colon, A., *Personal communication*. 2013, North Carolina Cape Fear Public Utility Authority.

- McKnight, D. M., Boyer, E. W., Westerhoff, P. K., Doran, P. T., Kulbe, T., Andersen, D. T. (2001). Spectrofluorometric Characterization of Dissolved Organic Matter for Indication of Precursor Organic Material and Aromaticity. *Limnology and Oceanography*, 46(1), 38-48.
- Membrane Systems Inc. Operations and Maintenance Manual for the Membrane Filtration System for the Water Treatment Plant and Maintenance Facility of New Hanover County Water and Sewer District. Received from John Malone, Cape Fear Public Utility Authority, 2011.
- Mi, B.; Coronell, O.; Mariñas, B.J.; Watanabe, F.; Cahill, D.G. (2006) Petrov, I. Physico-chemical characterization of NF/RO membrane active layers by Rutherford backscattering spectrometry. *Journal of Membrane Science*, 282, 71-81.
- Mulder, M. *Principles of Membrane Technology*; Second ed.; Kluwer Academic: Boston, MA, 1996.
- Munson, B. R., Young, D. F., Okiishi. (2005). *Fundamentals of Fluid Mechanics*. Hoboken, NJ: John Wiley and Sons.
- Mondal, S., Wickramasinghe, S. R. (2008). Produced water treatment by nanofiltration and reverse osmosis. *Journal of Membrane Science*, 322, 162-170.
- MWH Global; Crittenden, J. C., Trussell, R. R., Hand, D. W., Howe, K. J., Tchobanoglous, G. (2005). *Water Treatment: Principles and Design*. Hoboken, NJ: John Wiley & Sons, Inc.
- Nitto Denko – Hydranautics. (2011). *Foulants and Cleaning Procedures for composite polyamide RO Membrane Elements* [White Paper].
- North Carolina Department of Environment and Natural Resources (NCDENR) - What is Ground Water? Available at http://www.ncwater.org/Education_and_Technical_Assistance/Ground_Water/What/. (Accessed July 16, 2010a).
- North Carolina Division of Environment and Natural Resources - North Carolina Aquifers. Available at http://www.ncwater.org/Education_and_Technical_Assistance/Ground_Water/AquiferCharacteristics/. (Accessed July 16, 2010b).
- Peiris, R. H, Halle, C., Budman, H., Moresoli, C., Peldszus, S., Huck, P. M., Legge, R. L. (2010). Identifying fouling events in a membrane-based drinking water treatment process using principal component analysis of fluorescence excitation-emission matrices. *Water Research*, 44, 185-194.

- Pullin, M. J., Anthony, C., & Maurice, P. A. (2007). Effects of Iron on the Molecular Weight Distribution, Light Absorption, and Fluorescence Properties of Natural Organic Matter. *Environmental Engineering Science*, 24(8), 987-997.
- Russell, D., *Personal communication*. 2012, Professional Water Treatment Chemicals.
- Saikia, B. J. and Parthasarathy, G., (2010). Fourier transform infrared spectroscopic characterization of kaolinite from Assam and Meghalaya, Northeastern India. *Journal of Modern Physics*, (1) 206-210.
- Schafer, A. L., Fane, A. G., & Waite, T.D. (2006). *Nanofiltration: Principles and Applications*. Oxford, UK: Elsevier Advanced Technology.
- Song, W., Ravindran, V., Koel, B., Pirbazari, M. (2004). Nanofiltration of natural organic matter with H₂O₂/UV pretreatment: fouling mitigation and membrane surface characterization. *Journal of Membrane Science*, 241, 143-160.
- Stein, S. E., "Infrared Spectra" in NIST Chemistry WebBook, NIST Standard Reference Database Number 69, Eds. P.J. Linstrom and W.G. Mallard, National Institute of Standards and Technology, Gaithersburg MD, 20899, <http://webbook.nist.gov>, (retrieved June 1, 2012).
- Tang, C. Y.; Kwon, Y.-N.; Leckie, J. O., Effect of membrane chemistry and coating layer on physiochemical properties of thin film composite polyamide RO and NF membranes I. FTIR and XPS characterization of polyamide and coating layer chemistry. *Desalination* **2009**, 242, 149-167.
- United States Environmental Protection Agency, Office of Water. *Membrane Filtration Guidance Manual*, 2005.
- US Environmental Protection Agency (USEPA), *National Primary Drinking Water Regulations: Arsenic and clarifications to compliance and new source contaminants monitoring; Final Rule*. 2001, Federal Register. p. 6975-7066.
- US Environmental Protection Agency (USEPA), *National Primary Drinking Water Regulations: Long Term 2 Enhanced Surface Water Treatment Rule; Proposed Rule*. 1993, Federal Register. p. 47640-47795.
- US Environmental Protection Agency (USEPA), *National Primary Drinking Water Regulations: Stage 2 Disinfectants and Disinfection Byproducts Rule; Final Rule*. 2006, Federal Register. p. 388-493.
- Vaculikova, L., E. Plevova, S. Vallova, I. Koutnik. (2011). Characterization and differentiation of kaolinites from selected Czech deposits using infrared spectroscopy and differential thermal analysis. *Acta Geodyn. Geomater.*, 8(161) 59-67.

Weishaar, J. L., Fram, M. S., Fujii, R., Mopper, K., & Aiken, G. R. (2003). Evaluation of Specific Ultraviolet Absorbance as an Indicator of the Chemical Composition and Reactivity of Dissolved Organic Carbon. *Environmental Science & Technology*, 37(20), 4702-4708.

Yoon, J., Yoon, Y., Amy, G., & Her, N. (2005). Determination of Perchlorate Rejection and Associated Inorganic Fouling (Scaling) for Reverse Osmosis and Nanofiltration Membranes under Various Operating Conditions. *Journal of Environmental Engineering*, 131(5), 726-733.

Appendix 1: Abbreviations and Units

$\mu\text{S}/\text{cm}$ – Microsiemens per centimeter: Unit of resistance used in measuring conductivity (i.e., higher resistance, lower conductivity).

μm – Micrometers

ATR-FTIR – Attenuated Total Reflectance Fourier Transform Infrared Spectroscopy

CFPUA – Cape Fear Public Utility Authority

CHS1 – Castle Hayne Stage 1, referring to the lead element collected from the first stage of the Castle Hayne system

CHS2 – Castle Hayne Stage 2, referring to the tail element collected from the first stage of the Castle Hayne system

PDS1 – Peedee Stage 1, referring to the lead element collected from the first stage of the Peedee system

PDS2 – Peedee Stage 2, referring to the tail element collected from the first stage of the Peedee system

DC – Direct current

DOC – Dissolved organic carbon: Mass concentration of organic carbon that passes a $0.45\ \mu\text{m}$ filter (see TOC).

EDTA – Ethylene diaminetetraacetic acid

EDX – Energy-Dispersive X-Ray Spectroscopy

EEMs – Excitation-emission matrices

FI – Fluorescence index

GPM – Gallons per minute

HP – Horsepower

ICP-MS – Inductively coupled plasma mass spectroscopy

kDa – Kilodalton. A unit of molecular weight, one Dalton is the average mass of one proton or neutron.

KOH – Potassium hydroxide

kV – Kilovolt (1,000 volts)

kW – Kilowatt; one thousand watts; a standard unit of power

kWh – Kilowatt hour; power consumption of one thousand watts for a period of one hour; a standard unit of energy

mg/L – Milligrams per liter (parts per million, by mass)

nA – Nanoampere (one one-billionth of an ampere)

NaOH – Sodium hydroxide

NOM – Natural organic matter

NTU – Nephelometric turbidity unit: a measure of light-scattering particles in a sample.

psi – Pounds per square inch

RPM – Revolutions per minute

SCADA – Supervisory control and data acquisition

SDI – Silt density index

SDS – Sodium dodecyl sulfate

SEM – Scanning Electron Microscopy

STPP – Sodium tripolyphosphate

SUVA – Specific Ultraviolet Absorbance: ultraviolet absorbance (see UVA) divided by DOC.

TDH – Total dynamic head, expressed as height or pressure

TOC – Total organic carbon: Mass concentration of organic (i.e., cannot be removed by pH adjustment) combustible carbon.

TUNL – Triangle Universities Nuclear Laboratory, located on the Duke University campus.

UVA – Ultraviolet absorbance: absorbance of ultraviolet light with a wavelength of 254 nm.

XPS – X-Ray Photoelectron Spectroscopy

Appendix 2: Publications, Patents, Technology Transfer and Others

A2.1. Publications and Presentations

This research will become the Master's Technical Report of the graduate research assistant who completed the project, and will be submitted to scholarly journals for publication.

A portion of these results have been presented at the 2012 and 2013 North Carolina WRI Annual Conference and NCWRA symposium as cited below. These results will have also been submitted to the 2013 American Water Works Association Water Quality and Technology Conference.

Gorzalski, A.; Coronell, O. Identification of membrane foulants for NF and RO membranes treating groundwaters from the Castle Hayne and Peedee Aquifers. Presented at the 2012 WRI Annual Conference and NCWRA Symposium, North Carolina State University, March 28, 2012.

Gorzalski, A.; Coronell, O. Identification of Foulants and Optimum Cleaning Strategies for Nanofiltration and Reverse Osmosis Membranes Treating Groundwaters of Coastal North Carolina. Presented at the 2013 WRI Annual Conference and NCWRA Symposium, North Carolina State University, March 20, 2013.

A2.2. Patents, Data Sets, or Web Sites

No patents, data sets, or web sites to date.

A2.3. Technology Transfer

As a result of the execution of this project, there is ongoing communication with the supervisor and operator of the groundwater nanofiltration CFPWA treatment plant. Results and recommendations will also be shared with the plant personnel.

The graduate research assistant who completed the project received an Impact Award from the University of North Carolina's Graduate Education Advancement Board, which recognizes outstanding graduate research of particular benefit to the citizens of North Carolina. The graduate research assistant will showcase his research to state legislators and the campus community at the Graduate School's Student Recognition Celebration on April 10, 2013.

Appendix 3: Particle Size Distributions

Figures A3-1 and A3-2 show particle size distributions for filtered water samples from the Castle Hayne and Peedee waters, respectively. From these figures, it is evident that 1.2 μm filters have limited effect on the average particle size, indicating that most of the particulate matter entering the plant is less than 1.2 μm in diameter. Filters with 0.1 μm nominal diameter decreased the average particle size noticeably, and 100 kDa filtration reduced average particle diameter below the lower detection limit (i.e., a few nanometers) of the instrument.

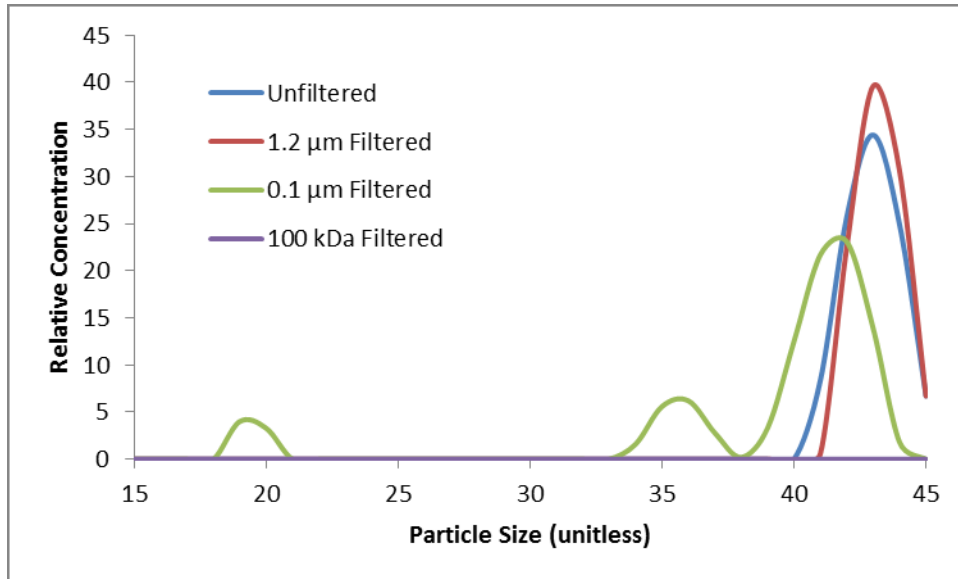


Figure A3-1. Particle size distributions for unfiltered and filtered water samples collected from the Castle Hayne aquifer.

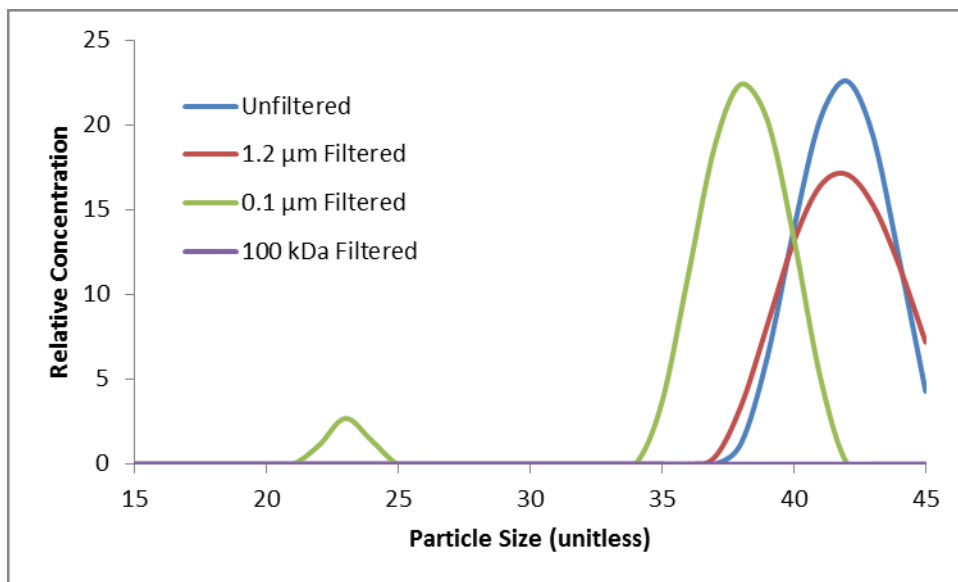


Figure A3-1. Particle size distributions for unfiltered and filtered water samples collected from the Peedee aquifer.

Appendix 4: Effect of Dissolved Iron on Fluorescence Measurements

To determine the influence of dissolved iron on fluorescence parameters, dissolved iron concentrations in unfiltered Castle Hayne and Peedee waters were doubled with a concentrated ferric chloride solution. Procedures for stock solution preparation and addition was similar to Pullin et al. (2007). Dissolved iron concentrations in samples collected on February 10, 2012 were 5.53 and 0.23 mg/L in the Castle Hayne and Peedee unfiltered waters, respectively. Iron concentrations were then increased to 11.06 mg/L in the Castle Hayne water and 0.46 mg/L in the Peedee water. Organic parameters, with the exception of DOC, were then measured and summarized in Table A4-1.

Table A4-1. Fluorescence parameters for unfiltered water from the Castle Hayne and Peedee waters with and without iron addition.

	Castle Hayne - no iron added	Castle Hayne - iron doubled	Peedee - no iron added	Peedee - iron doubled
UV254 (1/m)	14.7	16.5	14.1	15.1
Slope ratio	0.90	0.84	0.82	0.80
Fluorescence index	1.574	1.604	1.548	1.546
Peak C2:C1	0.098	0.089	0.113	0.110
Peak C3:C1	0.345	0.299	0.333	0.330

Table A4-1 shows that dissolved iron increases UV absorbance, and that this effect was stronger in Castle Hayne water which had a significantly higher iron concentration. Since UV absorbance at 254 nm increased but the DOC remained constant (i.e., no organic matter was added), then SUVA values also increased. Dissolved iron had a greater effect on fluorescence parameters in the Castle Hayne water than in the Peedee water. Both C2:C1 and C3:C1 peak ratios decreased, and the fluorescence intensity of peaks C1, C2, and C3 decreased by 19.3%, 8.7%, and 13.3%, respectively, in the Castle Hayne sample. This demonstrates that the impact of iron on fluorescence is non-uniform across the excitation-emission spectrum tested. Therefore, effects of dissolved iron on UV absorbance and fluorescence will be noted; however, attempts to decouple the influence of iron on measured parameters will be avoided.

Ionic strength and pH strongly influence UV absorbance and NOM fluorescence. Sample pH was measured before and after iron addition, and iron addition was found to have a negligible effect on pH. To prevent sample contamination via sorption/desorption of organic matter on the pH probe, samples used to measure pH were prepared in duplicate and used solely for that purpose. Given the high concentration of dissolved salts in both samples, iron addition increased ionic strength by 1.1%. Therefore, we can infer that changes in fluorescence were due to dissolved iron, and not potential changes in pH or ionic strength. Although not considered here, the addition of antiscalants can also affect UV absorption spectrum of iron (Kavita et al., 2011).

Appendix 5: Performance of Elements Collected from the Peedee Second Stage Cleaned with STPP+EDTA

Significant differences in permeability and conductivity rejection were observed between Peedee stage 2 elements cleaned in the dead-end apparatus and elements cleaned in the cross-flow system. Elements cleaned in the cross-flow system were then cut and retested in the dead-end apparatus. Results of these measurements are shown in Figure A5-1. Permeability results were very similar when tested in the dead-end cell. However, measurements of chloride rejection were reduced in the dead-end apparatus compared with the cross-flow system, yet significantly higher than measurements of dead-end cleaned samples. This demonstrates that a large portion of the discrepancy between Peedee stage 2 dead-end and cross-flow chloride rejection can be attributed to sample differences rather than differences in the two setups. These results support observations shown in Section 3.3 that both setups are comparable for measuring permeability, but that chloride rejection may be underestimated by the dead-end apparatus.

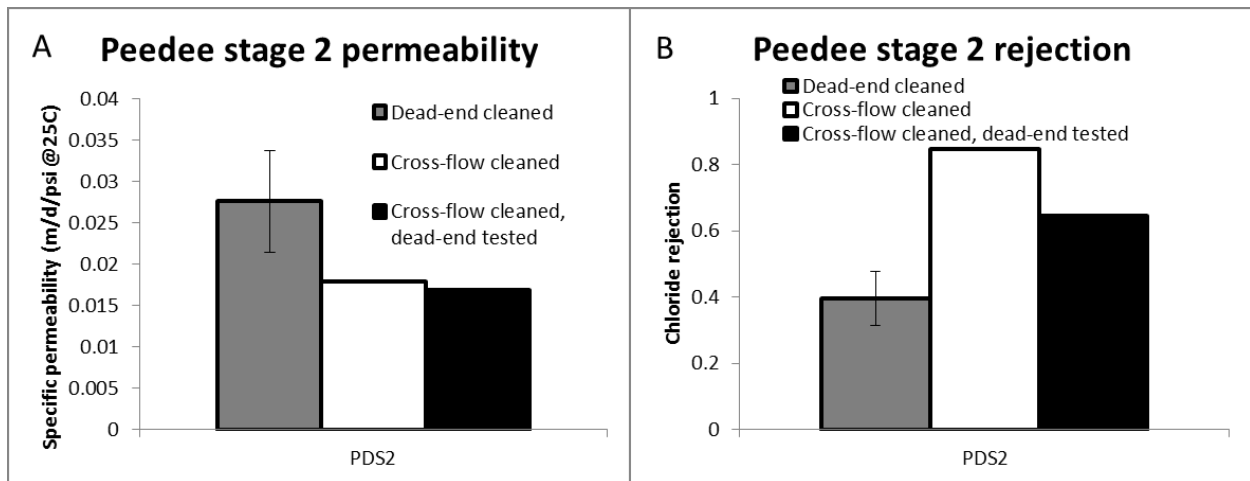


Figure A5-1. (A) Specific permeability and (B) chloride rejection of Peedee Stage 2 elements cleaned with STPP+EDTA. 'Cross-flow cleaned' and 'cross-flow cleaned, dead-end tested' measurements were taken from the same sample.

Appendix 6: Additional SEM Images of Fouled Membranes

While Figures 16-20 in Section 3.4.1 show SEM images taken perpendicular to the active layer surface, Figure A6-1 shows images taken from a grazing angle with respect to the membrane surface. Panel A shows a cross-section of an unfouled TFC-ULP membrane, including the polyester backing (at right), dense polysulfone support (center/left), and the active layer is the thin white edge of the image, which can be seen in higher resolution in Panel B. Panels C-F further demonstrate that each of the four fouling layers are unique in morphology.

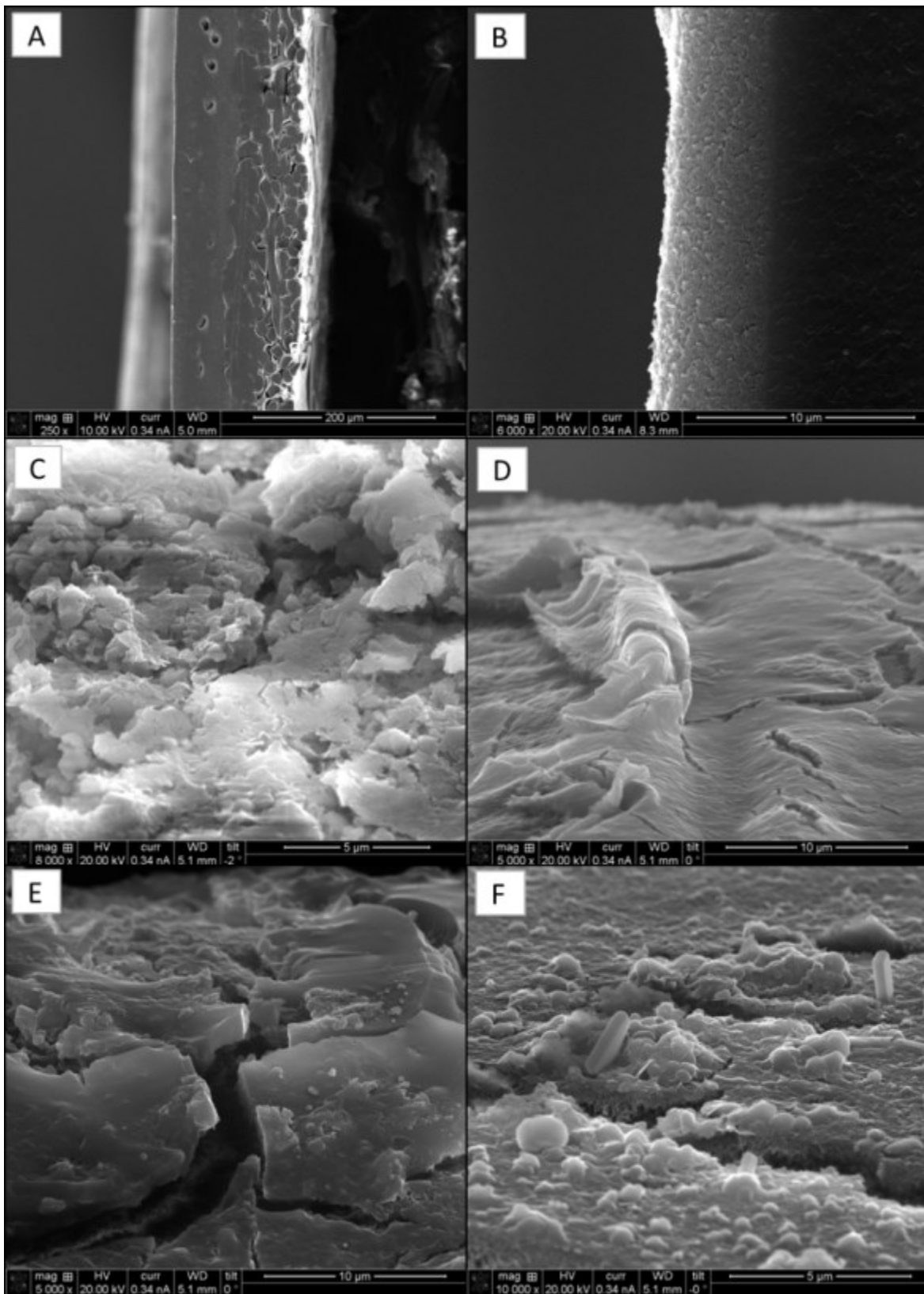


Figure A6-1. SEM images of an unfouled TFC-ULP membrane (A and B) and fouled (C) Castle Hayne stage 1, (D) Peedee stage 1, (E) Castle Hayne stage 2, and (F) Peedee stage 2 fouled membranes.

Appendix 7: Comparing EDX Results for Two Regions of the Same Sample

Figure A7-1 shows EDX results for two different regions of the fouling layer shown by SEM in Figure 20 (Section 3.4.1). The two fouling layers have different EDX spectra (Panels B and D), from which considerably different elemental composition was calculated (Panels E and F). The precipitate region indicated in Panel A is composed primarily of calcium and oxygen, while the region indicated in Panel C had a spectrum more similar to that of an unfouled membrane (see Figure 23 in Section 3.4.3). The elemental compositions determined by EDX for both fouled regions were significantly different from the compositions determined by XPS. XPS detected silicon, aluminum, and iron whereas EDX did not. This suggests that the fouled region in Panel C may be thin, and that XPS can characterize thin fouling layers better than EDX.

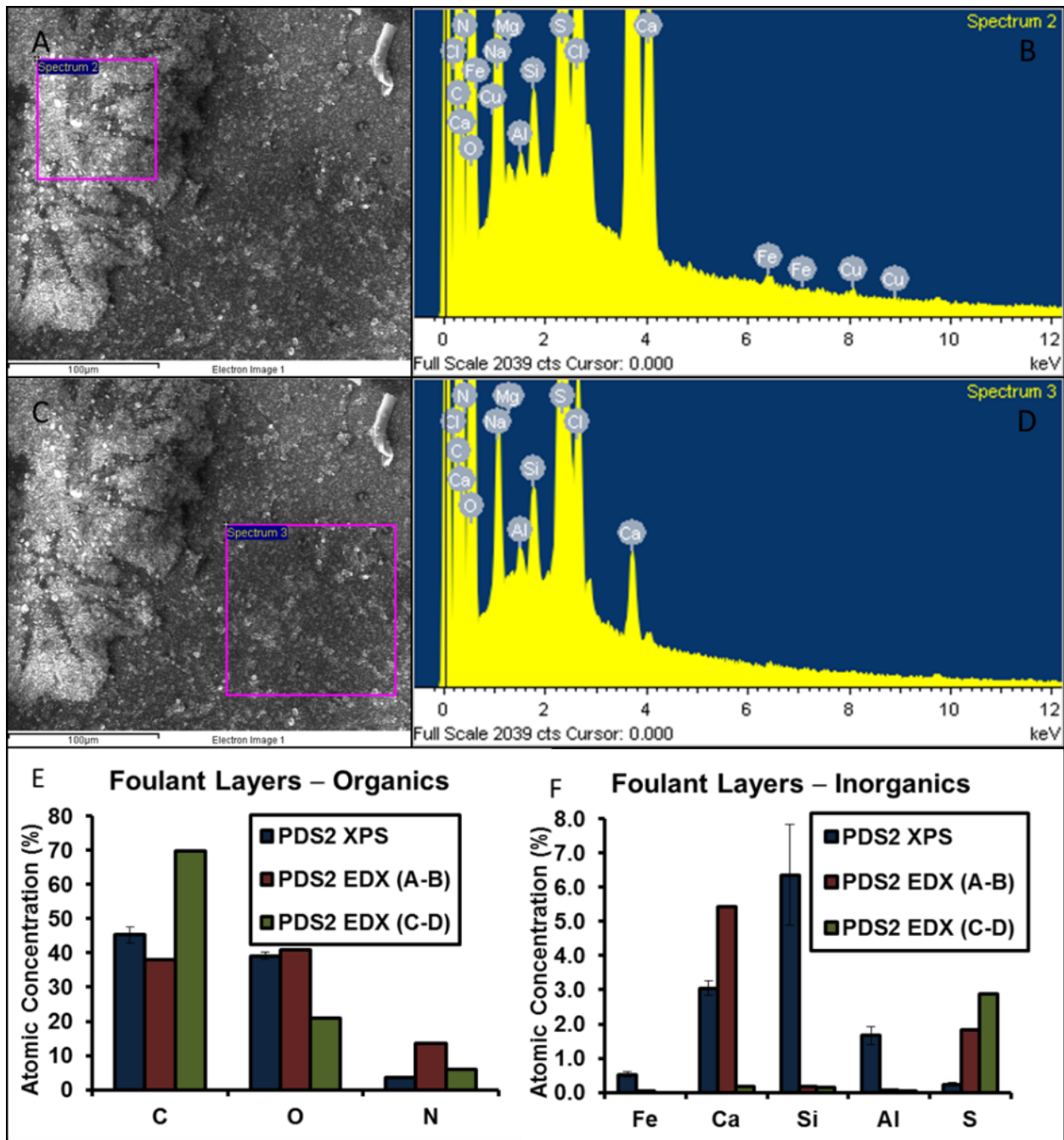


Figure A7-1. SEM images with regions of EDX analysis and corresponding EDX spectra for (A-B) a raised textured precipitate and (C-D) a relatively flat fouling region covering the surface of a fouled membrane from the Peedee second stage. EDX spectra were used to calculate atomic concentrations for comparison to XPS results for (E) organic and (F) inorganic foulants. Although sodium, chloride, copper, and magnesium appear in one or both spectra (B and D), these elements were removed from analysis and the other elemental concentrations recalculated for consistency with XPS results.

Appendix 8: Choosing a Clean Membrane Baseline – Comparison of TFC-ULP and TFC-S Elements

TFC-S membranes were unavailable from the manufacturer, and therefore characterization data for unfouled TFC-S membrane was obtained from unpublished data previously obtained by the PI. Figure A8-1 shows a comparison between the ATR-FTIR spectra obtained in this study for the TFC-ULP membrane and from previously obtained unpublished data for the TFC-S membrane. As shown in the figure, ATR-FTIR data for the TFC-S membrane were gathered for a more limited range of wavenumbers than for the TFC-ULP membrane. This limited range excluded the most prominent peak in the TFC-ULP membrane. However, the rest of the spectra matched closely. For this reason, ATR-FTIR spectra from TFC-ULP membranes were used as a clean membrane baseline for all fouled membranes tested. Similarly, RBS spectra for TFC-ULP and TFC-S membranes were collected using separate instruments (see Figure A8-2) with different energy resolutions; however, the general shape and height of the peaks corresponding to the main constituent elements (i.e., carbon, nitrogen, oxygen and sulfur) were similar. As a result, TFC-ULP membranes were used as the clean membrane baseline in the analyses of RBS results.

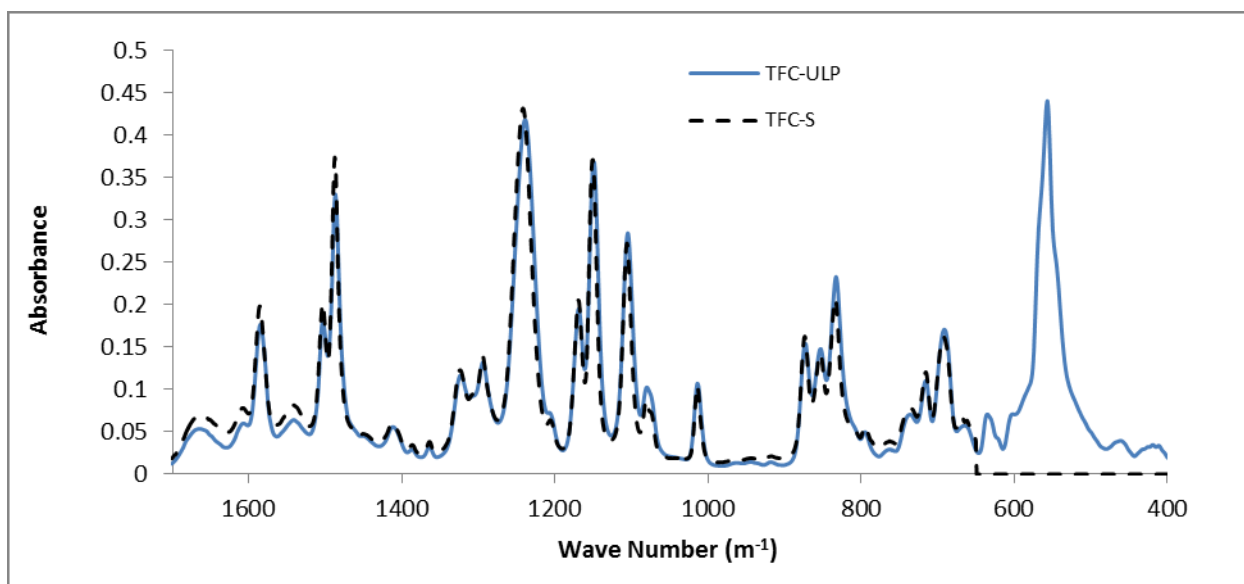


Figure A8-1. ATR-FTIR spectra for TFC-ULP membranes analyzed during this project, and for TFC-S membranes available from previously obtained unpublished data.

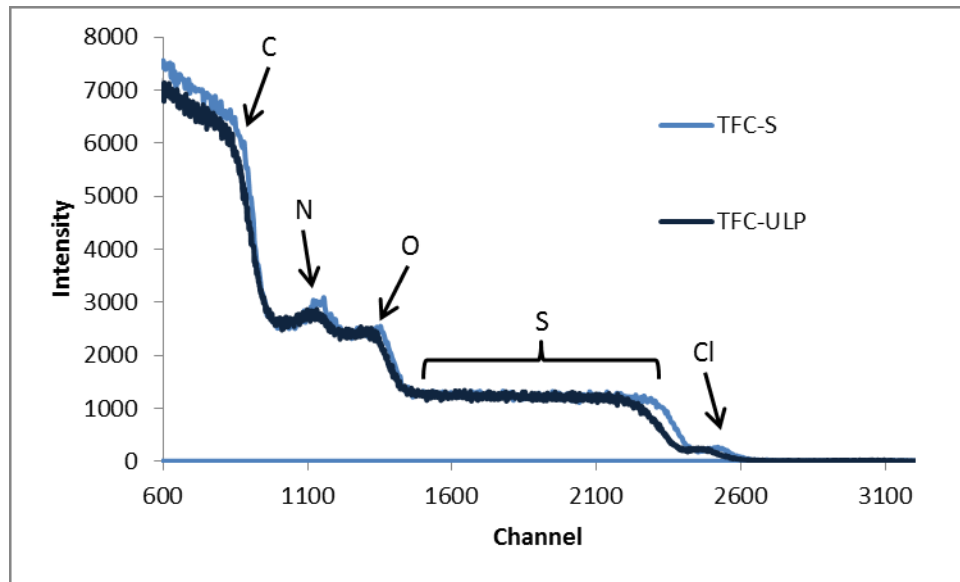


Figure A8-2. RBS spectra for TFC-ULP membranes analyzed during this project, and for TFC-S membranes available from previously obtained unpublished data.

Appendix 9: Individual RBS Spectra

Individual RBS spectra for unfouled TFC-ULP and TFC-S membranes are shown in Figures A9-1 and A9-2, respectively. Carbon, nitrogen, and oxygen peaks, as well as the characteristic sulfur plateau resulting from the polysulfone support layer, can be seen. RBS spectra for the four fouled membranes are shown in Figures A9-3 to A9-6. The location of aluminum, silicon, calcium, and iron peaks have been highlighted in these figures. While the results in this appendix show results for individual spectra for a single sample, the results in Sections 3.4.5. and 3.7.5. are composites of multiple spectra collected from multiple samples.

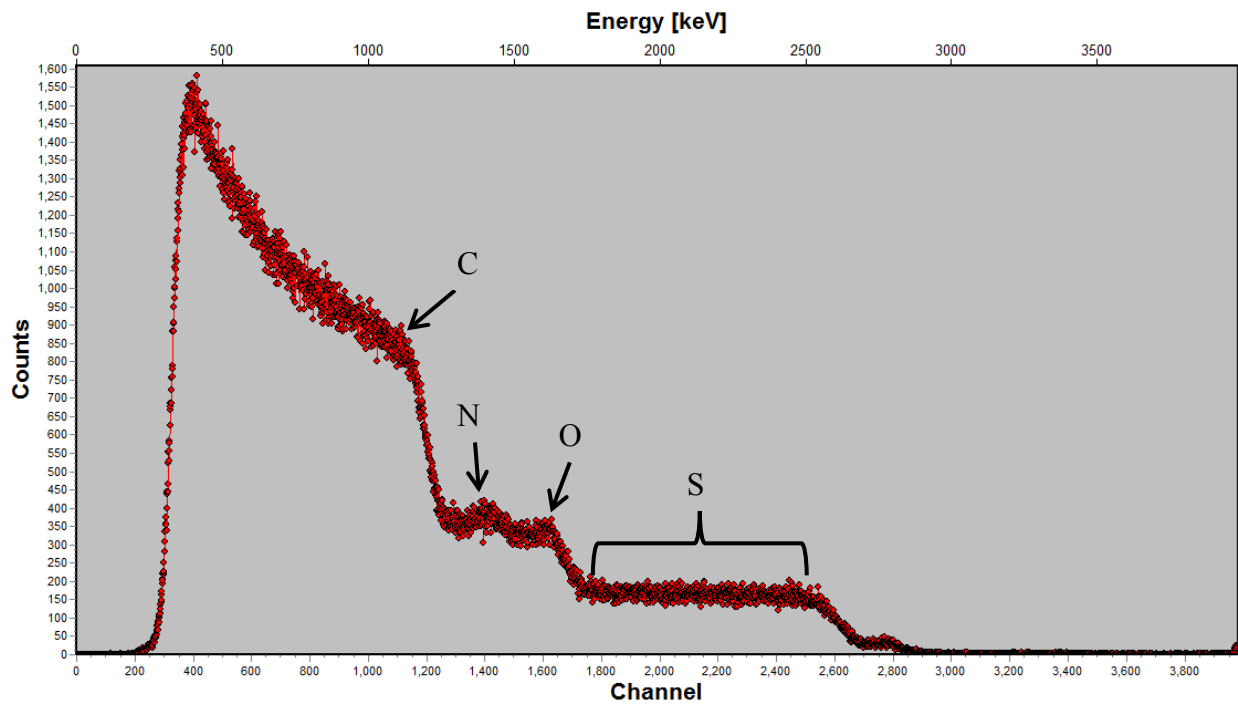


Figure A9-1. RBS spectrum for an unfouled TFC-ULP membrane.

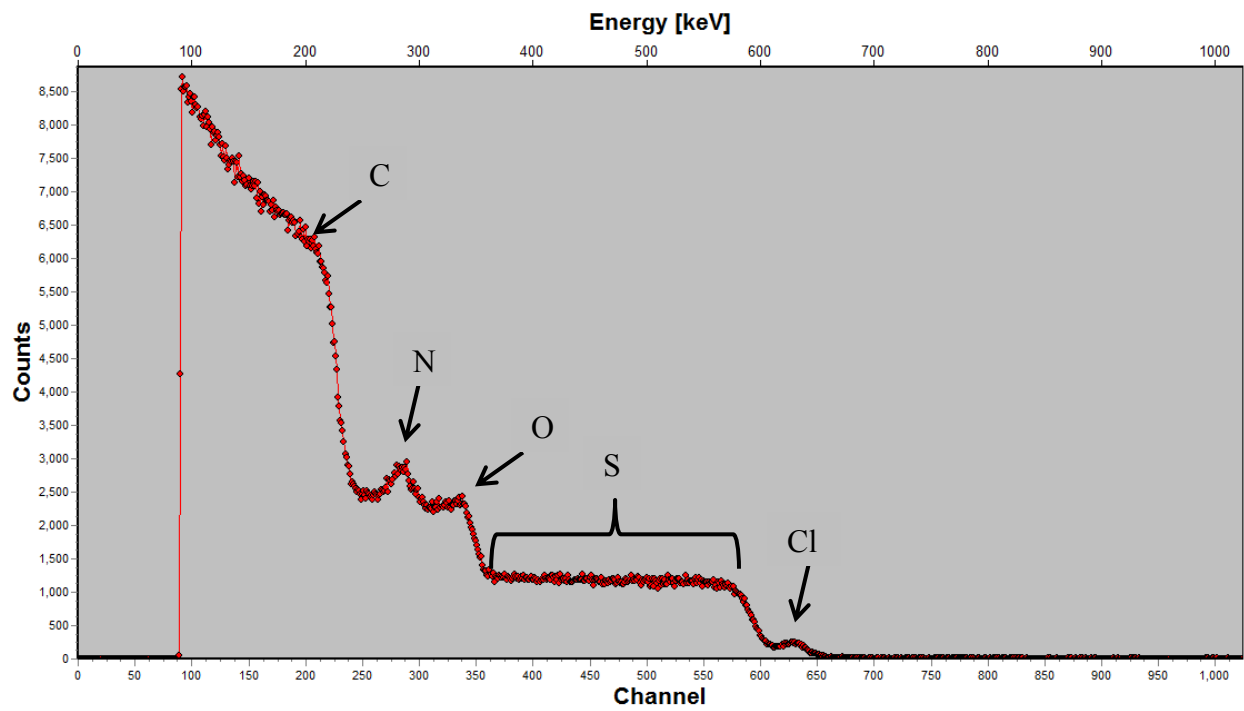


Figure A9-2. RBS spectrum for an unfouled TFC-S membrane.

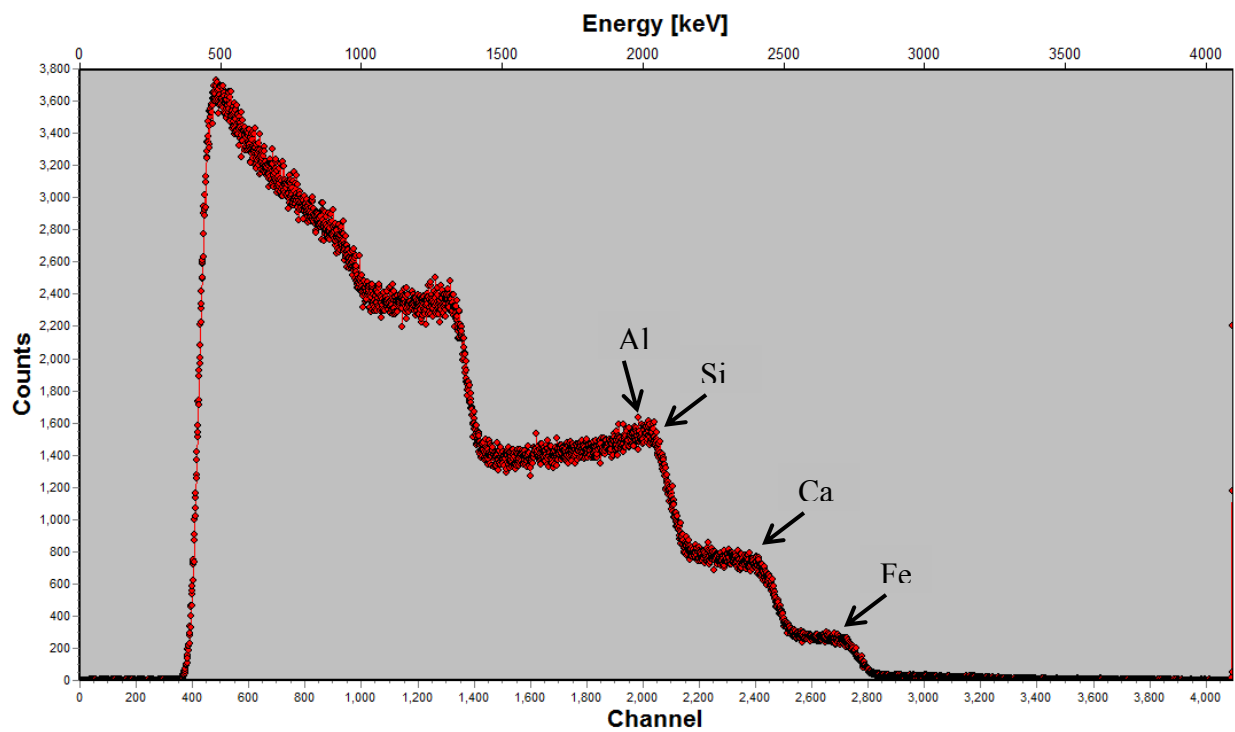


Figure A9-3. RBS spectrum for a fouled membrane from the Castle Hayne first stage.

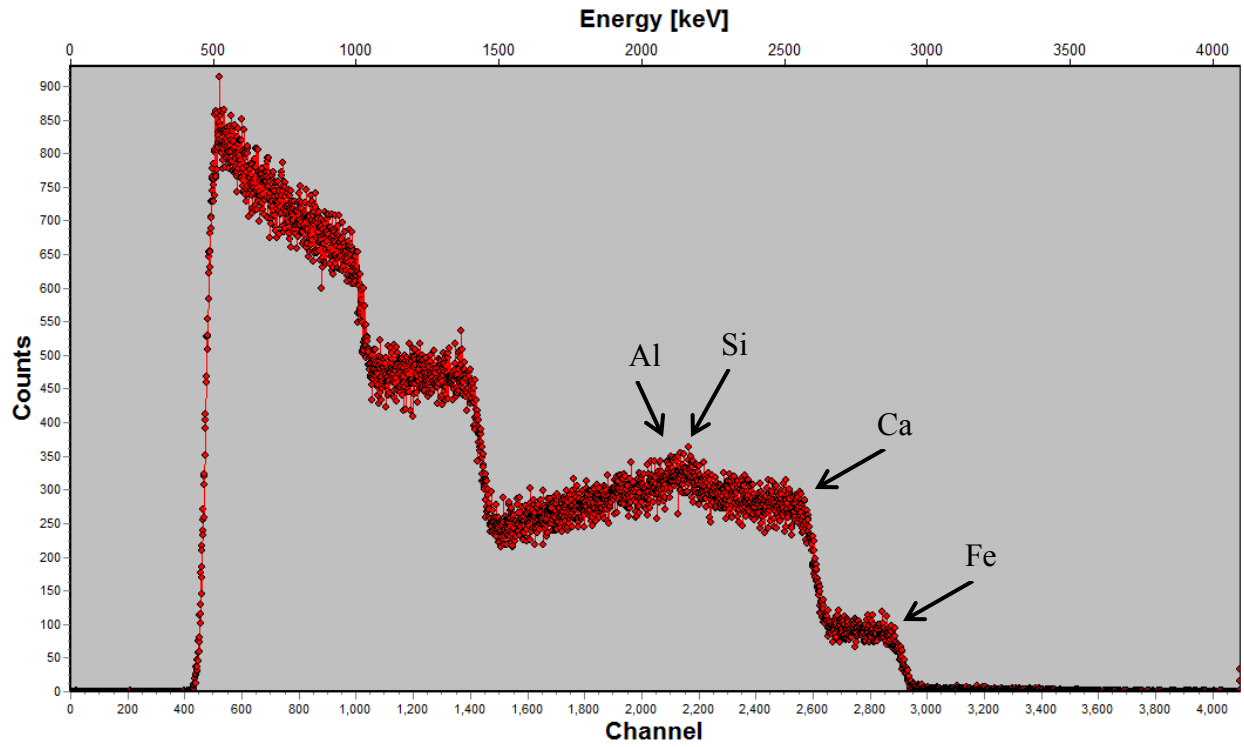


Figure A9-4. RBS spectrum for a fouled membrane from the Castle Hayne second stage.

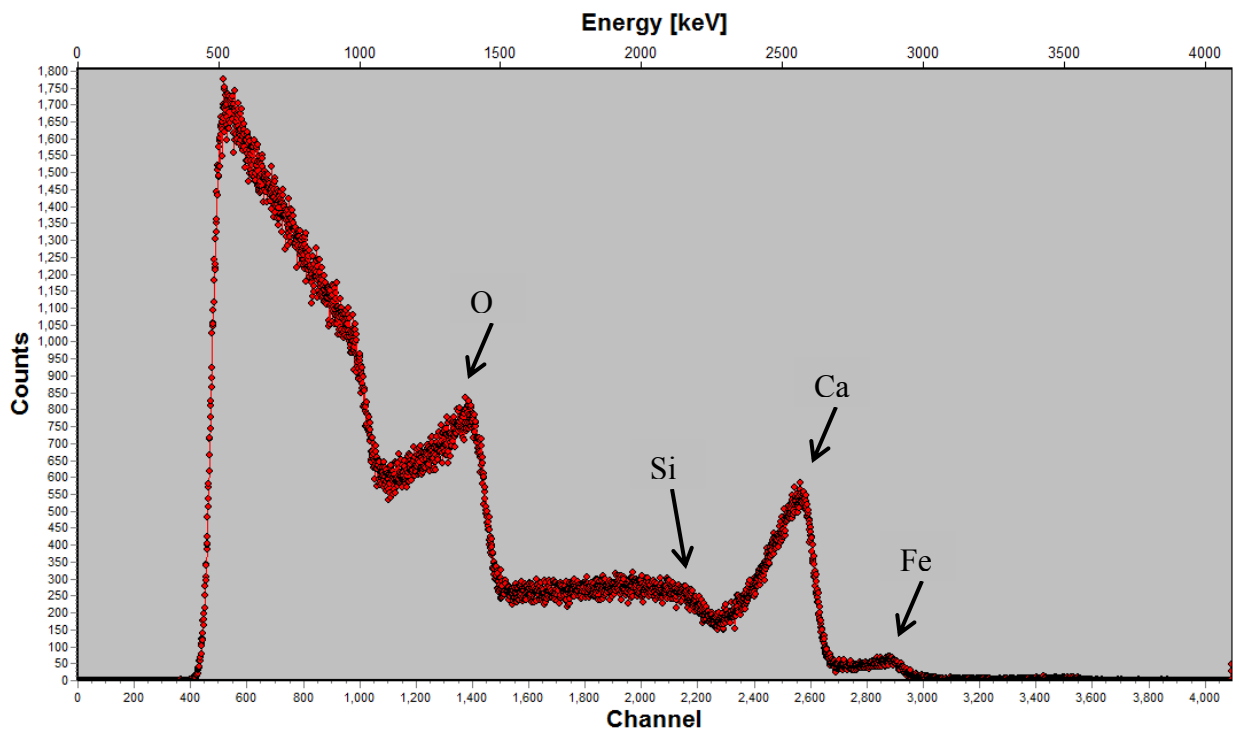


Figure A9-5. RBS spectrum for a fouled membrane from the Peedee first stage.

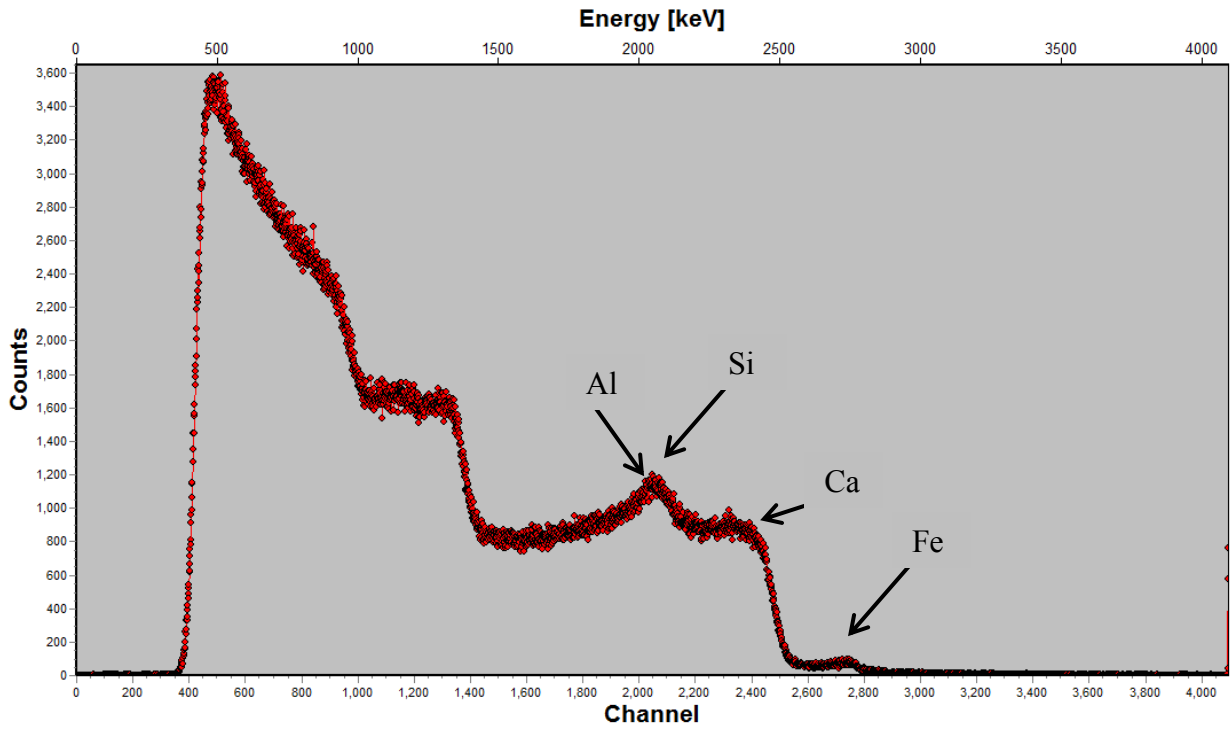


Figure A9-6. RBS spectrum for a fouled membrane from the Peedee second stage.

Appendix 10: Eluted Concentrations of Membrane Foulants Using Two Cleaning Solutions

Concentrations of inorganic elements present in cleaning solutions following cleaning were determined by ICP-MS and are shown in Table A10-1. Cleaning solutions that contained EDTA (STPP+EDTA and Lavasol 7) were more effective at removing inorganic foulants than an increase in pH alone. Given the high pH of cleaning solutions tested, there was the potential for precipitates to be filtered, as ICP-MS requires 0.2 μm filtration of samples prior to analysis.

Table A10-1. Concentration of membrane foulants eluted by cleaning with NaOH (pH=11) compared to cleanings with two effective cleaning solutions: STPP+EDTA (pH = 10.5) for the Castle Hayne elements and Lavasol 7 (pH=12.5) for the Peedee elements. Sample abbreviations are as follows: Castle Hayne first stage (CHS1), Castle Hayne second stage (CHS2), Peedee first stage (PDS1), and Peedee second stage (PDS2).

	Eluted concentration (mg/m ²)					
	Mg	Al	Si	Mn	Fe	Ca
CHS1 NaOH	2.58	2.27	58.9	0.08	9.30	30.7
CHS2 NaOH	3.11	2.07	58.6	0.27	37.4	30.8
PDS1 NaOH	2.75	2.43	65.3	0.02	1.27	34.0
PDS2 NaOH	2.40	2.17	65.0	0.04	0.51	33.7
CHS1 STPP w EDTA	121.4	64.7	1724	2.56	161.7	922.7
CHS2 STPP w EDTA	79.7	7.2	1031	2.32	205.9	555.1
PDS1 Lavasol 7	133.3	125.6	3630	0.97	26.3	1881.5
PDS2 Lavasol 7	127.9	118.5	3459	2.31	22.9	1793.6

Appendix 11: SEM Images of Cleaned Membranes

Figures A11-1 through A11-4 show SEM images of fouled membranes before and after cleaning with various solutions. Figures A11-1 and A11-2 (Panels D and F) show that acid cleaners were not effective at fully removing foulants on both elements from the Castle Hayne treatment train. From Figure A11-2 Panel E, it was evident that NaOH+SDS was not as effective at removing the fouling layer as the other basic cleaners tested. The Peedee first stage (see Figure A11-3) was returned to the original membrane state with all of the cleaning solutions tested. For the Peedee second stage, acidic cleaners and basic cleaners containing EDTA (STPP+EDTA and Lavasol 7) were found to be effective, with Lavasol 7 being the most effective. Basic cleaners without EDTA (NaOH+SDS and OptiClean F) were shown in Figure A11-4 to leave portions of the fouling layer remaining on the membrane.

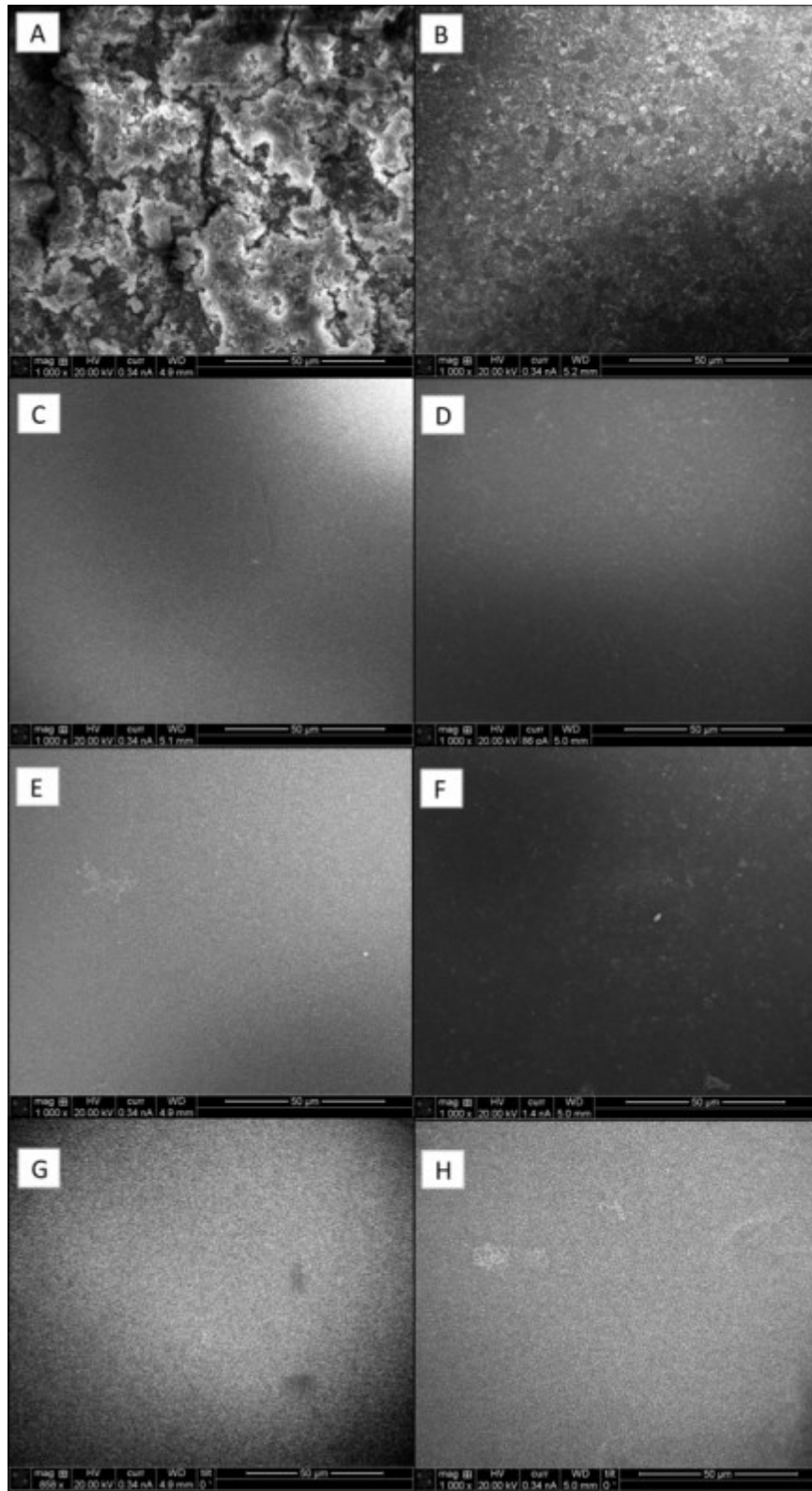


Figure A11-1. SEM images of a (A) fouled Castle Hayne first stage membrane and membranes cleaned by (B) sponge scrubbing with deionized water, (C) STPP+EDTA, (D) citric acid, (E) NaOH+SDS, (F) HCl, (G) Lavazol 7, and (H) OptiClean F at 50 µm scale.

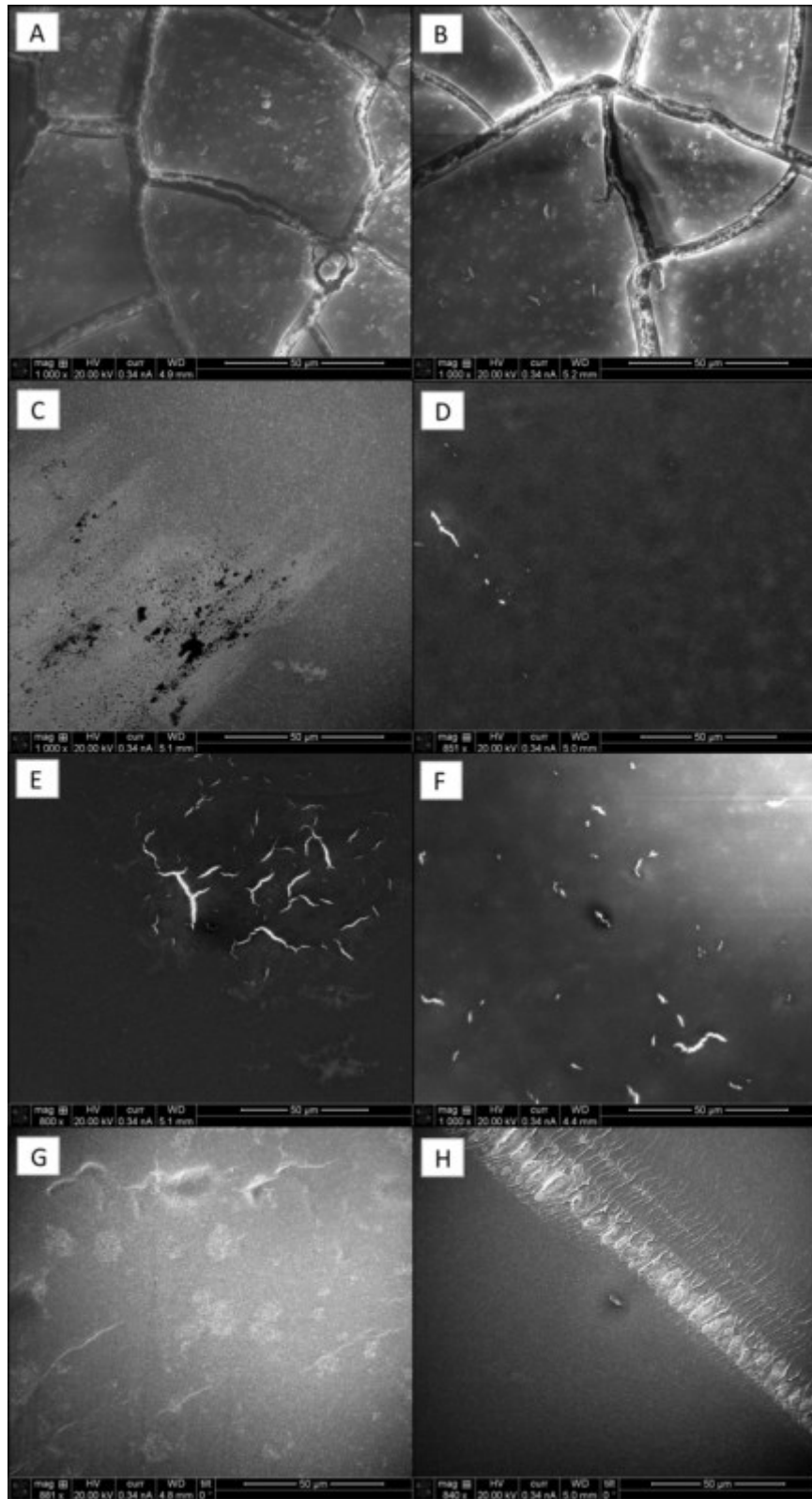


Figure A11-2. SEM images of a (A) fouled Castle Hayne second stage membrane and membranes cleaned by (B) sponge scrubbing with deionized water, (C) STPP+EDTA, (D) citric acid, (E) NaOH+SDS, (F) HCl, (G) Lavasol 7, and (H) OptiClean F at 50 µm scale.

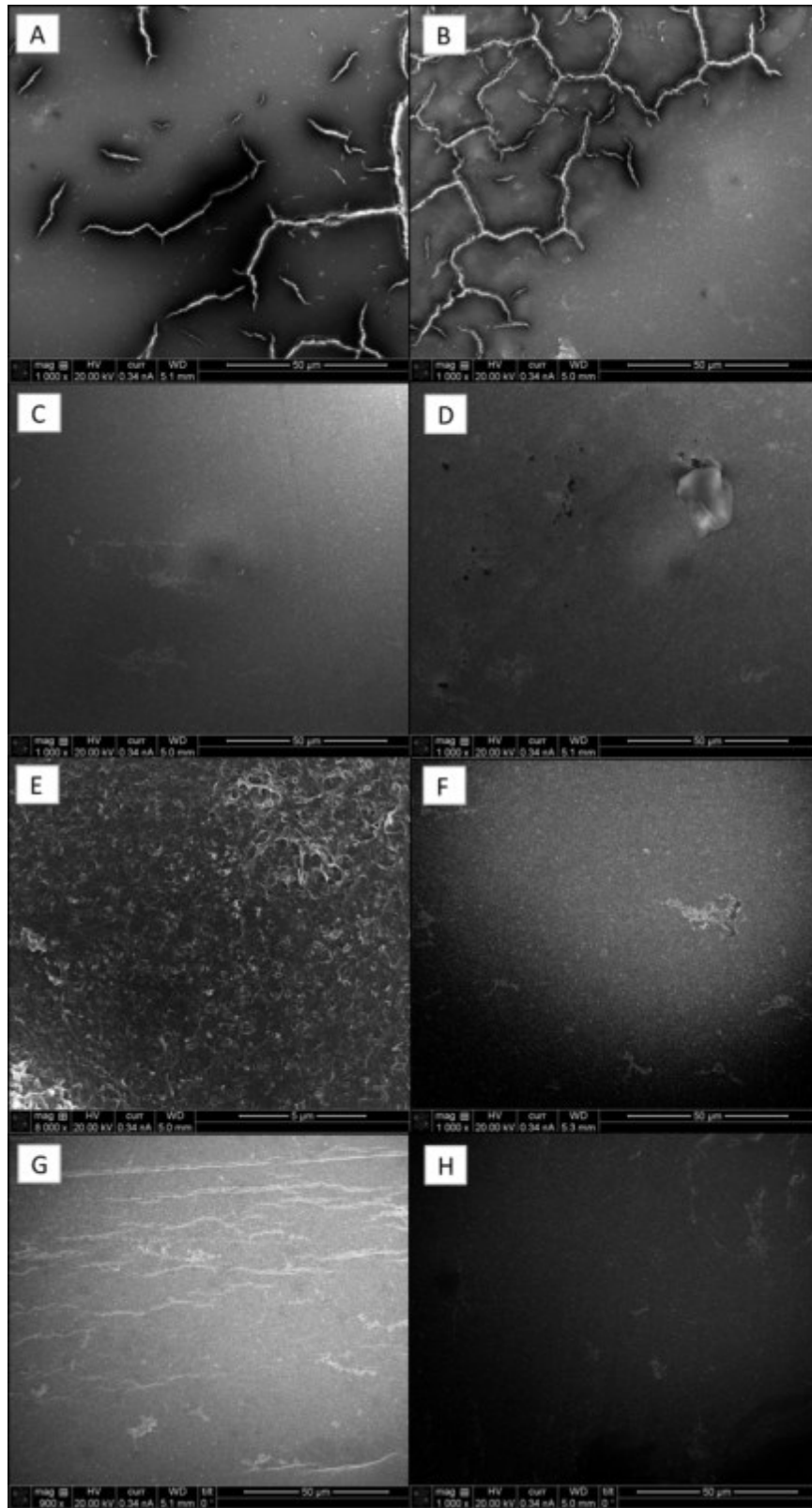


Figure A11-3. SEM images of a (A) fouled Peedee first stage membrane and membranes cleaned by (B) sponge scrubbing with deionized water, (C) STPP+EDTA, (D) citric acid, (E) NaOH+SDS, (F) HCl, (G) Lavasol 7, and (H) OptiClean F at 50 µm scale.

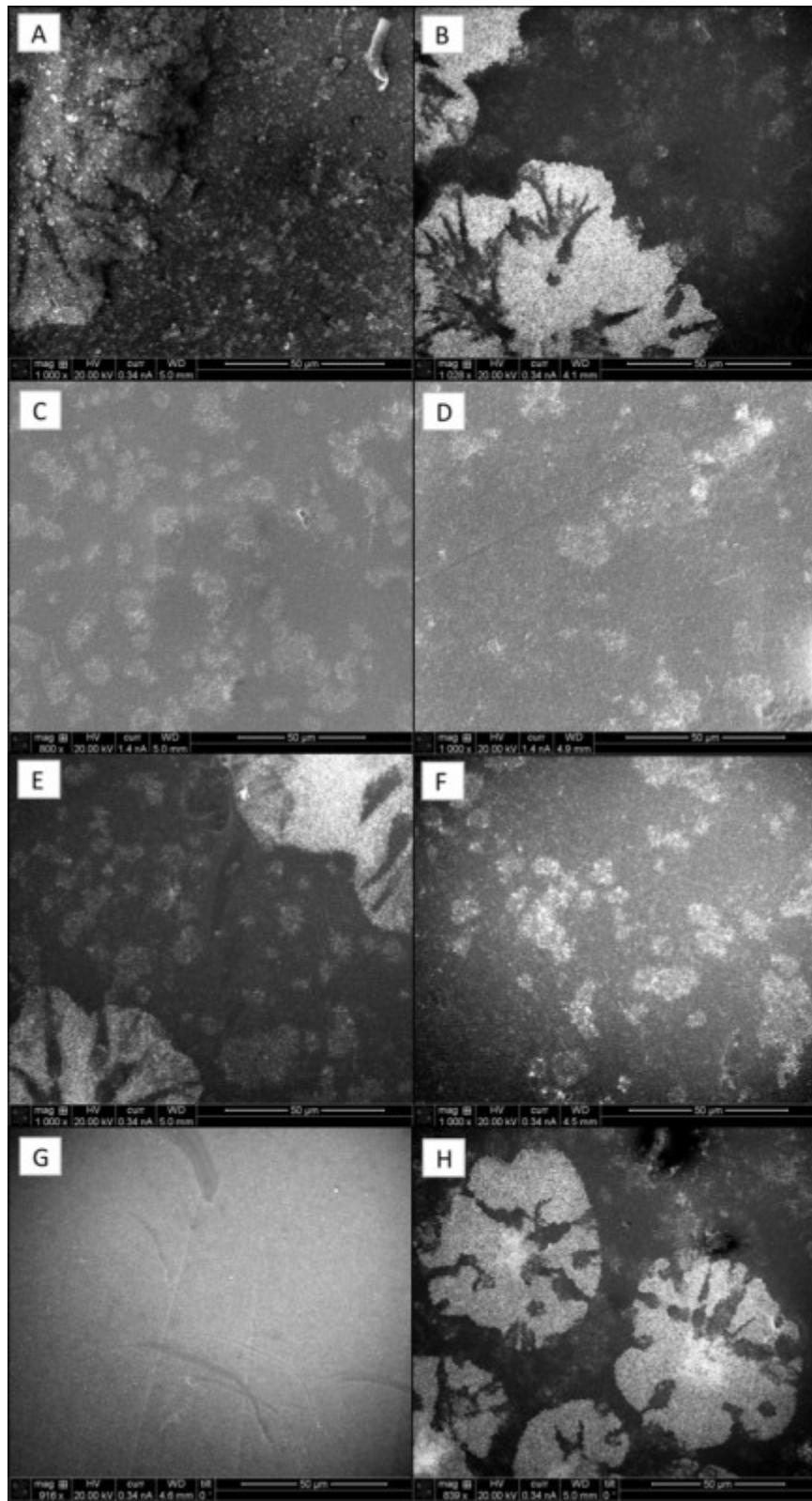


Figure A11-4. SEM images of a (A) fouled Peedee second stage membrane and membranes cleaned by (B) sponge scrubbing with deionized water, (C) STPP+EDTA, (D) citric acid, (E) NaOH+SDS, (F) HCl, (G) Lavasol 7, and (H) OptiClean F at 50 µm scale.

Appendix 12: XPS Results for Cleaned Membranes

Figures A12-1 through A12-4 show XPS results for membranes before and after cleaning with various cleaning solutions tested. For the Castle Hayne first stage, all basic cleaners tested were more effective at returning the membrane to its original composition than citric acid. The Castle Hayne second stage was best cleaned by basic solutions containing EDTA (STPP+EDTA and Lavasol 7). All solutions tested on the Peedee first stage were effective. For the Peedee second stage, both acids and bases containing EDTA were effective.

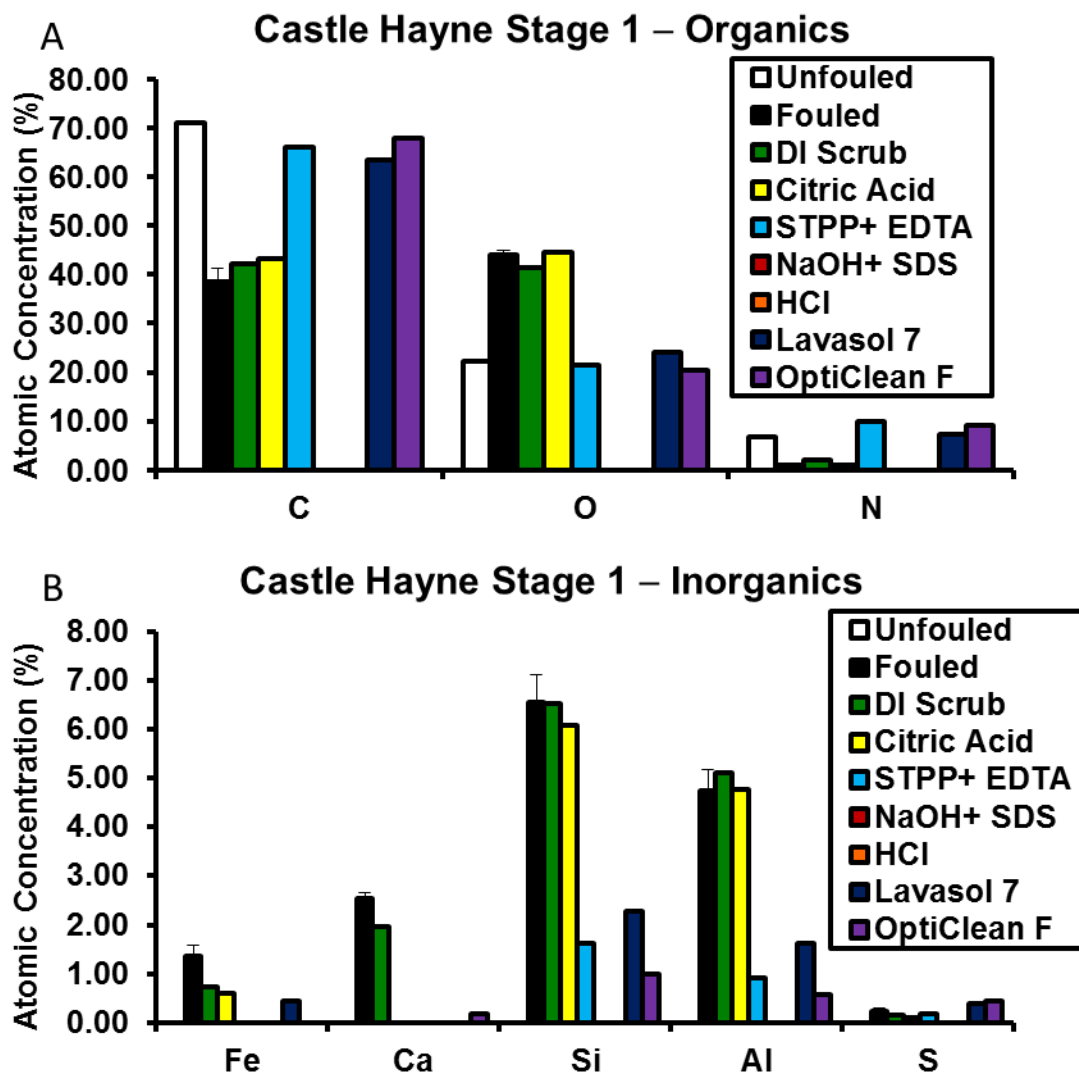


Figure A12-1. XPS results for fouled and cleaned elements from the Castle Hayne first stage. Only the unfouled reference (TFC-ULP) and the fouled sample were run in triplicate, and therefore the other measurements do not have error bars. Samples cleaned with NaOH+SDS and HCl cleaning solutions were not tested by XPS because other characterization methods showed that the membrane samples cleaned with less harsh cleaning solutions (STPP+EDTA and citric acid) were found to be more effectively cleaned.

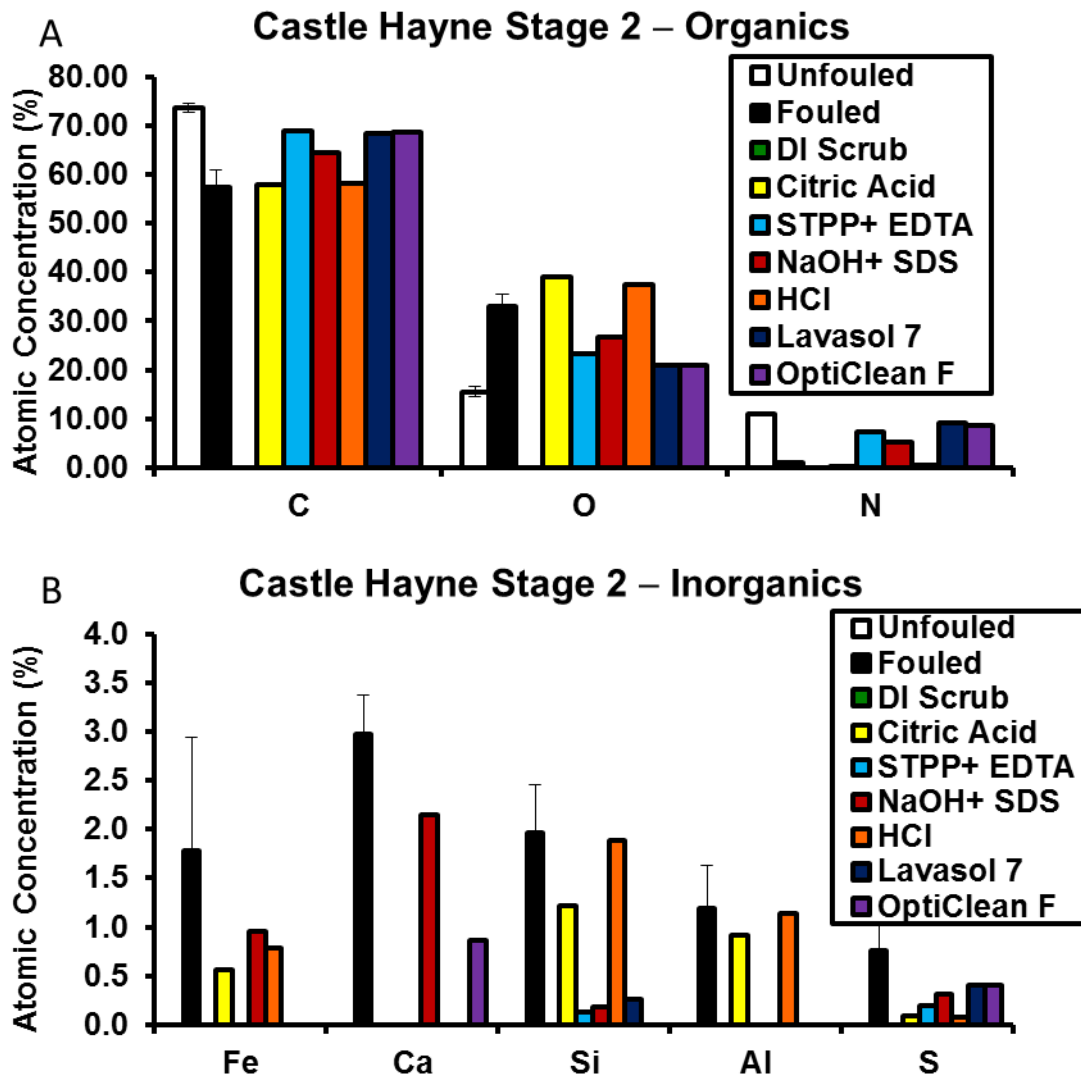


Figure A12-2. XPS results for fouled and cleaned elements from the Castle Hayne second stage. Only the unfouled reference (TFC-S) and the fouled sample were run in triplicate, and therefore the other measurements do not have error bars. Samples scrubbed with deionized water were not tested by XPS because no visible removal of the foulant was observed.

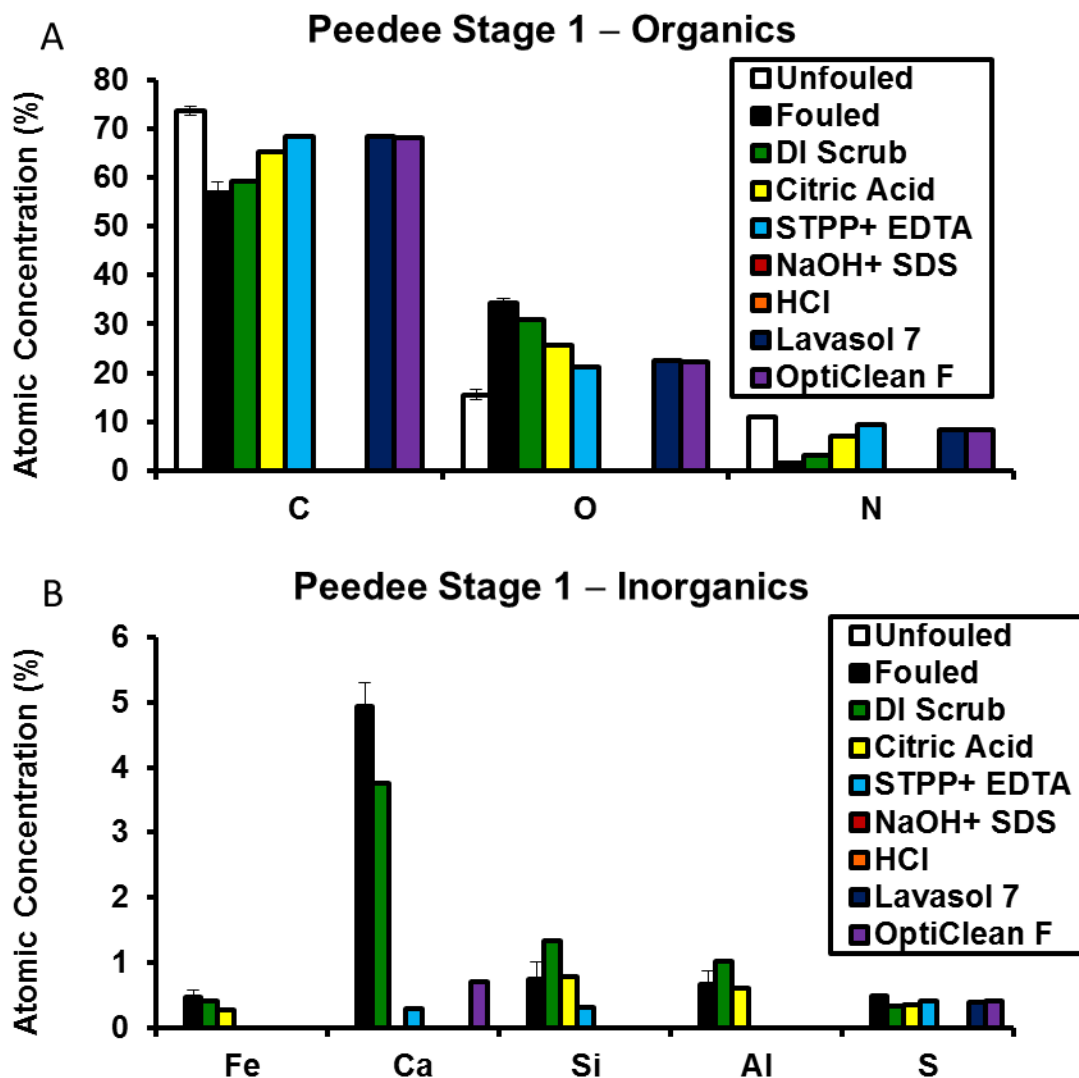


Figure A12-3. XPS results for fouled and cleaned elements from the Peedee first stage. Only the unfouled reference (TFC-S) and the fouled sample were run in triplicate, and therefore the other measurements do not have error bars. Samples cleaned with NaOH+SDS and HCl cleaning solutions were not tested by XPS because other characterization methods showed that the membrane samples cleaned with less harsh cleaning solutions (STPP+EDTA and citric acid) were found to be more effectively cleaned.

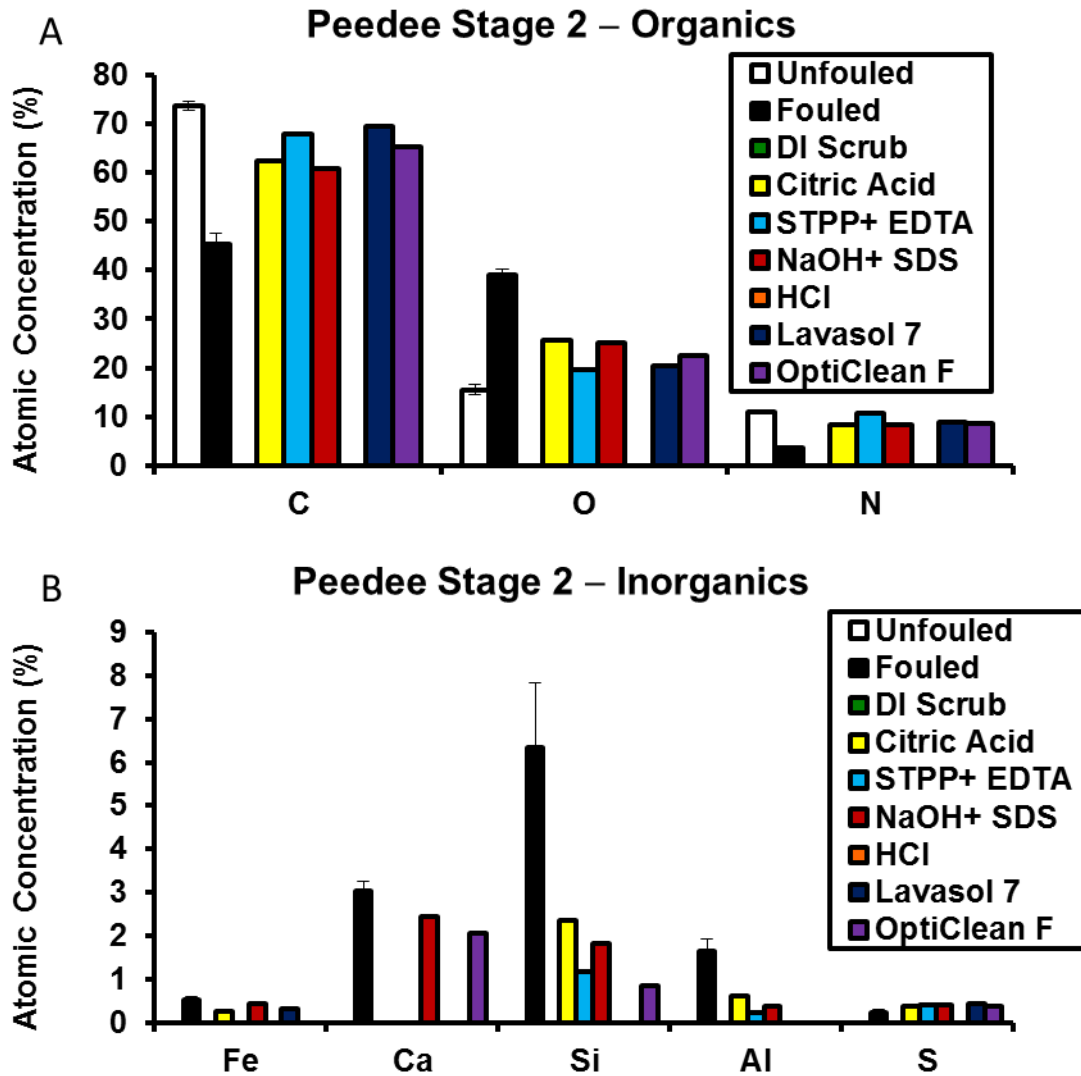


Figure A12-4. XPS results for fouled and cleaned elements from the Peedee second stage. Only the unfouled reference (TFC-S) and the fouled sample were run in triplicate, and therefore the other measurements do not have error bars. Samples scrubbed with deionized water were not tested by XPS because no visible removal of the foulant was observed.

Appendix 13: EDX Results for Cleaned Membranes

Figures A13-1 through A13-4 contain EDX results for various cleaning solutions. Most cleaning solutions appeared effective for all elements tested when the cleaned samples were analyzed by EDX, with the exception of the Peedee second stage cleaned by NaOH+SDS. EDX is less sensitive than XPS to thin fouling layers, and therefore EDX underestimates the concentration of inorganic foulants due to the sulfur signal from the polysulfone support layer.

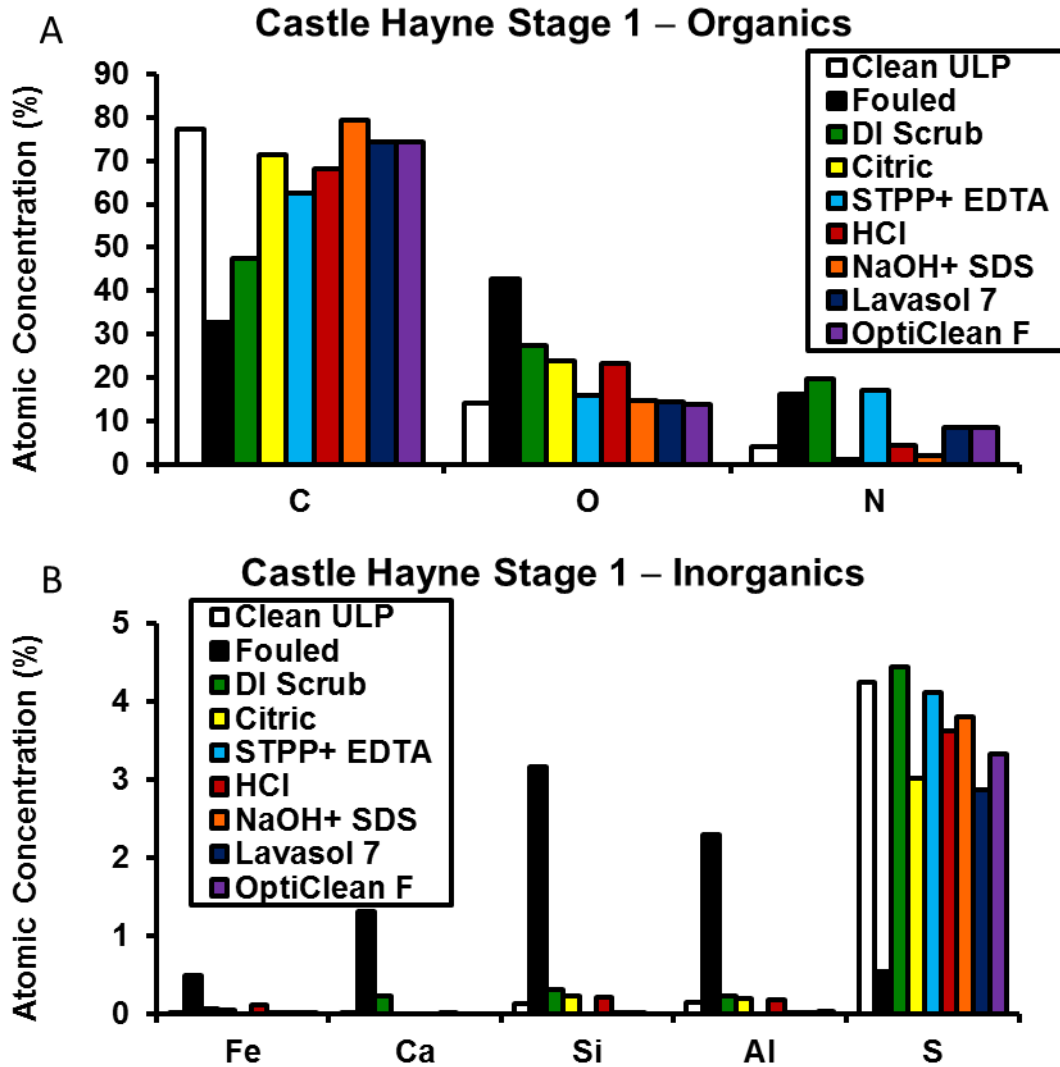


Figure A13-1. EDX results for fouled and cleaned elements from the Castle Hayne first stage.

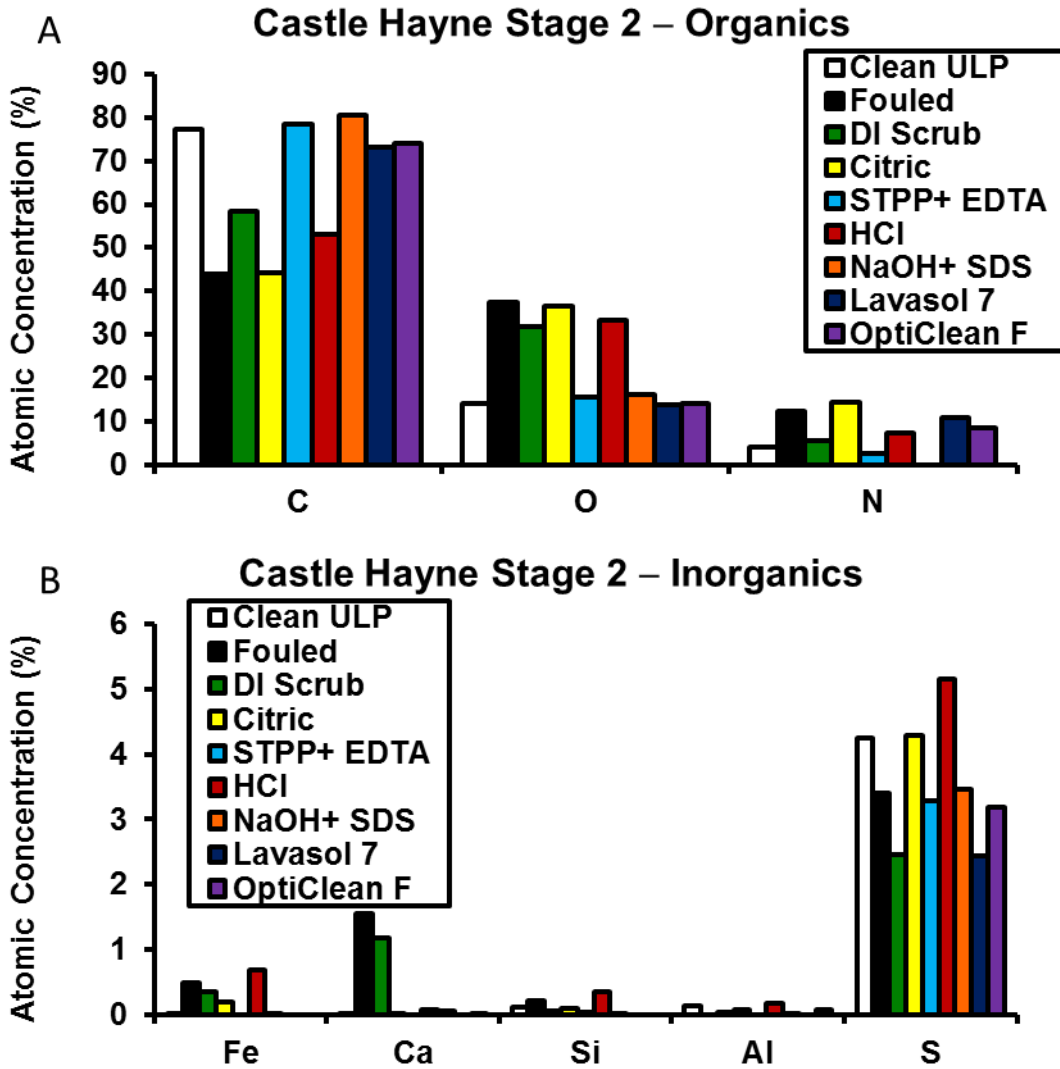


Figure A13-2. EDX results for fouled and cleaned elements from the Castle Hayne second stage. TFC-ULP was used as the clean element baseline because TFC-S was not available from the manufacturer at the time of analysis.

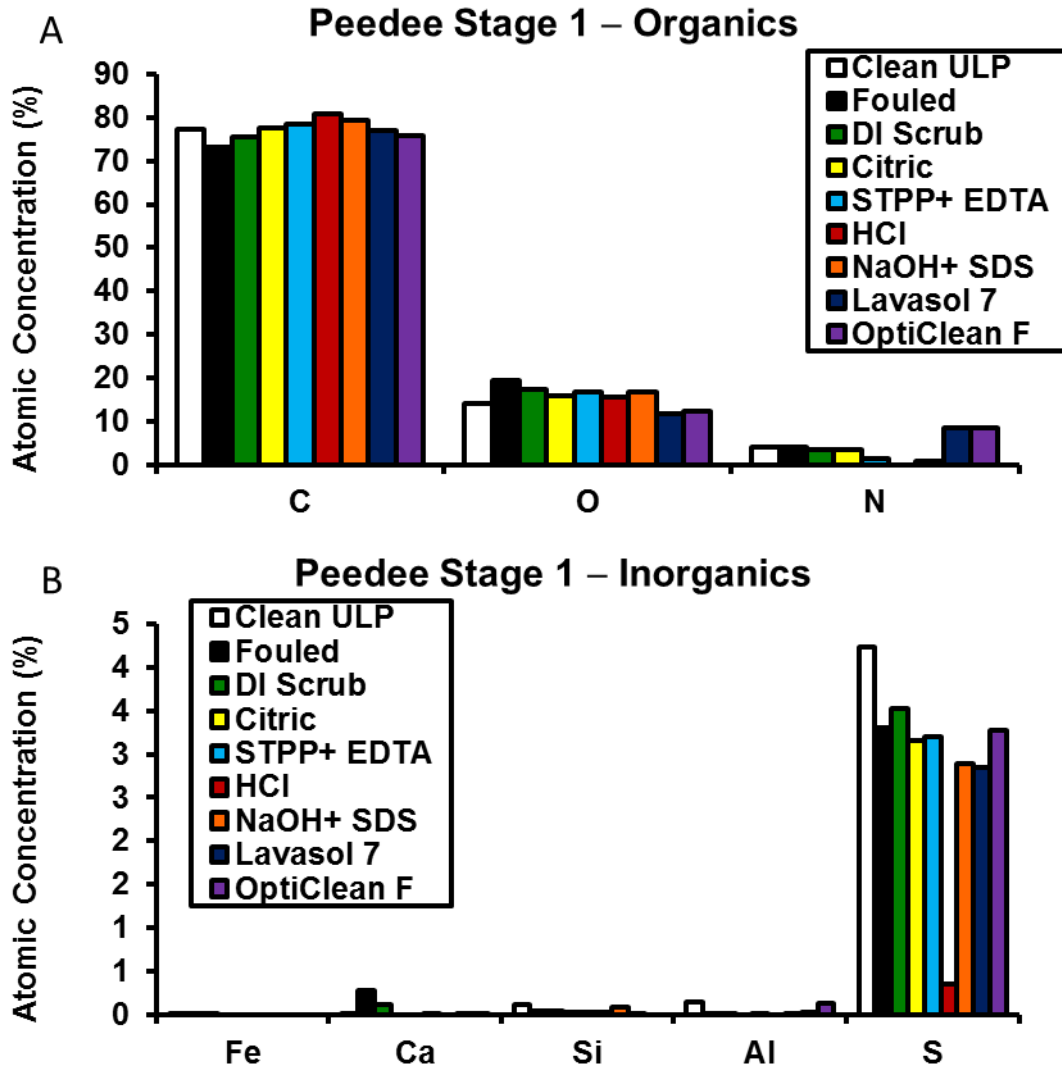


Figure A13-3. EDX results for fouled and cleaned elements from the Peedee first stage. TFC-ULP was used as the clean element baseline because TFC-S was not available from the manufacturer at the time of analysis.

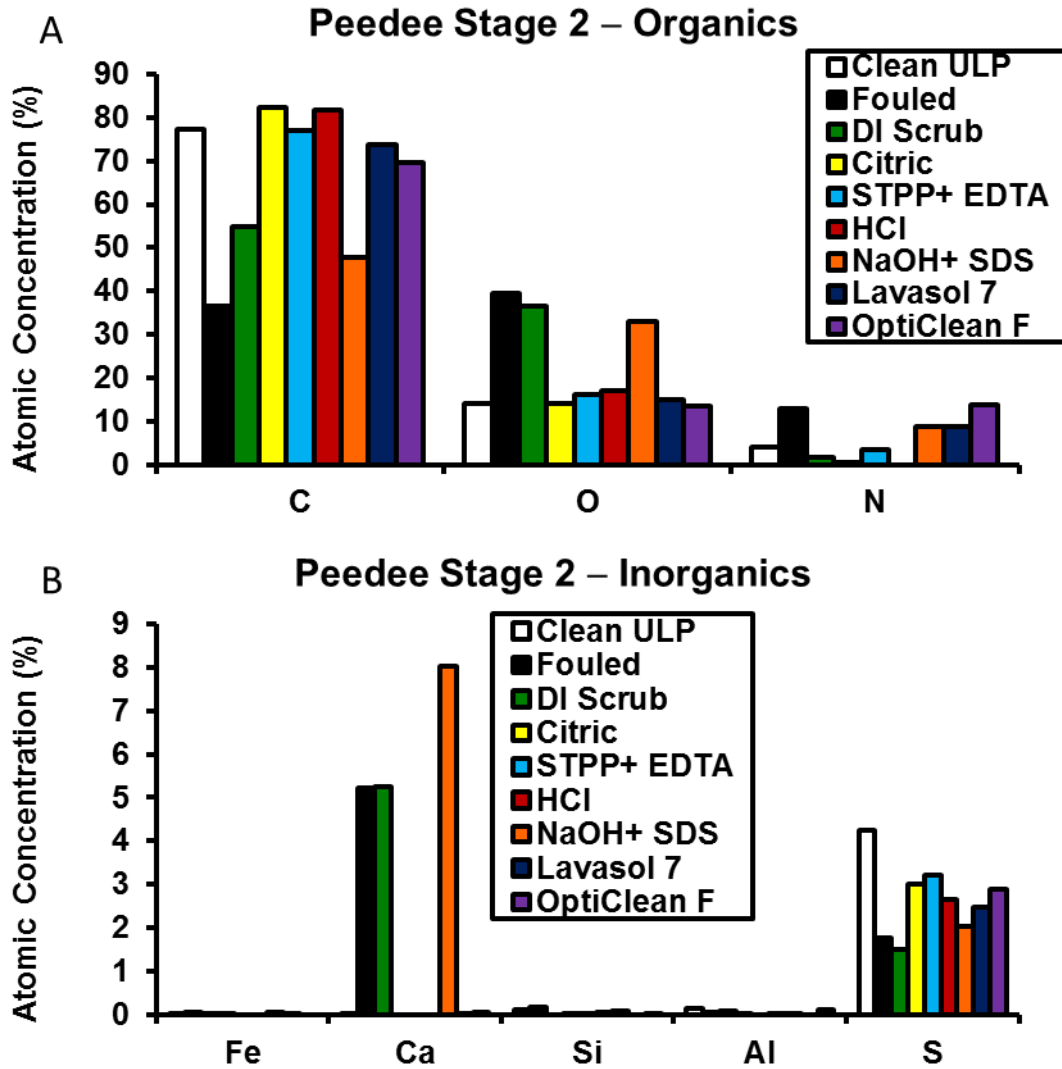


Figure A13-4. EDX results for fouled and cleaned elements from the Peedee second stage. TFC-ULP was used as the clean element baseline because TFC-S was not available from the manufacturer at the time of analysis.

Appendix 14: ATR-FTIR Results for Cleaned Membranes

ATR-FTIR was used to characterize membranes cleaned with every cleaning solution tested. Figures A14-1 through A14-8 along with Figure 37 (Section 3.7.4) contain ATR-FTIR spectra for all membranes after cleaning, which can be compared to fouled elements in Figure 24 (Section 3.4.4). Two cleaning solutions, STPP+EDTA and Lavasol 7, were the most effective at returning membranes to their original composition as determined by ATR-FTIR. Both of these cleaning solutions are basic and contain EDTA.

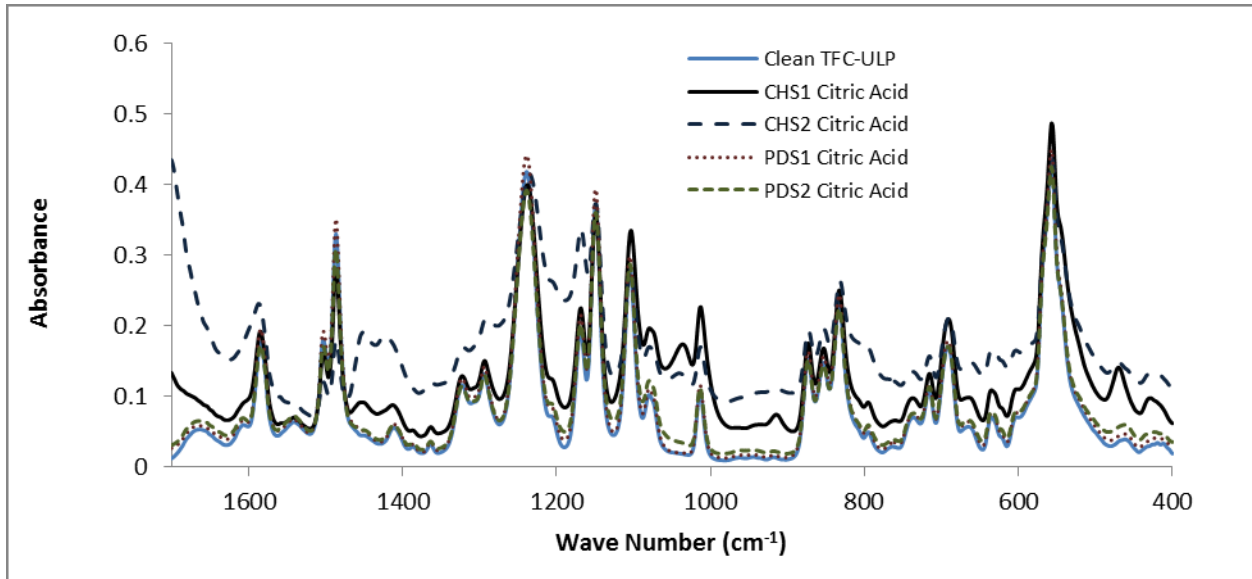


Figure A14-1. ATR-FTIR spectra for membranes cleaned with citric acid.

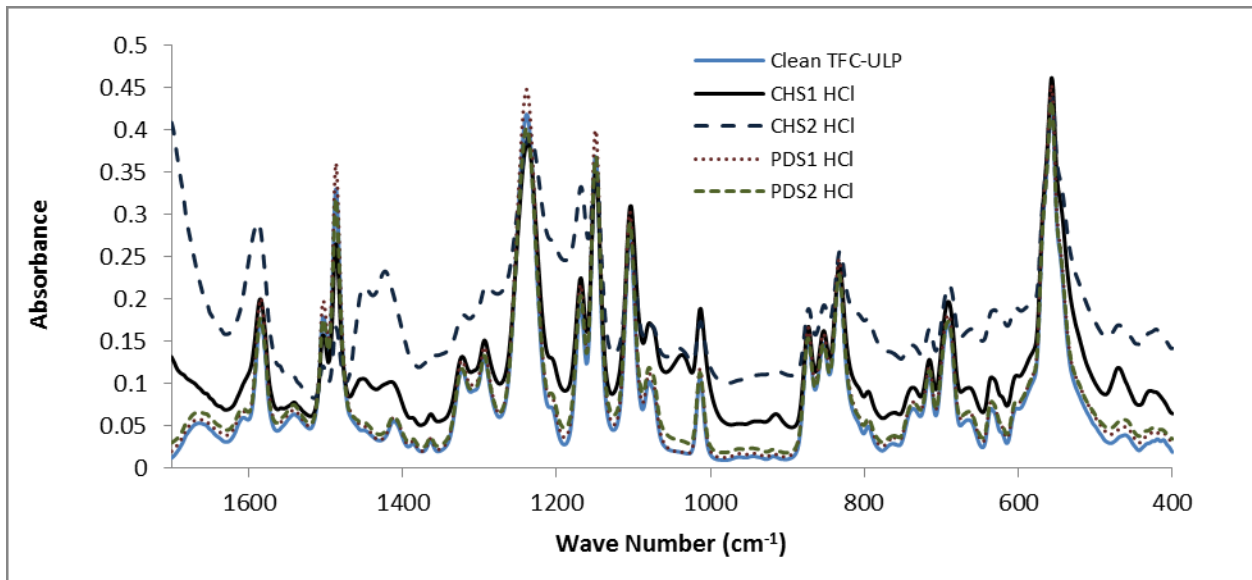


Figure A14-2. ATR-FTIR spectra for membranes cleaned with HCl.

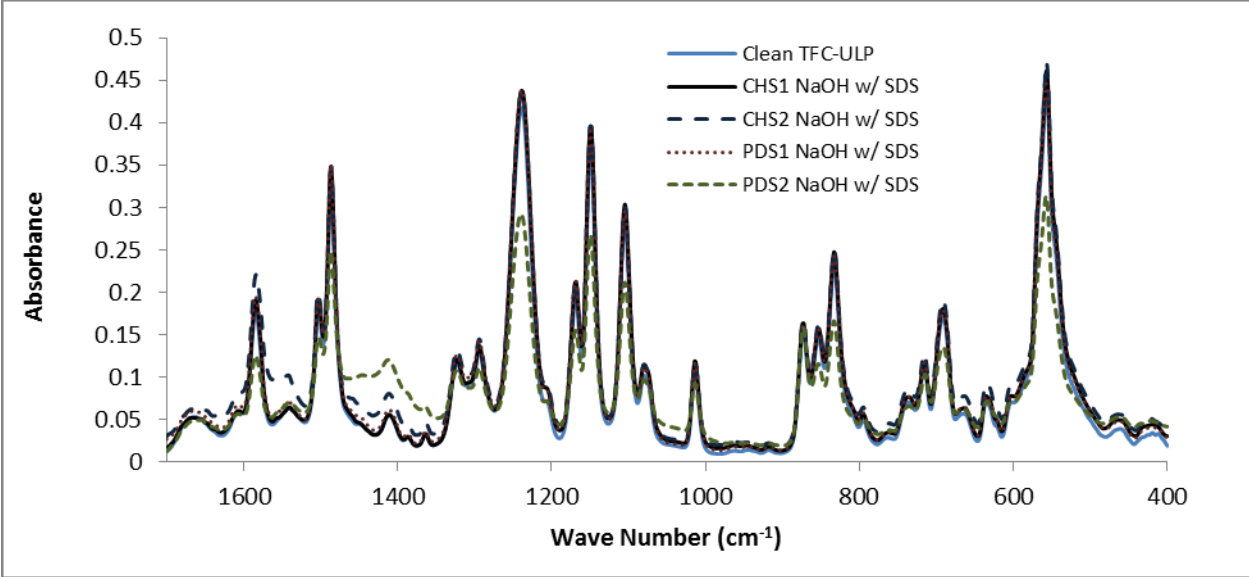


Figure A14-3. ATR-FTIR spectra for membranes cleaned with NaOH+SDS.

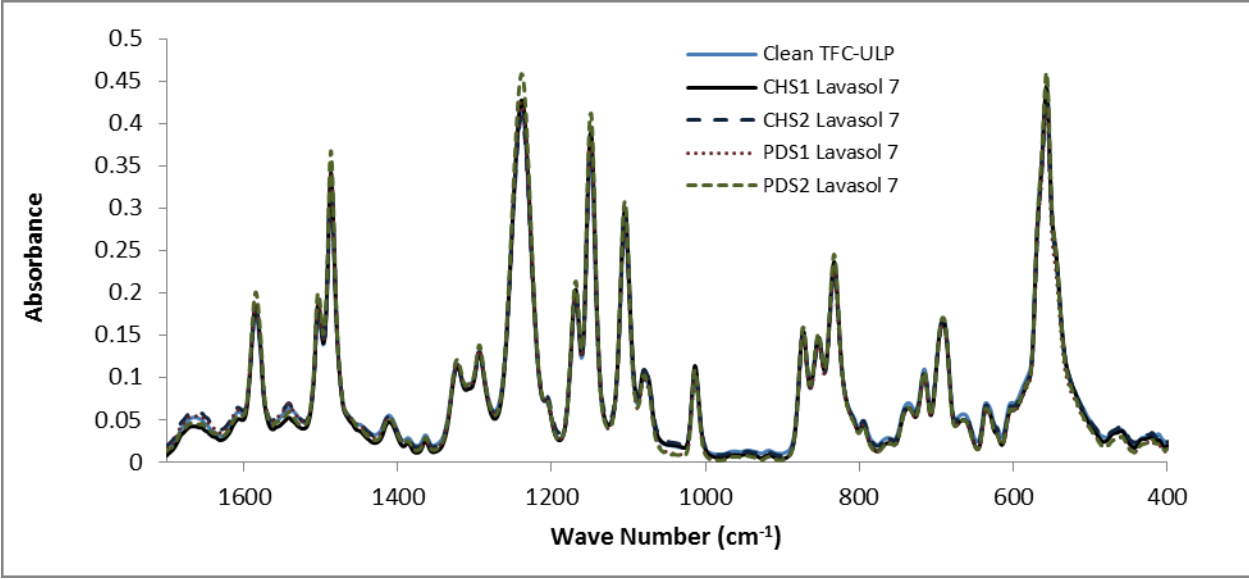


Figure A14-4. ATR-FTIR spectra for membranes cleaned with Lavasol 7 (pH =12.5).

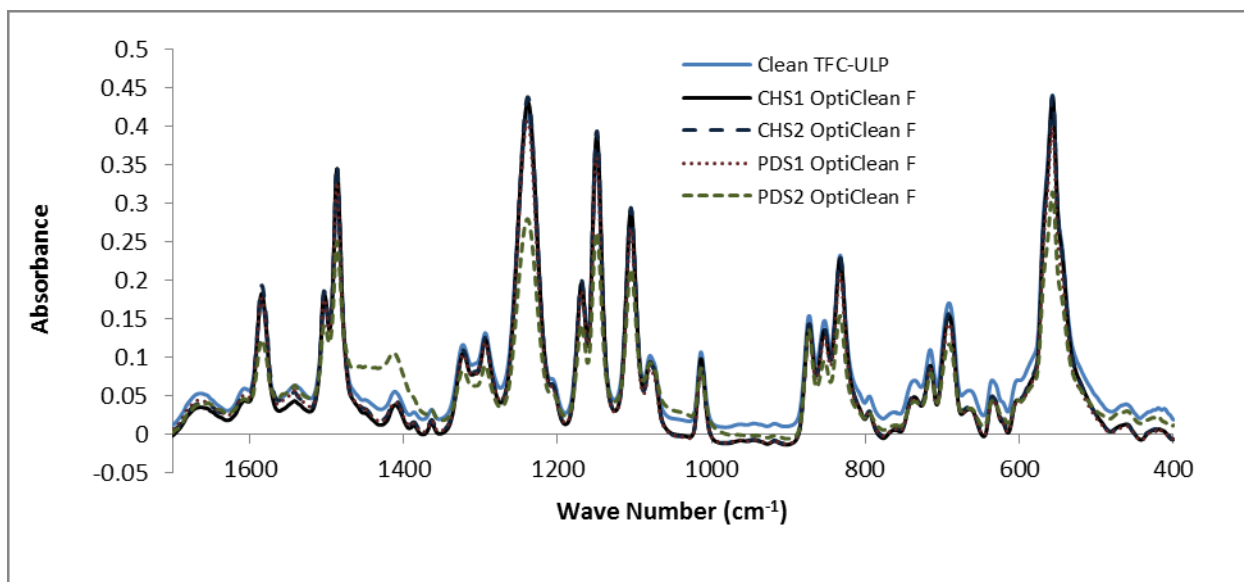


Figure A14-5. ATR-FTIR spectra for membranes cleaned with OptiClean F (pH =12.0).

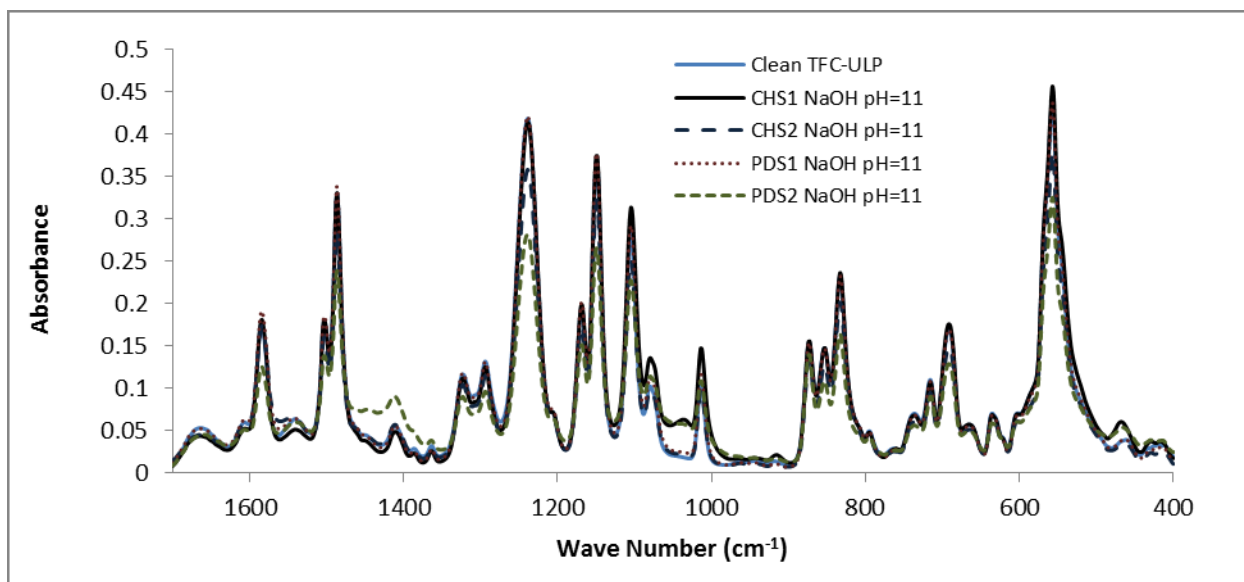


Figure A14-6. ATR-FTIR spectra for membranes cleaned with NaOH at a solution pH of 11.

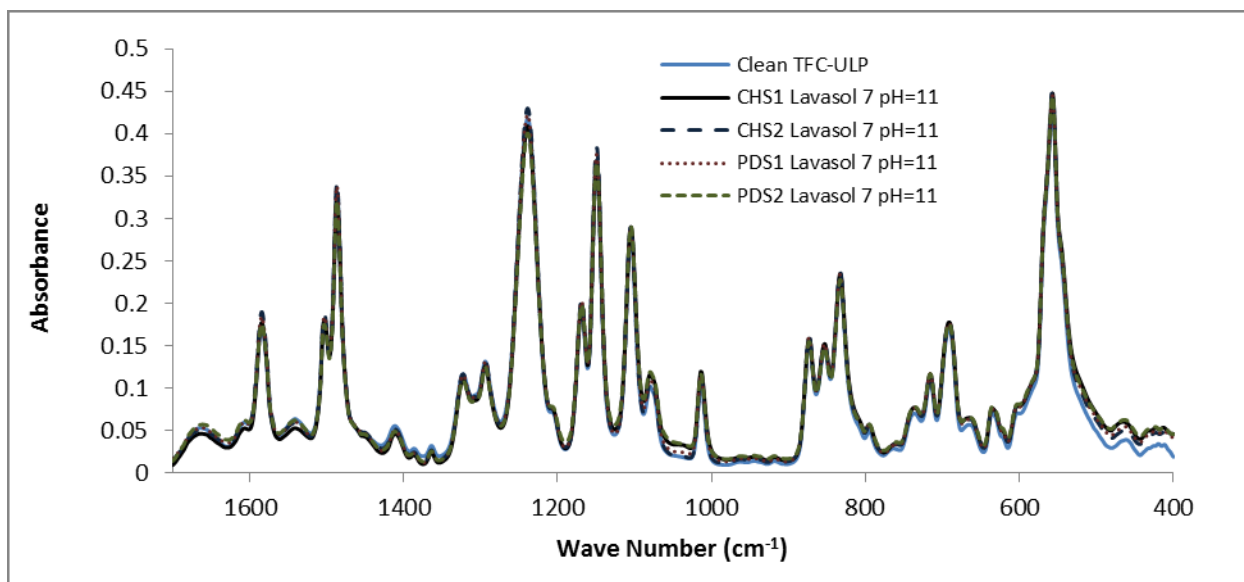


Figure A14-7. ATR-FTIR spectra for membranes cleaned with Lavasol 7 with the pH adjusted to 11 using HCl.

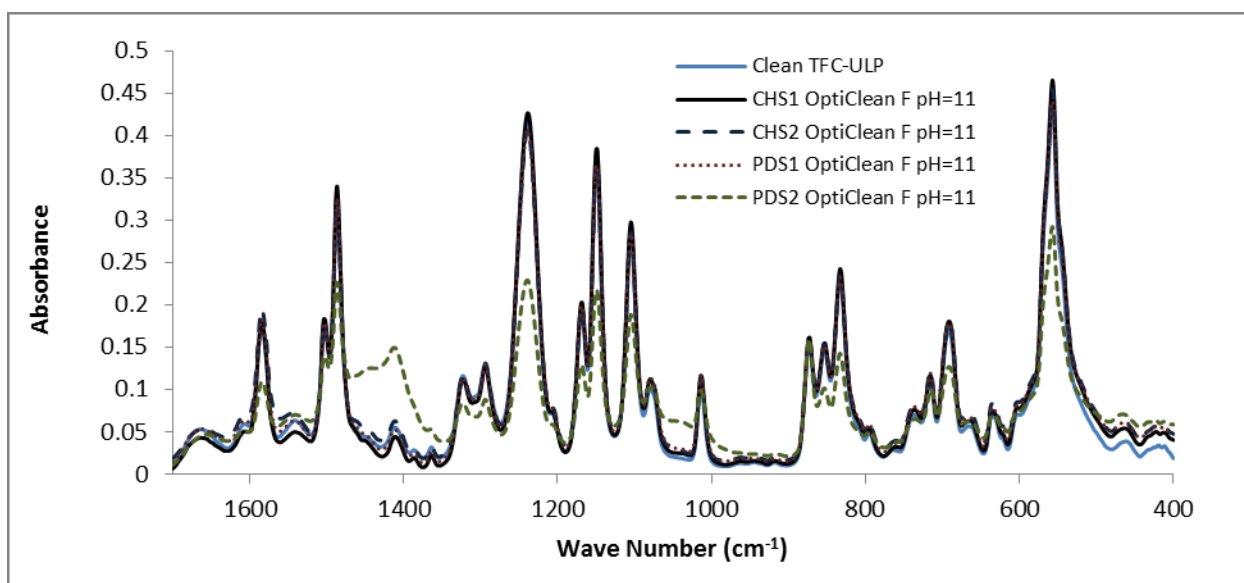


Figure A14-8. ATR-FTIR spectra for membranes cleaned with OptiClean F with the pH adjusted to 11 using HCl.

Appendix 15: Chloride Rejection by Cleaned Elements

Membrane performance was determined before and after cleaning, including water permeability (see Section 3.8) and chloride rejection. Chloride rejection following cleaning with various cleaning solutions is shown in Figures A15-1 to A15-4 for all four fouled membranes sampled. Cleaning did not significantly change chloride rejection in elements collected from the Castle Hayne first stage, Castle Hayne seconds stage, or Peedee first stage. Due to the variability in the performance of Peedee second stage membranes due to membrane damage, different chloride rejection values for different cleaning solutions should not be attributed to the effectiveness of the solutions (see note in the caption of Figure A15-4).

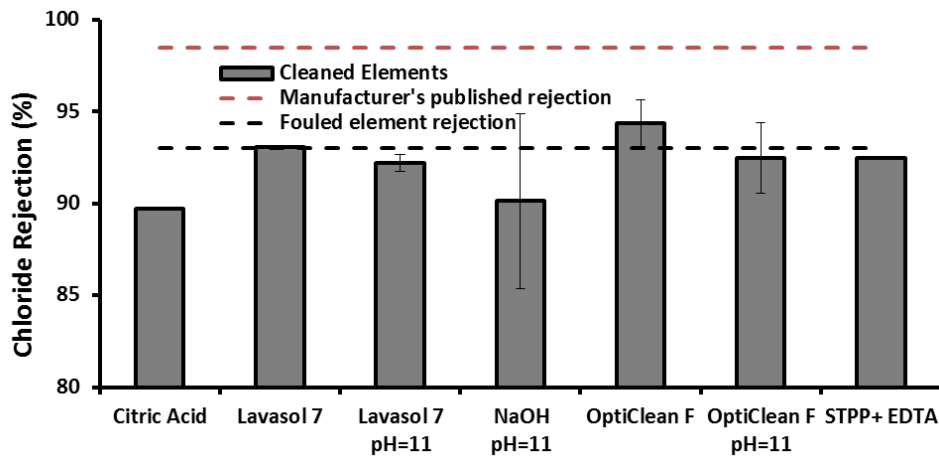


Figure A15-1. Chloride rejection of Castle Hayne first stage elements cleaned with various cleaning solutions. The red and black dashed lines represent the manufacturer's published chloride rejection and the observed chloride rejection of fouled elements, respectively.

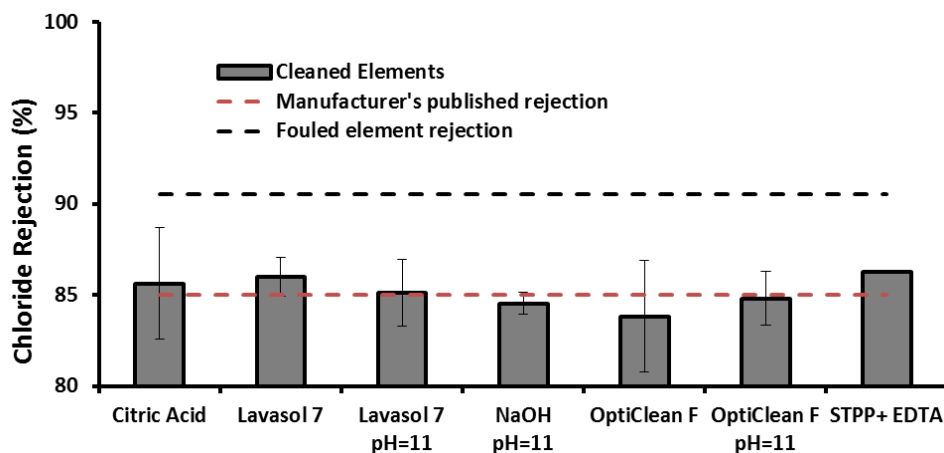


Figure A15-2. Chloride rejection of Castle Hayne second stage elements cleaned with various cleaning solutions. The red and black dashed lines represent the manufacturer's published chloride rejection and the observed chloride rejection of fouled elements, respectively.

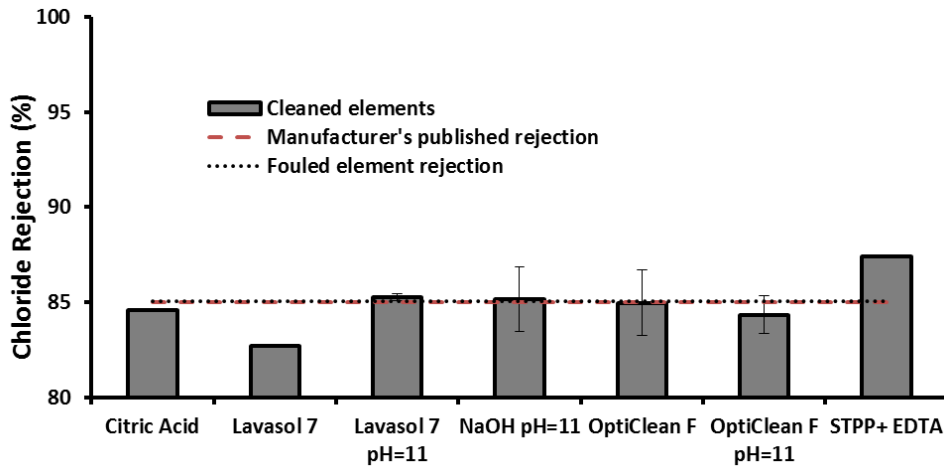


Figure A15-3. Chloride rejection of Peedee first stage elements cleaned with various cleaning solutions. The red and black dashed lines represent the manufacturer's published chloride rejection and the observed chloride rejection of fouled elements, respectively.

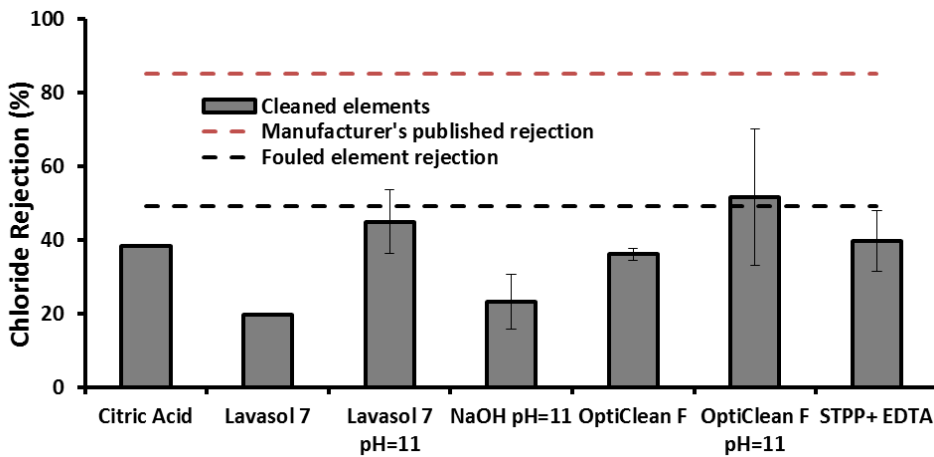


Figure A15-4. Chloride rejection of Peedee second stage elements cleaned with various cleaning solutions. The red and black dashed lines represent the manufacturer's published chloride rejection and the observed chloride rejection of fouled elements, respectively. Note: Peedee second stage membranes were damaged as evidenced by high flow rate and low chloride rejection, thus caution should be used when interpreting results for these membranes.

Evaluation of the P Balance of a Restored, Previously Farmed Wetland

Basic Information

Title:	Evaluation of the P Balance of a Restored, Previously Farmed Wetland
Project Number:	2012NC168B
Start Date:	3/1/2012
End Date:	2/28/2013
Funding Source:	104B
Congressional District:	04
Research Category:	Water Quality
Focus Category:	Water Quality, Nutrients, Surface Water
Descriptors:	None
Principal Investigators:	Michael J. Vepraskas, Jeffrey G White

Publications

There are no publications.

NC STATE UNIVERSITY

Campus Box 7619
Raleigh, NC 27695-7619

919.515.2655
919.515.2167 (fax)

MEMORANDUM

TO: Dr. David Genereux, Associate Director, WRRRI

FROM: M.J. Vepraskas, 

SUBJECT: Request for a one-year no cost extension for: Evaluation of the P-Balance of a Restored, Previously Farmed Wetland (NCSU PINS NO: 45227)

DATE: 4 February 2013

I am requesting a one year no-cost extension for the above-named grant. The proposed new end date would be 28 February 2014. Initial funding period from March 1, 2012 to February 28, 2013.

We have made substantial progress but more time is needed to complete the objectives. Progress to date has been summarized in the attached report. The main reason for the delay in completing the work is that the plant survey (task 2C in Table 1) took much longer than anticipated. That is now complete.

Evaluation of the P-Balance of a Restored, Previously Farmed Wetland

First Year's Progress Report

M.J. Vepraskas, Soil Science

4 February 2013

1. Period Covered: March 2012-January 2013

2. Project Objectives

- 1) Estimate the change in soil total P (TP_{soil}) over 8 years of a successful wetland restoration by comparing TP_{soil} concentrations in archived, pre-restoration samples, and present day samples taken from the same geo-referenced locations.
- 2) Estimate P fluxes into and out of Juniper bay, including:
 - a. Atmospheric deposition
 - b. Groundwater inflow and outflow and surface outflow
 - c. Plant uptake and forest floor accumulation
- 3) Combine objectives 1 and 2 to create a P balance for a Carolina Bay restored from soils previously under production agriculture, and
- 4) Evaluate the accuracy of the P balance in assessing fluxes in P within and out of the research site

3. Progress made to date:

Objective 1

Archived samples have been secured. A sampling scheme has also been designed to select 150 previously-sampled locations for resampling using an area-weighted, stratified random sampling scheme. Sampling of those locations has commenced, and will continue through the end of February. Laboratory analysis of these samples will begin thereafter.

Objective 2

Atmospheric deposition samplers were installed in June. Samples have been collected since then, and will continue to be collected through the conclusion of the study. Surface water outflow measurements and water samples have been collected throughout the study and will continue through the conclusion. For estimating groundwater and P fluxes into or out of the site, piezometer measurements have been made monthly from four previously-installed transects of piezometer nests. Water samples have been collected from each piezometer in the nests immediately outside of the perimeter ditch. These measurements and sample collections will continue to the completion of the study. A tree survey was completed using twenty square vegetation plots that were 30 by 30 m in size. Tree species, diameter at breast height, and height were recorded for each tree that was at least 10 cm DBH. Allometric equations from the literature will be used to estimate plant P uptake.

Objectives 3 and 4

Progress towards these objectives will begin once objectives 1 and 2 are complete.

Table 1. Timeline for grant extension. A “●” symbol indicates the task has been completed, while a “○” indicates a task that will be completed within the year

Task	Mar.-May	June-Aug.	Sept.-Dec.	Jan.-Feb.	Mar.-June	June-Feb. (2014)
	-----2012-----			-----2013-----		
1. Determine change in soil TP						
a) Sample Juniper Bay Soils				○		
b) Analyze TP in archived and present day samples					○	
2. Determine P fluxes						
a) Monitor atmospheric deposition	●	●	●	○	○	
b) Monitor surface outflow P	●	●	●	○	○	
c) Conduct tree survey		●	●			
3. Develop Final P-balance						○
4. Evaluate the accuracy of the P-balance						○

Nutrient retention and floodplain connectivity in restored Piedmont streams

Basic Information

Title:	Nutrient retention and floodplain connectivity in restored Piedmont streams
Project Number:	2012NC173B
Start Date:	3/1/2012
End Date:	2/28/2013
Funding Source:	104B
Congressional District:	NC-08
Research Category:	Water Quality
Focus Category:	Nutrients, Hydrogeochemistry, Surface Water
Descriptors:	None
Principal Investigators:	Sara K McMillan, Greg Jennings

Publications

There are no publications.

Nutrient Retention and Floodplain Connectivity in Restored Piedmont Streams

Sara McMillan (UNC Charlotte), Greg Noe (USGS), Greg Jennings (NCSU)

North Carolina Water Resources Research Institute
Project #12-03-W
Interim Report - April 2013

Introduction

The overall objective of this project is to quantify changes in sediment, nitrogen (N) and phosphorus (P) retention in the floodplains of restored streams. Floodplains and riparian zones are known to be important locations for sediment storage and nutrient transformations (Mayer et al. 2007, Noe and Hupp 2009, Vidon et al. 2010). While extensive research has been conducted on the capacity for riparian zones to buffer sediment and nutrient loads in natural systems, we know surprisingly little about the water quality function of floodplains in restored streams.

The two-stage channel design approach to river restoration has been implemented to enhance ecological functions during baseflow while maintaining channel stability during higher flows (Figure 1). Multiple flowpaths are included in this design approach: a low flow stream channel to maintain baseflow conditions, a low bench to transport bankfull discharge and a higher floodplain that is accessed during the largest storms. The low benches generally have dense herbaceous vegetation and high groundwater tables providing a potential sources of carbon (C) and promoting reducing conditions for N removal via denitrification (Kaushal et al. 2008). However, flashy hydrology typical of urban watersheds often results in high velocities in the low benches, which can limit their capacity to function as depositional sinks for sediment and nutrients. During the highest discharges, the upper floodplain is accessed, resulting in lower flow velocities, increased retention time and settling of fine sediment.

We hypothesized that increased frequency of floodplain connectivity would lead to increased sedimentation and nutrient transformations. During more frequently occurring high discharge events (i.e. 1-2 year return interval), the low benches would become inundated with surface water bringing along sediments, organic matter and nutrients. Because of the limited areal extents of the low benches (typically 1-2 meters) and flashy watershed hydrology, we hypothesized that discharge velocities would remain relatively high and that sedimentation would likely be of coarser sediment. While flooded less frequently, we also hypothesized

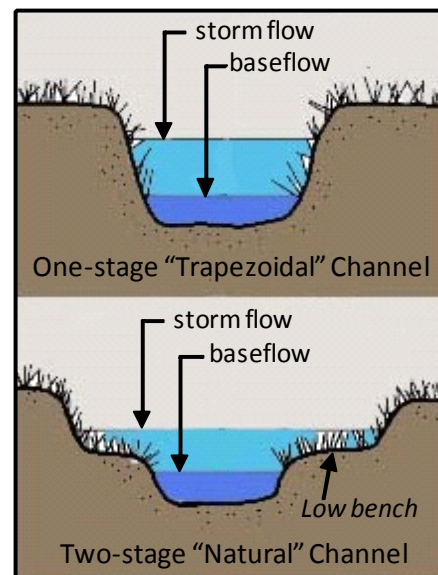


Figure 1: Two-stage natural channel typically found in stream restoration.

that higher floodplains would trap fine sediment due to significantly decreased flow velocities and thus be more important for particle-derived nutrient trapping. Greater nutrient content of fine organic-rich sediment could result in the upper floodplains functioning as hotspots of N sedimentation, mineralization, and denitrification. Finally, we predicted that restoration age would further enhance these effects. As the restoration project matures, establishment of riparian vegetation and enhanced biological activity in the rhizosphere of the riparian zone would accelerate soil biogeochemical processes.

Methods

Five study sites were selected to build upon ongoing research activities, particularly focusing on restored reaches with a range of floodplain connectivity (Table 1). To quantify the extent of connectivity, instream stage recorders were installed in June 2013. At the time of installation a preliminary geomorphic survey was completed at each site. We are currently finalizing a more detailed survey of each site that includes multiple cross sections (e.g. one for each tile location), stream pattern and longitudinal profile.

For each stream, 6 locations were established (3 in the upper floodplain and 3 in the low bench) for monthly determination of sedimentation rates and inorganic nutrient loading. Monthly sedimentation rates are currently being measured by weighing the dry mass of accumulated sediment on ceramic tiles (20×20 cm). Resin bags are also being used to quantify dissolved inorganic nutrient loading to the floodplain. Both have been collected monthly since May 2012.

Table 1: Restored streams included in the study.

Stream	Completed	Relative floodplain connectivity	Two-stage channel
Little Sugar Creek (LSC)	2004	Low	Yes
Dairy Branch (DB)	2006	High	Yes
Muddy Creek (MC)	2010	Medium	No
Winterfield Tributary (WT)	2011	Medium	No
Torrence Creek (TOR)	2012	Low	Yes

Net mineralization of N and P were be measured *in situ* in the surficial sediments (5 cm) from September through October 2012 using the resin core technique (DiStefano and Gholz 1986) modified for use in hydrologically dynamic wetland and floodplain sediments (Noe 2011). Modified resin cores allow water and gas exchange thereby tracking changes in the surrounding soil abiotic environment (Noe 2011). Mass of N and P in ambient soil were measured in a sample collected at the beginning of the one-month incubation and compared to mass at the end of the incubation. Changes in hydrology (e.g. overbank flooding and rising groundwater tables) deliver nutrients to floodplain soils. Mass loading to the soil was quantified as the mass retained in the outer resin bags of the in site core while biological transformations within the soil were captured by measuring changes in the two inner resin bags and soil core itself.

Potential denitrification rates were also measured during the Fall/Winter. Soils were incubated as soil/stream water slurries using the denitrification enzyme activity (DEA) assay (Tiedje et al. 1989, Groffman et al. 1999). Denitrification potential measures the intrinsic capacity for conversion of NO_3^- to N_2 by removing substrate limitation. Soil samples from low benches and upper floodplains were collected from November 2012 through January 2013.

Sedimentation rates, nutrient loadings and denitrification rates were compared across site ($n=5$) and elevation ($n=2$) using a two-way ANOVA with Tukey's HSD post-hoc comparison of means. Reported statistics were determined to be significant at $\alpha = 0.05$. Means of measured values are presented with error shown as the standard deviation. Relationships between response variables (e.g. denitrification rates) and hypothesized causal variables were tested using simple linear regressions.

Preliminary Results and Discussion

Average sedimentation rates from May-September 2012 were significantly greater in the low benches ($134.2 \pm 336.5 \text{ g m}^{-2} \text{ d}^{-1}$) compared to the high benches ($7.84 \pm 15.4 \text{ g m}^{-2} \text{ d}^{-1}$) when all sites were lumped together ($p=0.0047$, Figure 2). This difference was most evident at DB with total sediment sedimentation rates ranging from $124.0 - 1269.5 \text{ g m}^{-2} \text{ d}^{-1}$ at the locations in the low benches and $17.9 - 48.1 \text{ g m}^{-2} \text{ d}^{-1}$. However, this patterns was not universally observed, particularly at WT with similar sedimentation rates observed at all sites. Flashy hydrology and localized stream hydraulics in these urban sites controlled rates of sediment erosion and deposition.

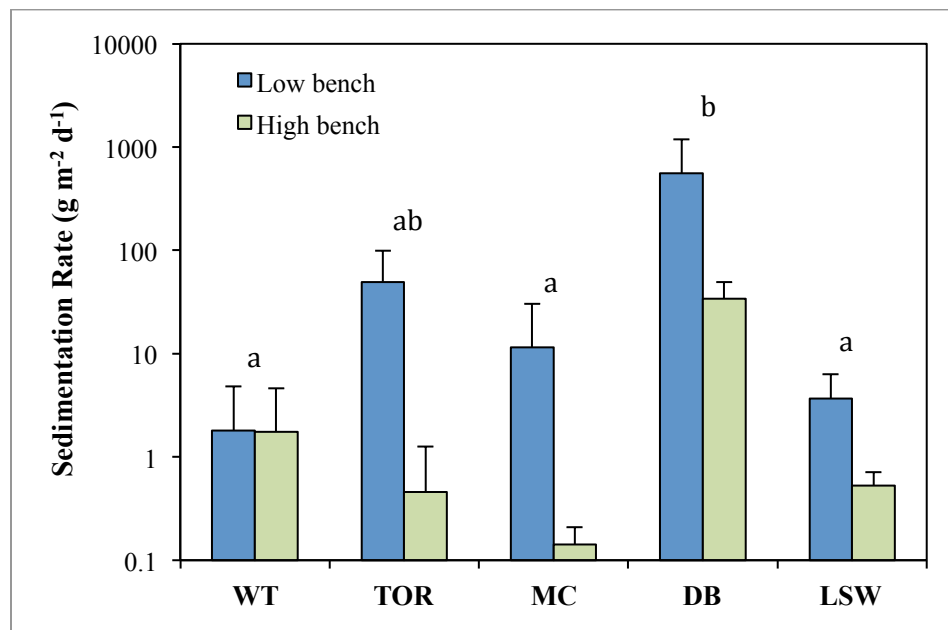


Figure 2: Sedimentation rates in the low and high benches from May – September 2012. Data are presented on a log scale and error bars indicated one standard deviation. Letters show significantly different rates by site ($p=0.0002$).

Potential denitrification rates were also measured at each of the sites during Fall/Winter 2012. Rates ranged from 1.2 – 80.4 mg m⁻² h⁻¹. No differences were observed between the low and high benches, however differences among sites were significant (p<0.0001, Figure 3). To better understand the factors controlling this variability, we performed simple linear regressions with potential causal variables. While this list is currently being expanded to include more soil and hydrologic metrics, two key variables emerged as significant. First, potential rates of denitrification were positively correlated with sedimentation rates (p=0.004; Figure 4). While the deposited sediment was not high in organic matter content, areas with high sedimentation rates also have well established vegetation and organic soils both of which contribute to increased bacterial activity in the rhizosphere. Restoration age was also an important factor controlling DEA. The oldest sites with mature vegetation exhibited highest rates of denitrification independent of elevation (R²=0.38, p<0.001). The correlation of denitrification rates with restoration age and sedimentation rates highlights the importance of vegetation and soil organic matter to fuel biogeochemical transformations.

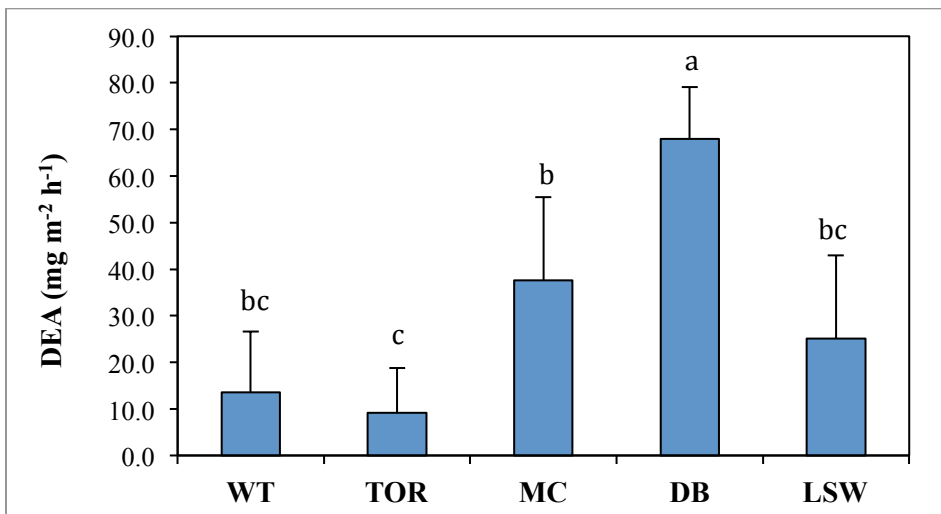


Figure 3: Denitrification potential (DEA) with error bars representing one standard deviation. Letters show significantly different rates by site (p<0.0001).

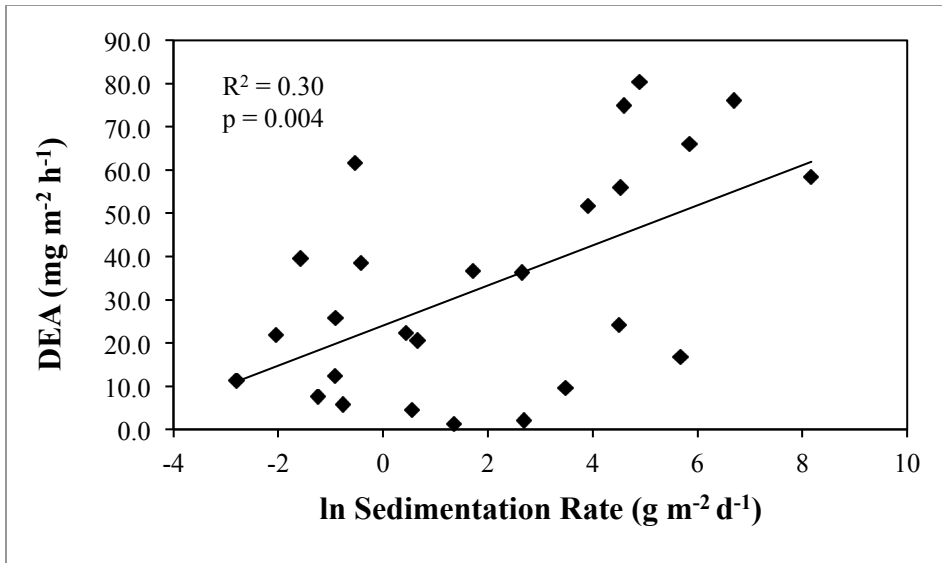


Figure 4: Linear regression of denitrification potential (DEA) as a function of ln transformed sedimentation rates.

Future work

There is a considerable amount of data collection and analysis yet to be completed for this project. We are currently analyzing data from the Fall/Winter *in situ* core experiments in which we measured net N and P mineralization rates. In addition, soil characteristics (including physical properties and chemical concentrations) are being quantified. Monthly nutrient loading as measured by extraction of inorganic nutrients (NH₄-N, NO₃-N and PO₄-P) from resin bags has recently been measured and data are currently being analyzed. Together these data will give us a greater understanding of loadings during storm events and biogeochemical processes in the restored floodplain soils.

A key component of this project is to link these data to hydrologic connectivity. At the start of the project, stage level recorders were installed and a preliminary geomorphic survey was completed at each site. We are currently finalizing a more detailed survey of each site that includes multiple cross sections (e.g. one for each tile location), stream pattern and longitudinal profile. This physical data will allow us to determine the time of inundation (indicator of connectivity) which will be tested as a predictor variable for nutrient and sediment loading as well as biogeochemical transformations in the floodplain soils.

We are requesting a no cost extension to complete these additional analyses and develop predictive statistical models of the system. We anticipate that this will be completed by December 31, 2013.

References

DiStefano, J. F. and H. L. Gholz. 1986. A proposed use of ion exchange resins to measure nitrogen mineralization and nitrification in intact soil cores. *Communications in soil science and plant analysis* **17**:989-998.

Groffman, P. M., E. A. Holland, D. D. Myrold, G. P. Robertson, and X. Zou. 1999. Denitrification. Pages 272-290 *in* G. P. Robertson, B. P. Bledsoe, D. C. Coleman, and P. Sollins, editors. *Standard Soil Methods for Long-Term Ecological Research*. Oxford University Press, New York.

Kaushal, S. S., P. M. Groffman, P. M. Mayer, E. Striz, and A. J. Gold. 2008. Effects of stream restoration on denitrification in an urbanizing watershed. *Ecological Applications* **18**:789-804.

Mayer, P. M. R., S. K. McCutchen, M. D. Canfield, and J. Timothy. 2007. Meta-analysis of nitrogen removal in riparian buffers. *Journal of Environmental Quality* **36**:1172.

Noe, G. B. 2011. Measurement of net nitrogen and phosphorus mineralization in wetland soils using a modification of the resin-core technique. *Soil Science Society of America Journal* **75**:760-770.

Noe, G. B. and C. R. Hupp. 2009. Retention of Riverine Sediment and Nutrient Loads by Coastal Plain Floodplains. *Ecosystems* **12**:728-746.

Tiedje, J. M., S. Simkins, and P. M. Groffman. 1989. Perspectives on measurement of denitrification in the field including recommended protocols for acetylene based methods. *Plant and Soil* **115**:261-284.

Vidon, P., C. Allan, D. Burns, T. Duval, N. Gurwick, S. Inamdar, R. Lowrance, J. Okay, D. Scott, and S. Sebestyen. 2010. Hot spots and hot moments in riparian zones: potential for improved water quality management. *Journal of the American Water Resources Association*:278-298.

Information Transfer Program Introduction

The Water Resources Research Institute (WRI) is heavily geared to providing water resources information to the water professional. WRI maintains a strong information transfer program by cooperating with various state agencies, municipalities, and professional organizations to sponsor workshops and other events and by seeking grants for relevant activities.

The professionals targeted by this program include private entrepreneurs, federal, state and local government staff and officials, and representatives of industry, agriculture, consulting, and environmental groups. The main forms of information transfer are through an Institute internet site, bi-monthly newsletter, conferences, seminars, forums, workshops, luncheons, and research publications.

The workshops conducted through WRI's partnership with the Department of Environment and Natural Resources Division of Energy, Mineral and Land Resources constitute the primary means by which the Division meets its educational obligations on sediment control under the state's Sediment Control Act.

WRI continues to be a sponsor of continuing education credits by the NC Board of Examiners of Engineers and Surveyors as an Approved Sponsor of Continuing Professional Competency activity for Professional Engineers and Surveyors licensed by the State of North Carolina. In addition, WRI also submits information for approval to the N.C. Board of Landscape Architects to offer contact hours to landscape architects. This allows WRI to offer Professional Development Hours (PDHs) to engineers and surveyors, and Continuing Education Units (CEUs) to landscape architects for attendance at the WRI Annual Conference and other workshops, seminars and forums that WRI sponsors.

During this reporting year, WRI provided 65.5 PDHs and 55.5 CEUs to 1048 people at 12 workshops, seminars, and other events described below.

WRRRI Information Transfer Program

Basic Information

Title:	WRRRI Information Transfer Program
Project Number:	2012NC174B
Start Date:	3/1/2012
End Date:	2/28/2013
Funding Source:	104B
Congressional District:	NC-02
Research Category:	Not Applicable
Focus Category:	None, None, None
Descriptors:	None
Principal Investigators:	Nicole Wilkinson

Publications

There are no publications.

FY 2012 Information Transfer Progress & Achievements

WRRI Sponsored Workshops, Forums and Seminars

Below is a list of the educational and training events WRRI sponsored during the project year, along with a description of each and the number of attendees. In total, through these workshops, WRRI offered 65.5 Professional Development Hours, 55.5 Continuing Education Units, and reached 1048 participants.

March 6, 2012 Water Audit Software Training

Best-practices for Water Auditing and Loss Control, as developed by the American Water Works Association, are beginning to take hold among water systems in the Southeast and across the nation. Water Auditing and Loss Control programs are the most effective ways for a utility to conserve water, save operating expenses, and increase revenues. To this end, the AWWA Water Loss Control Committee has made available a free software application as a useful and easy way for utilities to compile a basic, preliminary audit of water supply and billing operations, and begin to measure key performance indicators for water system efficiency. Join us on January 19th to learn how to use the software, to gain a thorough understanding of the data inputs and data validity, and to understand software outputs and how to apply them to your utility. Participants will benefit from team work, paper exercises, computer work, and a small amount of lecture, and will learn using real and simulated data from large and small utilities.

Attendance: 20

March 27-28, 2012 WRRI Annual Conference and NCWRA Symposium

Description: The WRRI annual conference is the premier research conference focusing on North Carolina's water resource issues, solutions, and opportunities. The NC Water Resources Association was again a key partner, with the NCWRA Annual Symposium "Mitigation Policy in NC: Is the Train on the Right Track?" being an integral element of the conference program. Local and state governments are under increasing pressure to protect and restore water resources and maintain the ecological integrity of aquatic habitats. Yet, experience has shown that restoring physical habitat alone may not be sufficient to achieve thriving biological communities, and that the interactions of a vast array of environmental variables and the complexities of ecosystem science make restoration needs difficult to understand and efforts costly to plan, implement, and regulate. The goal of the symposium was to help us better understand these complexities and prepare for the future restoration and protection of NC's water resources. In addition to this portion of the agenda, the symposium sparked a flood of conference abstracts that ended up creating a session track on stream restoration that spanned the length of the conference and was very well received. The conference offered 9.5 PDHs, 9.5 CEUs, and had 210 attendees. Over a 2-day period, the conference featured 110 presentations – 63 oral presentations over 15 concurrent sessions, 12 invited speakers in special sessions, and 35 poster presentations.

Attendance: 257

March 28, 2012 Progress Energy Seminar "Reality Check: Water Quality Management Perspectives from Scientists, Regulators, and the Regulated"

Description: Protection and restoration of surface waters from the impacts of non-point source pollution have received significant statewide and national attention in recent years. As price tags and regulations associated with water quality impairment and watershed rehabilitation

grow, there is an increasing need for research and data on aquatic ecosystems and what policies and strategies can realistically deliver desired results. The Progress Energy seminar brings together members of the scientific and environmental communities to discuss the realities of the ecological complexity of the ecosystems we seek to manage, as well as state regulators, and local governments to provide their perspectives on the reality of enforcing and complying with regulations designed to recover these ecosystems.

Attendance: 150

April 17-18, 2012 Erosion and Sedimentation Control Planning and Design Workshop

Description: These workshops are structured to educate and familiarize design professionals with the NC Sedimentation Pollution Control Act (SPCA), the rules implementing the Act, design standards for erosion and sedimentation control BMPs, and elements that are necessary to submit an erosion control plan. This comes directly from the source—the NC Division of Land Resources Land Quality Section and its partners to provide professionals with the information they need to submit an erosion control plan and prevent pollution by sedimentation.

Attendance: 102

May 7, 2012 NCWRA Seminar "Making Green Development a Reality in Coastal North Carolina"

Description: One of few authentic green communities in North Carolina, The Village of Woodsong, a Traditional Neighborhood Development (TND) near Shallotte, received the first ever Outstanding Recognition award for environmental excellence by The Lower Cape Fear Stewardship Program. Woodsong's stormwater plan was created to meet the triple bottom line of social, financial, and environmental values as it aimed to meet regulations and improve water quality. The presenter, Mr. Buddy Milliken, discussed his experience with getting innovative development ideas through the planning and permitting process and into reality in Woodsong, as well as potential barriers to future green development in the state.

Attendance: 41

September 10, 2012 NCWRA Seminar, "Water Quality Considerations for Shale Gas Development in North Carolina"

Description: In May 2012, the NC Department of Environment and Natural Resources completed a study of the potential for development of shale gas in North Carolina. With the passage of Senate Bill 820 in summer 2012, the NC General Assembly lifted prohibitions on technologies needed to exploit this potential resource and directed DENR to develop regulations for the shale gas exploration and production activities. Evan Kane presented an overview of some of the water quality considerations associated with potential shale gas development in North Carolina and a preview of the regulatory development process that lies ahead..

Attendance: 103

October 10, 2012 Erosion and Sedimentation Control Planning and Design Workshop, Swansboro NC

Description: These workshops are structured to educate and familiarize design professionals with the NC Sedimentation Pollution Control Act (SPCA), the rules implementing the Act, design standards for erosion and sedimentation control BMPs and elements that are necessary to submit an erosion control plan. This comes to directly from the source-the NC Division of Land Resources Land Quality Section and its partners providing you with the information you need to submit a plan and prevent pollution by sedimentation. The workshop focused on considerations

for land planning and enhancement of developing watersheds. Techniques will be discussed for channel design, conveyance of runoff, and surface dewatering. Design criteria for erosion control materials were demonstrated through use of online tools.

Attendance: 39

November 15, 2012 Erosion and Sedimentation Control Planning and Design Workshop, Hickory NC

Description: See description above.

Attendance: 89

December 3, 2012 NCWRA Seminar “The Role of Manufacturing and Industry in Promoting and Implementing Water Reuse in North Carolina”

Description: This program will focus on water reuse and non-traditional water sources such as municipal and industrial wastewater, harvested rainwater, stormwater, condensate, and remediated groundwater, and we will discuss the importance of these to holistic water supply planning and future resource management strategies for North Carolina. The presentation will include regulatory and statutory revisions enacted by the 2011 session of the General Assembly, as well as pertinent topics for upcoming sessions of the General Assembly, including Aquifer Storage & Recovery (ASRs), intrusion barriers, potable reuse, regulatory reform, and hydraulic fracturing. Local case studies of sustainable water practices implemented at commercial, institutional and industrial facilities will be highlighted.

Attendance: 31

December 4, 2012 Erosion and Sedimentation Control Planning and Design Workshop, Raleigh NC

Description: See description for previous Erosion and Sediment Control workshops.

Attendance: 90

February 5-6, 2013 Local Programs Erosion and Sediment Control Workshop

Description: The Local Programs Workshop provides training for local governments that have ordinance delegation and enforces the North Carolina Sedimentation Pollution Control Act. The training provides local programs an opportunity to be updated on the most current erosion and sedimentation control research and to get together with other local programs and exchange sedimentation and erosion control ideas and practices utilized at the local level. This training is helpful for landscape architects that may work for a local government that has an erosion and sedimentation control program. *Attendance:* 100

February 11, 2013 NCWRA Seminar “Clean Water Management Trust Fund: Understanding Programmatic Changes and the Future of North Carolina’s Surface Waters”

Description: The Clean Water Management Trust Fund was created to provide resources to protect and restore water quality across North Carolina. Current and evolving threats make our limited water resource of great importance to sustaining our state’s ability to adapt and meet the growing demands on this resource in a balanced way. This presentation provided an overview of the Clean Water Management Trust Fund and the programs that are in place to help communities protect, restore, and enhance surface waters in North Carolina.

Attendance: 26

Newsletter

Published the *WRRRI News* four times during the reporting period (April-June 2012 Issue #378, July-Sept 2012 Issue #379, Oct-Dec 2012 Issue #380 and Jan-Mar 2013 Issue #381). The WRRRI News is an 8-12 page newsletter that covers a wide range of water-related topics from current federal and state legislation and regulatory activities to new research findings, water-related workshops and conferences, and reviews of water-related publications. The WRRRI News is now sent electronically to 1008 federal and state agencies, university personnel, multi-county planning regions, city and local officials, environmental groups, consultants, businesses and individuals. It is also posted on the WRRRI website <http://www.ncsu.edu/wrri/code/publications/currentpublications.htm>

Internet Services

WRRRI continues to maintain a website, www.ncsu.edu/wrri. Overall, the goals of our website are:

- to provide access to information on upcoming events (seminars, workshops, etc) that are hosted by WRRRI and other events in the state related to water resources, as well as access to materials and resources from past events;
- to provide information to the research community about funding opportunities and state research priorities;
- to increase dissemination of information by providing access to research reports, the WRRRI newsletter, and other relevant publications;
- to provide information on key organizations with which WRRRI has strong partnerships and which play a key role in water resource research and management in the state;
- to provide background information about WRRRI at the state and federal levels, our roles, and what we can offer to different audiences throughout the state.

A related component of the website involves working with NC State University's DH Hill Library to increase and enhance WRRRI's use of their technical reports repository for all WRRRI publications. Through this collaboration, we are now able to direct people to this well organized, easily searchable site where they can access research reports from all WRRRI-funded projects as far back as the 1960s.

WRRRI Electronic Lists

WRRRI maintains the following electronic mail lists (listservs) for information transfer purposes:

- Water-Research list - 211 subscribers – inform water researchers from NC universities about calls for papers, grants, upcoming conferences, student internships, etc.;
- WRRRI-News list - 1008 subscribers - informs researchers, local governments, municipalities, interest groups etc. about calls for papers, grants, upcoming conferences and events, etc.;
- NCWRA-info list - 305 subscribers - provides information of the North Carolina Water Resources Association sponsored events;
- Urban Water Consortium (UWC) for Urban Water Consortium member communications;
- and UWC-Stormwater Group list for the UWC Stormwater Group member communications.

NC Urban Water Consortium

WRRI administers the NC Urban Water Consortium (UWC) and meets with the members quarterly. The consortium was established in 1985 by the Institute, in cooperation with several of North Carolina's larger cities to provide a program of research and development, and technology transfer on water problems that urban areas share. Through this partnership, WRRI and the State of North Carolina help individual facilities and regions solve problems related to local environmental or regulatory circumstances. Participants support the program through annual dues and enhancement funds and guide the program through representation on an advisory board, selection of research topics, participation in design of requests for proposals, and review of proposals. There are 12 member cities/special districts in North Carolina, and several members hosted quarterly meetings on the following dates: March 9, 2012 in Raleigh; June 22, 2012 in Greenville; September 7, 2012 in Carrboro; and December 7, 2012 in Cary.

The UWC also provided financial support to two research projects, which increased WRRI's ability to fund other high quality research with 104(b) funds. The two projects funded by the UWC were:

- "Bioavailability and fate of organic nitrogen loading to Neuse River Estuary phytoplankton" by PI Hans Paerl, UNC-Chapel Hill
- "Fats, Oil, and Grease Communications Implementation" by PI Regina Guyer, UNC-Charlotte

NC Urban Water Consortium - Stormwater Group

In 1998, several members of the NC UWC partnership formed a special group to sponsor research and technology transfer on issues related to urban stormwater and management. The Urban Water Consortium (UWC) Stormwater Group is administered by WRRI. Participants support the program through annual dues and enhancement funds. They guide the program through selective representation on the WRRI advisory board, determining stormwater-related research priorities, participation in the design of requests for proposals and review of proposals submitted to WRRI directly or to the SWG. During this reporting year, the SWG added their ninth member, the City of Burlington, to their membership. Quarterly meetings were held on the following dates: March 8, 2012 in Raleigh; June 21, 2012 in Greensboro; October 11, 2012 in High Point; and December 6, 2012 in Charlotte.

Individual members of the UWC-SWG provided funding for three research projects as enhancement projects through WRRI entitled:

- "Evaluating the Hydrologic and Water Quality Performance of Infiltrating Wet Ponds and Development of Supplemental Infiltrating Pond Design Guidance" by PI William Hunt
- "Implementing Permeable Pavement in Triassic Soils and Statewide to Reduce Runoff Volume and Nutrient Loads" by PI William Hunt
- "Downspout Disconnection & Rain Catchers Assistance" by PI William Hunt

USGS Summer Intern Program

None.

Student Support					
Category	Section 104 Base Grant	Section 104 NCGP Award	NIWR-USGS Internship	Supplemental Awards	Total
Undergraduate	7	0	0	0	7
Masters	3	0	0	0	3
Ph.D.	1	0	0	0	1
Post-Doc.	0	0	0	0	0
Total	11	0	0	0	11

Notable Awards and Achievements

1. Dr. Susan White Named New Director of NC WRI and NC Sea Grant

Ecologist Susan N. White was named the new executive director for Water Resources Research Institute of the University of North Carolina and North Carolina Sea Grant upon the retirement of Michael P. Voiland in December 2012.

"Susan brings a strong science background, as well as leadership working with a mix of partners and stakeholders," notes Vice Chancellor Terri L. Lomax of North Carolina State University, where the two state/federal partnership programs are headquartered.

"She will be a great leader for WRI and Sea Grant programs here that have strong traditions of assisting and guiding communities, businesses, organizations and the public," Lomax adds. Sea Grant focuses on the ecosystems and economies of the coastal region, while WRI supports research and training related to freshwater topics statewide.

White, who earned a doctorate from the University of Georgia, is returning to her home state. She grew up in Orange County and graduated from Duke University. She is eager to lead both University of North Carolina system programs that provide targeted research, outreach and education projects.

"I am excited to have this opportunity to work with the excellent teams associated with North Carolina Sea Grant and WRI to continue to address the current and future critical coastal, ocean, and water resource issues in the state and within the region," she says.

White's previous position was with the National Oceanic and Atmospheric Administration's Hollings Marine Laboratory in Charleston, SC. The Hollings lab is a Center of Excellence in Oceans and Human Health, working in partnership with the College of Charleston, Medical University of South Carolina, South Carolina Department of Natural Resources, and the National Institute of Standards and Technology.

As Hollings director since 2010, White had provided research vision and organizational management, including strategic planning with the partner agencies and universities. She previously served as deputy director, responsible for budgets and administration, with a focus on accountability and performance measures. The interdisciplinary facility provides science and technology research on coastal ecosystems, with an emphasis on linkages between the condition of coastal environments and human health and well-being.

"Her watershed approach — from the mountains to the sea — is a great fit for North Carolina, along with her knowledge of rapid-detection tools and technologies, and coastal health early warning systems," Lomax adds.

Formerly the national research coordinator for NOAA's Estuarine Reserves Division and National Estuarine Research Reserve System, White is a board member of The Coastal Society. She has served on national and regional steering committees on topics including technology transfer, integrated drought monitoring and early warning, and climate's connections to health.

"We are very fortunate to have a scientist, administrator and native North Carolinian of Susan's caliber and experience take on the leadership for Sea Grant and WRI. I am most confident that she will serve both programs well," notes Voiland, who has served with White on the NOAA in the Carolinas executive and steering committees.

2. NC WRII Coordinator for Research and Outreach Accepted to Fellowship Program Nicole Wilkinson, the Coordinator for Research and Outreach at NC WRII was accepted as a fellow in the Natural Resources Leadership Institute (NRLI) program in January 2013. NRLI brings together people from across North Carolina to develop leadership competencies for effectively engaging in today's complex, and often controversial policy environment. Since 1995, hundreds of professionals who are involved in natural resources policy, planning, education, and management have participated in the Institute, building skills and knowledge in conflict resolution and multi-party negotiation, critical thinking, and collaborative problem solving. The goal of the program is to enhance leadership in environmental management and policy development, leadership that will influence workable solutions to complex, often contentious environmental issues. The curriculum spans 18 months and includes approximately 140 hours of instruction time, as well as time spent outside of the classroom on a practicum project related to WRII's work and priorities. Mrs. Wilkinson will graduate from NRLI in June 2014.

3. WRII Hires New Newsletter Editor Science writer and editor Rhett Register recently joined the North Carolina Water Resources Research Institute. His duties also include writing for North Carolina Sea Grant's Coastwatch magazine. "We were lucky to find someone like Rhett with a strong background in science, policy and writing who also has the capacity to cover the range of issues – from the mountains to the coast – that our state and WRII must contend with," says Nicole Wilkinson, Coordinator for Research and Outreach at WRII. "Most people specialize in either freshwater or saltwater, so Rhett's diversity makes him a great fit for this position that we share with NC Sea Grant," she adds.

Register credits his birthplace, Jacksonville, Fla., for marking him with an early love for watery environments, with its easy access to beaches, rivers and Florida's massive springs. He has a background in writing about coastal planning and water resource issues. "Working with WRII and NC Sea Grant and has allowed me to combine my love for the aquatic environment with my interest in writing and communications," Register says.

Prior to joining WRII, Register worked as a researcher with National Geographic magazine and at National Geographic Traveler, researching and covering topics as varied as the American Civil War and marine protected areas. He also has worked with Oregon Sea Grant and a community newspaper. He has taught English, including three years in Japan. Register holds an undergraduate degree in English from the University of North Florida, and a master's degree from the marine resource management, or MRM, program at Oregon State University.

He joins the team as Jeri Gray, long-time newsletter editor and previous WRII education coordinator, leaves WRII. While Ms. Gray officially retired from WRII many years ago, she has stayed on as the organization's newsletter editor, covering water resource issues in our state with great skill, depth, and detailed analysis that has served to inform the state about priority topics for many years.

4. WRII Co-Produces Erosion and Sediment Control Needs Assessment WRII has had a long-standing relationship with North Carolina's Division of Energy, Mineral and Land Resources (DEMLR, previously the Division of Land Resources) in the state's Department of Environment and Natural Resources (DENR). WRII co-hosts annual erosion and sediment control workshops that help the division satisfy its mandate to provide education pursuant to the Sedimentation Pollution Control Act of 1973. As development slowed in the state during the economic downturn beginning in 2008, participation in training events decreased and professional needs changed as design professionals found themselves either without work or with increased job responsibilities where they needed to learn new skills and wear new hats. In order to ensure that the erosion and sediment control workshops continued to meet the present needs of professionals and continue to satisfy DEMLR's education provider requirements, WRII worked with the Center for Urban and Community Services at NC State University to conduct a statewide training needs assessment for erosion and sediment control professionals. A total of 713 respondents participated in the assessment, and the results have been used to inform the design and implementation of training in FY 12. While registration numbers were still low,

participant feedback indicated that presentation topics were very appropriate to the issues and training needs that professionals are faced with in today's environment. The assessment findings will continue to inform future trainings and it has been a very valuable resource at a time when funding and support for continuing education is tenuous.

5. Student Supported By USGS Funding Joins Wildlands Engineering Alea Tuttle, a graduate student supported by USGS Funds for project 2012NC173B "Nutrient retention and floodplain connectivity in restored Piedmont streams", under PI Sara McMillan, was hired as Project Scientist at Wildlands Engineering, an ecological engineering firm specializing in stream and wetland restoration. Ms. Tuttle's work with Dr. McMillan has been presented at WRRRI's annual research conference.

Publications from Prior Years

1. 2010NC147B ("Microbial Contaminants Associated with Urbanization of a Drinking Water Reservoir") - Articles in Refereed Scientific Journals - Rowny, JG and JR Stewart (2012). Characterization of nonpoint source microbial contamination in an urbanizing watershed serving as a municipal water supply. *Water Research*. 46(18):6143-6153.
2. 2010NC147B ("Microbial Contaminants Associated with Urbanization of a Drinking Water Reservoir") - Articles in Refereed Scientific Journals - Gentry-Shields, J, JG Rowny and JR Stewart (2012). HuBac and nifH source tracking markers display a relationship to land use but not rainfall. *Water Research*. 46(18):6163-6174.
3. 2010NC147B ("Microbial Contaminants Associated with Urbanization of a Drinking Water Reservoir") - Articles in Refereed Scientific Journals - Gentry-Shields, J, A Wang, RM Cory and JR Stewart (2013). Determination of specific types and relative levels of qPCR inhibitors in environmental water samples using excitation-emission matrix spectroscopy and PARAFAC. *Water Research*. Accepted. doi: 10.1016/j.watres.2013.03.049.